

DOCTORAL THESIS  
DIFFERENTIAL GEOMETRY

---

*Invariant Surfaces with Generalized  
Elastic Profile Curves*

---

Author:  
Álvaro Pámpano Llarena

Advisors:  
Prof. Óscar J. Garay Bengoechea  
Dr. Josu Arroyo Olea

September, 2018

Department of Mathematics  
University of the Basque Country (UPV/EHU)

eman la zabal zazu



Universidad del País Vasco    Euskal Herriko Unibertsitatea



# Acknowledgements

First of all, I would like to express my sincere gratitude to my supervisors Prof. Óscar J. Garay and Dr. Josu Arroyo for the continuous encouragement of my PhD and related research. Without their aid, patience and support I would not have been able to do this thesis. Actually, they have guided me in all the time of research and writing, always providing me with the tools needed to choose the right direction and successfully complete this memory.

Besides my advisors, I would also like to thank Prof. Stefano Montaldo for his warm hospitality during my research stay under his supervision at University of Cagliari, and for all the time he has spent introducing me in different geometric topics. In the same direction, I am profoundly grateful to Prof. Rafael López for friendly and generously receiving me at University of Granada, and for suggesting me new things to research.

However, the process of reaching this PhD started some years ago when I was an undergraduate student. As a matter of fact, my end of degree project was also related with Geometry.

In this sense, I would like to acknowledge the project advisors; on one hand, Dr. Jose J. Mencía who first introduced me to Geometry and taught me the basic notions, being not only my teacher but also my tutor; and, on the other hand, once more I owe Prof. Óscar J. Garay a debt of gratitude for enabling me to give my first steps in researching about Geometry and for helping me throughout the whole process. Being the advisor of all my projects during the degree, master and thesis he has also become a real mentor for me.

Last but not least, I must also thank the Programa Predoctoral de Formación de Personal Investigador No Doctor del Gobierno Vasco (2015) for the economic support. Moreover, this research has also been partially supported by MINECO-FEDER grant MTM2014-54804-P and Gobierno Vasco grant IT1094-16.



# Resumen

En esta memoria estamos principalmente interesados en estudiar la conexión entre las **curvas críticas** para energías de tipo elásticas adecuadas (lo que posteriormente llamaremos curvas elásticas generalizadas) y las **superficies invariantes** que posean ciertas propiedades geométricas interesantes (como por ejemplo, superficies de evolución binormal, superficies de curvatura media constante, superficies de Weingarten lineales,...). Además, se establecerá una conexión similar entre las superficies invariantes críticas para energías de tipo-Willmore (véase la definición de superficies tipo-Willmore en la página xiii) y curvas elásticas generalizadas. En el caso compacto, esta relación se basa en el Principio de Criticidad Simétrica de Palais, [117].

Más concretamente, vamos a estudiar las curvas críticas para algunos casos particulares de la siguiente familia de **energías elásticas generalizadas**

$$\Theta_{-\Phi}^{\epsilon,p}(\gamma) = \int_{\gamma} (\kappa^{\epsilon} + \Phi)^p ds,$$

donde  $\epsilon = 1, 2$ ,  $p \in \mathbb{R}$  y  $\Phi$  es un potencial. Como ya hemos mencionado, llamaremos **curvas elásticas generalizadas** a las curvas críticas de alguna de las energías anteriores; y, a partir de ellas vamos a construir superficies invariantes en espacios tridimensionales que posean propiedades geométricas atractivas para su estudio, como son las mencionadas anteriormente. Es decir, vamos a establecer un nexo entre las curvas elásticas generalizadas y diferentes tipos de superficies invariantes inmersas en ambientes tridimensionales.

El primer capítulo de la memoria está dedicado a la introducción de los objetos y fórmulas básicas, y al establecimiento de la notación y las convenciones que se usan a lo largo de la memoria. En efecto, vamos a recordar algunos aspectos de la geometría semi-Riemanniana, que van a resultar esenciales en el futuro desarrollo de la memoria. En concreto, nos vamos a centrar en superficies inmersas en los **modelos de espacio semi-Riemannianos de dimensión tres**. Así mismo, también vamos a recordar diversas herramientas y técnicas sobre problemas variacionales actuando en espacios de curvas donde los Lagrangianos dependen de las curvaturas de estas curvas. En particular, vamos a introducir las **líneas de centros de Kirchhoff generalizadas**, es decir, extremos de

la energía

$$\Theta(\gamma) = \int_{\gamma} (P(\kappa) + \mu \tau + \lambda) ds,$$

donde  $\kappa$  y  $\tau$  son la curvatura y torsión de  $\gamma$ , respectivamente,  $P(\kappa)$  es una función diferenciable y  $\lambda, \mu \in \mathbb{R}$  dos constantes. Debemos resaltar que las curvas críticas para cualquier tipo de funcionales energéticos dependientes de la curvatura poseen dos **campos de vectores de Killing** asociados. Entre ellos, se encuentra uno que es paralelo al campo de vectores binormal a la curva (y que denotaremos de ahora en adelante por  $\mathcal{I}$ ), tal y como se detalla en la Proposición 1.3.2 y en la Proposición 1.3.3 (véase también [58] y [94]).

Posteriormente, en el Capítulo 2, centraremos nuestra atención en las curvas elásticas generalizadas. En este capítulo trataremos de cubrir dos objetivos; por un lado, particularizando los resultados conocidos para casos más generales, en la primera parte del capítulo (Sección 2.1) estudiaremos las curvas elásticas generalizadas y fijaremos las ecuaciones de Euler-Lagrange, así como diversos resultados relacionados; y, por otro lado, en la segunda parte (Sección 2.2), describiremos una aplicación interesante de una elección particular de la energía elástica generalizada, dada por  $\epsilon = 2$  y  $p = 1/2$  para un potencial constante  $\Phi = a^2$ , a la compleción visual de curvas. Esta construcción justifica el estudio de este tipo de curvas, no sólo como objetos puramente matemáticos, si no que también ilustra sus diversas aplicaciones a otras áreas. Por ejemplo, se puede utilizar para resolver un problema surgido en visión computacional, ya que, reducimos el problema **sub-Riemanniano** de la compleción de imágenes mediante optimización a un problema variacional clásico. De hecho, tal y como sugieren diversos estudios neuro-biológicos, *existe una estructura sub-Riemanniana en el espacio de células visuales y, con el objetivo de completar una imagen parcialmente dañada o cubierta, el cerebro considera geodésicas sub-Riemannianas entre los puntos finales de la información que falta*. Esta estructura sub-Riemanniana ha sido recientemente modelada usando para ello el **fibrado unitario tangente** del plano, [124].

En la Sección 2.2.1, reduciremos el problema de hallar las geodésicas sub-Riemannianas, que se cree que usa el cerebro con fines de reconstrucción de imágenes, a la búsqueda de extremos de una familia de energías de tipo curvatura total (que en nuestro caso, se reducen a energías elásticas generalizadas para las elecciones  $\epsilon = 2$ ,  $p = 1/2$  y  $\Phi = a^2$ ) en el plano, es decir, a un problema variacional clásico. Entonces,

*Resolveremos estos problemas variacionales completamente, de forma geométrica, en la Sección 2.2.2, obteniendo de forma explícita las curvaturas de las curvas críticas.*

Teóricamente, esto resuelve el problema completamente, pues las curvaturas caracterizan a las curvas en el plano, salvo movimientos rígidos. Sin embargo, para objetivos prácticos resulta más conveniente utilizar un método numérico adecuado para aplicaciones

específicas y concretas. Por ello,

*En la Sección 2.2.3, describiremos un método numérico para obtener las curvas que minimicen la longitud. Esta aproximación, implementada en lo que llamamos plataforma XEL, está basada en el método del descenso del gradiente y se explicará brevemente en el Apéndice B.*

Por otro lado, como se explica al final de esa sección, el método que hemos desarrollado posee una gran ventaja en comparación con otros métodos numéricos, pues nos permite calcular la desviación de las soluciones numéricas con respecto a las analíticas. Nuestros resultados sobre este tema han sido principalmente publicados en [13], aunque el método del descenso del gradiente va a ser descrito con más detalle en [9].

Este resultado se puede ver como una primera aplicación de las elásticas generalizadas que sirve tanto como introducción, como motivación para el interés en este tipo de objetos por si solos. Del mismo modo, como ya hemos comentado anteriormente, uno de los principales objetivos de esta memoria es construir y/o caracterizar las superficies invariantes (es decir, superficies que quedan invariantes por la acción de un grupo uniparamétrico de isometrías) generadas por curvas elásticas generalizadas y que posean propiedades geométricas interesantes. Para este fin, se usan dos tipos de herramientas diferentes. Primero, si el espacio ambiente es un modelo de espacio semi-Riemanniano de dimensión tres, la técnica que vamos a desarrollar se llama **evolución binormal de curvas** y el Capítulo 3 nos servirá para introducir y explicar detalladamente esta idea; por otro lado, la segunda herramienta de construcción se basa en el uso de levantamientos totales de curvas bajo sumersiones de Killing, y será explicado en el Capítulo 6.

En 1972, Hasimoto [73], usando una transformación particular, obtuvo la reconocida ecuación de Schrödinger no-lineal en una aproximación del movimiento auto-inducido de un vórtice en un fluido viscoso, aunque este movimiento del vórtice viajando sin estiramiento fue descrito en primer lugar en 1906 por Da Rios, [130]. Para este modelo, Da Rios usó el movimiento de una curva, que representaba al filamento o vórtice, propagándose de acuerdo a la ecuación de inducción localizada. Además, Hasimoto relacionó este movimiento con las curvas elásticas, probando que *la evolución de la curva se realizaba en la dirección de la binormal*, [74]. Por ello, siguiendo estas ideas, empezaremos el Capítulo 3 estudiando la información geométrica de la evolución de curvas en la dirección de la binormal (con velocidades dependientes de la curvatura y la torsión de las mismas,  $\mathcal{F}(\kappa, \tau)$ ) y definiendo las **superficies de evolución binormal**, es decir, las superficies inmersas localmente generadas por esta evolución. Como consecuencia de aplicar la transformación de Hasimoto a nuestro estado más general, obtendremos una familia de ecuaciones diferenciales cuyas soluciones se corresponden con una onda compleja para diferentes evoluciones binormales (véase la Proposición 3.1.2 y [64]). A continuación, tras

calcular las ecuaciones de Gauss-Codazzi (véase la Sección 1.1.2) obtenemos el Teorema 3.1.3, [64]

*Las superficies de evolución binormal asociadas a soluciones de tipo onda viajera de las ecuaciones de Gauss-Codazzi se corresponden con la evolución (por isometrías y deslizamiento) de las líneas de centros de Kirchhoff generalizadas.*

En particular, una consecuencia esencial viene dada en el Corolario 3.1.4, [10], y da lugar al siguiente resultado,

*Una curva de Frenet de rango 2 ó 3 evoluciona bajo el flujo de la binormal mediante isometrías de un modelo de espacio semi-Riemanniano de dimensión tres,  $M_r^3(\rho)$ , si y sólo si, es un extremo de*

$$\Theta(\gamma) = \int_{\gamma} (P(\kappa) + \lambda) ds,$$

donde  $\mathcal{F}(\kappa, \tau) = \mathcal{F}(\kappa) := \frac{d}{d\kappa} (P(\kappa))$  es la velocidad de la evolución de la curva.

Por lo tanto, localmente, podemos construir superficies invariantes evolucionando curvas críticas bajo el campo de vectores de Killing en la dirección de la binormal,  $\mathcal{I}$ , cuya existencia está garantizada por la Proposición 1.3.2. Aún más, en este capítulo también veremos que en un sistema de coordenadas geodésico, toda superficie invariante es localmente de este tipo. Ahora, un caso especial de evolución binormal aparece cuando todos los filamentos tienen torsión nula. Este caso se estudia en la Sección 3.2 y, para nuestros objetivos, podemos resaltar la Proposición 3.2.1, [10], y el resultado principal que se deriva de ahí,

*Consideremos una superficie de evolución binormal cuyos filamentos tengan torsión nula. Entonces, el filamento inicial es un extremo de la energía*

$$\Theta(\gamma) = \int_{\gamma} (P(\kappa) + \lambda) ds$$

*y la superficie de evolución binormal es una superficie invariante de  $M_r^3(\rho)$ .*

Como caso particular, si  $M_r^3(\rho)$  es simplemente un modelo de espacio Riemanniano de dimensión tres,  $M^3(\rho)$ , entonces la Proposición 3.2.3 y la Proposición 3.2.4, [12], nos dicen que *la superficie de evolución binormal del resultado anterior es rotacional*. Además, para estas superficies rotacionales de evolución binormal, desarrollaremos las condiciones de cierre, que están resumidas en el Corolario 3.2.7 (que aparecerá en [14]). Estas condiciones de cierre están basadas en las correspondientes condiciones de cierre de las curvas



críticas, y se pueden encontrar, por ejemplo, en [5].

Ahora, usando estos resultados, las primeras superficies críticas invariantes que estudiaremos en profundidad son las superficies de curvatura media constante invariantes. Para este objetivo, a lo largo del Capítulo 4, consideraremos el caso particular de la energía elástica generalizada dado por  $\epsilon = 1$ ,  $p = 1/2$  y potencial constante  $\Phi = -\mu$ . Resulta que, cualquier superficie invariante con curvatura media constante puede ser descrita localmente (véase la Sección 1.2.3) como la evolución binormal de una de estas curvas elásticas generalizadas, tal y como se prueba en el Teorema 4.1.1, [12]. Más aún, el recíproco también es cierto; *la evolución binormal de estas curvas elásticas generalizadas particulares bajo el flujo de  $\mathcal{I}$ , localmente, genera superficies con curvatura media constante en cualquier modelo de espacio semi-Riemanniano de dimensión tres,  $M_r^3(\rho)$* . Este resultado se puede encontrar en el Teorema 4.2.6, [12]. Resumiendo, si combinamos ambos resultados tenemos

*Localmente, una superficie invariante de  $M_r^3(\rho)$  con curvatura media constante se puede describir, o bien como una superficie reglada, o bien como una superficie de evolución binormal con condición inicial una curva crítica para*

$$\Theta_\mu(\gamma) = \int_\gamma \sqrt{\kappa - \mu} ds,$$

*con  $\mu \in \mathbb{R}$ . Recíprocamente, la superficie invariante en  $M_r^3(\rho)$  obtenida mediante la evolución bajo el flujo de la binormal del campo de Killing asociado  $\mathcal{I}$  de una curva crítica para  $\Theta_\mu$  tiene curvatura media constante  $H = -\varepsilon_1\varepsilon_2\mu$ .*

En este punto, como todas las superficies invariantes con curvatura media constante de cualquier modelo de espacio semi-Riemanniano de dimensión tres se pueden ver localmente como superficies de evolución binormal, y en este caso se trata de productos alabeados, podemos obtener una relación entre las superficies invariantes de curvatura media constante y las soluciones de la ecuación de Ermakov-Milne-Pinney, [54] y [127]. El Teorema 4.1.2, [12], enuncia y prueba esta relación. De hecho, se puede resumir como sigue

*La función alabeada de una descripción local de cualquier superficie con curvatura media constante invariante de  $M_r^3(\rho)$  es una solución de la ecuación de Ermakov-Milne-Pinney con coeficientes constantes.*

Finalmente, explotamos esta caracterización local de las superficies invariantes con curvatura media constante como superficies de evolución binormal con curvas elásticas generalizadas como filamentos iniciales para obtener nuevas pruebas de ciertos resultados interesantes de la teoría de superficies con curvatura media constante. Por ejemplo, en la

Sección 4.2.2 obtenemos que las descripciones locales de superficies con curvatura media constante invariantes de  $M_r^3(\rho)$  forman una familia biparamétrica y, más aún, bajo las condiciones del Teorema 4.2.7, [12], existe una deformación isométrica y uniparamétrica de estas superficies con la misma curvatura media constante. Varias órbitas de estas deformaciones isométricas están dibujadas en las Figuras 4.1 a 4.5.

Como consecuencia de este resultado, en la Sección 4.2.3, se prueban dos teoremas. Primero, en el Teorema 4.2.8, [12], se da una versión de una correspondencia de tipo Lawson para superficies invariantes (para el caso general, se puede ver [96] en ambientes Riemannianos; y, [59] y [118] para ambientes Lorentzianos); y, segundo, si nos restringimos a modelos de espacio Riemannianos de dimensión tres,  $M^3(\rho)$ , (tal y como se explica al final de esta sección, el análogo para modelos de espacio Lorentzianos no tiene sentido) obtenemos una extensión del Lema de Bour, [35], en el Teorema 4.2.9, [12]. Este resultado enuncia que

*Localmente, cualquier superficie invariante con curvatura media constante de  $M^3(\rho)$  se puede deformar isométricamente en una superficie rotacional con la misma curvatura media.*

Por otro lado, como las superficies rotacionales con curvatura media constante de  $M^3(\rho)$  son de gran importancia, en la última parte del capítulo (Sección 4.3) estudiaremos la clasificación local de estas superficies y, en particular, buscaremos cerradas. Según se explica al final de la Sección 4.3.1, *en ambos, el espacio Euclídeo de dimensión tres y en el espacio hiperbólico de dimensión tres, las únicas superficies rotacionales cerradas con curvatura media constante son las esferas totalmente umbilicales.* No obstante, este no es el caso de la esfera de dimensión tres. Por ello, en la Sección 4.3.2, restringiremos nuestro análisis a este espacio. Aquí, usando la caracterización de las curvas perfil como elásticas generalizadas para los valores  $\epsilon = 1$ ,  $p = 1/2$  y  $\Phi = -\mu$ ; y, después de unas largas y tediosas cuentas que involucran a las integrales elípticas (que con el fin de simplificar al máximo los detalles, se resumirán en el Apéndice A) concluimos con el Corolario 4.3.8 (que aparecerá en [14]) sobre la existencia de curvas perfil cerradas y simples. Esto es, usando la maquinaria desarrollada para las superficies de evolución binormal, recuperamos los resultados de Andrews-Li, [3]; Perdomo, [121]; y Ripoll, [128]. Además, como observación final, también recuperamos la recientemente probada, [30], conjetura de Herbert Blaine Lawson Jr. sobre toros minimales en la esfera de dimensión tres; *el único toro minimal embebido es el toro de Clifford*, [97].

En las mismas condiciones, es decir, en espacios ambiente Riemannianos,  $M^3(\rho)$ , la curvatura media de una superficie se puede expresar como la suma de las curvaturas principales, salvo constante. Por este motivo, si la curvatura media es constante, esto nos da lugar a una relación afín entre las curvaturas principales de la superficie. Las superficies

que verifican algún tipo de relación diferenciable entre las curvaturas principales fueron introducidas por Julius Weingarten cuando intentaba estudiar deformaciones isométricas entre superficies preservando la curvatura media, [142]. En el caso particular de que la relación sea afín, estas superficies suelen ser conocidas como **superficies de Weingarten lineales** y generalizan a las de curvatura media constante, como se ha explicado anteriormente.

En el Capítulo 5, usaremos nuestro procedimiento de evolución binormal para estudiar las superficies de Weingarten lineales de  $M^3(\rho)$  invariantes a través de las elásticas generalizadas para los valores  $\epsilon = 1$  y potencial constante  $\Phi = -\mu$ . A lo largo de este capítulo, llamaremos curvas p-elásticas a las mismas, siguiendo la nomenclatura de [63]. Primero, de forma similar a lo que sucede con el caso de superficies invariantes con curvatura media constante, para estas p-elásticas podemos definir una función en términos de la curvatura, de tal forma que sea una solución de la ecuación de Ermakov-Milne-Pinney generalizada. De hecho, a partir de los Teoremas 5.1.1 y 5.1.2 (que representan una extensión de los correspondientes resultados incluidos en [63]) tenemos

*Dada una curva p-elástica es posible definir una función que solo dependa de la curvatura de la misma y que sea una solución de la ecuación de Ermakov-Milne-Pinney generalizada con coeficientes constantes. Más aún, para cada solución de esta ecuación diferencial, podemos construir una curva crítica para*

$$\Theta_{\mu}^p(\gamma) = \int_{\gamma} (\kappa - \mu)^p ds,$$

para algún  $\mu \in \mathbb{R}$ .

Obsérvese que la función solución de la ecuación de Ermakov-Milne-Pinney generalizada definida a partir de la curvatura de la curva p-elástica representará la velocidad de la superficie de evolución binormal, tal y como sucedía en el capítulo anterior. Ahora, si la curva p-elástica es plana, la combinación del Teorema 5.2.1 y Teorema 5.2.2 nos da

*La curva perfil de la descripción local de una superficie rotacional de Weingarten lineal de  $M^3(\rho)$  es, o bien una curva plana crítica para*

$$\Theta_{\mu}^p(\gamma) = \int_{\gamma} (\kappa - \mu)^p ds,$$

*o bien, una curva plana crítica para  $\Theta^{\nu}(\gamma) = \int_{\gamma} \exp(\nu\kappa) ds$ . Recíprocamente, la evolución binormal bajo el flujo del campo de Killing asociado  $\mathcal{I}$  de una curva plana crítica para,  $\Theta_{\mu}^p$  ó  $\Theta^{\nu}$ , es una superficie rotacional de Weingarten lineal.*

El Teorema 5.2.1 y el Teorema 5.2.2 son una generalización a los casos de modelos de espacio Riemannianos de dimensión tres con curvatura seccional no nula de los correspondientes resultados que se publicarán en [103]. En este artículo también se da la descripción geométrica de todas las superficies rotacionales de Weingarten lineales del espacio Euclídeo de dimensión tres, usando una técnica que queda fuera de los objetivos de esta memoria. No obstante, con ánimo de completar la misma y de fijar las ideas, enunciaremos esta clasificación en los Teoremas 5.2.4, 5.2.5 y 5.2.6. Todas las superficies de la clasificación se dibujaran en las Figuras 5.1 a 5.3.

Posteriormente, en la última parte del capítulo (Sección 5.3) aplicaremos los resultados obtenidos para estudiar soluciones de un problema variacional diferente, para ser más precisos, de las **superficies biconservativas**. A partir de los resultados de Caddeo, Montaldo, Oniciuc y Piu, [34]; y de Fu y Li, [60]; se tiene que una superficie biconservativa de un modelo de espacio Riemanniano de dimensión tres es, o bien, una superficie de curvatura media constante, o bien una superficie rotacional de Weingarten lineal para una elección particular de la relación afín entre las curvaturas principales. Por ello, como consecuencia de nuestra caracterización local como superficies de evolución binormal con condición inicial un curva p-elástica plana, concluimos con el Teorema 5.3.2 y el Teorema 5.3.3 (que se publicarán en [111]),

*La curva perfil de una superficie biconservativa con curvatura media no constante de  $M^3(\rho)$  es una curva plana crítica para*

$$\Theta_o^{1/4}(\gamma) = \int_{\gamma} \kappa^{1/4} ds.$$

*Recíprocamente, la superficie invariante de  $M^3(\rho)$  obtenida tras aplicar la evolución binormal bajo el flujo del campo de Killing asociado  $\mathcal{I}$  a una curva plana crítica para  $\Theta_o^{1/4}$  es una superficie biconservativa con curvatura media no constante.*

Así mismo, usando los argumentos presentados en el Capítulo 3, podemos estudiar el comportamiento topológico de estas curvas planas p-elásticas particulares, y, por lo tanto, traduciéndolo a las superficies de evolución binormal, somos capaces de probar que *no existen superficies cerradas biconservativas con curvatura media no constante ni en el espacio Euclídeo de dimensión tres, ni en el espacio hiperbólico de dimensión tres*, tal y como refleja la Proposición 5.3.2, [111]. Sin embargo, en la esfera de dimensión tres probamos la existencia de estas curvas planas p-elásticas con curvatura periódica y que no cruzan el eje de rotación. Por este motivo, la verificación de la condición de cierre (véase el Corolario 3.2.7) cobra especial interés. Esta comprobación requiere de largas y complicadas cuentas que involucran herramientas de análisis que omitiremos en la memoria con objeto de clarificar los resultados. Para más detalles al respecto se puede ver [111], donde

este análisis se publicará.

Nótese que todas las superficies invariantes con las que hemos trabajado hasta el momento están inmersas en modelos de espacio de dimensión tres, tanto Riemannianos como Lorentzianos. Para finalizar la memoria, consideraremos superficies invariantes inmersas en espacios ambiente con curvatura seccional no constante, pero que preserven ciertas simetrías. Por ejemplo, para los espacios Riemannianos homogéneos de dimensión tres, se sabe que la dimensión del grupo de isometrías debe ser 6, 4 ó 3. Los modelos de espacio se caracterizan por tener grupo de isometrías de dimensión seis. Por otro lado, los espacios de dimensión tres con grado de rigidez 4 se pueden describir localmente como espacios de Bianchi-Cartan-Vranceanu (véase la Sección 6.2.2). Más aún, *estos espacios se pueden ver como sumersiones de Killing con curvaturas del fibrado y de Gauss constantes*. Por lo tanto, parece natural considerar en este momento como espacios ambiente a los espacios totales  $M$  de **sumersiones de Killing**  $\pi : M \rightarrow B$  con superficie base  $B$  y campo de Killing vertical  $\xi$ .

Por estos motivos, en el Capítulo 6, estudiaremos superficies de los espacios totales  $M$  que queden invariantes por el flujo del campo de Killing  $\xi$  (superficies verticales) y tales que, al mismo tiempo, sean extremos de la **energía de tipo-Willmore**, es decir, de la energía de Willmore con potencial  $\xi$ -invariante  $\Phi$ ,  $\Phi \in C^\infty(M)$ . En primer lugar, calcularemos la Primera Fórmula de Variación y las ecuaciones de Euler-Lagrange para superficies compactas de tipo-Willmore. Posteriormente, usando el Principio de Criticidad Simétrica de Palais, [117], obtenemos en el Teorema 6.3.1, [25], una interesante conexión entre los toros verticales de tipo-Willmore en los espacios totales  $M$  de las sumersiones de Killing y las elásticas con potencial  $4\bar{\Phi}$  en las superficies base (donde  $\bar{\Phi}$  viene determinado por  $\Phi = \bar{\Phi} \circ \pi$ ). Más concretamente, probaremos que

*Un toro vertical generado a partir de una curva cerrada en la superficie base de una sumersion de Killing con fibras compactas es una superficie de tipo-Willmore con potencial  $\xi$ -invariante,  $\Phi \in C^\infty(M)$ , si y sólo si, la curva es crítica para*

$$\Theta_{4\bar{\Phi}}(\gamma) = \int_{\gamma} (\kappa^2 + 4\bar{\Phi}) ds,$$

donde  $\Phi = \bar{\Phi} \circ \pi$ .

Aunque, en general, las energías de tipo-Willmore con potencial y la energía de Chen-Willmore son diferentes funcionales actuando en el espacio de superficies inmersas, el carácter especial de la estructura que poseen las sumersiones de Killing nos permiten usar argumentos similares cuando trabajamos con ambos tipos de energías. Debido a ello, en el Teorema 6.3.3, [25], obtendremos una conexión entre los toros de Willmore verticales

en los espacios totales de sumersiones de Killing y las curvas elásticas generalizadas para las elecciones  $\epsilon = 2$  y  $p = 1$  en la superficie base  $B$ . Esto es,

*Un toro vertical generado a partir de una curva cerrada en la superficie base,  $B$ , de una sumersion de Killing es una superficie de Willmore en  $M$ , si y sólo si, la curva es crítica para*

$$\Theta_{4\tau_\pi^2}(\gamma) = \int_\gamma (\kappa^2 + 4\tau_\pi^2) ds,$$

donde  $\tau_\pi$  denota la curvatura del fibrado de la sumersion de Killing.

Particularizando este resultado al fibrado de referencias ortonormales de una superficie, llegamos al Corolario 6.3.5, [25], que enuncia que *un toro vertical en el fibrado de referencias ortonormales de una superficie es Willmore, si y sólo si, la curva perfil es una elástica con potencial  $K_B^2$ , donde  $K_B$  es la curvatura de Gauss de la superficie*. Entonces, en la última parte del capítulo (Sección 6.4), como ilustración de estos hallazgos describiremos dos métodos de construcción de sumersiones de Killing foliadas por toros de Willmore con curvatura media constante. La primera esta basada en la Proposición 6.4.2, [25], donde se obtienen todas las funciones alabeada de las superficies alabeadas,  $S_f$ , donde todas las fibras son elásticas con potencial  $K_{S_f}^2$  ( $K_{S_f}$  representando la curvatura de Gauss de  $S_f$ ). Por otro lado, la segunda construcción depende en gran medida del teorema de existencia de sumersiones de Killing (véase [107] y el Teorema 6.2.1, [25]).

# Contents

<b>Introduction</b>	<b>xix</b>
<b>1 Preliminaries</b>	<b>1</b>
1.1 Basic Facts of Semi-Riemannian Geometry . . . . .	1
1.1.1 Semi-Riemannian Manifolds . . . . .	2
1.1.2 Semi-Riemannian Submanifolds . . . . .	2
1.1.3 Curves in Semi-Riemannian Manifolds . . . . .	4
1.2 Semi-Riemannian 3-Space Forms . . . . .	5
1.2.1 Curves in 3-Space Forms . . . . .	6
1.2.2 Surfaces Immersed in 3-Space Forms . . . . .	7
1.2.3 Invariant Surfaces of 3-Space Forms . . . . .	10
1.3 Curvature Energies in Semi-Riemannian Manifolds . . . . .	12
1.3.1 Critical Curves in 3-Space Forms . . . . .	13
1.3.2 Generalized Kirchhoff Centerlines . . . . .	16
1.3.3 Curvature Energies with Potential . . . . .	17
<b>2 Generalized Elastic Curves: A First Application</b>	<b>19</b>
2.1 Generalized Elastic Curves in Semi-Riemannian Manifolds . . . . .	19
2.1.1 Generalized Elastic Curves in 3-Space Forms . . . . .	20
2.2 An Application to Image Reconstruction . . . . .	21
2.2.1 Sub-Riemannian Geodesics . . . . .	22
2.2.2 Total Curvature Type Extremals . . . . .	24
2.2.3 Minimizing Length . . . . .	27
<b>3 Binormal Evolution Surfaces in 3-Space Forms</b>	<b>35</b>
3.1 Binormal Motion of Curves . . . . .	36
3.1.1 Hasimoto Transformation and the Complex Wave Function . . . . .	39
3.1.2 Traveling Wave Solutions and Curvature Energies . . . . .	39
3.2 Evolution with Vanishing Torsion . . . . .	41
3.2.1 Parametrizations in Riemannian 3-Space Forms . . . . .	45
3.2.2 Closed Binormal Evolution Surfaces of $M^3(\rho)$ . . . . .	50

3.2.3	Parametrizations in Minkowski 3-Space . . . . .	51
3.3	Evolution with Non-Zero Constant Torsion . . . . .	53
3.4	A Few Consequences . . . . .	54
3.4.1	Pure Binormal Evolution and Hopf Cylinders . . . . .	54
3.4.2	Hasimoto Surfaces and Elasticae . . . . .	55
<b>4</b>	<b>Invariant Constant Mean Curvature Surfaces in 3-Space Forms</b>	<b>59</b>
4.1	Characterization as Binormal Evolution Surfaces . . . . .	61
4.2	Extension of Blaschke's Variational Problem . . . . .	65
4.2.1	Binormal Evolution of Extremal Curves . . . . .	69
4.2.2	Bour's Families of Invariant CMC Surfaces . . . . .	71
4.2.3	Lawson's Correspondence for Invariant CMC Surfaces . . . . .	75
4.3	Delaunay Surfaces in Riemannian 3-Space Forms . . . . .	77
4.3.1	Local Classification of CMC Rotational Surfaces . . . . .	79
4.3.2	Embedded CMC Tori in the Round 3-Sphere . . . . .	82
<b>5</b>	<b>Invariant Linear Weingarten Surfaces in 3-Space Forms</b>	<b>91</b>
5.1	The p-Elastic Energy of Curves in Riemannian 3-Space Forms . . . . .	93
5.1.1	A New Approach to the Generalized EMP Equation . . . . .	94
5.2	Planar p-Elasticae and Rotational Linear Weingarten Surfaces . . . . .	97
5.2.1	Rotational Linear Weingarten Surfaces in the Euclidean 3-Space . .	100
5.3	Application to Biconservative Surfaces . . . . .	105
5.3.1	Biconservative Surfaces in Riemannian 3-Space Forms . . . . .	107
5.3.2	Non-CMC Closed Biconservative Surfaces . . . . .	108
<b>6</b>	<b>Invariant Willmore Tori in Killing Submersions</b>	<b>113</b>
6.1	Willmore-Like Surfaces in Riemannian 3-Spaces . . . . .	115
6.1.1	Field Equations . . . . .	115
6.2	Killing Submersions . . . . .	117
6.2.1	Canonical Examples . . . . .	118
6.2.2	Bianchi-Cartan-Vranceanu Spaces . . . . .	119
6.2.3	Bundle-Like Metrics . . . . .	120
6.3	Willmore-Like Tori in Killing Submersions . . . . .	121
6.3.1	Vertical Willmore Tori in Killing Submersions . . . . .	122
6.4	Willmore Tori Foliations of Killing Submersions . . . . .	125
6.4.1	Willmore Tori Foliations of Orthonormal Frame Bundles . . . . .	125
6.4.2	Construction of Killing Submersions Foliated by Willmore Tori . . .	128
<b>A</b>	<b>Computations Involving Elliptic Integrals</b>	<b>131</b>
<b>B</b>	<b>Gradient-Descent Method</b>	<b>137</b>







# Introduction

Many mathematical and physical problems involve the determination of extremals. In fact, the development of Calculus was initially motivated in order to compute maxima and minima of functions, as the works of Gottfried Leibniz in 1684 prove. A natural generalization consists on the computation of stationary points of functionals acting on spaces of functions. Nowadays, this generalization is known as **Calculus of Variations** and it is based on the **Principle of Least Action**, which states that *any change in Nature is made by using the minimum amount of energy needed for it*. This principle is often attributed to Pierre Louis Maupertuis because he wrote about it in 1744 and 1746, although Leonhard Euler in 1744 and Gottfried Leibniz in 1705 stated it before. The principle remains central in Mathematics and Physics, where it is usually applied in Thermodynamics, Fluid Mechanics, Theory of Relativity, Quantum Mechanics, Particle Physics and String Theory, to mention some.

On the other hand, in Pure Mathematics, the Principle of Least Action plays an essential role in geometric Calculus of Variations. Actually, one of the first problems studied using the Calculus of Variations was to *determine the curve of minimum length among all the curves of a given surface that join two fixed points*, that is, roughly speaking, to obtain the shortest “path” between two points. In 1697, this problem was publicly proposed by Johan Bernoulli as a challenge to his brother Jacob Bernoulli. Since then, this problem has attracted the attention of many Differential Geometers and, up to day, many related problems are still open. If instead of curves with least length we just look for stationary points of the length functional, we deal with **geodesics**, provided they are parametrized by arc-length.

However, even before the problem of geodesics on surfaces, in 1691 Jacob Bernoulli formulated the problem of determining the shape of an ideal **elastic rod**. In modern terminology, by this is meant a thin elastic rod naturally straight and prismatic when unstressed, and which is being held bent and twisted by external forces and moments applied at its ends alone. The rod is supposed to be non-shearable, non-extendible and made of an isotropic material which has uniform elastic rigidities. Moreover, it is assumed that the strain energy, from which the stresses are derived, is a quadratic function of the

strains. To fix ideas we may think of a long straight curtain rod with uniform cross section, density and elasticity. Three rings are firmly attached to three given non-aligned points placed in the same wall and the rod is forced to pass through these three rings so as to cause the rod pass across a curved window. The curved rod itself is assumed to lie in the same plane parallel to the wall. In equilibrium, the elastic forces of resistant of the bent rod equal the external forces and the rod remains at rest. The point is to find out all possible shapes that the rod can take, [28].

In the same context, it is known that *the equilibrium equations of an ideal rod are equivalent to those describing the motion of a heavy body turning about a fixed point*, which is called Kirchhoff's kinetic analogy, [104]. If there is no twist and the rod is bent in a plane so that the central line becomes a planar curve, the kinetic analogous is a rigid pendulum, and the curve itself is nowadays called Euler-Bernoulli's planar elastica.

In 1738, Daniel Bernoulli, nephew of Jacob Bernoulli, used the results of his uncle, who had been investigating the bending of elastic rods from 1691 to 1705, to show that *the work of deformation done in bending an straight elastic rod is proportional to the square of the curvature of the resulting bent rod* (for more details, see [138]). That is, considering a regular curve  $\gamma$  with curvature  $\kappa$ , its **bending energy** is given by

$$\mathcal{BE}(\gamma) = \int_{\gamma} \kappa^2 ds,$$

where  $s$  is the arc-length parameter of  $\gamma$ . Hence, as suggested before, the work of deformation used in deforming the straight curtain rod into the elastica is proportional to the bending energy. This work done in deforming the rod is stored in the bent rod as potential energy of strain.

Later, in 1742, in a letter to Leonhard Euler, Daniel Bernoulli suggested that *an elastic rod should bend along the curve which minimizes the potential energy of the strain under suitable constraints* and proposed to study the **elastic curves**, or simply, elasticae, as minimizers of the bending energy, also referred as Bernoulli-Euler's elastic energy, or, total squared curvature energy. Using Daniel Bernoulli's setting of the elastica as a variational problem in terms of the stored energy, Leonhard Euler obtained in his book of 1744, [56], the ordinary differential equations for twistless planar rod configurations proving that *Daniel Bernoulli's principle of least potential energy of strain leads to the same differential equation for the elastica as is obtained directly from the principles of mechanics using Jacob Bernoulli's moments approach*, [99].

Moreover, in [56], Leonhard Euler also described the possible qualitative types of the twistless planar rod configurations classifying the different types of solutions for the case of a rod with both ends clamped, although Jacob Bernoulli had partially solved it between

1692 and 1694. It must be mentioned that the book of Leonhard Euler, [56], is considered as one of the fundamental basis for the development of the Calculus of Variations.

After the publication of [56] the topic of elastic curves was forgotten for many years, until in 1930 Tibor Radó classified free elastic curves in  $\mathbb{R}^3$ , that is, critical curves of the bending energy among all the curves joining two fixed points, no matter if they have the same length or no. However, it was not until the decade of 1980 that this topic gained interest again. In that decade, David Singer and Joel Langer classified closed elastic curves in bidimensional Riemannian space forms, [94]; and, they also studied issues concerning existence and stability of elasticae in the Euclidean 3-space, [92]. Then, in 1986, Robert Bryant and Phillip Griffiths introduced in [32] a different approach suitable, in particular, to analyze elastica in Riemannian space forms. Recently, the elastica problem has been generalized in several different aspects, giving rise to new and fruitful lines of research. Thus, for example, the functional defining the bending energy has been substituted by the integral of any smooth function depending on the curvatures of the curve (for more details one can see [4], [5], [82] and references therein). Moreover, different ambient spaces have been considered as background containers for elasticae, for instance, semi-Riemannian space forms, see [58], [82] and references therein. In addition, motivated by physical considerations, a bunch of different constraints have been imposed on the original problem. Indeed, elastic curve theory encompasses a broad range of mathematical and physical fruitful ideas and lies at the intersection of many different areas. For some examples see [11] and references therein.

On the other hand, many construction procedures to obtain solutions to geometric-variational problems defined on submanifolds have been devised by using elasticae (or some of their generalizations). Energies in this case are usually defined in terms of the mean curvature. In this setting, it is well-known that the analogue of the curvature of a curve in the Theory of Submanifolds is the mean curvature function,  $H$ . In particular, when the submanifold happens to be a surface in  $\mathbb{R}^3$ , the notion of mean curvature appeared around 1810 in elasticity problems studied by Marie-Sophie Germain, who coined the name, although it was Jean Baptiste Meusnier who first considered the sum of the principal curvatures to characterize surfaces that locally minimize area. In fact, in Differential Geometry, the mean curvature of a surface appears when we consider the classical isoperimetric problem of finding the surface of least area among all surfaces that enclose a given amount of volume. The answer to this problem is the round sphere, as it was shown by Hermann Amandus Schwarz using previous ideas of Jakob Steiner.

This variational problem can be understood as the bidimensional analogue of the minimum length problem for curves. However, the fixed enclosed volume condition makes a difference. Indeed, if we only look for infinitesimal solutions of above isoperimetric problem, we have that *the area of a compact surface immersed in the Euclidean 3-space is*

*stationary with respect to all volume preserving variations, if and only if, the immersion has constant mean curvature.* In other words, **surfaces with constant mean curvature** are the critical points of the area functional with respect to local deformations that preserve the enclosed volume. On the other hand, recall that geodesics, curves with vanishing curvature, are the curves that locally minimize the length, and that their bidimensional analogues are surfaces with vanishing mean curvature, which are called **minimal surfaces**. These surfaces appear precisely as critical points of the area functional without restricting the enclosed volume.

Moreover, the study of surfaces with constant mean curvature is interesting on itself, besides the isoperimetric problem, and it is a common topic in many works in Differential Geometry. Surfaces of constant mean curvature are used as mathematical models in physical settings where the energy is proportional to the surface area. For example, they are models of the rise of a liquid in a thin tube introduced into a tank of liquid in the absence of gravity that ascends, or descends, by the capillarity action. The first works on capillarity were initiated independently by Thomas Young and Pierre Simon Laplace in 1805, [146] and [95], respectively; but it was not until 1830 that Carl Friedrich Gauss derived the celebrated Young-Laplace equation after unifying the work of these two scientists.

Following the same idea, other examples in Physics where constant mean curvature surfaces arise are the so called **interfaces**. *An interface is the region generated between two immiscible materials*, for instance, where two liquids meet, or a liquid and the air. We may consider that the region separating both media has negligible thickness in such a way that the interface is modeled by a mathematical surface. In the absence of gravity, the shape of this interface changes until it attains a state of physical equilibrium. Once more, by the Principle of Least Action, this occurs when the interface minimizes the surface energy. If the interface occurs as the region between homogeneous materials in fluid phases, then the surface energy is proportional to the area of the interface, that is, mathematically, to its surface area. Moreover, the capillary pressure difference,  $\mathcal{P}_e - \mathcal{P}_i$ , sustained across the interface between the exterior and interior static fluids is governed by the Young-Laplace equation

$$\mathcal{P}_e - \mathcal{P}_i = 2 \lambda H ,$$

where  $\lambda$  is the surface tension, which is a constant depending only on the materials. In the case where the pressures are constant, the mean curvature  $H$  is also constant. Soap bubbles and soap films are examples of interfaces in this context. Furthermore, by the Young-Laplace equation, the mean curvature is zero on the interface, if the pressures on both sides are equal. Mathematically, this means that *a minimal surface is a critical point of the area for arbitrary variations without the need of preserving the volume*, as

explained before.

The case of minimal surfaces represents a special topic in Differential Geometry and is one of the oldest subjects. Therefore, during the years many generalizations have been introduced. For instance, a natural generalization of minimal surfaces, in the same sense elastic curves generalize the notion of geodesics, can be studied considering the integral along the surface of the square of the mean curvature. In 1811, Marie-Sophie Germain proposed to study this bending energy of a surface in order to study elastic plates. As we have mentioned, this energy can be expressed as

$$\mathcal{W}(N^2) = \int_{N^2} H^2 dA,$$

where  $N^2$  is any immersed surface in  $\mathbb{R}^3$  and  $H$  denotes the mean curvature function of the immersion. This functional was studied in the decade of 1920 by Wilhelm Blaschke, [29], and Gerhard Thomsen, [136]. In particular, Wilhelm Blaschke proved in his book, [29], that *the functional  $\mathcal{W}$  is conformal, that is, it stays invariant by conformal deformations*. This can be regarded as one of the most remarkable properties of this functional, which has yielded nice generalizations, such as, the Chen-Willmore functional, introduced by Bang-Yen Chen in [40].

Some years later, in 1968, Thomas James Willmore restarted the analysis of the functional  $\mathcal{W}$ , [144]. In fact, this functional is usually known as the **Willmore energy** and the stationary points under its action are often called **Willmore surfaces**. Moreover, among many other things, Thomas James Willmore conjectured that *for every smooth immersed torus, the Willmore energy is lower bounded by  $2\pi^2$  and that this lower bound is reached at the Clifford torus*, [144]. The study of this conjecture, as well as, many other related problems, made the Willmore functional to gain interest, up to day. Indeed, the conjecture was opened until it has been recently proved by Fernando Coda Marques and André Neves in 2014, [108].

At this point it must be observed that, in many cases, there is a strong connection between critical submanifolds for the Chen-Willmore energy and critical curves for some extended version of elastic curves. Under suitable symmetry conditions, these different critical objects can be closely related by means of a symmetry reduction procedure (for the simplest case see, for instance, [125]). In order to be able to apply this type of reduction procedures, critical objects must verify certain kinds of symmetries. For example, one may consider **invariant surfaces** within the space of immersed surfaces. These surfaces have rich symmetry what makes them ideal for modeling physical systems. Therefore, along the centuries the interest of many authors has been focused on studying invariant surfaces.

In this memory we are mainly interested in studying the connection between critical curves for suitable elastica-related energies (what we call below, generalized elastic curves) and invariant surfaces possessing nice geometric properties (such as, binormal evolution surfaces, constant mean curvature surfaces, linear Weingarten surfaces,...). Moreover, a similar connection between invariant surfaces that are critical for Willmore-like energies (for the definition of Willmore-like surfaces, see page xxxi below) and generalized elastic curves is established. In the compact case, this relation is based on the Symmetric Criticality Principle of Palais, [117].

More precisely, we will study critical curves for some particular cases of the following family of **generalized elastic energies**

$$\Theta_{-\Phi}^{\epsilon,p}(\gamma) = \int_{\gamma} (\kappa^{\epsilon} + \Phi)^p ds,$$

where  $\epsilon = 1, 2$ ,  $p \in \mathbb{R}$  and  $\Phi$  is a potential. Critical curves of any of above energies will be called **generalized elastic curves** and, by using them, we are going to construct invariant surfaces in 3-spaces that have nice geometric properties, such as those referred above. Moreover, we are going to establish a link between these generalized elastic curves and different types of invariant surfaces in some 3-dimensional ambient spaces.

The first chapter of the memory is devoted to the introduction of basic facts and to the establishment of the notation and conventions that are used along the whole memory. In fact, we recall a few aspects about semi-Riemannian geometry, which are going to be essential in the future development of the memory, focusing on surfaces immersed in **semi-Riemannian 3-space forms**. Furthermore, we also recall many tools about variational problems over curves where the Lagrangians depend on the curvatures of the curves. In particular, we introduce the **generalized Kirchhoff centerlines**, that is, extremals of the energy

$$\Theta(\gamma) = \int_{\gamma} (P(\kappa) + \mu \tau + \lambda) ds,$$

$\kappa$  and  $\tau$  being the curvature and torsion of  $\gamma$ , respectively,  $P(\kappa)$  a smooth function and  $\lambda, \mu \in \mathbb{R}$  two constants. It must be highlighted that critical curves of these general curvature energies have naturally associated two **Killing vector fields**, and that one of them (from now on denoted as  $\mathcal{I}$ ) is parallel to the Frenet binormal as detailed in Proposition 1.3.2 and Proposition 1.3.3 (see also [58] and [94]).

Then, in Chapter 2, we center our attention on generalized elastic curves. Along this chapter we want to fulfill two objectives; on one hand, by particularizing general tools known for more ample settings, along the first part of the chapter (Section 2.1) we study generalized elastic curves and fix the Euler-Lagrange equations and related results; and,



on the other hand, in the second part (Section 2.2), we describe a nice application of a particular choice of generalized elastic energy, given by the choices  $\epsilon = 2$  and  $p = 1/2$  for constant potential  $\Phi = a^2$ , to visual curve completion. This construction not only justifies the study of these curves as a pure mathematical subject, but it also illustrates their many application to other fields. As an example, it can be used to solve a problem arising in computer vision, since we reduce the **sub-Riemannian** problem of completion of images by optimization to a classical variational problem. In fact, as many neuro-biological researches suggest, *there is some sub-Riemannian structure on the space of visual cells and in order to complete a partially spoiled or broken image the brain considers sub-Riemannian geodesics between the endpoints of the missing data*. This sub-Riemannian structure has been recently modeled using the **unit tangent bundle** of the plane, [124].

In Section 2.2.1, we reduce the problem of finding sub-Riemannian geodesics, which are believed to be used by the brain for image completion purposes, to the search of extremals of a family of *total curvature type* energies (which reduce in our case to generalized elastic energies for the choices  $\epsilon = 2$ ,  $p = 1/2$  and  $\Phi = a^2$ ) in the plane, that is, to a classical variational problem. Then,

*We completely solve these variational problems geometrically in Section 2.2.2, explicitly obtaining the curvatures of the critical curves.*

Theoretically, this completely solves the problem, since the curvatures characterized the curves in the plane, up to rigid motions. However, for practical purposes it is much better to devise a numerical procedure suitable to be used in specific and concrete applications. Thus,

*In Section 2.2.3, we describe a direct numerical approach in order to obtain energy minimizers. This procedure, which is implemented in what we call the XEL-platform, is based on the gradient descent method, briefly explained in Appendix B.*

Moreover, as explained at the end of that section, the method we have developed has an advantage in comparison with other numerical methods, since it allows us to compute the deviation of numerical solutions from being analytical. Our results about this topic have been basically published in [13], although the gradient descent method is going to be more deeply explained in [9].

This result can be seen as a first application of generalized elastic curves that serves as both, introduction and motivation for our interest in these objects on their own. Moreover, as we have already mentioned, one of the main goals of this memory is to construct and/or characterize invariant surfaces (by which we mean surfaces invariant by a one-parameter group of isometries) “shaped” on generalized elastic curves and possessing interesting ge-

ometric properties. To this end, two different main tools are used. First, if the ambient space is a semi-Riemannian 3-space form, the technique we are going to develop is called the **binormal evolution of curves** and Chapter 3 is devoted to introduce and explain this idea; the second construction tool is based on the use of total lifts of curves under Killing submersions as it is going to be explained in Chapter 6.

In 1972, Hasimoto [73], using a particular transformation involving the curvature and torsion of a curve, derived the celebrated nonlinear Schrödinger equation in an approximation to the self-induced motion of a thin vortex filament in a viscous fluid, although this movement of vortex filaments traveling without stretching was first modeled in 1906 by Da Rios, [130]. For this model, Da Rios used the motion of a curve, which represents the filament, propagating according to the localized induction equation. Moreover, Hasimoto related this motion with elastic curves proving that the evolution of the curve is done in the direction of the binormal, [74]. Therefore, following these ideas, we begin Chapter 3 studying geometric information of binormal motion of curves (with velocity depending on the curvature and torsion,  $\mathcal{F}(\kappa, \tau)$ ) and defining the **binormal evolution surfaces**, that is, the immersed surfaces that are locally generated by this evolution. As a consequence of applying Hasimoto transformation to our more general setting, we get a family of differential equations whose solutions correspond to the complex wave function for different binormal evolutions (see Proposition 3.1.2 and [64]). Then, after computing the Gauss-Codazzi equations (see Section 1.1.2) we obtain Theorem 3.1.3, [64],

*The binormal evolution surfaces associated to traveling wave solutions of the Gauss-Codazzi equations correspond to the evolution (by isometries and slippage) of generalized Kirchhoff centerlines.*

In particular, an essential consequence is given in Corollary 3.1.4, [10], and gives rise to the following result,

*A Frenet curve of rank 2 or 3 evolves under the binormal flow by isometries of a semi-Riemannian 3-space form,  $M_r^3(\rho)$ , if and only if, it is an extremal of*

$$\Theta(\gamma) = \int_{\gamma} (P(\kappa) + \lambda) ds,$$

where  $\mathcal{F}(\kappa, \tau) = \mathcal{F}(\kappa) := \frac{d}{d\kappa}(P(\kappa))$  is the velocity of the curve evolution.

Therefore, we can locally construct an invariant surface by evolving any critical curve under the Killing vector field  $\mathcal{I}$  in the direction of the binormal, whose existence is guaranteed by Proposition 1.3.2. Moreover, in this chapter we also see that in a geodesic coordinate system, any invariant surface is locally of this type. Now, a special case of

binormal evolution appears when all the filaments have vanishing torsion. This case is studied in Section 3.2 and, for our purposes, we highlight Proposition 3.2.1, [10], and the main consequence that can be obtained from it,

*Consider a binormal evolution surface all whose filaments have vanishing torsion. Then, the initial filament is an extremal for the energy*

$$\Theta(\gamma) = \int_{\gamma} (P(\kappa) + \lambda) ds$$

*and the binormal evolution surface is an invariant surface of  $M_r^3(\rho)$ .*

As a particular case, if  $M_r^3(\rho)$  is simply a Riemannian 3-space form,  $M^3(\rho)$ , then Proposition 3.2.3 and Proposition 3.2.4, [12], tell us that *the binormal evolution surface given in the above result is rotational*. Moreover, for these rotational binormal evolution surfaces, we develop closure conditions, which are summarized in Corollary 3.2.7 (to appear in [14]). These closure conditions are based on the corresponding closure conditions of the critical curves, that can be found for instance in [5].

Now, using these results, the first critical invariant surfaces that we deeply study are invariant constant mean curvature surfaces. For this objective, along Chapter 4, we consider the particular generalized elastic energies given by  $\epsilon = 1$ ,  $p = 1/2$  and with constant potential  $\Phi = -\mu$ . It turns out that any invariant constant mean curvature surface can be locally (see Section 1.2.3) described as the binormal evolution of these generalized elastic curves as it is proved in Theorem 4.1.1, [12]. Furthermore, the converse is also true; *the binormal evolution of these particular generalized elastic curves under the flow of  $\mathcal{I}$ , locally, generates surfaces with constant mean curvature in any semi-Riemannian 3-space form,  $M_r^3(\rho)$* . This result can be found in Theorem 4.2.6, [12]. To sum up, combining both results we have

*Locally, an invariant surface of  $M_r^3(\rho)$  with constant mean curvature can be described either as a ruled surface or as a binormal evolution surface with initial condition a critical curve of*

$$\Theta_{\mu}(\gamma) = \int_{\gamma} \sqrt{\kappa - \mu} ds,$$

*where  $\mu \in \mathbb{R}$ . Conversely, the invariant surface in  $M_r^3(\rho)$  obtained by evolving a critical curve of  $\Theta_{\mu}$  under the binormal flow of the associated Killing field  $\mathcal{I}$  has constant mean curvature  $H = -\varepsilon_1 \varepsilon_2 \mu$ .*

Now, since all invariant constant mean curvature surfaces of semi-Riemannian 3-space forms can be locally seen as binormal evolution surfaces, which in this case are warped

products, we obtain a link between invariant constant mean curvature surfaces and solutions of the Ermakov-Milne-Pinney equation, [54] and [127]. Theorem 4.1.2, [12], states and proves this link. Moreover, it can be summarized as follows

*The warping function of a local description of an invariant constant mean curvature surface of  $M_r^3(\rho)$  is a solution of the Ermakov-Milne-Pinney equation with constant coefficients.*

Finally, we exploit the local characterization of invariant constant mean curvature surfaces as binormal evolution surfaces with generalized elastic curves as initial filaments to get new proofs of some interesting results of the theory of constant mean curvature surfaces. For instance, in Section 4.2.2 we obtain that local descriptions of invariant constant mean curvature surfaces of  $M_r^3(\rho)$  form a biparametric family and, what is more, under the conditions of Theorem 4.2.7, [12], there exists a one-parameter isometric deformation of these surfaces with the same constant mean curvature. Some orbits of these isometric deformations are drawn in Figures 4.1 to 4.5.

As a consequence of this result, in Section 4.2.3, two theorems are proved. First, in Theorem 4.2.8, [12], a version of the Lawson's type correspondence for invariant surfaces is given (for the general case, one can see [96] for Riemannian backgrounds; and, [59] and [118] for Lorentzian ambient spaces); and, second, by restricting ourselves to Riemannian 3-space forms,  $M^3(\rho)$ , (as it is explained at the end of the section, the analogue for Lorentzian 3-space forms makes no sense) we get an extension of Bour's Lemma, [35], in Theorem 4.2.9, [12]. This result states that

*Locally, any invariant constant mean curvature surface in  $M^3(\rho)$  can be isometrically deformed into a rotational surface with the same constant mean curvature.*

On the other hand, rotational constant mean curvature surfaces in  $M^3(\rho)$  are of special interest. Hence, in the last part of the chapter (Section 4.3) we study the local classification of rotational constant mean curvature surfaces and, in particular, we search for closed ones. As explained at the end of Section 4.3.1, *in both the Euclidean 3-space and the hyperbolic 3-space the only closed rotational surface with constant mean curvature is the totally umbilical sphere.* However, this is not the case in the round 3-sphere. Thus, we restrict our analysis to this space in Section 4.3.2. Here, using the characterization of profile curves as generalized elastic curves for  $\epsilon = 1$ ,  $p = 1/2$  and  $\Phi = -\mu$ ; and, after lengthy computations involving elliptic integrals (that have been summarized in Appendix A, for the sake of clearness) we conclude with Corollary 4.3.8 (to appear in [14]) about the existence of closed and simple planar profile curves. That is, using the machinery we have developed for binormal evolution surfaces we recover the results of Andrews and Li, [3]; Perdomo, [121]; and Ripoll, [128]. Moreover, as a final remark, we also recover the

recently proved, [30], conjecture of Herbert Blaine Lawson Jr. about minimal tori in the round 3-sphere; *the only embedded minimal tori is the Clifford torus*, [97].

In the same setting, that is, in Riemannian ambient spaces,  $M^3(\rho)$ , the mean curvature of a surface can be expressed, up to a constant, as the sum of the principal curvatures. Therefore, if the mean curvature is constant, this gives rise to a particular affine relation between the principal curvatures. Surfaces that verify any type of smooth relation between their principal curvatures were introduced by Julius Weingarten when trying to study isometric deformations between surfaces preserving the mean curvature, [142]. In the particular case of an affine relation they are often called **linear Weingarten surfaces** and they generalize constant mean curvature ones, as explained above.

In Chapter 5, we use our binormal evolution procedure to study invariant linear Weingarten surfaces of  $M^3(\rho)$  via generalized elastic curves with  $\epsilon = 1$  and constant potential  $\Phi = -\mu$ . Along this chapter, they are also called **p-elastic curves**, following the notation of [63]. First, similar to what happened in the invariant constant mean curvature case, for these p-elastic curves we can define a function in terms of the curvature, such that, it is a solution of a generalization of the Ermakov-Milne-Pinney equation. Indeed, from Theorem 5.1.1 and Theorem 5.1.2 (which represent an extension of the corresponding results that are included in [63]) we get

*Given a p-elastic curve it is possible to define a function depending only on its curvature which is a solution of the generalized Ermakov-Milne-Pinney equation with constant coefficients. Furthermore, for any solution of this differential equation, we can construct a critical curve of*

$$\Theta_{\mu}^p(\gamma) = \int_{\gamma} (\kappa - \mu)^p ds,$$

for some  $\mu \in \mathbb{R}$ .

Observe that the function solution of the generalized Ermakov-Milne-Pinney equation defined from the curvature of the p-elastic curve will represent the velocity of the binormal evolution surface, as happened in previous chapter. Now, if the p-elastic curve happens to be planar, combination of Theorem 5.2.1 and Theorem 5.2.2 gives us

*The profile curve of a local description of a rotational linear Weingarten surface of  $M^3(\rho)$  is either, a planar critical curve of*

$$\Theta_{\mu}^p(\gamma) = \int_{\gamma} (\kappa - \mu)^p ds,$$

*or, a planar critical curve of  $\Theta^{\nu}(\gamma) = \int_{\gamma} \exp(\nu\kappa) ds$ . Conversely, the binormal evolution along the flow of the associated Killing field  $\mathcal{I}$  of a planar critical curve of either,  $\Theta_{\mu}^p$  or*

$\Theta^\nu$ , is a rotational linear Weingarten surface.

Theorem 5.2.1 and Theorem 5.2.2 are a generalization to non-zero constant sectional curvature Riemannian 3-space forms of the corresponding results that will appear in [103]. In this article the geometric description of all rotational linear Weingarten surfaces of the Euclidean 3-space is also given, using a technique that is out of the purposes of this memory. However, for the sake of completeness and, in order to fix ideas, we state this classification in Theorem 5.2.4, Theorem 5.2.5 and Theorem 5.2.6. All the surfaces of this classification have been drawn in Figures 5.1 to 5.3.

Then, in the last part of the chapter (Section 5.3) we apply our findings to study solutions of a different variational problem, more precisely, to **biconservative surfaces**. From the results of Caddeo, Montaldo, Oniciuc and Piu, [34]; and of Fu and Li, [60]; we get that a biconservative surface of a Riemannian 3-space form is either, a constant mean curvature surface, or a rotational linear Weingarten surface for a particular choice in the affine relation between the principal curvatures. Therefore, as a consequence of our local characterization as binormal evolution surfaces with planar p-elastic curves as initial conditions, we conclude with Theorem 5.3.2 and Theorem 5.3.3 (to appear in [111]),

*The profile curve of a non-constant mean curvature biconservative surface of  $M^3(\rho)$  is a planar critical curve of*

$$\Theta_o^{1/4}(\gamma) = \int_\gamma \kappa^{1/4} ds.$$

*Conversely, the invariant surface in  $M^3(\rho)$  obtained by evolving a planar critical curve of  $\Theta_o^{1/4}$  under the binormal flow of the associated Killing field  $\mathcal{I}$  is a non-constant mean curvature biconservative surface.*

Furthermore, using the arguments introduced in Chapter 3, we can study the topological behavior of these particular planar p-elastic curves, and, therefore, translating to the binormal evolution surfaces, we are able to prove that *there are no closed non-constant mean curvature biconservative surfaces in neither, the Euclidean 3-space nor in the hyperbolic 3-space*, as it is stated in Proposition 5.3.4, (to appear in [111]). However, in the round 3-sphere we prove the existence of this particular planar p-elastic curves with periodic curvature and that they never cross the axis of rotation. Thus, the verification of the closure condition (see Corollary 3.2.7) plays an essential role. This verification requires hard computations involving analytical tools that are omitted here for the sake of clearness. For more details one can check [111], where this analysis is going to appear.

Notice that all the invariant surfaces we have been working with up to now are immersed in either Riemannian or Lorentzian 3-space forms. To finish this memory we are

also going to consider invariant surfaces immersed in ambient spaces with non-constant sectional curvature having suitable symmetries. For instance, for Riemannian homogeneous 3-spaces, it is known that the dimension of the isometry group must be 6, 4 or 3. Space forms are characterized by having six-dimensional isometry group. On the other hand, those 3-spaces with degree of rigidity 4 can be locally described as Bianchi-Cartan-Vranceanu spaces (see Section 6.2.2). What is more, *these spaces can be seen as Killing submersions with constant bundle and Gaussian curvatures*. Therefore, it seems natural at this step to consider as ambient spaces the total spaces  $M$  of **Killing submersions**  $\pi : M \rightarrow B$  with base surface  $B$  and vertical Killing field  $\xi$ .

Thus, in Chapter 6, we study surfaces of the total space  $M$  which are invariant by the flow of the Killing field  $\xi$  (vertical surfaces) and which, at the same time, are extremals of a **Willmore-like energy**, that is, a Willmore energy weighted with a  $\xi$ -invariant potential  $\Phi$ ,  $\Phi \in C^\infty(M)$ . We first compute the First Variation Formula and Euler-Lagrange equations for compact Willmore-like surfaces. Then, by using the Symmetric Criticality Principle of Palais [117] we obtain in Theorem 6.3.1, [25], a nice connection between Willmore-like vertical tori in the total space  $M$  of a Killing submersion and elastica with potential  $4\bar{\Phi}$  in the base surface  $B$  ( $\bar{\Phi}$  being determined by  $\Phi = \bar{\Phi} \circ \pi$ ). More precisely, we can show

*A vertical torus shaped on a closed curve of the base surface  $B$  of a Killing submersion with compact fibers is a Willmore-like surface in  $M$  with  $\xi$ -invariant potential  $\Phi \in C^\infty(M)$ , if and only if, the curve is a critical curve of*

$$\Theta_{4\bar{\Phi}}(\gamma) = \int_{\gamma} (\kappa^2 + 4\bar{\Phi}) \, ds,$$

where  $\Phi = \bar{\Phi} \circ \pi$ .

Although, in general, Willmore-like energies with potential and the Chen-Willmore energy are different functionals acting on the space of immersed surfaces, the special structure of Riemannian submersions allows us to use similar arguments when dealing with both types of energies. Thus, in Theorem 6.3.3, [25], we obtain the connection between vertical Willmore tori in the total space  $M$  of Killing submersions and generalized elastic curves for the choices  $\epsilon = 2$  and  $p = 1$  in the base surface  $B$ . More precisely,

*A vertical torus shaped on a closed curve of the base surface,  $B$ , of a Killing submersion is a Willmore surface of  $M$ , if and only if, the curve is a critical curve of*

$$\Theta_{4\tau_\pi^2}(\gamma) = \int_{\gamma} (\kappa^2 + 4\tau_\pi^2) \, ds,$$

where  $\tau_\pi$  denotes the bundle curvature of the Killing submersion.

Particularizing this result to the orthonormal frame bundle of a surface, we conclude with Corollary 6.3.5, [25], which states that *a vertical torus in the orthonormal frame bundle of a surface is Willmore, if and only if, the profile curve is an elastic curve with potential  $K_B^2$ , where  $K_B$  is the Gaussian curvature of the base surface,  $B$* . Then, in the last part of the chapter (Section 6.4), as an illustration of our findings we describe two constructions of Killing submersions foliated by Willmore tori with constant mean curvature. The first one is based on Proposition 6.4.2, [25], where the warping functions of warped product surfaces,  $S_f$ , all whose fibers are elastic curves with potential  $K_{S_f}^2$  ( $K_{S_f}$  denoting the Gaussian curvature of  $S_f$ ) are obtained. The second construction strongly depends on the existence theorem of Killing submersions (see [107] and Theorem 6.2.1, [25]).



# Chapter 1

## Preliminaries

The Calculus of Variations has played a major role in the analysis of many problems in Differential Geometry, as we have highlighted along the introduction. In particular, if Lagrangians are described in terms of geometric invariants, these variational problems are usually referred as *geometric-variational problems*, and the search of stationary points of these energies has yielded great results. Therefore, both the energies themselves and, also, the ambient spaces where the minimizing objects live have been generalized in the last decades. For the former, one can see [5] and the references therein, while for the latter, one of the most frequent generalizations consists on considering semi-Riemannian ambient spaces, (see, for instance, [82]), due to the unnumbered applications semi-Riemannian manifolds have, for instance, in Physics.

For these reasons, this chapter is going to be devoted to introductory notions and well-known facts about semi-Riemannian geometry. Moreover, in the last part we are also going to describe the main tools about different types of curvature energies in semi-Riemannian ambient spaces.

### 1.1 Basic Facts of Semi-Riemannian Geometry

Although in this PhD memory we are going to be mainly interested in low dimensions, as this chapter has an introductory objective, and as there is no extra cost for the presentation of these facts in more general settings, we are going to begin by introducing the main objects, of arbitrary dimension, of semi-Riemannian geometry, that is, manifolds and submanifolds, as well as their most commonly used formulas. In particular, we will put emphasis on the case of curves. This section is mainly based on [39].

### 1.1.1 Semi-Riemannian Manifolds

Along this PhD memory, we will understand that a *manifold* is a connected smooth manifold of dimension greater or equal than two without boundary. We will denote it by  $M^n$ , where  $n$  represents the *dimension* of the manifold.

A *semi-Riemannian metric tensor*,  $g$ , on a manifold  $M^n$  is a symmetric non-degenerate  $(0, 2)$  tensor field on  $M^n$  of constant index. Very often, we will use the notation  $\langle \cdot, \cdot \rangle$  to denote  $g$ . Moreover,  $g$  is sometimes referred as the *first fundamental form*. Then, a *semi-Riemannian manifold* is a manifold equipped with a metric tensor  $g$ . The common value  $r$  ( $0 \leq r \leq n$ ) of index on  $M^n$  is called the *index* of  $M^n$ . Thus, from now on, we will denote by  $M_r^n$  to a  $n$ -dimensional semi-Riemannian manifold of index  $r$ , keeping the notation  $M^n = M_0^n$  to denote Riemannian manifolds of dimension  $n$ .

As it is usual, the *Levi-Civita connection* on  $M_r^n$  is going to be denoted by  $\nabla$ . Moreover, for a semi-Riemannian manifold  $M_r^n$  with Levi-Civita connection  $\nabla$ , we will define the *Riemann curvature tensor* as the  $(1, 3)$  tensor field defined by

$$R(X, Y)Z = \nabla_Y \nabla_X Z - \nabla_X \nabla_Y Z + \nabla_{[X, Y]} Z, \quad (1.1)$$

where  $X, Y$  and  $Z$  are any vector fields tangent to  $M_r^n$ . Furthermore, if  $W$  is another tangent vector field, following this notation we will write  $R(X, Y, Z, W) = \langle R(X, Y)Z, W \rangle$ . Observe that some authors use a different convention for the curvature tensor  $R$ , which differs from our convention in the sign. Finally, if we denote by  $\pi$  any *plane section* of  $M_r^n$ , its *sectional curvature*,  $K(\pi)$ , is given by

$$K(u, v) = \varepsilon_u \varepsilon_v \langle R(u, v)u, v \rangle, \quad (1.2)$$

where  $\{u, v\}$  represents any orthonormal basis of  $\pi$ , and,  $\varepsilon_u$  and  $\varepsilon_v$  are the causal characters of the vectors  $u$  and  $v$ , respectively. Take into account that, even if in other works the definition of the curvature tensor may have the opposite sign, the sectional curvature coincides.

### 1.1.2 Semi-Riemannian Submanifolds

An immersion  $\varphi : N_\nu^m \rightarrow M_r^n$  of a semi-Riemannian manifold,  $N_\nu^m$ , into another semi-Riemannian manifold,  $M_r^n$ , is said to be *isometric* if

$$\langle u, v \rangle_p = \langle \varphi_{*p} u, \varphi_{*p} v \rangle_{\varphi(p)}$$

holds for all  $u, v$  in  $T_p N_\nu^m$  and for all  $p \in N_\nu^m$ . Let's assume now that  $\varphi : N_\nu^m \rightarrow M_r^n$  is an isometric immersion. We will denote by  $\nabla$  and  $\tilde{\nabla}$  the Levi-Civita connections of  $N_\nu^m$  and  $M_r^n$ , respectively.

Assume also, that  $X$  and  $Y$  are vector fields tangent to  $N_\nu^m$ , then  $\tilde{X}$  and  $\tilde{Y}$  will be the *extensions* of  $X$  and  $Y$  to vector fields on  $M_r^n$ , respectively. Thus, we have the following *formula of Gauss*

$$\tilde{\nabla}_{\tilde{X}}\tilde{Y} = \nabla_X Y + h(X, Y). \quad (1.3)$$

The bilinear form  $h$  is called the *second fundamental form* of  $N_\nu^m$  for the immersion  $\varphi$ . When there is no doubt, we will just write  $X, Y$  for the tangent vectors of  $N_\nu^m$  and for their extensions to  $M_r^n$ .

On the other hand, if  $\eta$  is a normal vector field of  $N_\nu^m$  in  $M_r^n$ , the decomposition of the Levi-Civita connection into its tangential and normal parts gives us also the *formula of Weingarten*

$$\tilde{\nabla}_X \eta = -A_\eta(X) + D_X^\perp \eta, \quad (1.4)$$

where  $A_\eta$  stands for the *shape operator* and  $D^\perp$  denotes the connection on the normal bundle of  $N_\nu^m$ .

Finally, let's denote by  $R$  and  $\tilde{R}$  the curvature tensors of  $N_\nu^m$  and  $M_r^n$ , respectively. Then we have the *Gauss-Codazzi equations*

$$\langle \tilde{R}(X, Y)Z, W \rangle = \langle R(X, Y)Z, W \rangle - \langle h(X, W), h(Y, Z) \rangle + \langle h(X, Z), h(Y, W) \rangle, \quad (1.5)$$

$$(\nabla h)(X, Y, Z) = (\nabla h)(Y, X, Z), \quad (1.6)$$

where  $\nabla h$  is defined by

$$(\nabla h)(X, Y, Z) = D_X^\perp h(Y, Z) - h(\nabla_X Y, Z) - h(Y, \nabla_X Z).$$

It is also possible to obtain the *Ricci equation*, however, when the codimension of the submanifold is one, Ricci equation is just an identity (see, for instance, [39]). Notice that this would be the case along this PhD memory, since we are going to work mainly with surfaces immersed in 3-spaces. Therefore, for the sake of simplicity we omit this equation. Usually, the three systems of equations of Gauss, Codazzi and Ricci are known as the *fundamental equations*. Indeed, they are the essential conditions that the first and second fundamental forms must satisfy in order to assure the existence and uniqueness of submanifolds. For more details, see §2.7 of [39].

Finally, if we restrict ourselves to *semi-Riemannian space forms*,  $M_r^n(\rho)$ , that is, complete, connected, simply-connected semi-Riemannian manifolds with constant sectional curvature,  $\rho$ , we are going to see that it is possible to reduce the codimension for a given isometric immersion. In fact, let  $N_\nu^m$  be a semi-Riemannian manifold isometrically immersed in a semi-Riemannian space form,  $M_r^n(\rho)$ , of arbitrary dimension  $n$ . For a given  $p \in N_\nu^m$ , the *first normal space*  $\mathcal{N}_1(p)$  is defined to be the subspace of the normal space spanned by the vector valued second fundamental form of the immersion. A normal subbundle  $\mathcal{N}$  is called *parallel* if, for each section  $\eta$  of  $\mathcal{N}$  and each tangent vector  $X \in TN_\nu^m$ , the covariant derivative of  $\eta$  in the direction of  $X$ , with respect to the normal connection, remains in  $\mathcal{N}$ . The following result is basically known

**Theorem 1.1.1.** *Let  $\varphi : N_\nu^m \rightarrow M_r^n(\rho)$  be an isometric immersion of a semi-Riemannian manifold,  $N_\nu^m$ , into a semi-Riemannian space form,  $M_r^n(\rho)$ . Assume that  $(N_\nu^m, \varphi)$  has a parallel normal subbundle  $\mathcal{N}_2$  of rank  $q < n - m$  containing the first normal space  $\mathcal{N}_1$ . Then, there exists a totally geodesic submanifold  $E^{m+q}$  embedded in  $M_r^n(\rho)$  such that  $\varphi(N_\nu^m) \subset E^{m+q}$ .*

If  $\rho = 0$  the result can be found in [105] for  $\mathcal{N}_1 = \mathcal{N}_2$  (see also [39], Theorem 2.6). If  $\rho = -1$  a proof is given in [87]. A general proof for any  $\rho$  can be made by adapting to the semi-Riemannian case the arguments of [39], Theorem 2.6 and of [44], Theorem 4.1. In the Riemannian case, the above result is due to Erbacher, [53]. Therefore, quite often, above Theorem is called *Erbacher's Reduction Theorem*.

From now on, we will resort to the standard abuse of notation and identification tricks in the Theory of Submanifolds.

### 1.1.3 Curves in Semi-Riemannian Manifolds

Let  $M_r^n$  be a semi-Riemannian manifold with metric  $g \equiv \langle \cdot, \cdot \rangle$  and Levi-Civita connection  $\nabla$ . If  $\gamma : \bar{I} \rightarrow M_r^n$  is a smooth immersed curve in  $M_r^n$ ,  $\gamma'(t)$  will represent its velocity vector  $\frac{d\gamma(t)}{dt}$  and the covariant derivative of a vector field  $X(t)$  along  $\gamma$  will be denoted by  $\nabla_{\gamma'} X(t)$ .

A  $\mathcal{C}^1$  immersed curve in a semi-Riemannian manifold is *spacelike* (respectively, *timelike*; respectively, *lightlike*) if  $\langle \gamma'(t), \gamma'(t) \rangle > 0, \forall t \in \bar{I}$  (respectively,  $\langle \gamma'(t), \gamma'(t) \rangle < 0, \forall t \in \bar{I}$ ; respectively,  $\langle \gamma'(t), \gamma'(t) \rangle = 0, \forall t \in \bar{I}$ ). Of course, there exist curves whose causal character changes as  $t$  moves along the parameter interval, but this kind of curves will not be considered in this memory. We recall that, a non-null curve can be parametrized by the arc-length and this natural parameter is called *proper time*. From now on this natural parameter is going to be denoted by  $s$  and, therefore, the tangent to the curve is going to be represented by  $T(s) = \gamma'(s)$ .

For a non-null immersed curve, the *first Frenet curvature*, or simply, *the curvature*, is defined as the positive root of  $\kappa_1^2 = \varepsilon_2 \langle \nabla_T T(s), \nabla_T T(s) \rangle$ , where  $\varepsilon_2$  denotes the causal character of  $\nabla_T T(s)$ . A *geodesic* is a constant speed curve whose tangent vector is parallel propagated along itself, that is, a curve whose tangent,  $\gamma'(s) = T(s)$ , satisfies the equation  $\nabla_T T(s) = 0$ . Obviously, geodesics have zero curvature. Along this memory, geodesics will be equivalently called *Frenet curves of rank 1*.

An arc-length parametrized immersed curve in a semi-Riemannian manifold  $\gamma : I \rightarrow M_r^n$  is called a *Frenet curve of rank  $m$* ,  $2 \leq m \leq n$ , if  $m$  is the highest integer for which there exists an orthonormal frame defined along  $\gamma$ ,  $\{e_1(s) = T(s) = \gamma'(s), e_2(s), \dots, e_m(s)\}$  and non-negative smooth functions on  $\gamma$ ,  $\kappa_i(s)$ ,  $s \in I$ ,  $1 \leq i \leq m - 1$  (*Frenet curvatures*),

such that the following equations are satisfied (*Frenet-Serret equations*)

$$\nabla_T e_1(s) = \nabla_T T(s) = \varepsilon_2 \kappa_1(s) e_2(s), \tag{1.7}$$

$$\begin{aligned} & \dots\dots\dots, \\ \nabla_T e_h(s) &= -\varepsilon_{h-1} \kappa_{h-1}(s) e_{h-1}(s) + \varepsilon_{h+1} \kappa_h(s) e_{h+1}(s), \quad h \in \{2, 3, \dots, m-1\}, \tag{1.8} \\ & \dots\dots\dots, \end{aligned}$$

$$\nabla_T e_m(s) = -\varepsilon_{m-1} \kappa_{m-1}(s) e_{m-1}(s), \tag{1.9}$$

where  $\varepsilon_i := \langle e_i(s), e_i(s) \rangle$  denotes the causal character of  $e_i(s)$ ,  $i \in \{1, \dots, m\}$ . For a Frenet curve of rank  $m < n$  the Frenet curvatures of index higher than  $m - 1$  are considered to be zero,  $\kappa_i(s) = 0$ ,  $s \in I$ ,  $m \leq i \leq n - 1$ .

## 1.2 Semi-Riemannian 3-Space Forms

Consider the Euclidean semi-space  $\mathbb{E}_{\mathfrak{D}}^m$ . That is,  $\mathbb{R}^m$  endowed with the canonical metric of index  $\mathfrak{D}$ , denoted by  $\langle \cdot, \cdot \rangle$ , and the corresponding Levi-Civita connection, denoted by  $\nabla$ . A *semi-Riemannian 3-space form* is a complete, connected, simply connected semi-Riemannian 3-manifold of index  $r = 0, 1$ , with constant sectional curvature  $\rho$ . These spaces are going to be denoted by  $M_r^3(\rho)$ ,  $r = 0, 1$ . If  $r = 0$ ,  $M_0^3(\rho)$  is a Riemannian 3-space form (usually, simply denoted by  $M^3(\rho)$ ) and if  $r = 1$ ,  $M_1^3(\rho)$  is a Lorentzian 3-space form.

Notice that,  $M_r^3(\rho)$ ,  $r = 0, 1$ , can be isometrically immersed in  $\mathbb{E}_{\mathfrak{D}}^4$ , the 4-dimensional Euclidean semi-space, in a standard way. In fact, the flat case,  $M_r^3(\rho) = \mathbb{E}_r^3$ ,  $\rho = 0$ ,  $r = 0, 1$ , corresponds to either the Euclidean 3-space,  $\mathbb{R}^3$ , or to the Minkowski 3-space,  $\mathbb{R}_1^3 \equiv \mathbb{L}^3$ . They can be isometrically immersed in  $\mathbb{L}^4 = \mathbb{R}_1^4$  endorsed with the metric

$$g = dx_1^2 + dx_2^2 + dx_3^2 - dx_4^2,$$

in an obvious manner;

$$\mathbb{R}^3 = \{(x_1, x_2, x_3, x_4) \in \mathbb{L}^4 \mid x_4 = 0\}, \quad \mathbb{L}^3 = \{(x_1, x_2, x_3, x_4) \in \mathbb{L}^4 \mid x_1 = 0\}.$$

When  $\rho > 0$ ,  $M_r^3(\rho)$  corresponds to the round 3-sphere  $\mathbb{S}^3(\rho)$ , if  $r = 0$ , and to the de Sitter 3-space  $\mathbb{S}_1^3(\rho)$ , if  $r = 1$ , which are defined by

$$\mathbb{S}_r^3(\rho) = \{\mathbf{x} \in \mathbb{E}_r^4 \mid \langle \mathbf{x}, \mathbf{x} \rangle = \frac{1}{\rho}\},$$

where  $\mathbf{x} = (x_1, x_2, x_3, x_4)$ . Finally, for  $\rho < 0$  we obtain the hyperbolic 3-space,  $\mathbb{H}^3(\rho)$  if  $r = 0$ , and the anti de Sitter 3-space,  $\mathbb{H}_1^3(\rho)$ , if  $r = 1$

$$\mathbb{H}_r^3(\rho) = \{\mathbf{x} \in \mathbb{E}_{r+1}^4 \mid \langle \mathbf{x}, \mathbf{x} \rangle = \frac{1}{\rho}\}.$$

The standard isometric immersions of  $M_r^3(\rho)$  into  $\mathbb{E}_3^4$  ([39], p. 20) will be all denoted by  $i$  and the induced metrics also by  $\langle \cdot, \cdot \rangle$ , while the Levi-Civita connections on  $\mathbb{E}_3^4$  and  $M_r^3(\rho)$  are denoted by  $\bar{\nabla}$  and  $\tilde{\nabla}$ , respectively.

As usual, the cross product of two vector fields  $X, Y$  in  $M_r^3(\rho)$ , denoted by  $X \times Y$ , is defined so that  $\langle X \times Y, Z \rangle = \det(X, Y, Z)$  for any other vector field  $Z$  of  $M_r^3(\rho)$ , where  $\det(X, Y, Z)$  stands for the determinant.

### 1.2.1 Curves in 3-Space Forms

Let's denote by  $\gamma$  an arc-length parametrized non-null curve immersed in  $M_r^3(\rho)$ , and let  $\kappa(s)$  represent the curvature of  $\gamma$  in the 3-space form.

If  $\kappa(s) = 0$ , then  $\gamma$  is a geodesic in  $M_r^3(\rho)$ . On the other hand, if  $\gamma(s)$  is a unit speed non-geodesic smooth curve immersed in  $M_r^3(\rho)$  with non-null velocity  $\gamma'(s) = T(s)$  and non-null acceleration,  $\tilde{\nabla}_T T(s)$ , then  $\gamma(s)$  is a *Frenet curve* of rank 2 or 3 and the standard *Frenet frame* along  $\gamma(s)$  is given by  $\{T, N, B\}(s)$ , where  $N$  and  $B$  are the *unit normal* and *unit binormal* to the curve, respectively, and  $B$  is chosen so that  $\det(T, N, B) = 1$ . Then the *Frenet equations* (see formulas (1.7)-(1.9))

$$\tilde{\nabla}_T T(s) = \varepsilon_2 \kappa(s) N(s), \quad (1.10)$$

$$\tilde{\nabla}_T N(s) = -\varepsilon_1 \kappa(s) T(s) + \varepsilon_3 \tau(s) B(s), \quad (1.11)$$

$$\tilde{\nabla}_T B(s) = -\varepsilon_2 \tau(s) N(s), \quad (1.12)$$

define the *curvature*,  $\kappa(s)$  ( $\kappa(s) > 0$  if  $n = 3$ ), and *torsion*,  $\tau(s)$ , along  $\gamma(s)$ , where  $\varepsilon_i$ ,  $1 \leq i \leq 3$  are the causal characters of  $T$ ,  $N$  and  $B$ , respectively. Notice that  $\{\varepsilon_i, i = 1, 2, 3\}$  are three numbers satisfying

$$i) \text{ at most one of them is negative, } \quad ii) \varepsilon_i = \pm 1, \quad iii) \varepsilon_1 \varepsilon_2 \varepsilon_3 = (-1)^r. \quad (1.13)$$

Now, the following relations hold

$$T = \varepsilon_1 N \times B, \quad N = \varepsilon_2 B \times T, \quad B = \varepsilon_3 T \times N.$$

Notice that, even if the rank of  $\gamma$  is 2 (that is,  $\tau = 0$ ), the binormal  $B = \varepsilon_3 T \times N$  is still well defined and above formulas (1.10)-(1.12) still make sense when  $\tau = 0$ . A curve with vanishing torsion,  $\tau = 0$ , is going to be referred as a *planar curve*. On the other hand, if a curve has constant curvature and torsion is called a *Frenet helix*. Moreover, a *Lancret helix* is a curve whose unit tangent vector makes a constant angle with a Killing vector field of  $M_r^3(\rho)$  of constant length.

Finally, we recall that, in a semi-Riemannian space form any local geometrical scalar defined along Frenet curves can always be expressed as a function of their curvatures and derivatives.

### 1.2.2 Surfaces Immersed in 3-Space Forms

Let's consider a given isometric immersion of a surface in a 3-space form,  $\varphi : N_\nu^2 \rightarrow M_r^3(\rho)$ , where  $\nu \in \{0, 1\}$  represents the index of the surface. Recall that  $M_r^3(\rho)$  is immersed in a Euclidean semi-space of dimension 4 for suitable index,  $\mathbb{E}_\delta^4$ , see Section 1.2. We denote by  $\nabla$  the Levi-Civita connection of the surface  $N_\nu^2$ . As it is also customary, for a surface  $N_\nu^2$  in any 3-dimensional space form  $M_r^3(\rho)$ , we require the first fundamental form to be non-degenerate. Take  $X, Y, Z, W$  tangent vector fields to  $N_\nu^2$  and choose  $\eta$  a local normal vector field to  $N_\nu^2$  in  $M_r^3(\rho)$ . Then the *formulas of Gauss and Weingarten*, (1.3) and (1.4), are, respectively

$$\bar{\nabla}_X Y = \tilde{\nabla}_X Y - \rho \langle X, Y \rangle x = \nabla_X Y + h(X, Y) - \rho \langle X, Y \rangle x, \quad (1.14)$$

$$\tilde{\nabla}_X \eta = -A_\eta X + D_X^\perp \eta, \quad (1.15)$$

where  $x = i \circ \varphi$  can be seen as the position vector,  $h$  denotes the second fundamental form of  $N_\nu^2$  in  $M_r^3(\rho)$ , and  $D^\perp$  denotes the connection on the normal bundle of  $N_\nu^2$ . We remind that  $A_\eta$  is the notation we are using for the *shape operator*.

A surface is said to be *isoparametric* if the shape operator  $A_\eta$  has the same characteristic polynomial at all points of the surface. As proved in [71], this definition coincides with the classical definition due to Cartan; *a surface is said to be isoparametric if locally all parallel surfaces have constant mean curvature*. Notice that in the Riemannian case,  $A_\eta$  is diagonalizable and, therefore, an isoparametric surface has constant eigenvalues, usually called *principal curvatures*, with constant algebraic multiplicities. In [37], Cartan classified isoparametric surfaces in Riemannian 3-space forms and showed that *they are either totally umbilical or spherical cylinders*. In Lorentzian backgrounds, Magid [106] studied hypersurfaces whose shape operator has constant minimal polynomial in Lorentz-Minkowski space  $\mathbb{L}^n$  and called them also isoparametric; Li and Wang [100] studied these isoparametric surfaces in the de Sitter space  $\mathbb{S}_1^3(\rho)$ ,  $\rho > 0$ ; and, Xiao [145] studied these isoparametric hypersurfaces in the anti de Sitter space  $\mathbb{H}_1^n(\rho)$ ,  $\rho < 0$ .

Now, for any isometric immersion, by using (1.14) and (1.15), and denoting by  $R$  and  $\tilde{R}$  the Riemann curvature tensors associated to  $\nabla$  and  $\tilde{\nabla}$ , respectively, the following relation holds

$$\tilde{R}(X, Y)Z = \rho(\langle Y, Z \rangle X - \langle X, Z \rangle Y), \quad (1.16)$$

while the *equations of Gauss and Codazzi* are given respectively by (1.5) and (1.6). Choosing an adapted local orthonormal frame  $\{e_1, e_2, e_3\}$  in  $M_r^3(\rho)$  such that the vectors  $e_1, e_2$  are tangent to  $N_\nu^2$  and  $e_3$  is normal to  $N_\nu^2$  in  $M_r^3(\rho)$ , the intrinsic *Gaussian curvature* of  $N_\nu^2$  is given by (1.2)

$$K = \tilde{\varepsilon}_1 \tilde{\varepsilon}_2 \langle R(e_1, e_2)e_1, e_2 \rangle, \quad (1.17)$$

where  $\tilde{\varepsilon}_j = \langle e_j, e_j \rangle$  is the causal character of  $e_j$ . Now, denoting by  $\{\omega^1, \omega^2, \omega^3\}$  the dual

frame of  $\{e_1, e_2, e_3\}$ , the *Cartan connection forms* are defined by

$$\tilde{\nabla}_X e_i = \sum_j \tilde{\varepsilon}_j \omega_i^j(X) e_j,$$

for  $i, j \in \{1, 2, 3\}$ . Then,  $\omega_i^j = -\omega_j^i$  and

$$h(e_i, e_j) = \tilde{\varepsilon}_3 h_{ij} e_3, \quad h_{ij} = -\langle \tilde{\nabla}_{e_i} e_3, e_j \rangle = \omega_j^3(e_i), \quad (1.18)$$

$i, j \in \{1, 2\}$ .

Moreover, the *mean curvature vector*  $\mathbf{H}$  of a surface  $N_\nu^2$  isometrically immersed in  $M_r^3(\rho)$  is defined by  $\mathbf{H} = \frac{1}{2} \text{trace } h$  while the *mean curvature function*,  $H$ , is defined so that the following equation is verified

$$\mathbf{H} = \tilde{\varepsilon}_3 H e_3. \quad (1.19)$$

For a local parametrization of  $N_\nu^2$ , take  $p \in N_\nu^2$  and let  $\alpha : \bar{I} \rightarrow N_\nu^2$  be an immersed non-null curve  $\alpha(t)$  with causal character  $\varepsilon_\alpha$ , such that  $\alpha(\bar{I})$  is contained in a local chart around  $p$  and  $\alpha(0) = p$ . For any  $t_o \in \bar{I}$ , take  $V_{t_o}$  as a unit vector tangent to  $N_\nu^2$  at  $\alpha(t_o)$  so that  $\{(d\alpha/dt)(t_o), V_{t_o}, \eta(t_o)\}$  form an orthonormal basis and consider the geodesic  $\gamma^{t_o}(s)$  with initial data;  $\gamma^{t_o}(0) = \alpha(t_o)$  and  $(d\gamma^{t_o}/ds)(0) = V_{t_o}$ . Thus, in a neighborhood of  $p$  in  $N_\nu^2$  we can find a local parametrization  $(U, x)$  (called a *geodesic parametrization*) defined by

$$x(s, t) = \gamma^t(s), \quad (1.20)$$

$t \in \bar{I}$ . Therefore, calling  $\gamma = \gamma^o(s)$ , the coefficients of the metric with respect to  $(U, x)$  are (reparametrizing the geodesics if needed)  $g_{11} = \langle x_s, x_s \rangle = \varepsilon_\gamma$ ,  $g_{12} = \langle x_s, x_t \rangle = 0$ , and  $g_{22} = \langle x_t, x_t \rangle$ , which, for simplicity, is denoted by  $g_{22} = \varepsilon_\alpha \mathcal{F}^2(s, t)$ . That is, with respect to this parametrization, (1.20), the metric can be written as

$$g = \varepsilon_\gamma ds^2 + \varepsilon_\alpha \mathcal{F}^2 dt^2. \quad (1.21)$$

Let's assume that  $\gamma$  is not a geodesic of the ambient space. Then, by using the Frenet frame defined in Section 1.2.1 we have that  $\varepsilon_\gamma = \varepsilon_1$  and  $\varepsilon_\alpha = \varepsilon_3$  (since,  $\gamma$  is a geodesic on the surface). Therefore, (1.21) can be equivalently expressed as

$$g = \varepsilon_1 ds^2 + \varepsilon_3 \mathcal{F}^2 dt^2. \quad (1.22)$$

In this setting, the Gauss and Weingarten formulas (1.14) and (1.15), in combination with the Gauss and Codazzi equations (1.5) and (1.6), will give us all the relevant geometric information about the immersion  $(U, x)$ . Indeed, the Christoffel symbols of the Levi-Civita connection of (1.22) with respect to the parametrization (1.20) (see, for instance [39], Proposition 1.1) can be computed from the metric coefficients  $g_{ij}$ . In our case, we have

$$\Gamma_{11}^1 = \Gamma_{11}^2 = \Gamma_{12}^1 = 0, \quad \Gamma_{12}^2 = \frac{\mathcal{F}_s}{\mathcal{F}}, \quad \Gamma_{22}^1 = -\varepsilon_1 \varepsilon_3 \mathcal{F} \mathcal{F}_s, \quad \Gamma_{22}^2 = \frac{\mathcal{F}_t}{\mathcal{F}},$$



where subscripts  $s$  and  $t$  mean partial derivative with respect to  $s$  and  $t$ , respectively. This makes it possible to know the expression for the Levi-Civita connection of  $x(U)$  ([39], §1.4), denoted here by  $\nabla$ ,

$$\nabla_{\frac{\partial}{\partial s}} \frac{\partial}{\partial s} = 0, \quad \nabla_{\frac{\partial}{\partial s}} \frac{\partial}{\partial t} = \frac{\mathcal{F}_s}{\mathcal{F}} \frac{\partial}{\partial t}, \quad \nabla_{\frac{\partial}{\partial t}} \frac{\partial}{\partial t} = -\varepsilon_1 \varepsilon_3 \mathcal{F} \mathcal{F}_s \frac{\partial}{\partial s} + \frac{\mathcal{F}_t}{\mathcal{F}} \frac{\partial}{\partial t}. \quad (1.23)$$

As before,  $\{T(s, t), N(s, t), B(s, t)\}$  represent the Frenet frames along  $\gamma^t(s)$ , and we choose the following local adapted frame on  $x(U)$

$$e_1 = x_s = T, \quad e_2 = \frac{x_t}{\mathcal{F}} = B, \quad e_3 = \eta = -\varepsilon_2 N, \quad (1.24)$$

where  $\eta$  is the unit normal to  $x(U)$  (locally defined). Then, combining (1.10)-(1.12), (1.14), (1.15) and (1.18), one gets

$$\omega_1^2(e_1) = 0, \quad \omega_1^2(e_2) = \varepsilon_3 \frac{\mathcal{F}_s}{\mathcal{F}}, \quad \omega_1^3(e_1) = h_{11} = -\varepsilon_2 \kappa, \quad (1.25)$$

$$\omega_1^3(e_2) = \omega_2^3(e_1) = h_{12} = \varepsilon_2 \tau, \quad \omega_2^3(e_2) := h_{22}, \quad (1.26)$$

where,  $\kappa(s, t)$  and  $\tau(s, t)$  denote the curvature and torsion of the curves  $\gamma^t(s)$ .

The second fundamental form can be considered as a quadratic form given by  $h(X) := \langle A_\eta X, X \rangle$ , therefore, we obtain from (1.18), (1.25) and (1.26) that

$$h = -\varepsilon_2 \kappa ds^2 + 2\varepsilon_2 \tau \mathcal{F} ds dt + \mathcal{F}^2 h_{22} dt^2, \quad (1.27)$$

with respect to the parametrization (1.20), where  $h_{22}$  is the coefficient of the second fundamental form ([39], §2.3) of  $x(U)$  in  $M_r^3(\rho)$  given by  $h_{22} := -\varepsilon_2 \langle \tilde{\nabla}_B B, N \rangle$ . Since  $\nabla$  is determined by  $g$ ,  $h_{22}$  can be computed with the aid of (1.23) and the Gauss formula (1.14) giving

$$h_{22} = \frac{1}{\kappa} \left\{ \varepsilon_3 \frac{\mathcal{F}_{ss}}{\mathcal{F}} - \varepsilon_2 \tau^2 + \varepsilon_1 \varepsilon_3 \rho \right\}. \quad (1.28)$$

Using again the Gauss and Weingarten formulas (1.14) and (1.15), it can be shown that  $x : U \rightarrow M_r^3(\rho) \rightarrow \mathbb{E}_3^4$  satisfies the following PDE system

$$x_{ss} = -\frac{\kappa}{\mathcal{F}} x_s \times x_t - \varepsilon_1 \rho x, \quad (1.29)$$

$$x_{ts} = \frac{\mathcal{F}_s}{\mathcal{F}} x_t - \frac{\tau \mathcal{F}}{\kappa} x_{ss} - \varepsilon_1 \frac{\tau \mathcal{F}}{\kappa} \rho x, \quad (1.30)$$

$$x_{tt} = -\varepsilon_1 \varepsilon_3 \mathcal{F} \mathcal{F}_s x_s - \varepsilon_2 \frac{h_{22} \mathcal{F}^2}{\kappa} x_{ss} - \left( \frac{\varepsilon_1 \varepsilon_2 h_{22}}{\kappa} + \varepsilon_3 \right) \mathcal{F}^2 \rho x + \frac{\mathcal{F}_t}{\mathcal{F}} x_t. \quad (1.31)$$

### 1.2.3 Invariant Surfaces of 3-Space Forms

An immersed surface  $N_\nu^2$  in a 3-space form,  $M_r^3(\rho)$ , is said to be an *invariant surface* if it stays invariant under the action of a one-parameter group of isometries of  $M_r^3(\rho)$ . One-parameter groups of isometries of  $M_r^3(\rho)$  are determined by the flow of Killing vector fields of  $M_r^3(\rho)$ .

If the Killing field  $\xi$  is null, then  $N_\nu^2$  is isometric to the Minkowski 2-space,  $\mathbb{L}^2$ . Isometric immersions of  $\mathbb{L}^2$  into  $M_1^3(\rho)$  have been studied in [45] and [69]. Thus, let's consider that  $\xi$  is a non-null Killing vector field on  $M_r^3(\rho)$ . Since  $M_r^3(\rho)$  is complete, we can consider that the flow of  $\xi$  is  $\{\phi_t, t \in \mathbb{R}\}$ . Therefore,  $N_\nu^2$  is a  $\xi$ -invariant surface of  $M^3(\rho)$  if we have  $\phi_t(N_\nu^2) = N_\nu^2$ . However, if  $\xi$  changes its causal character, there may exist points such that for all their neighborhoods there are orbits of different causal characters, see [33]. Thus, along the whole memory we are also going to assume that we are working in any local neighborhood of a point,  $p$ , such that  $\langle \xi(p), \xi(p) \rangle$  is non-zero. More precisely, if we call  $S = N_\nu^2 - \{p \in N_\nu^2 \mid \langle \xi(p), \xi(p) \rangle = 0\}$ , then  $S$  is a  $\xi$ -invariant surface, which can be locally parametrized as  $(U, x)$  given by

$$x(s, t) := \phi_t(\gamma(s)), \quad (1.32)$$

where  $\gamma(s)$  is a curve in  $S$  everywhere orthogonal to the Killing vector field  $\xi$ , called the *profile curve*. That is, locally, any  $\xi$ -invariant surface of  $M_r^3(\rho)$  can be described as a surface  $S_\gamma = x(U)$  with profile curve  $\gamma$ . From now on, we will say that the surface constructed as above is a *local description of a  $\xi$ -invariant surface  $N_\nu^2$* .

From above parametrization, (1.32), it is clear that we have a family of congruent copies of the profile curve,  $\{\gamma^t(s)\}$ . Moreover, if the profile curve  $\gamma$  is arc-length parametrized, then all the curves in this family are also unit speed parametrized. Notice that in this case  $\mathcal{F}^2(s, t) = \tilde{\varepsilon}\langle x_t, x_t \rangle = \tilde{\varepsilon}\langle \xi, \xi \rangle$ , where  $\tilde{\varepsilon}$  denotes the constant causal character of  $\xi$ , only depends on the parameter  $s$ . Therefore, let's call from now on,  $G(s) = \mathcal{F}(s)$  which represents the length of the Killing vector field  $\xi$ .

Now, if the profile curve,  $\gamma$ , is a geodesic of the 3-space form,  $M_r^3(\rho)$ , then  $S_\gamma$  will be a *ruled surface*, that is, a surface locally foliated by geodesics of the ambient space. In this case, we call  $\delta_s(t)$  to the integral curve of  $\xi$  through  $\gamma(s)$  and consider the orthonormal frame  $\{T_\gamma, T_\delta, n\}$  where  $T_\gamma$  and  $T_\delta$ , are unit tangent fields to  $\gamma$  and  $\delta_s(t)$ , respectively, and  $n$  is determined by the cross product of both. We are going to use  $\epsilon_1$  for the causal character of  $\gamma$ ,  $\epsilon_3$  for that of  $\delta_s$ , and finally,  $\langle n, n \rangle = \epsilon_2$ . Then, by standard computations we obtain the following Frenet-type equations,

$$\tilde{\nabla}_{T_\gamma} T_\gamma = 0, \quad \tilde{\nabla}_{T_\gamma} T_\delta = -\epsilon_2 f(s)n, \quad \tilde{\nabla}_{T_\gamma} n = \epsilon_3 f(s)T_\delta, \quad (1.33)$$

for some smooth function  $f(s)$ . Moreover, we also have

$$\tilde{\nabla}_{T_\delta} T_\delta = -\epsilon_1 \epsilon_3 \frac{G_s}{G} T_\gamma + \epsilon_2 h_{22} n, \quad \tilde{\nabla}_{T_\delta} n = \epsilon_2 \tilde{\nabla}_{T_\delta} (T_\gamma \times T_\delta) = \epsilon_1 f T_\gamma - \epsilon_2 \epsilon_3 h_{22} T_\delta.$$

Thus,  $S_\gamma$  is completely determined by its first fundamental form,

$$g = \epsilon_1 ds^2 + \epsilon_3 G^2 dt^2. \quad (1.34)$$

and the second following fundamental form  $h = -2f(s)G(s)dsdt + h_{22}G^2(s)dt^2$ . The functions involved in both fundamental forms are connected by the Gauss-Codazzi equations (1.5) and (1.6), which, in this case, can be written as

$$f^2(s) = (-1)^r \rho + \epsilon_2 \epsilon_3 \frac{G_{ss}}{G}, \quad (1.35)$$

$$f'(s) + 2 \frac{G_s}{G} f(s) = 0, \quad (1.36)$$

$$h'_{22}(s) + 2 \frac{G_s}{G} h_{22}(s) = 0. \quad (1.37)$$

On the other hand, if the profile curve,  $\gamma$ , is a Frenet curve, we obtain that all congruent copies of the profile curve have well defined Frenet frame satisfying (1.10)-(1.13). Moreover, since  $\gamma^t(s) = x(s, t)$  is not a geodesic in  $M_r^3(\rho)$  and  $\tilde{\nabla}_{x_s} x_s$  is not null, then, for sufficiently small  $s$ , the unit Frenet normal to  $\gamma^t(s)$ ,  $N(s, t)$ , is parallel to a (local) unit normal to  $S_\gamma$ ,  $\eta$ . This means that  $\gamma^t(s)$  are geodesics in  $S_\gamma$  for any  $t$  and the parametrization (1.32) determines a *geodesic coordinate system* (see Section 1.2.2) with respect to which the metric  $\langle \cdot, \cdot \rangle \equiv g$  can be written as (1.22), while the second fundamental form is given in (1.27), in both cases with  $\mathcal{F}(s, t) = G(s)$ .

Finally, from the definition of the Riemannian curvature tensor, (1.1), and (1.17), one can check that the Gaussian curvature,  $K$ , of a local description,  $S_\gamma$ , of any  $\xi$ -invariant surface in terms of the natural parametrization, (1.32), is given by

$$K(s, t) = -\epsilon_1 \frac{G_{ss}(s)}{G(s)}. \quad (1.38)$$

In this case, it is also possible to give the explicit formula for the mean curvature function,  $H$ , (1.19). In fact, we obtain

$$H(s, t) = \frac{1}{2\kappa(s)G(s)} (G_{ss}(s) - \epsilon_1 \epsilon_2 G(s)(\kappa^2(s) + \epsilon_1 \epsilon_3 \tau^2(s) - \epsilon_2 \rho)). \quad (1.39)$$

That is, looking at both (1.38) and (1.39) we can see that the Gaussian and mean curvature functions of a local description of any  $\xi$ -invariant surface,  $K$  and  $H$  respectively, only depend on the parameter of the profile curve, that is, on  $s$ . Roughly speaking, this is the reason why studying invariant surfaces simplifies the equations, translating PDEs to ODEs.

### 1.3 Curvature Energies in Semi-Riemannian Manifolds

Let's assume along this section that all our curves are Frenet curves, and let's consider the following *curvature energy functional*

$$\Theta(\gamma) := \int_{\gamma} P(\kappa) = \int_0^L P(\kappa(s)) ds, \quad (1.40)$$

where  $P(\kappa)$  is a smooth function in an adequate domain and where, as usual, the arc-length or natural parameter is represented by  $s \in [0, L]$ ,  $L$  being the length of  $\gamma$ . For more details in this section we refer the reader to, for instance, [4], [5], [7], [8], [58], [82], [93] and [94].

Then, we consider  $\Theta$  acting on the following spaces of curves, satisfying given boundary conditions in  $(M_r^n, \langle \cdot, \cdot \rangle)$ . We shall denote by  $\Omega_{p_0 p_1}^r$  the space of smooth immersed Frenet curves of  $M_r^n$ , joining two given points of it, that is:

$$\Omega_{p_0 p_1}^r = \{\beta : [0, 1] \rightarrow M_r^n \mid \beta(i) = p_i, i \in \{0, 1\}, \frac{d\beta}{dt}(t) \neq 0, \forall t \in [0, 1]\}, \quad (1.41)$$

where  $p_i \in M_r^n, i \in \{0, 1\}$ , are arbitrary given points of  $M_r^n$ .

We take  $\Theta$  acting on  $\Omega_{p_0 p_1}^r$ . For a Frenet curve  $\gamma : [0, 1] \rightarrow M_r^n$ , we take a variation of  $\gamma$ ,  $\Gamma = \Gamma(t, \varsigma) : [0, 1] \times (-\varepsilon, \varepsilon) \rightarrow M_r^n$  with  $\Gamma(t, 0) = \gamma(t)$ . Associated to this variation we have the vector field  $W = W(t) = \frac{\partial \Gamma}{\partial \varsigma}(t, 0)$  along the curve  $\gamma(t)$ . We also write  $V = V(t, \varsigma) = \frac{\partial \Gamma}{\partial t}(t, \varsigma)$ ,  $W = W(t, \varsigma)$ ,  $v = v(t, \varsigma) = |V(t, \varsigma)|$ ,  $T = T(t, \varsigma) = e_1(t, \varsigma)$ ,  $N = N(t, \varsigma) = e_2(t, \varsigma)$ , with the obvious meanings and put  $V(s, \varsigma)$ ,  $W(s, \varsigma)$ ,... for the corresponding reparametrizations by arc-length. The following general formulas for the variations of  $v$  and  $\kappa_1$  in  $\gamma$  in the direction of  $W$  can be obtained using standard computations that involve the Frenet equations (1.7)-(1.9) (see [58] and [94])

$$W(v) = \varepsilon_1 v \langle \tilde{\nabla}_T W, T \rangle, \quad (1.42)$$

$$W(\kappa_1) = \langle \tilde{\nabla}_T^2 W, N \rangle - 2\varepsilon_1 \kappa_1 \langle \tilde{\nabla}_T W, T \rangle + \langle R(W, T)T, N \rangle, \quad (1.43)$$

Then, after a standard computation involving integrating by parts and formulae (1.42) and (1.43), the *First Variation Formula* is obtained

$$\frac{d}{d\varsigma} \Theta(\varsigma)|_{\varsigma=0} = \int_0^L \langle \mathcal{E}(\gamma), W \rangle ds + \mathcal{B}[W, \gamma]_0^L, \quad (1.44)$$

with  $\mathcal{E}(\gamma)$ ,  $\mathcal{B}[W, \gamma]_0^L$  denoting the *Euler-Lagrange operator* and *boundary term*, respectively. These are given by

$$\mathcal{E}(\gamma) = \tilde{\nabla}_T \mathcal{J} + R(\mathcal{K}, T)T, \quad (1.45)$$

$$\mathcal{B}[W, \gamma]_0^L = \left[ \langle \mathcal{K}, \tilde{\nabla}_T W \rangle - \langle \mathcal{J}, W \rangle \right]_0^L. \quad (1.46)$$

where

$$\mathcal{K}(\gamma) = \dot{P}(\kappa) N, \quad (1.47)$$

$$\mathcal{J}(\gamma) = \tilde{\nabla}_T \mathcal{K} + \varepsilon_1 \left( 2\kappa \dot{P}(\kappa) - P(\kappa) \right) T, \quad (1.48)$$

where  $\dot{P}$  represents the derivative of  $P(\kappa)$  with respect to  $\kappa$ .

We will call *critical curve* (or, also, *extremal curve*) to any curve  $\gamma \subset \Omega_{p_0 p_1}^r$ , (1.41), such that  $\mathcal{E}(\gamma) = 0$ . Notice that this is an abuse of notation, since proper criticality depends on the boundary conditions, (1.46), as it can be checked from the First Variation Formula, (1.44). However, under suitable boundary conditions, curves verifying  $\mathcal{E}(\gamma) = 0$  are going to be proper critical curves. Therefore, since for the purposes of this memory we just need to consider curves that verify  $\mathcal{E}(\gamma) = 0$ , for the sake of simplicity, from now on, we are going to use the name critical curve to denote any curve  $\gamma \subset \Omega_{p_0 p_1}^r$  verifying  $\mathcal{E}(\gamma) = 0$ .

Let's assume now that  $M_r^n$  is an  $n$ -dimensional space form, that is,  $M_r^n = M_r^n(\rho)$ . Then, from the Reduction Theorem, Theorem 1.1.1, it is enough to study critical curves of our functional when acting on the space of smooth immersed curves of  $M_r^3(\rho)$  since, it can be seen that a curve critical for  $\Theta$  must lie in a totally geodesic  $M_r^3(\rho) \subset M_r^n(\rho)$ . Indeed, we have

**Proposition 1.3.1.** *Let's consider the curvature energy functional  $\Theta$ , (1.40), acting on the space of curves immersed in a space form of dimension  $n$ , that is, acting on  $\Omega_{p_0 p_1}^r$ , (1.41), where  $M_r^n = M_r^n(\rho)$ , then a critical point of  $\Theta$  must lie in a totally geodesic 3-dimensional submanifold of  $M_r^n(\rho)$ , namely,  $M_r^3(\rho)$ .*

For a proof of above Proposition, just adapt the computations of Proposition 3 of [65].

### 1.3.1 Critical Curves in 3-Space Forms

Let's consider the *curvature energy functional*  $\Theta$ , (1.40), acting on  $\Omega_{p_0 p_1}^{r\rho}$ , where we denote by  $\Omega_{p_0 p_1}^{r\rho}$  the space of smooth immersed Frenet curves of  $M_r^3(\rho)$ , joining two given points of it, that is:

$$\Omega_{p_0 p_1}^{r\rho} = \left\{ \beta : [0, 1] \rightarrow M_r^3(\rho) \mid \beta(i) = p_i, i \in \{0, 1\}, \frac{d\beta}{dt}(t) \neq 0, \forall t \in [0, 1] \right\}, \quad (1.49)$$

where  $p_i \in M_r^3(\rho)$ ,  $i \in \{0, 1\}$ , are arbitrary given points of  $M_r^3(\rho)$ .

Then, apart from the general formulas for the variations of  $v$  and  $\kappa_1 = \kappa$  in  $\gamma$  in the direction of the variation vector field,  $W$ , (1.42) and (1.43), we can also obtain the formula for the variation of  $\kappa_2 = \tau$  in  $\gamma$  in the direction of  $W$  ([82] p. 59 and [58])

$$W(\tau) = \varepsilon_2 \left( \frac{1}{\kappa} \langle \tilde{\nabla}_T^2 W + \varepsilon_1 \rho W, B \rangle \right) - \varepsilon_1 \tau \langle \tilde{\nabla}_T W, T \rangle + \varepsilon_1 \kappa \langle \tilde{\nabla}_T W, B \rangle, \quad (1.50)$$

where the subscript  $s$  here denotes differentiation with respect to the arc-length.

In this case, the Euler-Lagrange operator, (1.45), can be written as

$$\mathcal{E}(\gamma) = \tilde{\nabla}_T \mathcal{J} + R(\mathcal{K}, T)T = \tilde{\nabla}_T \mathcal{J} + \varepsilon_1 \rho \mathcal{K}, \quad (1.51)$$

where  $\mathcal{K}$  and  $\mathcal{J}$  are given in (1.47) and (1.48), respectively. Now, using the Gauss formula (1.14) and the Frenet-Serret equations (1.10)-(1.12), we can see that  $\mathcal{E}(\gamma)$  has no component in  $T$  while its normal and binormal components can be expressed in terms of the curvature and torsion. Thus, after long straightforward computations,  $\mathcal{E}(\gamma) = 0$ , (1.51), boils down to

$$\dot{P}_{ss} + \varepsilon_1 \varepsilon_2 \dot{P} (\kappa^2 - \varepsilon_1 \varepsilon_3 \tau^2 + \varepsilon_2 \rho) - \varepsilon_1 \varepsilon_2 \kappa P = 0, \quad (1.52)$$

$$2\tau \dot{P}_s + \tau_s \dot{P} = 0, \quad (1.53)$$

which are the *Euler-Lagrange* equations of the curvature energy functional  $\Theta$ , (1.40), acting on  $\Omega_{p_0 p_1}^{r\rho}$ , (1.49). Therefore, the only curve, up to rigid motions (see §2.7 of [39]), determined by the curvature,  $\kappa$ , and torsion,  $\tau$ , solution of (1.52) and (1.53) is a critical curve of  $\Theta$ , (1.40), acting on  $\Omega_{p_0 p_1}^{r\rho}$ , (1.49), in the sense of previous section.

### Associated Killing Vector Fields

Along this section we are going to consider that  $\gamma$  is a critical Frenet curve of  $\Theta$ , (1.40), acting on  $\Omega_{p_0 p_1}^{r\rho}$ , (1.49). Then, a vector field  $W$  along  $\gamma$ , which infinitesimally preserves unit speed parametrization is said to be a *Killing vector field along  $\gamma$*  (in the sense of [94]) if  $\gamma$  evolves in the direction of  $W$  without changing shape, only position. In other words, the following equations must hold

$$W(v)(s, 0) = W(\kappa)(s, 0) = W(\tau)(s, 0) = 0, \quad (1.54)$$

( $v = |\gamma'| = \left| \frac{d\gamma}{ds} \right|$  being the speed of  $\gamma$ ) for any variation of  $\gamma$  having  $W$  as variation field.

It turns out that these extremals of  $\Theta$ , (1.40), have naturally associated Killing vector fields defined along them. Let us define the following vector field,  $\mathcal{I}$ , along  $\gamma$

$$\mathcal{I} = \varepsilon_3 T \times \mathcal{K},$$

where  $\times$  denotes the cross product and  $\mathcal{K}$  is defined in (1.47). Combining the Frenet equations (1.10)-(1.12) and (1.47), we see that  $\mathcal{I}$  is given by

$$\mathcal{I} = \varepsilon_3 T \times \mathcal{K} = \dot{P}(\kappa) B. \quad (1.55)$$

Then, we have (see also [58])

**Proposition 1.3.2.** *Assume that  $\gamma$  is an immersed curve in  $M_r^3(\rho)$  with non-null velocity and acceleration which is an extremal of  $\Theta$ , (1.40). Consider the vector fields (1.48) and (1.55) given by*

$$\mathcal{I} = \dot{P}B, \quad \mathcal{J} = \varepsilon_1 \left( \kappa \dot{P} - P \right) T + \dot{P}_s N + \varepsilon_3 \tau \dot{P}B, \quad (1.56)$$

defined on  $\gamma$ ,  $\{T, N, B\}$  being its Frenet frame. Then  $\mathcal{I}$  and  $\mathcal{J}$  are Killing vector fields along  $\gamma$ .

*Proof.* Assume that  $\gamma$  is an extremal of  $\Theta$ , (1.40), which, without loss of generality we can assume  $\gamma$  to be arc-length parametrized. Then the curvature and torsion of  $\gamma$  must satisfy (1.52) and (1.53). Take any variation of  $\gamma$  in  $\Omega_{p_0 p_1}^{r\rho}$ , (1.49),  $\Gamma(s, \varsigma)$ , with variation vector field  $\mathcal{I}$  and denote by  $v(s, \varsigma) = \left| \frac{d}{ds} \Gamma(s, \varsigma) \right|$  the speed of the variation curves. By substituting  $W = \mathcal{I}$  in (1.42), we have

$$\mathcal{I}(v) = \varepsilon_1 \langle \tilde{\nabla}_T \mathcal{I}, T \rangle v,$$

and then, the Frenet equations (1.10)-(1.12) give  $\mathcal{I}(v)(t, 0) = 0$ . Similarly, when  $W = \mathcal{I}$ , the equation (1.43) gives

$$\mathcal{I}(\kappa) = \varepsilon_2 \frac{1}{\kappa} \langle \tilde{\nabla}_T^2 \mathcal{I}, \tilde{\nabla}_T \mathcal{I} \rangle - 2\varepsilon_1 \kappa \langle \tilde{\nabla}_T \mathcal{I}, T \rangle + \varepsilon_1 \rho \langle \mathcal{I}, N \rangle,$$

which combined with the Euler-Lagrange equation (1.53) shows that  $\mathcal{I}(\kappa)(t, 0) = 0$ . Finally, a combination of (1.50)

$$\mathcal{I}(\tau) = \varepsilon_2 \left( \frac{1}{\kappa} \langle \tilde{\nabla}_T^2 \mathcal{I} + \varepsilon_1 \rho \mathcal{I}, B \rangle \right)_s - \varepsilon_1 \tau \langle \tilde{\nabla}_T \mathcal{I}, T \rangle + \varepsilon_1 \kappa \langle \tilde{\nabla}_T \mathcal{I}, B \rangle$$

and (1.52), gives also  $\mathcal{I}(\tau)(t, 0) = 0$ . Hence, we see from (1.54) that  $\mathcal{I}$  is a Killing vector field along  $\gamma$ . A similar argument works for the vector field  $\mathcal{J}$ , which proves the statement.  $\square$

Thus, using an argument similar to that of [94] we can extend  $\mathcal{I}$  and  $\mathcal{J}$ , (1.56), to Killing vector fields on the whole  $M_r^3(\rho)$ . We are going to denote them again by  $\mathcal{I}$  and  $\mathcal{J}$ , respectively.

### First Integrals of Euler-Lagrange Equations

The Euler-Lagrange equations, (1.52) and (1.53), represent a system of second order ordinary differential equations, ODEs. However, if  $\dot{P}_s$  does not vanish, we can compute a first integral of this system making use of the Killing vector fields along the critical curves,  $\mathcal{I}$  and  $\mathcal{J}$ , (1.56) (see [5], [58] and [82]).

In fact, a direct long computation using the Frenet equations (1.10)-(1.12), formulas (1.47) and (1.48), and the Euler-Lagrange equations (1.52) and (1.53), shows that the derivatives of the functions  $\langle \mathcal{J}, \mathcal{I} \rangle$  and  $\langle \mathcal{J}, \mathcal{J} \rangle + \varepsilon_1 \varepsilon_2 \varepsilon_3 \rho \langle \mathcal{I}, \mathcal{I} \rangle$  along the critical curve are both zero. Thus,

$$\langle \mathcal{J}, \mathcal{I} \rangle = e, \quad (1.57)$$

$$\langle \mathcal{J}, \mathcal{J} \rangle + \varepsilon_1 \varepsilon_2 \varepsilon_3 \rho \langle \mathcal{I}, \mathcal{I} \rangle = d, \quad (1.58)$$

with  $d$  and  $e$  being real constants. Now, if we substitute the values of both Killing vector fields along any critical curve, (1.56), we get the expression of the first integrals of the Euler-Lagrange equations, (1.52) and (1.53), in terms of the curvature and torsion of the critical curve,

$$\tau \dot{P}^2 = e, \quad (1.59)$$

$$\dot{P}_s^2 + \varepsilon_1 \varepsilon_2 (\kappa \dot{P} - P)^2 + \varepsilon_2 \varepsilon_3 \tau^2 \dot{P}^2 + \varepsilon_1 \rho \dot{P}^2 = \varepsilon_2 d. \quad (1.60)$$

### 1.3.2 Generalized Kirchhoff Centerlines

Along this section, we are going to study a generalization of the curvature energy functionals  $\Theta$ , (1.40). More precisely, let's consider a functional of the following form

$$\Theta(\gamma) = \int_{\gamma} P(\kappa) + \mu\tau + \lambda = \int_0^L (P(\kappa)(s) + \mu\tau(s) + \lambda) ds, \quad (1.61)$$

acting on Frenet curves immersed in space forms, where  $\mu$  and  $\lambda \in \mathbb{R}$ . As one can check, in this case the Reduction Theorem, Theorem 1.1.1, also works, therefore, again it is enough to study critical curves of above variational problem among immersed curves in  $M_r^3(\rho)$ .

Now, by computing the first variation formula for (1.61) acting on  $\Omega_{p_0 p_1}^{r\rho}$ , (1.49), (under arbitrary boundary conditions) and using the Frenet equations (1.10)-(1.12), the Euler-Lagrange equations can be written as

$$\dot{P}_{ss} + \varepsilon_1 \varepsilon_2 \dot{P} (\kappa^2 - \varepsilon_1 \varepsilon_3 \tau^2 + \varepsilon_2 \rho) - \varepsilon_1 \varepsilon_2 \kappa (P - \mu\tau + \lambda) = 0, \quad (1.62)$$

$$2\tau \dot{P}_s + \tau_s \dot{P} - \varepsilon_1 \varepsilon_3 \mu \kappa_s = 0, \quad (1.63)$$

For reasons that will be clear later (see Section 3.4.2), along this memory curves satisfying above equations (1.62) and (1.63) will be called *generalized Kirchhoff centerlines*. Notice that generalized Kirchhoff centerlines are a particular case of extremals of energies depending on the curvature and torsion of the curves,  $P(\kappa, \tau)$ . The Euler-Lagrange of these energies in semi-Riemannian 3-space forms have been obtained, for instance, in [4], [58] and [82].

An important fact about generalized Kirchhoff centerlines is that the correspondence version of Proposition 1.3.2 is also true. In particular, we have



**Proposition 1.3.3.** *The vector field  $\mathcal{I} = \varepsilon_1 \varepsilon_3 \mu T + \dot{P}B$  is a Killing vector field along  $\gamma$ , if and only if,  $\gamma$  is a generalized Kirchhoff centerline.*

For a proof of above result, we refer to [64].

### 1.3.3 Curvature Energies with Potential

A different generalization of the curvature energies  $\Theta$ , (1.40), can be done by considering a potential defined on the manifold. Along this section, let's assume that  $\Phi$  is a smooth function on the semi-Riemannian manifold  $M_r^n$ . Then, we consider the following *curvature energy functional with potential*

$$\Theta_\Phi(\gamma) = \int_\gamma P(\kappa) + \Phi = \int_o^L (P(\kappa) + \Phi)(s) ds, \quad (1.64)$$

acting on  $\Omega_{p_0 p_1}^r$ , (1.41). Arguing as before we can get the Euler-Lagrange operator, which, in this case is

$$\mathcal{E}_\Phi(\gamma) = \tilde{\nabla}_T \mathcal{J}_\Phi + R(\mathcal{K}_\Phi, T)T + \text{grad } \Phi, \quad (1.65)$$

where now  $\mathcal{J}_\Phi$  is given by

$$\mathcal{J}_\Phi(\gamma) = \tilde{\nabla}_T \mathcal{K}_\Phi + \varepsilon_1 \left( 2\kappa \dot{P}(\kappa) - P(\kappa) - \Phi \right) T,$$

while  $\mathcal{K}_\Phi = \mathcal{K}$ , (1.47). Moreover, as in the potential free case, (1.40), critical curves under suitable boundary conditions of  $\Theta_\Phi$ , (1.64), are going to be characterized by the equation  $\mathcal{E}_\Phi(\gamma) = 0$ .

#### Elasticae with Potential in Riemannian Surfaces

If we consider  $P(\kappa) = \kappa^2$ ,  $\Phi = \lambda \in \mathbb{R}$  and  $\lambda = 0$  in (1.64), we are dealing with the bending energy and its critical curves are *elastic curves* (or, simply, *elasticae*). The study of elasticae is a classical variational problem initiated in 1691 when Bernoulli proposed to determine the final shape of a flexible rod. If  $n = 2$ , the problem of elastic curves in surfaces has a long history but it is really well understood only when  $M^2$  is a real 2-space form,  $M^2(\rho)$ . In fact, Euler published in 1744 his classification of the planar elastic curves in the Euclidean plane  $\mathbb{R}^2$ , [56], and, much more recently, Langer and Singer have classified the closed elastic curves in the 2-sphere,  $\mathbb{S}^2(\rho)$ , and in the hyperbolic plane,  $\mathbb{H}^2(\rho)$ , [94], but, in general, little is known for elastic curves in surfaces with non-constant curvature.

On the other hand, if  $\lambda \neq 0$ , the functional  $\Theta_\lambda$ , (1.64), is also a bending-type energy. However, in this case, by a version of the Lagrange's Multipliers Principle, critical curves are elastic curves with a restriction on the length. Notice that the constant  $\lambda$  can be

generalized. For instance, following the notation of Section 1.3.3, consider that  $\Phi$  is a general smooth function defined on a Riemannian surface  $M_r^n = N^2$ , and we are going to consider the curvature energy with potential (1.64) for  $P(\kappa) = \kappa^2$ , that is

$$\Theta_\Phi(\gamma) = \int_\gamma (\kappa^2 + \Phi) ds \quad (1.66)$$

acting on smooth immersed curves in  $N^2$ . Then, following the computations of Section 1.3.3, the Euler-Lagrange equations for this case, (1.65), simplifies to (see also [25])

$$2\kappa_{ss} + \kappa (\kappa^2 + 2K - \Phi) + N(\Phi) = 0, \quad (1.67)$$

where  $K$  denotes the Gaussian curvature of  $N^2$ . Observe that above Euler-Lagrange equation, (1.67), generalizes the Euler-Lagrange equation of classical elastic curves. Thus, solutions of (1.67) are going to be referred as *elasticae with potential*.

## Chapter 2

# Generalized Elastic Curves: A First Application

The determination of the shape of elastic curves or rods is not only one of the oldest problems in the geometric Calculus of Variations, as it has been explained in the introduction, but during the years it has been also showed to be one of the most interesting. In fact, it has a huge range of applications, not only in Differential Geometry, but also in Physics, Biophysics, Fluid Dynamics,... (see [11] and the references therein).

In this chapter we consider a possible generalization of elastic curves, that also includes many other classical variational problems (see, for instance, [5], [7], [29],...). We are going to call *generalized elastic curves* to these curves for obvious reasons, and they are going to play an essential role along the whole memory. Indeed, most of the critical curves that are going to appear in the memory fall inside this family. Therefore, in the first part of the chapter, we are going to fix all the details of the variational problem related with generalized elastic curves.

Finally, in the second part, we are going to completely describe a first nice application of these curves to visual curve completion, that is, to image reconstruction.

## 2.1 Generalized Elastic Curves in Semi-Riemannian Manifolds

Along this section we are going to consider the particular choice of the function  $P(\kappa)$  given by

$$P(\kappa) = (\kappa^\epsilon - \mu)^p, \quad (2.1)$$

in the curvature energy functional (1.40), where  $\epsilon = 1, 2$  and  $p$  and  $\mu \in \mathbb{R}$ . That is, we are going to consider the curvature energy

$$\Theta_{\mu}^{\epsilon,p}(\gamma) = \int_{\gamma} (\kappa^{\epsilon} - \mu)^p = \int_0^L (\kappa^{\epsilon}(s) - \mu)^p ds, \quad (2.2)$$

where  $s$  denotes the arc-length parameter and  $L$  is the length of  $\gamma$ .

When  $p = 0$ , (2.2) is nothing but the *length functional* whose arc-length parametrized critical curves are geodesics, therefore, in what follows, we are not going to allow  $p$  to be zero. Moreover, if  $p = 1$ , then (2.2) is, basically, the *total curvature functional*, if  $\epsilon = 1$ ; or, the *bending energy* with a penalty on the length, if  $\epsilon = 2$ . In the latter, extremals of (2.2) are called *elastic curves*. Therefore, from now on, we are going to call *generalized elasticae* to critical curves of (2.2).

We first notice that for any positive  $p$ , curves with  $\kappa^{\epsilon} = \mu$  will be global minima among curves with  $(\kappa^{\epsilon} - \mu)^p \in L^1([0, L])$ . Then, for all the cases, we consider  $\Theta_{\mu}^{\epsilon,p}(\gamma) \geq 0$  acting on the following spaces of curves, satisfying given boundary conditions in  $(M_r^n, \langle \cdot, \cdot \rangle)$ , with  $\kappa^{\epsilon}$  greater than  $\mu$ . We shall denote by  $\Omega_{p_0 p_1}^{r*}$  the space of smooth immersed Frenet curves of  $M_r^n$ , joining two given points of it and verifying that  $\kappa^{\epsilon} > \mu$ , that is:

$$\Omega_{p_0 p_1}^{r*} = \{\beta : [0, 1] \rightarrow M_r^n \mid \beta(i) = p_i, i \in \{0, 1\}, \frac{d\beta}{dt}(t) \neq 0, \forall t \in [0, 1], \kappa^{\epsilon} > \mu\}, \quad (2.3)$$

where  $p_i \in M_r^n, i \in \{0, 1\}$ , are arbitrary given points of  $M_r^n$ .

Then, if  $W$  is a proper vector field along a curve  $\gamma \in \Omega_{p_0 p_1}^r$ , (1.41), then it is known that there exists a variation of  $\gamma$  by immersed curves in  $M_r^n, \Gamma : [0, 1] \times (-\varepsilon, \varepsilon) \rightarrow M_r^n, (t, \varsigma) \rightarrow \Gamma(t, \varsigma)$ , whose variation vector field is  $\frac{d\Gamma}{d\varsigma} = W$ , as we have already explained in Section 1.3 of Chapter 1. Moreover, if  $\gamma \in \Omega_{p_0 p_1}^{r*}$ , (2.3), smoothness of  $\Gamma$  and  $\kappa$  implies that there exists a “subvariation”  $\widehat{\Gamma} : [0, 1] \times (-\widehat{\varepsilon}, \widehat{\varepsilon}) \rightarrow M_r^n, \widehat{\varepsilon} < \varepsilon$  and  $\widehat{\Gamma}$  being the restriction of  $\Gamma$ , such that any variation curve in  $\widehat{\Gamma}$  belongs to  $\Omega_{p_0 p_1}^{r*}$ , (2.3). Observe that both variations have the same variation vector field  $W$ , and therefore, the derivation of the Euler-Lagrange equations is the same.

That is, a critical curve  $\gamma \in \Omega_{p_0 p_1}^{r*}$ , (2.3), of  $\Theta_{\mu}^{\epsilon,p}$ , (2.2), must satisfy  $\mathcal{E}(\gamma) = 0$ , where  $\mathcal{E}$  is the Euler-Lagrange operator defined in (1.45), for the adequate value of  $P(\kappa)$ , (2.1).

### 2.1.1 Generalized Elastic Curves in 3-Space Forms

If the ambient space is a semi-Riemannian space form of arbitrary dimension  $n$ ,  $M_r^n(\rho)$ , then by Proposition 1.3.1, it is enough to consider critical curves among curves immersed in  $M_r^3(\rho)$ . Thus, in this section we are going to study the Euler-Lagrange equations of a generalized elastica immersed in a semi-Riemannian 3-space form,  $M_r^3(\rho)$ .

Following the notation of Section 1.3.1 and 2.1, we denote by  $\Omega_{p_0 p_1}^{r\rho*}$  to the subspace of  $\Omega_{p_0 p_1}^{r\rho}$ , (1.49), where  $\kappa^{\epsilon} > \mu$ . Now, if we consider  $\Theta_{\mu}^{\epsilon,p}$ , (2.2), acting on  $\Omega_{p_0 p_1}^{r\rho*}$ , substituting

the value of  $P(\kappa)$ , (2.1), in (1.52) and (1.53),  $\mathcal{E}(\gamma) = 0$  boils down to

$$\frac{d}{ds^2} (\kappa^{\epsilon-1} (\kappa^\epsilon - \mu)^{p-1}) + \varepsilon_1 \varepsilon_2 \kappa^{\epsilon-1} (\kappa^\epsilon - \mu)^{p-1} (\kappa^2 - \varepsilon_1 \varepsilon_3 \tau^2 + \varepsilon_2 \rho) - \varepsilon_1 \varepsilon_2 \frac{\kappa}{\epsilon p} (\kappa^\epsilon - \mu)^p = 0, \quad (2.4)$$

$$2 \frac{d}{ds} (\kappa^{\epsilon-1} (\kappa^\epsilon - \mu)^{p-1}) \tau + \kappa^{\epsilon-1} (\kappa^\epsilon - \mu)^{p-1} \frac{d\tau}{ds} = 0, \quad (2.5)$$

which are the Euler-Lagrange equations of  $\Theta_\mu^{\epsilon,p}$ , (2.2), acting on  $\Omega_{p_0 p_1}^{r\rho*}$ . Moreover, applying Proposition 1.3.2 we obtain that the following vector fields along  $\gamma$ ,

$$\mathcal{I} = \epsilon p \kappa^{\epsilon-1} (\kappa^\epsilon - \mu)^{p-1} B, \quad (2.6)$$

$$\begin{aligned} \mathcal{J} &= \varepsilon_1 (\kappa^\epsilon - \mu)^{p-1} ((\epsilon p - 1) \kappa^\epsilon + \mu) T \\ &+ \epsilon p \frac{d}{ds} (\kappa^{\epsilon-1} (\kappa^\epsilon - \mu)^{p-1}) N + \varepsilon_3 \epsilon p \kappa^{\epsilon-1} (\kappa^\epsilon - \mu)^{p-1} \tau B, \end{aligned} \quad (2.7)$$

are Killing vector fields along  $\gamma$ . And, therefore, as explained in Section 1.3.1 they have unique extensions to Killing vector fields on  $M_r^3(\rho)$  (which will be denoted by the same letters).

Finally, by making use of equations (1.59) and (1.60), we also have the following first integrals of the Euler-Lagrange equations (2.4) and (2.5)

$$p^2 \kappa^{2(\epsilon-1)} (\kappa^\epsilon - \mu)^{2(p-1)} \tau = e, \quad (2.8)$$

$$\begin{aligned} \left( \frac{d}{ds} (\kappa^{\epsilon-1} (\kappa^\epsilon - \mu)^{p-1}) \right)^2 + \varepsilon_1 \varepsilon_2 \frac{1}{\epsilon^2 p^2} (\kappa^\epsilon - \mu)^{2(p-1)} ((\epsilon p - 1) \kappa^\epsilon + \mu)^2 \\ + (\varepsilon_2 \varepsilon_3 \tau^2 + \varepsilon_1 \rho) \kappa^{2(\epsilon-1)} (\kappa^\epsilon - \mu)^{2(p-1)} = \varepsilon_2 \frac{d}{\epsilon^2 p^2}, \end{aligned} \quad (2.9)$$

where  $d$  and  $e$  are the constants of integration appearing in (1.57) and (1.58), respectively.

## 2.2 An Application to Image Reconstruction

In this second part of the chapter, we are going to show how a certain family of generalized elastic curves can be applied to image reconstruction. In particular, we are mainly interested in the application to visual curve completion. This section is going to be based on [13].

Neuro-biologic research over the past few decades has greatly clarified the functional mechanisms of the first layer V1 of the visual cortex (*primary visual cortex*). Such layer contains a variety of types of cells, including the so-called simple cells. Researchers found that V1 constitutes of orientation selective cells at all orientations for all retinal positions

so simple cells are sensitive to orientation specific brightness gradients (for details see [26] and [50]). Recently, this structure of the primary visual cortex has been modeled using sub-Riemannian geometry, [124]. In particular, the unit tangent bundle of the plane can be used as an abstraction to study the organization and mechanisms of V1.

According to this model, in the space  $\mathbb{R}^2 \times \mathbb{S}^1$  each point  $(x, y, \theta)$  represents a column of cells associated to a point of *retinal data*  $(x, y) \in \mathbb{R}^2$ , all of which are adjusted to the *orientation* given by the angle  $\theta \in \mathbb{S}^1$ . In other words, the vector  $(\cos \theta, \sin \theta)$  is the direction of maximal rate of change of brightness at point  $(x, y)$  of the picture seen by the eye. Such vector can be seen as the normal to the boundary of the picture. Thus, when the cortex cells are stimulated by an image, the border of the image gives a curve inside the 3-space  $\mathbb{R}^2 \times \mathbb{S}^1$ , but such curves are restricted to be tangent to the distribution spanned by the vector fields

$$X_1 = \cos \theta \frac{\partial}{\partial x} + \sin \theta \frac{\partial}{\partial y}, \quad X_2 = \frac{\partial}{\partial \theta}. \quad (2.10)$$

It is believed that, if a piece of the contour of a picture is missing to the eye vision (or maybe it is covered by an object), then the brain tends to “complete” the curve by minimizing some kind of energy, being length the simplest (but not the only) of such (for other possible options see [13]). In short, *there is some sub-Riemannian structure on the space of visual cells and the brain considers a sub-Riemannian geodesic between the endpoints of the missing data.*

### 2.2.1 Sub-Riemannian Geodesics

Let  $M^3$  be a smooth 3-manifold. A subbundle of the tangent bundle  $TM^3$  is called a *distribution*  $\mathcal{D}$  on  $M^3$ . Once we have chosen  $\mathcal{D}$ , a  $\mathcal{D}$ -*curve* on  $M^3$  is a smooth immersed curve  $\delta : [a, b] \rightarrow M^3$  which is always tangent to  $\mathcal{D}$ ; that is,  $\delta'(t) \in \mathcal{D}_{\delta(t)}$  for all  $t \in [a, b]$ . A distribution  $\mathcal{D}$  is said to be *bracket-generating* if for every  $p \in M^3$  the sections of  $\mathcal{D}$  near  $p$  together with all their commutators span the tangent space of  $M^3$  at  $p$ ,  $T_p M^3$ . By a well-known Theorem of Chow-Rashevskii, *there is a  $\mathcal{D}$ -curve joining any two points of  $M^3$  if  $\mathcal{D}$  is bracket-generating* (check [27] for the smooth version of this Theorem).

Now, a *sub-Riemannian metric* is a smoothly varying positive definite bilinear form  $\langle \cdot, \cdot \rangle$  on  $\mathcal{D}$ . Thus, if  $\mathcal{D}$  were equal to the whole tangent bundle,  $\langle \cdot, \cdot \rangle$  would give a Riemannian metric on  $M^3$ . A *sub-Riemannian 3-manifold*,  $(M^3, \mathcal{D}, \langle \cdot, \cdot \rangle)$ , is a smooth 3-dimensional manifold  $M^3$  equipped with a sub-Riemannian metric  $\langle \cdot, \cdot \rangle$  on a bracket-generating distribution  $\mathcal{D}$  of rank  $m > 0$ . In this setting, the *length* of a  $\mathcal{D}$ -curve  $\delta$  is defined to be

$$\mathcal{L}(\delta) = \int_a^b \langle \delta'(t), \delta'(t) \rangle^{\frac{1}{2}} dt.$$

Since  $\mathcal{D}$  is bracket-generating, it is possible to endow  $M^3$  with a *distance*  $d$ . The distance

$d(p, q)$  between any two points  $p$  and  $q$  of  $M^3$  is defined by

$$d(p, q) = \inf_{\delta} \{L(\delta) \mid \delta \text{ is a } \mathcal{D}\text{-curve joining } p \text{ to } q\}.$$

To construct a sub-Riemannian structure on  $M^3 = \mathbb{R}^2 \times \mathbb{S}^1$  we take the distribution  $\mathcal{D} = \ker(\sin \theta dx - \cos \theta dy)$ , where  $x$  and  $y$  are the coordinates on  $\mathbb{R}^2$  and  $\theta$  is the coordinate on  $\mathbb{S}^1$ . This distribution is spanned by the vector fields described in (2.10). Consider on  $\mathcal{D}$  the inner product  $\langle \cdot, \cdot \rangle$  for which the two vectors (2.10) are everywhere orthonormal.

Now, notice that every  $\mathcal{D}$ -curve  $\gamma(t) = (x(t), y(t), \theta(t))$  with  $\gamma^*(\cos \theta dx + \sin \theta dy) \neq 0$  is the lift of a regular curve  $\alpha(t) = (x(t), y(t))$  in the plane whose tangent vector  $\alpha'(t)$  forms the angle  $\theta(t)$  with the  $x$ -axis, that is,

$$\alpha'(t) = v(t) \cos \theta \frac{\partial}{\partial x} + v(t) \sin \theta \frac{\partial}{\partial y},$$

where  $v(t)$  is the speed of  $\alpha(t)$ . Conversely, every regular curve  $\alpha(t)$  in the plane may be lifted to a  $\mathcal{D}$ -curve  $\gamma(t) = (x(t), y(t), \theta(t))$  by setting  $\theta(t)$  equal to the angle between  $\alpha'(t)$  and the  $x$ -axis. Now, the tangent vector  $\gamma'(t)$  of the  $\mathcal{D}$ -curve  $\gamma(t)$  has squared length

$$\langle \gamma'(t), \gamma'(t) \rangle = v^2(t) + (\theta')^2(t) = v^2(t) \left( 1 + \left( \frac{\theta'(t)}{v(t)} \right)^2 \right) = v^2(t)(1 + \kappa^2(t)),$$

where  $\kappa(t)$  is the curvature of  $\alpha$ . Thus, the  $\mathcal{D}$ -curves with  $\gamma^*(\cos \theta dx + \sin \theta dy) \neq 0$  that cover the distance between two points  $(x_0, y_0, \theta_0)$  and  $(x_1, y_1, \theta_1)$  of  $M^3$  are the lifts of curves  $\alpha$  in the plane joining  $(x_0, y_0)$  to  $(x_1, y_1)$  with initial angle  $\theta_0$  and final angle  $\theta_1$  that minimize the functional

$$L(\alpha) = \int_{\alpha} (1 + \kappa^2(s))^{\frac{1}{2}} ds, \quad (2.11)$$

$s$  being the arc-length parameter, among all such curves in the plane. In other words, *geodesics in  $V1$  are obtained by lifting to  $M^3 = \mathbb{R}^2 \times \mathbb{S}^1$  minimizers of (2.11) in  $\mathbb{R}^2$* . Finally, as indicated in [26], the hypercolumnar organization of the visual cortex suggests that the cost of moving one orientation unit is not necessarily the same as to moving spatial units, then the curve completion problem should consider the functional

$$\Theta_a(\gamma) = \int_{\gamma} \sqrt{\kappa^2 + a^2} ds \quad (2.12)$$

for any real constant  $a$ , acting on planar curves instead. Observe that  $\Theta_a$ , (2.12) is included in our family of generalized elastic functionals, (2.2), for  $p = 1/2$ ,  $\epsilon = 2$  and  $\mu = -a^2$ .

### 2.2.2 Total Curvature Type Extremals

Let us consider along this section the energy functional  $\Theta_a: \Omega_{pq} \rightarrow \mathbb{R}$  defined in (2.12) where,  $a \in \mathbb{R}$ ,  $s$  is the arc-length parameter and  $\kappa(s) \equiv \kappa_1(s)$  is the first Frenet curvature of  $\gamma(s)$ , acting on the space of immersed curves  $\gamma(t)$  in  $\mathbb{R}^3$  with fixed endpoints  $p, q \in \mathbb{R}^3$ ,  $\Omega_{pq}$ .

Observe that geodesics (curves of rank 0) are minima of  $\Theta_a$ , (2.12). Now, since geodesics are always critical for  $\Theta_a$ , (2.12) (for suitable boundary conditions) in the following we may assume, in addition, that  $\gamma \in \Omega_{pq}$  is a non-geodesic curve, namely, that it is a curve of rank at least 1. Then, from (1.51), we obtain that the Euler-Lagrange operator is given by

$$\begin{aligned} \mathcal{E}(\gamma) &= \frac{1}{(\kappa^2 + a^2)^{\frac{1}{2}}} T^{(3)} + 2 \frac{d}{ds} \left( \frac{1}{(\kappa^2 + a^2)^{\frac{1}{2}}} \right) T'' \\ &\quad + \left( \frac{d^2}{ds^2} \left( \frac{1}{(\kappa^2 + a^2)^{\frac{1}{2}}} \right) + \frac{\kappa^2 - a^2}{(\kappa^2 + a^2)^{\frac{1}{2}}} \right) T' + \frac{d}{ds} \left( \frac{\kappa^2 - a^2}{(\kappa^2 + a^2)^{\frac{1}{2}}} \right) T. \end{aligned}$$

Now, if  $\gamma$  is an extremal of  $\Theta_a$ , (2.12), then  $\mathcal{E}(\gamma) = 0$  and, therefore, (2.4) and (2.5), reduce to

$$\frac{d^2}{ds^2} \left( \frac{\kappa}{(\kappa^2 + a^2)^{\frac{1}{2}}} \right) + \frac{\kappa}{(\kappa^2 + a^2)^{\frac{1}{2}}} (\kappa^2 - \tau^2) - \kappa (\kappa^2 + a^2)^{\frac{1}{2}} = 0, \quad (2.13)$$

$$\frac{d}{ds} \left( \frac{\kappa^2}{\kappa^2 + a^2} \tau \right) = 0. \quad (2.14)$$

Case  $a = 0$  corresponds to the *total curvature functional*. This is the reason why along this section we call *total curvature type energy* to  $\Theta_a$ , (2.12). Moreover, this is also the name given to the functional  $\Theta_a$  in [15], where it was studied in any space form. In the proper total curvature functional case, if  $\gamma \in \Omega_{pq}$  is critical then (2.13) and (2.14) imply that the torsion vanishes,  $\tau = 0$  and, therefore,  $\gamma$  is a planar curve. Then,

$$\int_{\gamma} \kappa = \theta(1) - \theta(0) + 2\pi m, \quad (2.15)$$

where  $\theta(i) \in [0, 2\pi)$ ,  $i = 1, 2$ , denotes the angle that  $v_i$ ,  $i = 1, 2$ , makes with the line determined by  $p$  and  $q$ , and  $m \in \mathbb{Z}$  is an integer representing the number (taking orientation into account) of loops that the trace of  $\gamma$  has between  $p$  and  $q$ . Since (2.15) is constant within any regular homotopy class of  $\Omega_{pq}$  having the same tangent vectors at  $p$  and  $q$ , we see that the corresponding variational problem is trivial, that is, any  $\gamma \in \Omega_{pq}$  with adequate tangent vectors at  $p$  and  $q$  is critical for  $\Theta_a$ , (2.12), when  $a = 0$ .

So we assume from now on that  $a \neq 0$ . Notice that above equations (2.13) and (2.14) imply that there are no helices (nor even Lancret helices) critical for  $\Theta_a$ , (2.12) (see the



corresponding definitions in Section 1.2.1). On the other hand, if  $\gamma \in \Omega_{pq}$  is critical for  $\Theta_a$  under arbitrary boundary conditions, then it satisfies  $\mathcal{E}(\gamma) = 0$  and, therefore, we conclude that the first integrals of the Euler-Lagrange equations, (2.13) and (2.14), are

$$\left(\frac{d\kappa}{ds}\right)^2 = \left(\frac{a^2 + \kappa^2}{a^2\kappa}\right)^2 ((\kappa^2 + a^2)(d\kappa^2 - e^2(\kappa^2 + a^2)) - \kappa^2 a^4), \quad (2.16)$$

$$\tau = e \left(\frac{\kappa^2 + a^2}{\kappa^2}\right), \quad (2.17)$$

where  $d > 0$  and  $e \in \mathbb{R}$ , due to the constraints of (1.57) and (1.58).

Moreover, by using the symmetries of  $\mathbb{R}^3$ , the coordinates of a critical curve  $\gamma$  can also be obtained by quadratures. In fact,  $\gamma$  being critical means that  $\mathcal{I}$  and  $\mathcal{J}$ , which are the extensions of (2.6) and (2.7), are Killing fields (see Section 2.1.1, Proposition 1.3.2 and the argument after it), which must come from one-parameter groups of helicoidal motions. Then, choosing  $z$  as the axis of the helicoidal motion associated to  $\mathcal{I}$ , introducing cylindrical coordinates  $r, \theta, z$ , and taking into account the first integrals of the Euler-Lagrange equations given before, (2.16) and (2.17), we get ([5] and [92])

$$\mathcal{J} = \sqrt{d} \partial_z, \quad (2.18)$$

$$\mathcal{I} = \mathcal{J} \times \gamma + \frac{e}{d} \mathcal{J} = \frac{e}{\sqrt{d}} \partial_z + \sqrt{d} \partial_\theta, \quad (2.19)$$

where  $d > 0$  and  $e \in \mathbb{R}$  are the constants of integration appearing in (1.57) and (1.58). Since  $|\partial_\theta|^2 = r^2(s)$ , then (1.55) and (2.19) give

$$r^2(s) = \frac{\kappa^2}{d(\kappa^2 + a^2)} - \frac{e^2}{d^2}. \quad (2.20)$$

Moreover,  $T(s) = r' \partial_r + \theta' \partial_\theta + z' \partial_z$  so (2.6), (2.7) and (2.18) imply

$$z'(s) = \frac{-a^2}{(d(\kappa^2 + a^2))^{\frac{1}{2}}}. \quad (2.21)$$

Finally, combining  $\langle T, \mathcal{I} \rangle = 0$  and (2.19) we obtain

$$\theta'(s) = \frac{e z'}{d r^2}. \quad (2.22)$$

Therefore, from (2.20)-(2.22) we see that, once the curvature of the critical curve,  $\gamma$ , is known (for which we need to solve (2.16)) the coordinates of  $\gamma$  can be obtained by quadratures. Notice also that (2.21) implies that  $z(s)$  is monotonic, thus, there are no periodic solutions of the Euler-Lagrange equations (2.13) and (2.14), so that we cannot have closed critical curves.

Extremals in  $\mathbb{R}^2$  are totally determined by their curvature,  $\kappa$ , which, in our case, can be obtained explicitly. In fact, making  $\tau = 0$  in the Euler-Lagrange equation (2.13) we get

$$\frac{d^2}{ds^2} \left( \frac{\kappa}{(\kappa^2 + a^2)^{\frac{1}{2}}} \right) - \frac{a^2 \kappa}{(\kappa^2 + a^2)^{\frac{1}{2}}} = 0,$$

from which we have

$$\frac{\kappa}{(\kappa^2 + a^2)^{\frac{1}{2}}}(s) = c_1 \exp(as) + c_2 \exp(-as),$$

for some integration constants  $c_1$  and  $c_2$ . Then, solving for  $\kappa$  one obtains

$$\kappa(s) = \frac{a(c_1 \exp(as) + c_2 \exp(-as))}{(1 - (c_1 \exp(as) + c_2 \exp(-as))^2)^{\frac{1}{2}}}. \quad (2.23)$$

From this equation, (2.23), we see that there is at most one point where the curvature may change sign, so the curvature is always positive (or negative) except for at most one inflection point. Moreover  $\kappa'(s)$  has at most one zero (a vertex), hence, either the curvature is monotonic, or it monotonically decreases up to reaching the vertex where it starts to monotonically increase (or viceversa). This means that planar critical curves are a family of “short time” spirals in the plane.

This is a case relevant in image restoration as we mentioned in Section 2.2 and a parametrization of extremal curves, using as parameter,  $\theta$ , the angle which the curve makes with a fixed line, was given in [26], under the assumption that the curves have no inflection points. But, as we have just noticed, these extremals have at most one vertex, hence, the argument of [26] applies and an explicit parametrization of extremals for this variational problem can be obtained in terms of elliptic integrals of the first and second kind (see Appendix A for details about these elliptic integrals). Alternatively, one may use our previous computations to get different parametrizations of extremals, at least, by quadratures. In fact, as it is very well-known, a parametrization in terms of the curvature and arc-length parameter of a planar curve is given by  $(\int \cos \int \kappa, \int \sin \int \kappa)$ , then, using (2.23) we can also get a parametrization of the extremals of  $\Theta_a$  in  $\mathbb{R}^2$  in terms of the arc-length parameter after two quadratures. Observe that another parametrization can also be explicitly obtained from (2.20) and (2.21).

However, for any possible choice of a parametrization method, a specific determination of the solution curves implies that the integration constants must be determined. This can be tried by imposing the solutions to satisfy the given boundary conditions, but this requires, at the best, solving a highly nonlinear system for which an explicit parameters expression looks unlikely. Hence, a numerical approach seems to be a reasonable strategy. Our numerical treatment will be developed in next section and it is based on the gradient descent method. For more details, see Appendix B.

### 2.2.3 Minimizing Length

As explained in Section 2.2.1, the problem of minimizing the functional (2.11) acting on the space of plane curves joining two given points of  $\mathbb{R}^2$  with prescribed initial and final angles is equivalent to that of finding  $\mathcal{D}$ -curves minimizing the sub-Riemannian length. Even better adapted to the curve completion demands is the variational problem associated to the functional  $\Theta_a$ , (2.12), which has been discussed in Section 2.2.2. Thus, once we translate it to the language of the unit tangent bundle, we are led to the following variational problem.

Denote by  $\mathfrak{X}$  the space of curves

$$\beta: [a, b] \longrightarrow \mathbb{R}^2 \times \mathbb{S}^1; \quad \beta(t) = (x(t), y(t), \theta(t)),$$

joining two given points  $(x_a, y_a, \theta_a)$  and  $(x_b, y_b, \theta_b)$  of  $\mathbb{R}^2 \times \mathbb{S}^1$ , that is

$$(x(a), y(a), \theta(a)) = (x_a, y_a, \theta_a), \quad (x(b), y(b), \theta(b)) = (x_b, y_b, \theta_b),$$

and satisfying the following admissibility condition

$$y'(t) = x'(t) \tan \theta(t), \quad t \in [a, b],$$

where  $'$  denotes derivative with respect to the curve parameter  $t \in [a, b]$ , hereafter. On  $\mathfrak{X}$  we consider the functional  $\mathcal{L}$  defined by

$$\mathcal{L}(\beta) = \int_a^b \sqrt{(x')^2 + (y')^2 + h^2 (\theta')^2} dt, \quad (2.24)$$

where  $h \in \mathbb{R}$  is a proportionality constant introduced by accuracy of the physical model [26]. Then, our problem is to find the minimizers or, more generally, extremals of  $\mathcal{L} : \mathfrak{X} \rightarrow \mathbb{R}$ .

We first translate the problem to our settings. The sub-Riemannian metric defined on  $\mathbb{R}^2 \times \mathbb{S}^1$  in Section 2.2.1 is extended to the whole space by considering the vector field

$$X_3 = -\sin \theta \frac{\partial}{\partial x} + \cos \theta \frac{\partial}{\partial y},$$

and declaring orthonormal the family  $\{X_1, X_2, X_3\}$ , where  $X_1, X_2$  are given in (2.10). It is easy to check that the induced metric is nothing but the standard product metric in  $\mathbb{R}^2 \times \mathbb{S}^1$ .

Now, consider the exponential map

$$\exp : \mathbb{R} \rightarrow \mathbb{S}^1; \quad \exp(t) = (\cos t, \sin t).$$

Then  $\pi := Id \times \exp : \mathbb{R}^3 \rightarrow \mathbb{R}^2 \times \mathbb{S}^1$ ,  $\pi(x, y, z) = (x, y, \exp z)$  is a Riemannian covering map with respect to the product metrics in both spaces and, in particular, it is a local

isometry. For any  $\beta \in \mathfrak{X}$  choose a point  $(x_a, y_a, \tilde{\theta}_a) \in \mathbb{R}^3$  such that  $\pi((x_a, y_a, \tilde{\theta}_a)) = (x_a, y_a, \theta_a)$  and take the unique lifting  $\tilde{\beta}: [a, b] \rightarrow \mathbb{R}^3$  of  $\beta$  to  $\mathbb{R}^3$  with  $\tilde{\beta}(a) = (x_a, y_a, \tilde{\theta}_a)$ . Define  $(x_b, y_b, \tilde{\theta}_b) = \tilde{\beta}(b)$ . Then any variation of  $\beta$  within  $\mathfrak{X}$  can be uniquely lifted to a variation of  $\tilde{\beta}$  with endpoints  $(x_a, y_a, \tilde{\theta}_a)$  and  $(x_b, y_b, \tilde{\theta}_b)$  satisfying the constraint  $y'(t) = x'(t) \tan \tilde{\theta}(t)$ ,  $t \in [a, b]$ .

Thus, on the space of curves  $\tilde{\mathfrak{X}}$

$$\tilde{\beta}: [a, b] \rightarrow \mathbb{R}^3; \quad \tilde{\beta}(t) = (x(t), y(t), \tilde{\theta}(t)),$$

joining the two points  $(x_a, y_a, \tilde{\theta}_a), (x_b, y_b, \tilde{\theta}_b)$  of  $\mathbb{R}^3$ ,

$$(x(a), y(a), \tilde{\theta}(a)) = (x_a, y_a, \tilde{\theta}_a), \quad (x(b), y(b), \tilde{\theta}(b)) = (x_b, y_b, \tilde{\theta}_b),$$

and satisfying the admissibility condition

$$y'(t) = x'(t) \tan \tilde{\theta}(t), \quad t \in [a, b],$$

we can define the functional

$$\tilde{\mathcal{L}}(\tilde{\beta}) = \int_a^b \sqrt{(x')^2 + (y')^2 + h^2 (\tilde{\theta}')^2} dt.$$

Then,  $\tilde{\mathcal{L}}(\tilde{\beta}) = \mathcal{L}(\beta)$ , and, therefore  $\beta$  is critical for  $\mathcal{L}$ , if and only if,  $\tilde{\beta}$  is critical for  $\tilde{\mathcal{L}}$ . Observe also that regular curves in  $\mathbb{R}^2 \times \mathbb{S}^1$  are lifted to regular curves in  $\mathbb{R}^3$  with the same curvature and torsion and that they have the same projection,  $\alpha(t) = (x(t), y(t))$ , on  $\mathbb{R}^2$ .

Therefore, the original problem boils down to study extremals for  $\tilde{\mathcal{L}}$  in  $\tilde{\mathfrak{X}}$  and we are in position to apply our algorithm based on the gradient descent model to locate minima (see Appendix B) with  $m = 3$ ,  $n = 1$ ,  $A = B = 0$  to the functional  $\tilde{\mathcal{L}}$  acting on  $\tilde{\mathfrak{X}}$  (however, by abuse of notation we are going to denote both, the functional and the space of curves, without the tilde  $\sim$ ). Moreover, for computational simplicity, it is better to work with plane curves  $\alpha(t) = (v(t), \theta(t))$  which are parametrized by using its speed  $v(t)$ , and the angle that its tangent makes with the  $x$ -axis direction,  $\theta(t)$ . Hence, our energy functional becomes

$$\mathcal{L}(\beta) = \int_a^b \sqrt{v^2(t) + h^2 (\theta')^2} dt,$$

and will be considered acting on the space  $\hat{\mathfrak{X}}$  formed by curves (we are abusing again of the notation by using the same letter  $\beta$  as before)

$$\beta: [a, b] \rightarrow \mathbb{R}^2; \quad \beta(t) = (v(t), \theta(t)),$$

satisfying the affine conditions

$$\theta(a) = \theta_a, \quad \theta(b) = \theta_b,$$

along with the following isoperimetric conditions

$$x_b - x_a = \int_a^b v \cos \theta dt, \quad y_b - y_a = \int_a^b v \sin \theta dt.$$

Observe that the relations

$$x'(t) = v(t) \cos \theta(t), \quad y'(t) = v(t) \sin \theta(t),$$

enable us to recover the original minimizing curve  $\beta$ . Finally, the choice of our metric will be

$$\langle \beta(t), \bar{\beta}(t) \rangle = \langle \beta(a), \bar{\beta}(a) \rangle + \int_a^b \langle \beta'(t), \bar{\beta}'(t) \rangle dt,$$

for curves  $\beta, \bar{\beta} \in \widehat{\mathfrak{X}}$ .

In order to make the XEL-platform [9] work on the functional  $\mathcal{L} : \widehat{\mathfrak{X}} \rightarrow \mathbb{R}$  just defined, we can take, without loss of generality, our curves defined in the unit interval, that is,  $a = 0, b = 1$ , and assume also that the ends of the curves are chosen to be

$$p_0 = (0, 0, \theta_0), \quad p_1 = (1, 0, \theta_1), \quad \theta_0, \theta_1 \in \mathbb{R}.$$

As an strategy to speed up the convergence of the algorithm we will restrict our analysis to curves  $\beta$  satisfying additionally  $\theta(t) = \theta_0 + t(\theta_1 - \theta_0)$ ,  $t \in [0, 1]$ . Notice that this is a quite reasonable assumption in image reconstruction, since we do not expect our image filling curves to have loops, and its inclusion does not alter the conclusions. Rewriting our functional in this context we have

$$\mathcal{L}(\beta) = \int_0^1 \sqrt{v^2(t) + h^2(\theta_1 - \theta_0)^2} dt,$$

with

$$\begin{aligned} \theta(0) &= \theta_0, & \theta(1) &= \theta_1, \\ x_1 - x_0 &= \int_0^1 v \cos \theta dt, & y_1 - y_0 &= \int_0^1 v \sin \theta dt, \\ x'(t) &= v(t) \cos \theta(t), & y'(t) &= v(t) \sin \theta(t). \end{aligned}$$

To start with the gradient descent process we need to choose an initial curve  $\alpha_o$  in the space of functions defined just above. For  $a = 0, b = 1$ , we determine  $\alpha_o$  by selecting functions

$$\theta(t) = (\theta_1 - \theta_0)t + \theta_0, \quad v(t) = \lambda + \nu t, \tag{2.25}$$

where the parameters  $\lambda$  and  $\eta$  are obtained by using the isoperimetric constraints, that is

$$1 = \int_0^1 v(t) \cos \theta(t) dt, \quad 0 = \int_0^1 v(t) \sin \theta(t) dt.$$

In other words, denoting by  $\Delta\theta = \theta_1 - \theta_0$ , we have

$$1 = \frac{\lambda}{\Delta\theta} (\sin(\theta(t)))_0^1 + \nu \left( \frac{t}{\Delta\theta} \sin(\theta(t)) + \frac{\cos \theta(t)}{(\Delta\theta)^2} \right),$$

and

$$0 = \frac{\lambda}{\Delta\theta} (-\cos(\theta(t)))_0^1 + \nu \left( -\frac{t}{\Delta\theta} \cos(\theta(t)) + \frac{\sin \theta(t)}{(\Delta\theta)^2} \right).$$

This gives a linear system  $\mathbf{A} \begin{pmatrix} \lambda \\ \nu \end{pmatrix} = \begin{pmatrix} 1 \\ 0 \end{pmatrix}$ , with associated matrix

$$\mathbf{A} = \begin{pmatrix} \frac{\sin \theta_1 - \sin \theta_0}{\Delta\theta} & \frac{\sin \theta_1}{\Delta\theta} + \frac{\cos \theta_1 - \cos \theta_0}{(\Delta\theta)^2} \\ \frac{\cos \theta_0 - \cos \theta_1}{\Delta\theta} & \frac{\sin \theta_1 - \sin \theta_0}{(\Delta\theta)^2} - \frac{\cos \theta_1}{\Delta\theta} \end{pmatrix}$$

whose solutions are

$$\lambda = \frac{1}{\det(\mathbf{A})} \left\{ \frac{\sin \theta_1 - \sin \theta_0}{(\Delta\theta)^2} - \frac{\cos \theta_1}{\Delta\theta} \right\}, \quad \nu = \frac{1}{\det(\mathbf{A})} \left\{ \frac{\cos \theta_1 - \cos \theta_0}{\Delta\theta} \right\}.$$

Now, substitution of these values in (2.25) gives us the curve  $\alpha_o$  to start with the method. Of course, this can be done for any choice of initial conditions  $\theta_0, \theta_1$ .

Figure 2.1 shows a family of minimizers which have been obtained via the XEL-platform for different choices of end angles  $\theta_0, \theta_1$  detailed in Table 2.1. The minimizer painted in blue in Figure 2.1 corresponds with the first row of Table 2.1. The initial and final data of the minimizer in red is described in the second row, and, finally, the green and brown curves correspond with the third and fourth rows of the Table 2.1, respectively.

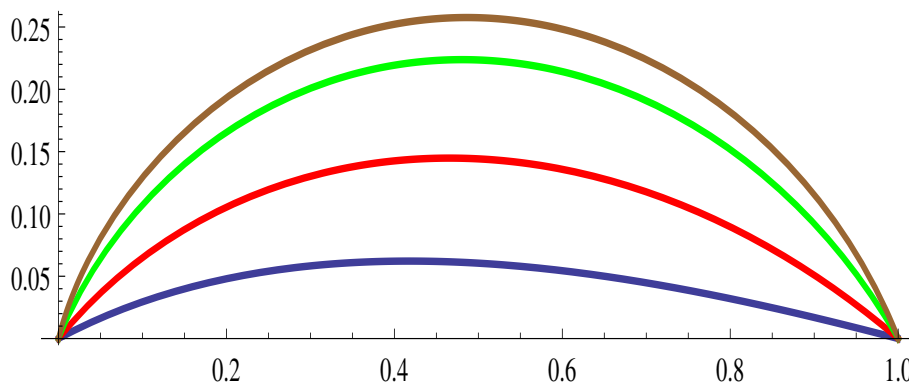


Figure 2.1: Some projections of minimizers of (2.24) obtained via XEL.

One may wish to compare extremals obtained by our method with those got in [26], where the authors used a different numerical approach. For example, Table 2.1 also shows the length of extremal curves obtained with both methods for identical initial data. Thus, although both numerical approaches are conceptually very different, it is remarkable that the results obtained by each method are very close concerning both shape and length of the extremals.

However, the numerical procedure, XEL, briefly described in Appendix B (for more details one can see [9]), is based mainly on numerical integration and it is free of numerical derivations. This fact is very important when numerical algorithms are developed because it is well-known that integration is more forgiving than differentiation.

Table 2.1: Some values of four minimizers of (2.24) in  $\mathbb{R}^2 \times \mathbb{S}^1$ .

$\theta_0$	$\theta_1$	[26]	XEL	$\text{dev}(\mathcal{L})$	$\text{err}(\mathcal{G})$
$20^\circ$	$-10^\circ$	1.1687	1.16917677	$4 \times 10^{-7}$	$2 \times 10^{-8}$
$40^\circ$	$-30^\circ$	1.6287	1.62896057	$7 \times 10^{-8}$	$2 \times 10^{-8}$
$60^\circ$	$-50^\circ$	2.2435	2.24363232	$8 \times 10^{-7}$	$3 \times 10^{-9}$
$70^\circ$	$-60^\circ$	2.5758	2.57613001	$2 \times 10^{-9}$	$2 \times 10^{-8}$

Our model deals with two different types of boundary conditions, affine and isoperimetric conditions. The former ones do not accumulate errors during the process, while for the latter ones, the design of the numerical procedure looks for the minimization of the possible error that can be accumulated during the implementation. Furthermore, as it is deeply explained in [9], this way of constructing the solution via numerical integrations gives rise to a way of measuring the deviation between numerical and real solutions. In other words, once that boundary conditions are satisfied, it is possible to measure how far the numerical solution, obtained with this method, is from satisfying the differential

equation. Notice that this remark represents a huge advantage in comparison with other numerical methods used for image reconstruction.

For instance, for the variational problem we are studying along this section, (2.24), let's consider the differential equation (2.13) with  $\tau = 0$  written in terms of a general parameter  $t \in [0, 1]$ , that is,

$$\frac{1}{v(t)} \frac{d}{dt} \left( \frac{1}{v(t)} \frac{d}{dt} \left( \frac{\kappa(t)}{\sqrt{\kappa^2(t) + a^2}} \right) \right) - \frac{a^2 \kappa(t)}{\sqrt{\kappa^2(t) + a^2}} = 0,$$

where  $v(t) = \frac{ds}{dt}$  is the velocity of the curve. Then, manipulating it, we formally obtain a first integral

$$\frac{d}{dt} \left( \frac{\kappa(t)}{\sqrt{\kappa^2(t) + a^2}} \right) - a^2 v(t) \int_o^t \frac{\kappa(u) v(u)}{\sqrt{\kappa^2(u) + a^2}} du = c v(t),$$

for any constant of integration  $c \in \mathbb{R}$ . Moreover, it is also possible to obtain formally a second integral, that is

$$\left( \frac{\kappa(u)}{\sqrt{\kappa^2(u) + a^2}} \right)_o^t - a^2 \int_o^t \left( \int_o^w \frac{\kappa(u) v(u)}{\sqrt{\kappa^2(u) + a^2}} du \right) v(w) dw = c \int_o^t v(u) du. \quad (2.26)$$

Observe that in the experiments of Table 2.1 we have chosen  $a = 1$ , for simplicity.

Now, as explained above, the XEL-platform gives both tabulated functions and their corresponding integrals, that is, everything we need to substitute in (2.26). As a consequence, we can also measure the deviation. For this purpose, let's define the *point-wise deviation* by

$$\Psi(t) = \left( \frac{\kappa(u)}{\sqrt{\kappa^2(u) + a^2}} \right)_o^t - a^2 \int_o^t \left( \int_o^w \frac{\kappa(u) v(u)}{\sqrt{\kappa^2(u) + a^2}} du \right) v(w) dw - c \int_o^t v(u) du.$$

Then, the *deviation* between the theoretical solution and the approximate one will be considered to be the  $L^2$  norm of the function  $\Psi(t)$ , that is

$$\text{dev}(\mathcal{L}) = \left( \int_o^1 \Psi^2(t) dt \right)^{\frac{1}{2}}.$$

Take into account that the theoretical solution verifies  $\Psi(t) = 0$ , and, therefore,  $\text{dev}(\mathcal{L}) = 0$ . We collect the deviations of the solutions given by XEL in the column  $\text{dev}(\mathcal{L})$  of Table 2.1. On the other hand, in the column  $\text{err}(\mathcal{G})$  we compute the accumulated error for each case, due to the isoperimetric boundary conditions. In conclusion, it can be checked that both columns have really small values, which makes our method quite accurate.



In Figures 2.2 and 2.3, we plot some examples of curve completion via minimum length in the unit tangent bundle of the plane. In Figure 2.2, we have two *modal* completions (their completed boundary curves give illusory and subjective objects) and in Figure 2.3 one *amodal* completion (the object is fragmented due to occlusion) is represented.

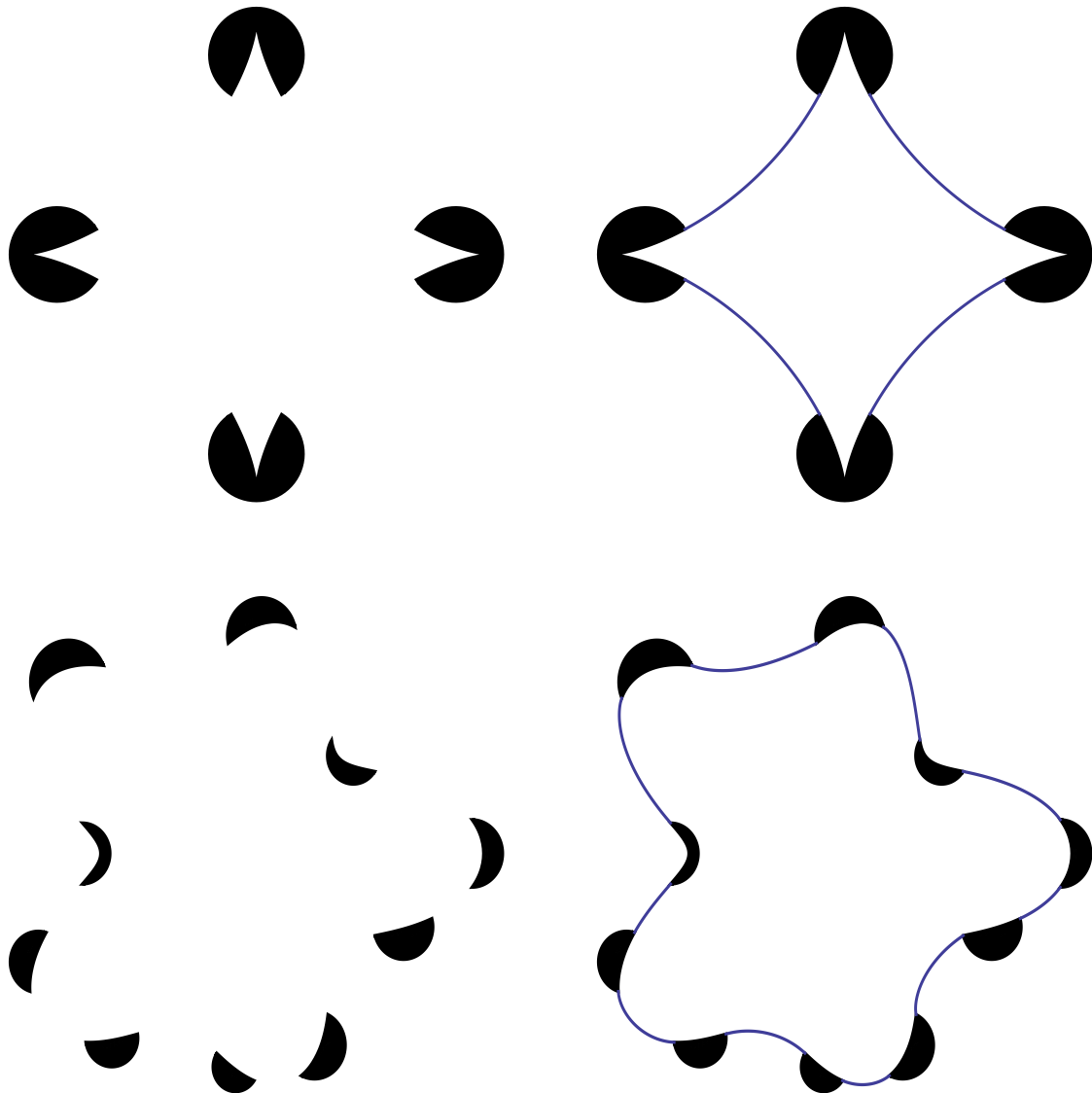


Figure 2.2: Two modal completions.

Finally, notice that another advantage of our XEL-platform is that it is easily adaptable to a huge family of functionals satisfying the required conditions. For instance, it has been pointed out in [26] (and also suggested in [112]) that investigation of extremals

for the elastic energy in the unit normal bundle might be important for examining combinations of image plane properties. See [13] for some results obtained considering the elastic energy (and others) using this XEL-platform.

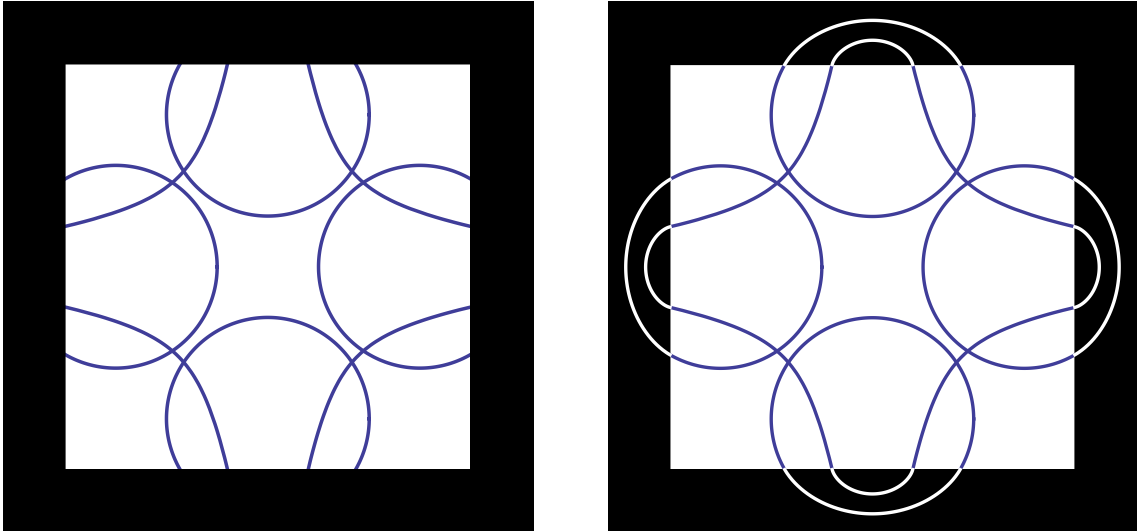


Figure 2.3: One amodal completion.

## Chapter 3

# Binormal Evolution Surfaces in 3-Space Forms

A large class of physical systems are modeled in terms of motion of curves and surfaces in the Euclidean 3-space,  $\mathbb{R}^3$ . A remarkable example is the so called *localized induction equation*

$$x_t = x_s \times x_{ss}, \quad (3.1)$$

which is a soliton equation used to model the dynamics of a thin vortex filament in an incompressible, inviscid, homogeneous, 3-dimensional fluid, [49], [130] and [132]. Locally, this motion determines an immersed surface in  $\mathbb{R}^3$ . On the other hand, by choosing a geodesic coordinate system in an isometrically immersed surface  $(U, x)$  of  $\mathbb{R}^3$ , one can check that the following equation is satisfied on  $U$

$$x_t = \zeta x_s \times x_{ss},$$

where  $\zeta$  is a function which depends on the surface metric coefficients with respect to  $(U, x)$ . If  $\zeta = 1$ , we recover the localized induction equation, (3.1), and as we will see later, Gauss-Codazzi equations, (1.5) and (1.6), boil down to Da Rios equations found in 1906, [130].

Quite often, by resorting to the underlying geometry one can gain considerable insight into the dynamics of physical systems, [89] and [132]. In the first part of this chapter, we use a geometrical approach to investigate an extension of (3.1) obtained by considering a smooth map  $x : U \subset \mathbb{R}^2 \rightarrow M_r^3(\rho)$ ,  $x(s, t)$  (recall that  $M_r^3(\rho)$  is isometrically immersed in  $\mathbb{E}_0^4$ ), verifying

$$x_t = \zeta \left( |\tilde{\nabla}_{x_s} x_s|, \frac{\det(x_s, \tilde{\nabla}_{x_s} x_s, \tilde{\nabla}_{x_s}^2 x_s)}{|\tilde{\nabla}_{x_s} x_s|^2} \right) x_s \times \tilde{\nabla}_{x_s} x_s, \quad (3.2)$$

where  $\zeta$  is a suitable smooth function and  $\tilde{\nabla}$  is the Levi-Civita connection on  $M_r^3(\rho)$ .

Under mild conditions we will see that a curve motion following (3.2) describes a curve  $\gamma$  evolving under the binormal flow, with velocity depending on the curvature and torsion of  $\gamma$ , and determines an immersed surface,  $x(U)$ , in  $M_r^3(\rho)$ . Then, fundamental results of the Theory of Submanifolds can be applied and it will be seen that solving geometrically (3.2) amounts to solve the Gauss-Codazzi equations (1.5) and (1.6), since that would give us the curvature and torsion of a geodesic foliation of  $x(U)$ . Alternatively, one can determine the evolution by finding a single solution, working as initial condition  $x(s, 0) = \gamma(s)$ , and then giving a geometrical description of the binormal flow.

In the second part of this chapter, we focus on traveling wave solutions of the Gauss-Codazzi equations and we will show that the initial condition for this type of solutions is a generalized Kirchhoff centerline. In particular, we study curves evolving by (3.2) with constant torsion and use the Gauss-Codazzi equations to construct solutions by means of extremal curves for curvature dependent energies and associated one-parameter groups of isometries.

Finally, in the last part, we are going to apply our findings to some special families of surfaces of 3-space forms.

### 3.1 Binormal Motion of Curves

Let's consider a smooth map  $x : U \subset \mathbb{R}^2 \rightarrow M_r^3(\rho)$ ,  $x(s, t)$ , satisfying (3.2) and let's assume that the *initial condition*  $\gamma(s) := x(0, s)$  is a unit speed Frenet curve of rank 2 or 3, then  $\gamma^t(s) := x(s, t)$ , which will be called *the filament at time t*, is also unit speed parametrized  $\forall t$ . In fact, we have  $\frac{\partial}{\partial t} \langle x_s(s, t), x_s(s, t) \rangle = 2 \langle \tilde{\nabla}_{x_s} x_t, x_s \rangle = 0$ , where the last equality is obtained from (3.2). So, since  $\langle x_s(s, 0), x_s(s, 0) \rangle = \langle \frac{d\gamma}{ds}, \frac{d\gamma}{ds} \rangle = \langle T, T \rangle = \varepsilon_1$ , then so is  $\forall t$ , that is, (3.2) is a length-preserving evolution. Assuming also that  $\tilde{\nabla}_{x_s} x_s(s, t)$  is non-null everywhere, the associated Frenet frame,  $\{x_s = T(s, t), N(s, t), B(s, t)\}$ , will be defined for all  $\gamma^t$  and combining (3.2) and (1.10)-(1.12) we obtain

$$\begin{aligned} x_t &= \zeta(\kappa, \tau) x_s \times \tilde{\nabla}_{x_s} x_s = \zeta(\kappa, \tau) T \times \tilde{\nabla}_T T = \\ &= \varepsilon_2 \kappa \zeta(\kappa, \tau) T \times N = \varepsilon_2 \varepsilon_3 \kappa \zeta(\kappa, \tau) B = \mathcal{F}(\kappa, \tau) B. \end{aligned} \quad (3.3)$$

This means that  $\gamma(s)$  evolves by the binormal flow with *velocity*  $\mathcal{F}(\kappa, \tau)$ . We are going to suppose also that  $\zeta$  is never zero so that  $(U, x)$  defines an immersed surface in  $M_r^3(\rho)$  swept out by  $\gamma(s)$ . It will be called a *binormal evolution surface with initial condition  $\gamma$  and velocity  $\mathcal{F}$* . In conclusion, a surface  $x : U \rightarrow M_r^3(\rho)$ ,  $x(s, t)$ , immersed in any Riemannian or Lorentzian 3-space form is a binormal evolution surface with velocity  $\mathcal{F}(\kappa, \tau)$  if the following conditions are verified;

- (i) The initial condition  $\gamma(s) = x(s, 0)$  is an arc-length parametrized Frenet curve of rank 2 or 3,

(ii) All the filaments  $\gamma^t(s) = x(s, t)$  are Frenet curves, and

(iii) Equation  $x_t = \mathcal{F}(\kappa, \tau) B$ , (3.3), is verified.

The curves  $\delta_s(t) := x(s, t)$ , perpendicular to the filaments, are called *fibers* of  $(U, x)$ . The time variation of the Frenet frames is described in the following Proposition (compare with (3.15) of [132] for surfaces in  $\mathbb{R}^3$ )

**Proposition 3.1.1.** ([10]) *Let  $(U, x)$  be a binormal evolution surface of  $M_r^3(\rho)$  with velocity  $\mathcal{F}$ . Then,*

$$\tilde{\nabla}_{\frac{\partial}{\partial s}} \begin{pmatrix} T \\ N \\ B \end{pmatrix} (s, t) = \begin{pmatrix} 0 & \kappa & 0 \\ -\kappa & 0 & \tau \\ 0 & -\tau & 0 \end{pmatrix} \begin{pmatrix} \varepsilon_1 T \\ \varepsilon_2 N \\ \varepsilon_3 B \end{pmatrix} (s, t), \quad (3.4)$$

$$\tilde{\nabla}_{\frac{\partial}{\partial t}} \begin{pmatrix} T \\ N \\ B \end{pmatrix} (s, t) = \begin{pmatrix} 0 & -\tau \mathcal{F} & \varepsilon_3 \mathcal{F}_s \\ \tau \mathcal{F} & 0 & \varepsilon_2 h_{22} \mathcal{F} \\ -\varepsilon_3 \mathcal{F}_s & -\varepsilon_2 h_{22} \mathcal{F} & 0 \end{pmatrix} \begin{pmatrix} \varepsilon_1 T \\ \varepsilon_2 N \\ \varepsilon_3 B \end{pmatrix} (s, t), \quad (3.5)$$

where  $h_{22} = \frac{1}{\kappa} \{ \varepsilon_3 \frac{\mathcal{F}_{ss}}{\mathcal{F}} - \varepsilon_2 \tau^2 + \varepsilon_1 \varepsilon_3 \rho \}$ , and  $\kappa(s, t)$  and  $\tau(s, t)$  denote the curvature and torsion of the curves  $\gamma^t(s)$ .

*Proof.* It is clear from (3.3) and (3.4) that the filaments  $\gamma^t(s)$  are geodesics of  $(U, x)$  and, then,  $(U, x)$  defines a geodesic coordinate system (see Section 1.2.2). Thus, it must verify the PDE system (1.29)-(1.31). This system can be expressed equivalently in terms of the time variation of the Frenet frame. In fact, from the Gauss formula (1.14) and (1.29), we have

$$\tilde{\nabla}_{\frac{\partial}{\partial t}} T = -\varepsilon_2 \mathcal{F} \tau N + \mathcal{F}_s B. \quad (3.6)$$

So, differentiating  $x_t = \mathcal{F} B$  and using once more Gauss and Weingarten formulas, (1.14) and (1.15), we have

$$x_{tt} = \mathcal{F}_t B + \mathcal{F} \left( \tilde{\nabla}_{\frac{\partial}{\partial t}} B - \varepsilon_3 \rho \mathcal{F} x \right),$$

which combined with (1.31) gives

$$\tilde{\nabla}_{\frac{\partial}{\partial t}} B = -\varepsilon_1 \varepsilon_3 \mathcal{F}_s T - h_{22} \mathcal{F} N. \quad (3.7)$$

Finally, from (3.6), (3.7) and the cross product relations (see Section 1.2.1), one obtains

$$\tilde{\nabla}_{\frac{\partial}{\partial t}} N = \varepsilon_1 \tau \mathcal{F} T + \varepsilon_2 \varepsilon_3 h_{22} \mathcal{F} B,$$

which ends the proof.  $\square$

Now, combining (1.16) and Gauss and Codazzi equations, (1.5) and (1.6), with (1.23)-(1.26), we obtain after a long computation

$$\frac{\mathcal{F}_{ss}}{\mathcal{F}} = \varepsilon_3 \kappa h_{22} + \varepsilon_2 \varepsilon_3 \tau^2 - \varepsilon_1 \rho, \quad (3.8)$$

$$\kappa_t = -2\mathcal{F}_s \tau - \tau_s \mathcal{F}, \quad (3.9)$$

$$\tau_t = \varepsilon_1 \varepsilon_3 \kappa \mathcal{F}_s + \varepsilon_2 (h_{22} \mathcal{F})_s. \quad (3.10)$$

From the Gauss equation (3.8) we have (1.28)

$$h_{22} = \frac{1}{\kappa} \left( \varepsilon_2 \frac{\mathcal{F}_{ss}}{\mathcal{F}} - \varepsilon_2 \tau^2 + \varepsilon_1 \varepsilon_3 \rho \right).$$

By substitution of (1.28) in (3.10) we get that the Codazzi equations, (3.9) and (3.10), for  $(U, x)$  boil down to

$$\kappa_t = -2\mathcal{F}_s \tau - \tau_s \mathcal{F}, \quad (3.11)$$

$$\tau_t = \varepsilon_1 \varepsilon_3 \kappa \mathcal{F}_s + \varepsilon_2 \left( \frac{\mathcal{F}}{\kappa} \left( \varepsilon_3 \frac{\mathcal{F}_{ss}}{\mathcal{F}} - \varepsilon_2 \tau^2 + \varepsilon_1 \varepsilon_3 \rho \right) \right)_s. \quad (3.12)$$

Observe that, if  $\mathcal{F} = \kappa$ , (3.11) and (3.12) are precisely Da Rios equations for the vortex filament, [130]. So Da Rios equations can be seen as the Gauss-Codazzi equations of a binormal evolution surface with velocity  $\kappa$ .

Notice that (3.11) and (3.12) are the compatibility conditions of the PDE system (1.29)-(1.31). Thus, from the Fundamental Theorem of Submanifolds (see §2.7 of [39]), given functions  $\kappa(s, t)$ ,  $\tau(s, t)$  and  $\mathcal{F}(s, t)$ , smoothly defined on a connected domain  $U$  and satisfying (3.11) and (3.12), there exists a solution of (1.29)-(1.31) (and, consequently, of (3.4) and (3.5)) determining a smooth isometric immersion  $(U, x)$  (unique up to rigid motions, if  $U$  is simply connected) of a surface in  $M_r^3(\rho)$  whose metric and the second fundamental form are given, respectively, by  $g = \varepsilon_1 ds^2 + \varepsilon_3 \mathcal{F}^2 dt^2$  and  $\varepsilon_2 h = -\kappa ds^2 + 2\tau \mathcal{F} ds dt + \varepsilon_2 \mathcal{F}^2 h_{22} dt^2$ , (1.22) and (1.27), where  $h_{22}$  is obtained from (1.28).

Moreover, computing the Christoffel symbols from the metric coefficients for such an immersion,  $(U, x)$ , we see that  $\gamma^t(s)$  are arc-length parametrized geodesics  $\forall t$ . Then, a combination of the Gauss formula (1.14) and equations (1.10)-(1.12) for the Frenet frame along the coordinate curves  $\gamma^t(s)$ ,  $\{x_s = T(s, t), N(s, t), B(s, t)\}$ , shows that the unit Frenet normals  $N(s, t)$  are perpendicular to the surface  $(U, x)$ . Hence,  $x_t = \lambda(s, t)B(s, t)$ , but then the second coefficient of  $g$  (1.22) implies that  $\mathcal{F}(s, t) = \lambda(s, t)$  and  $(U, x)$  is a solution of (3.3). Since  $(U, x)$  is foliated by geodesics  $\gamma^t(s)$  having  $\kappa^t(s) := \kappa(s, t)$  and  $\tau^t(s) := \tau(s, t)$  as curvature and torsion, respectively, the immersion itself,  $x$ , is geometrically determined by  $\kappa^t(s) := \kappa(s, t)$  and  $\tau^t(s) := \tau(s, t)$ , because, from the Fundamental Theorem of Curves, for any fixed  $t$ , there exists a unique curve  $\gamma^t(s)$  (up to congruences and causal character of the Frenet frame) having  $\kappa^t(s)$  and  $\tau^t(s)$  as curvature and torsion.

Then, an smooth assembling of these curves  $\gamma^t(s)$ ,  $t \in \bar{I}$  would give  $x$ . So, geometrically solving (3.3) amounts to solve the system (3.11) and (3.12).

From now on, it will be convenient to choose a smooth function  $P(\kappa, \tau)$  so that,  $\dot{P}(\kappa, \tau) := \frac{\partial P}{\partial \kappa}(\kappa, \tau) = \mathcal{F}(\kappa, \tau)$ .

### 3.1.1 Hasimoto Transformation and the Complex Wave Function

To end up this section, we rewrite the Gauss-Codazzi equations (3.11) and (3.12) in terms of the *complex wave function*. The *Hasimoto transformation* [73] maps any curve  $\gamma(s)$  with positive curvature  $\kappa > 0$  and torsion  $\tau$  into its complex wave function  $\Psi$  defined by

$$\Psi(s, t) = \kappa(s, t) \exp \left( i \int_{s_0}^s \tau(s^*, t) ds^* \right). \quad (3.13)$$

Moreover, the curve can be recovered (up to congruences in  $M_r^3(\rho)$ ) from its complex wave function  $\Psi$ , in terms of its curvature and torsion, by taking

$$\kappa = \langle \Psi, \Psi \rangle^{\frac{1}{2}}, \quad \tau = \text{Im} \left( \frac{\Psi_s}{\Psi} \right). \quad (3.14)$$

Using this transformation and a choice of a suitable  $s_0$  (such that,  $\int \tau_t ds^*|_{s_0} = 0$ ), we can see that the Gauss-Codazzi equations (3.11) and (3.12) are equivalent to

$$\dot{P}_{ss}(1 - \varepsilon_2 \varepsilon_3) \frac{\Psi}{|\Psi|} = i \Psi_t + \left( \dot{P} \frac{\Psi}{|\Psi|} \right)_{ss} + \varepsilon_1 \varepsilon_3 \left( \frac{\dot{P}}{|\Psi|} (|\Psi|^2 + \varepsilon_3 \rho) - P \right) \Psi. \quad (3.15)$$

Thus, we have that each solution of (3.15) gives rise to two functions defined in (3.14), such that a smooth assembly of the only curves having them as curvature and torsion (up to rigid motions in  $M_r^3(\rho)$ ) give a foliation of a binormal evolution surface with velocity  $\dot{P}$ , (3.3). The converse is clear, so we have

**Proposition 3.1.2.** ([64]) *Let  $\gamma(s)$  be a unit speed Frenet curve of rank 2 or 3. Then,  $\gamma(s)$  is the initial condition of a evolution under (3.3), if and only if, the complex wave function  $\Psi$ , (3.13), evolves by (3.15).*

### 3.1.2 Traveling Wave Solutions and Curvature Energies

As mentioned in Section 3.1, geometrically solving the binormal flow (3.3) is equivalent to solve the Gauss-Codazzi equations given by the system (3.11) and (3.12). Thus, along this section we are going to analyze traveling wave solutions of the Gauss-Codazzi equations (3.11) and (3.12) associated to a binormal evolution surface with respect to the parametrization  $x(s, t) = \gamma^t(s)$ , (1.20).

Here, *traveling wave* is understood to be a function  $u(s, t)$  of the form  $u(s, t) = \psi(s - \varpi t)$ ,  $\varpi \in \mathbb{R}$  for some smooth function  $\psi$ . Let's define  $\iota = s - \varepsilon_1 \varepsilon_3 \mu t$  for some real constant  $\mu$ , and take  $\kappa(s, t) = \kappa(\iota)$  and  $\tau(s, t) = \tau(\iota)$ . Differentiating the Gauss-Codazzi equations (3.11) and (3.12) we get

$$\dot{P}\tau_\iota + 2\dot{P}_\iota\tau - \varepsilon_1 \varepsilon_3 \mu \kappa_\iota = 0, \quad (3.16)$$

$$\dot{P}_\iota + \varepsilon_1 \varepsilon_2 \dot{P}(\kappa^2 - \varepsilon_1 \varepsilon_3 \tau^2 + \varepsilon_2 \rho) - \varepsilon_1 \varepsilon_2 \kappa(P - \mu\tau + \varepsilon_1 \varepsilon_3 c) = 0, \quad (3.17)$$

for some  $c \in \mathbb{R}$ . Then, calling  $\lambda = \varepsilon_1 \varepsilon_3 c$ , it is easy to verify that (3.16) and (3.17) are precisely the Euler-Lagrange equations, (1.62) and (1.63), for  $\Theta(\gamma) = \int_\gamma (P(\kappa) + \mu\tau + \lambda)$ . In other words, *a solution  $(\kappa, \tau)$  of (3.16) and (3.17) determines a curve  $\gamma$  that must be a generalized Kirchhoff centerline*. Hence, the next theorem shows how to construct solutions of binormal evolution surfaces in  $M_r^3(\rho)$

**Theorem 3.1.3.** ([64]) *Traveling wave solutions of Gauss-Codazzi equations (3.11) and (3.12) correspond to the curvature and torsion of generalized Kirchhoff centerlines. Moreover, generalized Kirchhoff centerlines evolve following (3.3) by isometries of  $M_r^3(\rho)$  and slippage.*

*Proof.* The first part has just been stated. As for the second one, consider  $\gamma(s)$  a generalized Kirchhoff centerline. Then, by Proposition 1.3.3,  $\mathcal{I} = \varepsilon_1 \varepsilon_3 \mu T + \dot{P}B$  is a Killing vector field along  $\gamma$ . Denote by  $\xi$  the Killing vector field on  $M_r^3(\rho)$  which extends  $\mathcal{I}$  (as explained in Section 1.3.1) and denote by  $\{\phi_t, t \in \mathbb{R}\}$ , the one-parameter group of isometries associated to  $\xi$ , that is, the flow of  $\xi$ . Define the surface  $y(s, t) := \phi_t(\gamma(s))$ . Since  $\{\phi_t, t \in \mathbb{R}\}$  are isometries, we have  $y_t = \varepsilon_1 \varepsilon_3 \mu T + \dot{P}B$  and we see that, after reparametrizations,  $y(s, t)$  evolves by (3.3).  $\square$

Therefore, traveling wave solutions of the Gauss-Codazzi equations represent binormal evolution surfaces  $(U, x)$ , where the initial condition  $\gamma$  is a generalized Kirchhoff centerline. In this case  $\gamma$  evolves by rigid motions and slippage.

On the other hand, among traveling wave solutions there is a special case where initial filaments evolve by congruences. These solutions correspond to traveling wave solutions with  $\mu = 0$  and it is a straightforward computation to verify that the Gauss-Codazzi equations (3.11) and (3.12) are equivalent to the Euler-Lagrange equation for  $\Theta(\gamma) = \int_\gamma (P(\kappa) + \lambda) ds$ . Then,

**Corollary 3.1.4.** ([10]) *A Frenet curve  $\gamma$  of rank 2 or 3 evolves under (3.3) by isometries of  $M_r^3(\rho)$ , if and only if,  $\gamma$  is an extremal of  $\Theta(\gamma) = \int_\gamma (P(\kappa) + \lambda) ds$ .*

In this case, we get a foliation of the binormal evolution surface by critical points of  $\Theta$ , (1.40), (as curves in  $M_r^3(\rho)$ ) that are also geodesics of the surface  $(U, x)$ .

In the following sections we are going to study binormal evolution surfaces all whose filaments have the same constant torsion. Moreover, since  $\tau = \tau_o \in \mathbb{R}$ ,  $\mathcal{F}(s, t) = \mathcal{F}(\kappa(s, t), \tau_o)$ . Thus, we can choose a smooth function  $P(\kappa)$  so that  $\dot{P}(\kappa) := \frac{dP}{d\kappa} = \mathcal{F}(\kappa)$ .



## 3.2 Evolution with Vanishing Torsion

Let's assume along this section that the torsion of all filaments of the evolution vanishes, that is,  $\tau(s, t) = 0$ . Now,

**Proposition 3.2.1.** ([10]) *Let  $(U, x)$  be a binormal evolution surface all whose filaments satisfy  $\tau = 0$ . Then, the initial filament  $\gamma = x(s, 0)$  is extremal for the energy  $\Theta(\gamma) := \int_{\gamma} (P(\kappa) + \lambda) ds$  and  $x(U) = S_{\gamma} = \{\phi_t(\gamma), t \in \mathbb{R}\}$ , where  $\{\phi_t, t \in \mathbb{R}\}$  is a one-parameter group of isometries of  $M_r^3(\rho)$ .*

*Proof.* By substituting  $\tau = 0$  in (3.11) we have  $\kappa(s, t) = \kappa(s)$  and the metric with respect to the chosen coordinate system is  $g = \varepsilon_1 ds^2 + \varepsilon_3 \mathcal{F}^2(s) dt^2$ . This means that  $(U, x)$  is a warped product surface [39], and, since  $\frac{\partial g_{ij}}{\partial t} = 0$ , we have that  $x_t(s, t) = \mathcal{F}(s)B(s, t) = \dot{P}(s)B(s, t)$  is a Killing field of  $(U, x)$ . Now, integrating (3.12) we get

$$0 = \dot{P}_{ss} + \varepsilon_1 \varepsilon_2 \dot{P}(\kappa^2 + \varepsilon_2 \rho) - \varepsilon_1 \varepsilon_2 \kappa(P + \lambda), \quad (3.18)$$

for some  $\lambda \in \mathbb{R}$ . Moreover, since  $\tau = 0$ , we have that (3.18) is the Euler-Lagrange equation for  $\Theta$ , (1.40), (see Section 1.3.1) and  $\gamma^t$  must be an extremal of  $\Theta$  in  $M_r^2(\rho)$ ,  $\forall t$ . Then, by Proposition 1.3.2,  $x_t$  is Killing along  $\gamma^t$ .

Hence, the associated one-parameter group  $\{\phi_t, t \in \mathbb{R}\}$  is formed by isometries of  $M_r^3(\rho)$  and  $x(U) = S_{\gamma}$  is obtained as  $S_{\gamma} = \{\phi_t(\gamma(s)), t \in \mathbb{R}\}$ , where  $\gamma(s) = x(s, 0)$ .  $\square$

Moreover, under the conditions of above Proposition

**Proposition 3.2.2.** ([10]) *The fibers of  $S_{\gamma}$  have constant curvature and zero torsion (if they are not geodesics) in  $M_r^3(\rho)$ .*

*Proof.* Since  $x_s = T(s, t)$ ,  $x_t = \dot{P}(\kappa(s))B(s, t)$ , and  $\tilde{\nabla}_{x_s} B(s, t) = -\varepsilon_2 \tau N(s, t) = 0$ , we get that  $B(s, t)$  does not depend on  $s$ . Moreover, as fibers are orbits of a Killing field of  $M_r^3(\rho)$ , they have constant curvature in  $M_r^3(\rho)$ . Now, for any  $s_o$  take an arc-length parametrization,  $\delta_{s_o}(t)$ , of the fiber of  $S_{\gamma}$  through  $s_o$ . With the subscript  $\delta$  denoting the geometric elements associated to the curve  $\delta_{s_o}(t)$ , we have  $T_{\delta}(t) = B(\frac{t}{P(\kappa(s_o))})$  and, using the last equation of (3.5), we obtain

$$\varepsilon_2^{\delta} \kappa_{\delta} N_{\delta} = -\varepsilon_1 \varepsilon_3 \frac{\dot{P}_s}{P} T - h_{22} N, \quad (3.19)$$

if  $\delta_{s_o}(t)$  has non-null acceleration. Thus, differentiating (3.19) with respect to  $t$  and using again (3.5), we have that  $\delta_{s_o}(t)$  must verify

$$\kappa_{\delta}(s_o, t) = \kappa_{\delta}(s_o), \quad \kappa_{\delta} \tau_{\delta} = 0, \quad \varepsilon_2^{\delta} \kappa_{\delta}^2 = \varepsilon_1 \frac{\dot{P}_s^2}{P^2} + \varepsilon_2 h_{22}^2,$$

from which we see that either  $\kappa_\delta = 0$ , and  $\delta_{s_o}(t)$  is a geodesic in  $M_r^3(\rho)$ , or  $\kappa_\delta \neq 0$ , and  $\delta_{s_o}(t)$  is a planar circle.

On the other hand, if  $\delta_{s_o}(t)$  has null acceleration and is not a geodesic, then we can consider the following frame along  $\gamma$ . Define  $N_\delta(t)$  as the lightlike field on  $\delta_{s_o}(t)$  given by  $\tilde{\nabla}_{\frac{\partial}{\partial t}} T_\delta(t) = N_\delta(t)$  and denote by  $B_\delta(t)$  the only lightlike vector such that  $\langle N_\delta, B_\delta \rangle = 1$  and  $\langle T_\delta, B_\delta \rangle = 0$ . In this case, we have the following Frenet-type equations

$$\tilde{\nabla}_{\frac{\partial}{\partial t}} T_\delta(t) = N_\delta(t), \quad \tilde{\nabla}_{\frac{\partial}{\partial t}} N_\delta(t) = \tau_\delta(t)N_\delta(t), \quad \tilde{\nabla}_{\frac{\partial}{\partial t}} B_\delta(t) = -T(t) - \tau_\delta(t)B_\delta(t),$$

for certain function  $\tau_\delta(t)$  which will be also called the *torsion* of  $\gamma$  (here, the ‘‘curvature’’ is considered to be 1). Then, from the second equation of (3.5), it is clear that  $\tau_\delta(t) = 0$ .  $\square$

In particular, if the curvature of the filaments,  $\kappa(s, t)$ , is also constant, then  $S_\gamma$  is a flat isoparametric surface.

**Proposition 3.2.3.** ([12]) *Let  $S_\gamma$  be a binormal evolution surface and assume that  $\gamma$  has constant curvature,  $\kappa_o$ , and vanishing torsion,  $\tau = 0$ . Then,  $S_\gamma$  is a flat isoparametric surface.*

*Proof.* Take  $\gamma$  a planar curve of  $M_r^3(\rho)$  with constant curvature  $\kappa(s) = \kappa_o$ . Then, the function  $\dot{P} = \mathcal{F} = G$  is independent of the arc-length parameter  $s$ . Therefore, from equation (1.38), we have that the Gaussian curvature of  $S_\gamma$  vanishes, that is,  $S_\gamma$  is a flat surface. Furthermore, substituting this information in equation (1.39), we get that the mean curvature of  $S_\gamma$ ,  $H$ , is constant. Thus, we conclude that  $S_\gamma$  is a flat isoparametric surface.  $\square$

Assume now that  $r = 0$ , that is,  $S_\gamma$  is immersed in a Riemannian 3-space form  $M^3(\rho)$ . If  $S_\gamma$  has planar filaments ( $\tau = 0$ ) and the curvature of  $\gamma$  is not constant, then  $S_\gamma$  would be a rotational surface. In fact, any Killing vector field  $\xi$  defined on  $M^3(\rho)$  can be assumed to be of the form  $\xi = \lambda_1 X_1 + \lambda_o V_o$  where  $\lambda_i \in \mathbb{R}$  for  $i = 0, 1$  and

$$X_1 = x_1 \partial_{x_2} - x_2 \partial_{x_1}, \quad V_o = \partial_{x_3}, \quad (3.20)$$

if  $M^3(\rho) = \mathbb{R}^3$ . In the case that,  $M^3(\rho) = \mathbb{S}^3(\rho) \subset \mathbb{R}^4$ , any Killing vector field  $\xi$  can be written as  $\xi = \lambda_1 X_1 + \lambda_2 X_2$  where  $\lambda_2 \in \mathbb{R}$ ,  $X_1$  is given in (3.20) and

$$X_2 = x_3 \partial_{x_4} - x_4 \partial_{x_3}. \quad (3.21)$$

And, in the last case,  $M^3(\rho) = \mathbb{H}^3(\rho) \subset \mathbb{L}^4$ , a Killing vector field  $\xi$  can be assumed to be either  $\xi = \lambda_1 X_1 + \lambda_3 X_3$  where  $\lambda_3 \in \mathbb{R}$ ,  $X_1$  is defined in (3.20) and

$$X_3 = x_4 \partial_{x_3} + x_3 \partial_{x_4}, \quad (3.22)$$

or  $\xi = \lambda_4 X_4$  where  $\lambda_4 \in \mathbb{R}$ , with

$$X_4 = (x_4 - x_3)\partial_{x_2} + x_2\partial_{x_3} + x_2\partial_{x_4}. \quad (3.23)$$

We say that the Killing vector field  $V_o$ , (3.20), is a *translational vector field*. Notice that the orbits of  $V_o$  are straight lines. On the other hand, the Killing vector fields  $X_1$  and  $X_2$ , given in (3.20) and (3.21), respectively, are called *spherical rotational vector fields* and their orbits are Euclidean circles. Moreover, we call *hyperbolic rotational vector field* to  $X_3$ , (3.22), while we refer as *parabolic rotational vector field* to  $X_4$ , (3.23). The orbits of  $X_3$  and  $X_4$  are *hypercycles* and *horocycles*, respectively.

Finally, we say that a surface  $N^2$  immersed in a Riemannian 3-space form,  $M^3(\rho)$ , is a *rotationally symmetric surface* (or simply a *rotational surface*) if it is congruent to a  $\xi$ -invariant surface and  $\xi = \lambda_i X_i$ , for some  $i = 1, 2, 3, 4$ , that is, for some rotational Killing vector field. If  $N^2$  is a rotational surface, then there exist a planar ( $\tau = 0$ ) curve,  $\gamma$ , in  $M^3$  such that  $N^2 = \{\phi_t(\gamma), t \in \mathbb{R}\}$ , where  $\{\phi_t, t \in \mathbb{R}\}$  represents the one-parameter group of isometries associated to  $\xi$ . Therefore, we use the notation  $N^2 = S_\gamma$  (see Section 1.2.3). Now, in the case that  $\xi$  is a real multiple of  $X_1$  or  $X_2$ , we will say that  $S_\gamma$  is a *spherical rotational surface*; if  $\xi$  is a multiple of  $X_3$ , then  $S_\gamma$  will be referred as a *hyperbolic rotational surface*, and, finally, if  $\xi$  is a multiple of  $X_4$  we have that  $S_\gamma$  is a *parabolic rotational surface*.

**Proposition 3.2.4.** ([12]) *Let  $S_\gamma \subset M^3(\rho)$  be a binormal evolution surface all whose filaments have zero torsion. Then, if they also have non-constant curvature,  $S_\gamma$  is a rotational surface.*

*Proof.* In this case, from the proof of Proposition 3.2.2 we know that the Frenet binormal is a constant vector field on  $\gamma$ , which can be written as

$$B(s) = \sum_{i=1}^4 a_i \partial_{x_i}, \quad (3.24)$$

where  $a_i \in \mathbb{R}$ . From Proposition 3.2.1 we know that  $S_\gamma$  is invariant by a one-parameter group of isometries associated to a Killing vector field  $\xi$ . Moreover, from Proposition 1.3.2 we also know that the restriction of the Killing vector field  $\xi$  to the surface is

$$\mathcal{I} = \xi = \dot{P}B, \quad (3.25)$$

where  $\dot{P}$  denotes the function  $\dot{P} = \frac{dP}{d\kappa}$ .

Case (i).  $M^3(\rho) = \mathbb{R}^3$ . In this case, since  $\xi$  is a Killing field, we can assume  $\xi = \lambda_1 X_1 + \lambda_o V_o$ , (3.20). Then, comparing (3.24) and (3.25) we obtain that  $\dot{P} a_3 = \lambda_o$ . If  $a_3 \neq 0$ , then  $\dot{P}$  (and, therefore,  $\kappa$ ) would be constant, which is not possible. Hence  $a_3 = \lambda_o = 0$ , what implies that  $S_\gamma$  is rotational.

Case (ii).  $M^3(\rho) = \mathbb{S}^3(\rho)$ ,  $\rho > 0$ . In this case, since  $\xi$  is a Killing field, we can assume  $\xi = \lambda_1 X_1 + \lambda_2 X_2$ , (3.21). Now, comparing (3.24) and (3.25) we obtain that

$$\dot{P} a_1 = -\lambda_1 \gamma_2(s), \quad \dot{P} a_2 = \lambda_1 \gamma_1(s), \quad \dot{P} a_3 = -\lambda_2 \gamma_4(s), \quad \dot{P} a_4 = \lambda_2 \gamma_3(s). \quad (3.26)$$

If  $\lambda_1, \lambda_2 \neq 0$ , then, combining  $\sum_{i=1}^4 \gamma_i^2 = 1/\rho$  and (3.26), we would obtain that  $\dot{P}$  (and, therefore,  $\kappa$ ) would be constant, which is not possible. Hence, either  $\lambda_1 = 0$  or  $\lambda_2 = 0$ . In both cases,  $S_\gamma$  is rotational.

Case (iii).  $M^3(\rho) = \mathbb{H}^3(\rho)$ ,  $\rho < 0$ . In this case the Killing field  $\xi$  can be assumed to be either  $\xi = \lambda_1 X_1 + \lambda_3 X_3$  or  $\xi = \lambda_4 X_4$ , (3.22) or (3.23).

In the first case, comparing (3.24) and (3.25) we obtain that

$$\dot{P} a_1 = -\lambda_1 \gamma_2(s), \quad \dot{P} a_2 = \lambda_1 \gamma_1(s), \quad \dot{P} a_3 = \lambda_3 \gamma_4(s), \quad \dot{P} a_4 = \lambda_3 \gamma_3(s). \quad (3.27)$$

If  $\lambda_1, \lambda_3 \neq 0$ , then, combining  $\sum_{i=1}^3 \gamma_i^2 - \gamma_4^2 = 1/\rho$  and (3.27), we would obtain that  $\dot{P}$  (and, therefore,  $\kappa$ ) would be constant, which is not possible. Hence, either  $\lambda_1 = 0$  or  $\lambda_3 = 0$ .

Assume first that  $\lambda_3 = 0$ . Then (3.27) implies  $a_3 = a_4 = 0$ , and  $a_1^2 + a_2^2 = 1$ . Thus, without loss of generality we may take  $B = (0, 1, 0, 0)$ . From this and (3.27), we have that  $\gamma_2 = 0$  and  $\dot{P} = \lambda_1 \gamma_1$ . After reparametrization if needed, we have that the flow of  $\xi = \lambda_1 X_1$  is formed by the curves  $\beta(t) = (b_1 \cos(\lambda_1 t), b_1 \sin(\lambda_1 t), b_3, b_4)$ , for certain scalars  $b_i \in \mathbb{R}$ ,  $i = 1, 3, 4$ . Taking  $\gamma(s)$  as initial condition for the flow, we have the following parametrization of  $S_\gamma$

$$x(s, t) = (\gamma_1(s) \cos(\lambda_1 t), \gamma_1(s) \sin(\lambda_1 t), \gamma_3(s), \gamma_4(s)).$$

Call  $P^2$  the plane spanned by  $e_3 = (0, 0, 1, 0)$  and  $e_4 = (0, 0, 0, 1)$ . Analogously, denote by  $P^3$  the 3-space spanned by  $e_3, e_4$  and  $e_1 = (1, 0, 0, 0)$ . If  $\{\phi_t, t \in \mathbb{R}\}$  denotes the one-parameter group of isometries associated to  $\xi$ , then we see that the Lorentzian plane  $P^2$  is point-wise invariant by the action of  $\{\phi_t, t \in \mathbb{R}\}$  and that  $P^3 \cap S_\gamma = \gamma$ . Hence,  $S_\gamma$  is a spherical rotational surface in  $\mathbb{H}^3(\rho)$ , [36].

Assume now that  $\lambda_1 = 0$ . Then (3.27) implies  $a_1 = a_2 = 0$ , and we may take  $B = (0, 0, 1, 0)$ . Combining this and (3.27), we have that  $\gamma_3 = 0$  and  $\dot{P} = \lambda_3 \gamma_4$ . After reparametrization if needed, we have that the flow of  $\xi = \lambda_3 X_3$  is formed by the curves  $\beta(t) = (b_1, b_2, b_3 \cosh(\lambda_3 t), b_3 \sinh(\lambda_3 t))$ , for certain scalars  $b_i \in \mathbb{R}$ ,  $i = 1, 2, 3$ . Taking  $\gamma(s)$  as initial condition for the flow, we have the following parametrization of  $S_\gamma$

$$x(s, t) = (\gamma_1(s), \gamma_2(s), \gamma_4(s) \sinh(\lambda_3 t), \gamma_4(s) \cosh(\lambda_3 t)).$$

Call  $P^2$  the plane spanned by  $e_1 = (1, 0, 0, 0)$  and  $e_2 = (0, 1, 0, 0)$ . Analogously, denote by  $P^3$  the 3-space spanned by  $e_1, e_2$  and  $e_4 = (0, 0, 0, 1)$ . If  $\{\phi_t, t \in \mathbb{R}\}$  denotes the one-parameter group of isometries associated to  $\xi = \lambda_3 X_3$ , then we see that the Riemannian plane  $P^2$  is point-wise invariant by the action of  $\{\phi_t, t \in \mathbb{R}\}$  and that  $P^3 \cap S_\gamma = \gamma$ . Hence,

$S_\gamma$  is a hyperbolic rotational surface in  $\mathbb{H}^3(\rho)$ , [36].

Finally, assume that  $\xi = \lambda_4 X_4$ , (3.23). Then, comparing (3.24) and (3.25) we obtain

$$\dot{P} a_1 = 0, \quad \dot{P} a_2 = \lambda_4(\gamma_4(s) - \gamma_3(s)), \quad \dot{P} a_3 = \lambda_4\gamma_2(s), \quad \dot{P} a_4 = \lambda_4\gamma_2(s). \quad (3.28)$$

For simplicity, we take  $\lambda_4 = 1$ . Thus, relations (3.28) imply  $a_1 = 0$  and, since  $a_2^2 + a_3^2 - a_4^2 = 1$ , we may assume  $a_2 = a_3 = a_4 = 1$ . Again, we compute the integral curves of  $\xi$  with initial conditions  $\gamma(s)$  obtaining the following parametrization of  $S_\gamma$

$$x(s, t) = (\gamma_1(s), \gamma_2(s)t + \gamma_2(s), \frac{\gamma_2(s)}{2}t^2 + \gamma_2(s)t + \gamma_3(s), \frac{\gamma_2(s)}{2}t^2 + \gamma_2(s)t + \gamma_4(s)).$$

On the other hand (3.28) imply also  $\gamma_2(s) = \gamma_4(s) - \gamma_3(s)$ , so that, choosing the following pseudo-orthonormal coordinate system  $\mathcal{B} := \{v_1 = (0, 1, 0, 1), v_2 = (0, 1, 1, 1), v_3 = (0, 0, -1, -1), v_4 = (1, 0, 0, 0)\}$ , we see that above parametrization reduces to

$$x(s, t) = (\gamma_2(s), \gamma_2(s)t, -\frac{1 + \gamma_1^2(s) + \gamma_2(s)^2 t^2}{2\gamma_2(s)}, \gamma_1(s)).$$

Moreover, the plane  $P^2 = \text{span}\{v_3, v_4\}$  is a degenerate point-wise invariant plane by the action of the group of isometries associated to  $\xi$ , and if  $P^3 = \text{span}\{v_1, v_3, v_4\}$  we have  $P^3 \cap S_\gamma = \gamma$ . Hence,  $S_\gamma$  is a parabolic rotational surface in  $\mathbb{H}^3(\rho)$ , [36].  $\square$

### 3.2.1 Parametrizations in Riemannian 3-Space Forms

Observe that the proof of Proposition 3.2.4 provides a standard way of finding local parametrizations of binormal evolution surfaces with planar initial conditions in Riemannian 3-space forms, provided that  $\gamma$  is a critical curve of  $\Theta$ , (1.40), with non-constant curvature. However, in what follows we are going to use a technique based on Killing vector fields associated to  $\gamma$  (as described in Proposition 1.3.2) to obtain the local parametrizations of  $S_\gamma$  in Riemannian 3-space forms,  $M^3(\rho)$ , with  $\dot{P}_s \neq 0$ .

#### The Euclidean 3-Space, $\mathbb{R}^3$

If  $M^3(\rho) = \mathbb{R}^3$ , the Euclidean 3-space, we are going to work with cylindrical coordinates, that is,

$$x(r, \theta, z) = (r \cos \theta, r \sin \theta, z).$$

In these coordinates, we obtain that the Killing vector fields  $X_1$  and  $V_o$ , (3.20), simplify to  $\partial_\theta$  and  $\partial_z$ , respectively.

Now, take  $\mathcal{I}$  and  $\mathcal{J}$  the Killing vector fields along  $\gamma$  defined in Proposition 1.3.2 which can be extended to Killing vector fields on the whole  $M^3(\rho)$  (denoted by the same letter).

Moreover,  $\mathcal{I}$  is rotational as we have seen in Proposition 3.2.4 and  $\mathcal{I}$  and  $\mathcal{J}$  commute, [5]. Therefore, we may assume that

$$\mathcal{I} = a \partial_\theta, \quad \mathcal{J} = \tilde{a} \partial_\theta + \tilde{b} \partial_z,$$

with  $a, \tilde{a}$  and  $\tilde{b}$  real constants. Then, from equations (1.57) and (1.58), we conclude that,

$$\mathcal{I} = \sqrt{d} \partial_\theta, \quad \mathcal{J} = \sqrt{d} \partial_z, \quad (3.29)$$

for positive real  $d$ . Notice that above fields coincide with (2.18) and (2.19) for  $e = 0$ . In these coordinates, the curve  $\gamma$  can be parametrized as,  $\gamma(s) = x(r(s), \theta(s), z(s))$ . Now, assuming without loss of generality that  $s$  represents the arc-length parameter, we have that  $T(s) = r'(s)\partial_r + \theta'(s)\partial_\theta + z'(s)\partial_z$ .

Therefore, from (3.29) and the definition of  $\mathcal{I}$  and  $\mathcal{J}$ , (1.56),  $\theta(s)$  can be assumed to be zero, and

$$z(s) = \int \frac{\kappa \dot{P} - P}{\sqrt{d}} ds.$$

Thus, the binormal evolution surface,  $S_\gamma$ , in the Euclidean 3-space can be parametrized as

$$x(s, \theta) = \frac{1}{\sqrt{d}} \left( \dot{P} \cos \theta, \dot{P} \sin \theta, \int (\kappa \dot{P} - P) ds \right), \quad (3.30)$$

where the curvature of  $\gamma$  is denoted by  $\kappa(s)$ ,  $P = P(\kappa(s))$  and  $\dot{P} = \frac{dP}{d\kappa}$ . Then, we have that  $\gamma$  can be parametrized as  $x(s, 0)$ .

### The Round 3-Sphere, $\mathbb{S}^3(\rho)$

In the case that  $M^3(\rho) = \mathbb{S}^3(\rho)$  is the 3-dimensional round sphere, we are going to use the following spherical coordinates,

$$x(\theta, \sigma, \psi) = \frac{1}{\sqrt{\rho}} (\cos \theta \cos \sigma, \cos \theta \sin \sigma, \sin \theta \sin \psi, \sin \theta \cos \psi).$$

The Killing vector fields  $X_1$  and  $X_2$ , (3.20) and (3.21), are  $\partial_\sigma$  and  $\partial_\psi$ , respectively. Notice that in the 3-sphere there are only rotational Killing vector fields, so both of them are of the same type.

Again, as  $\mathcal{I}$  and  $\mathcal{J}$  given in Proposition 1.3.2 are commuting Killing vector fields in  $\mathbb{S}^3(\rho)$ , [5]. Then, by a similar argument to that used in the Euclidean case, they are a linear combination of  $\partial_\sigma$  and  $\partial_\psi$ . Moreover, we may assume that  $\mathcal{I}$  is a real multiple of  $\partial_\sigma$ , since it must be rotational.

Therefore, arguing as in the Euclidean case and using equations (1.57) and (1.58), we obtain that,

$$\mathcal{I} = \sqrt{d} \partial_\sigma, \quad \mathcal{J} = \sqrt{\rho d} \partial_\psi.$$

Now, we parametrize  $\gamma(s) = x(\theta(s), \sigma(s), \psi(s))$  using these spherical coordinates introduced above. Then, computing the tangent vector of  $\gamma$  and combining with (1.56), we have that without loss of generality  $\sigma(s) = 0$  and

$$\psi(s) = \sqrt{\rho d} \int \frac{\kappa \dot{P} - P}{d - \rho \dot{P}^2} ds. \quad (3.31)$$

Therefore, taking into account that  $\gamma$  is arc-length parametrized we have that the binormal evolution surface  $S_\gamma$  in  $\mathbb{S}^3(\rho)$  can be parametrized as,

$$x(s, \phi) = \frac{1}{\sqrt{\rho d}} \left( \sqrt{\rho \dot{P}} \cos \phi, \sqrt{\rho \dot{P}} \sin \phi, \sqrt{d - \rho \dot{P}^2} \sin \psi(s), \right. \\ \left. \sqrt{d - \rho \dot{P}^2} \cos \psi(s) \right), \quad (3.32)$$

where  $\kappa(s)$  represents the curvature of  $\gamma$ ,  $\dot{P} = \frac{dP}{d\kappa}(\kappa(s))$  and  $\psi(s)$  is given in (3.31). Moreover, we also have  $\gamma(s) = x(s, 0)$ . Observe that  $\gamma(s)$  crosses the pole of the parametrization,  $(1/\sqrt{\rho}, 0, 0, 0)$ , if and only if,  $d = \rho \dot{P}^2$ .

### The Hyperbolic 3-Space, $\mathbb{H}^3(\rho)$

Finally, if  $M^3(\rho) = \mathbb{H}^3(\rho)$  is the hyperbolic 3-space, we need to work slightly different since there are three different types of rotations. For a rotational binormal evolution surface in  $\mathbb{H}^3(\rho)$ , the type of rotation is completely characterized by the constant of integration  $d$ , (1.58). For any velocity, we get,

**Proposition 3.2.5.** ([14]) *Let  $S_\gamma \subset \mathbb{H}^3(\rho)$  be a rotational binormal evolution surface with velocity  $\dot{P}$ , and let the initial condition  $\gamma$  be a planar extremal curve of  $\Theta$ , (1.40). Then, if  $d > 0$ ,  $S_\gamma$  is a spherical rotational surface; if  $d = 0$ ,  $S_\gamma$  is a parabolic rotational surface; and, if  $d < 0$ ,  $S_\gamma$  is a hyperbolic rotational surface.*

*Proof.* For any  $s_o$  take an arc-length parametrization,  $\delta_{s_o}(t)$ , of the fiber of  $S_\gamma$  through  $s_o$ . Notice that since  $\gamma$  is planar, the binormal along  $\gamma$  does not depend on  $s$ , see Proposition 3.2.2. Now, from equation (3.19) we can compute the curvature of  $\delta_{s_o}$ . Moreover, using (1.28), (1.52) and (1.60), we obtain

$$\kappa_\delta^2(s_o) = \frac{\dot{P}_s^2}{\dot{P}^2} + h_{22}^2 = \frac{d}{\dot{P}^2} - \rho. \quad (3.33)$$

Therefore,  $d > 0$ , if and only if,  $\kappa_\delta^2 > -\rho$ , that is, if and only if,  $\delta_{s_o}$  is a Euclidean circle. Similarly,  $d = 0$  is equivalent to  $\delta_{s_o}$  being an horocycle; and, finally,  $\delta_{s_o}$  represents an hypercycle, if and only if,  $d < 0$ .  $\square$

**Case (i). Cyclical Case** ( $d > 0$ )

For the spherical rotational case, we are going to use the upper sheet hyperboloid model, see Section 1.2. In this model we are going to pick up the following coordinates in order to parametrize it,

$$x(u, \theta, v) = \frac{1}{\sqrt{-\rho}} (\sinh u \cos \theta, \sinh u \sin \theta, \cosh u \sinh v, \cosh u \cosh v) .$$

Then, we have the following simplifications,  $\partial_\theta$  and  $\partial_v$ , of the Killing vector fields  $X_1$  and  $X_3$ , (3.20) and (3.22), respectively. As in the other 3-space forms, we may assume  $\mathcal{I}$  to be a multiple of  $\partial_\theta$ , since for this case we want a spherical rotation. Notice that  $\mathcal{J}$  must be orthogonal to  $\mathcal{I}$ , therefore it must be a linear combination of  $\partial_\theta$  and  $\partial_v$ . The Killing vector field  $X_4$ , (3.23), does not appear here due to this orthogonality condition.

Using one more time equations (1.57) and (1.58), we conclude that

$$\mathcal{I} = \sqrt{d} \partial_\theta, \quad \mathcal{J} = \sqrt{-\rho d} \partial_v .$$

Now, if we combine (1.56) with the tangent vector of  $\gamma$ , after reparametrizing it by arc-length using above coordinates, we may assume without loss of generality that  $\theta(s) = 0$  and that

$$v(s) = \sqrt{-\rho d} \int \frac{\kappa \dot{P} - P}{d - \rho \dot{P}^2} ds . \quad (3.34)$$

Thus, a binormal evolution surface in  $\mathbb{H}^3(\rho)$  for  $d > 0$  admits the parametrization,

$$x(s, \theta) = \frac{1}{\sqrt{-\rho d}} \left( \sqrt{-\rho \dot{P}} \cos \theta, \sqrt{-\rho \dot{P}} \sin \theta, \sqrt{d - \rho \dot{P}^2} \sinh v(s), \sqrt{d - \rho \dot{P}^2} \cosh v(s) \right), \quad (3.35)$$

where  $\kappa(s)$  is the curvature of  $\gamma$ ,  $v(s)$  is given in (3.34) and  $\dot{P} = \frac{dP}{d\kappa}(\kappa(s))$ . The generating curve  $\gamma$  can be parametrized as  $x(s, 0)$ .

**Case (ii). Hypercyclical Case** ( $d < 0$ )

The case of hyperbolic rotational surfaces is similar to above case ( $d > 0$ ). Indeed, we are going to use the same coordinates as before. Now, we want  $\mathcal{I}$  to be a hyperbolic rotational vector field, so it must be a scalar multiple of  $\partial_v$ . By the same argument as before, we get that,

$$\mathcal{I} = \sqrt{-d} \partial_v, \quad \mathcal{J} = \sqrt{\rho d} \partial_\theta .$$

Combining again this and (1.56) with the tangent vector of  $\gamma$ , we conclude that  $v(s) = 0$  and that

$$\theta(s) = \sqrt{\rho d} \int \frac{\kappa \dot{P} - P}{d - \rho \dot{P}^2} ds . \quad (3.36)$$



Therefore, rotational binormal evolution surfaces in  $\mathbb{H}^3(\rho)$  for  $d < 0$  can be parametrized as,

$$x(s, \phi) = \frac{1}{\sqrt{\rho d}} \left( \sqrt{d - \rho \dot{P}^2} \cos \theta(s), \sqrt{d - \rho \dot{P}^2} \sin \theta(s), \sqrt{-\rho \dot{P}} \sinh \phi, \sqrt{-\rho \dot{P}} \cosh \phi \right), \quad (3.37)$$

where  $\kappa(s)$  is the curvature of the profile curve  $\gamma$ , which is  $\gamma(s) = x(s, 0)$ ,  $\dot{P} = \frac{dP}{d\kappa}(\kappa(s))$  and  $\theta(s)$  is given by (3.36).

### Case (iii). Horocyclical Case ( $d = 0$ )

The last case in the hyperbolic 3-space corresponds to parabolic rotational surfaces. The orbits here are horocycles, and computations involving horocycles in the upper sheet hyperboloid model are quite hard. Moreover, as the ball model is just a conformal transformation of the hyperboloid model, it is also hard to deal with computations. That is, it will be convenient to use here a different model, for instance, the semi-space model.

Therefore, just for the next lines we are going to consider the definition of the hyperbolic 3-space given by

$$\mathbb{H}^3(\rho) = \{(x_1, x_2, x_3) \in \mathbb{R}^3 \mid x_3 > 0\}$$

endowed with the metric

$$g = -\frac{1}{\rho x_3^2} (dx_1^2 + dx_2^2 + dx_3^2). \quad (3.38)$$

Now, we choose a parametrization of the space by horospheres,

$$x(u, v, w) = \left( \frac{2u \exp(2w)}{(u^2 + v^2) \exp(2w) + 4}, \frac{2v \exp(2w)}{(u^2 + v^2) \exp(2w) + 4}, \frac{4 \exp w}{(u^2 + v^2) \exp(2w) + 4} \right).$$

In this parametrization the frame of coordinate vector fields is an orthogonal frame where the metric (3.38) becomes

$$g_{11} = g_{22} = -\frac{\exp(2w)}{4\rho}, \quad g_{33} = -\frac{1}{\rho}.$$

Moreover, the parabolic rotational vector field  $X_4$ , (3.23), simplifies to  $\partial_u$ . And, then we can assume that  $\mathcal{I} = a \partial_u$ , which necessarily gives us that  $\mathcal{J} = b \partial_v$ . Since it must be orthogonal to  $\mathcal{I}$ . Now, equation (1.58) tells us that  $b^2 = -\rho a^2$ . Moreover, if we compute the tangent vector of  $\gamma$ ,  $T(s) = u'(s) \partial_u + v'(s) \partial_v + w'(s) \partial_w$ , and, since  $\mathcal{I}$  is a vector field in the direction of the binormal of  $\gamma$ , we can suppose that  $u(s) = 0$ . That is, the tangent

vector of  $\gamma$  is just  $T(s) = v'(s)\partial_v + w'(s)\partial_w$ , and we can obtain the expression of the normal vector field of  $\gamma$ ,

$$N(s) = -\frac{2w'(s)}{\exp w}\partial_v + \frac{\exp w v'(s)}{2}\partial_w.$$

Using (1.56), together with the above descriptions of  $T(s)$  and  $N(s)$ , we also have that  $a^2 \exp(2w) = -4\rho\dot{P}^2$  and,

$$v(s) = -\frac{b}{\rho} \int \frac{\kappa\dot{P} - P}{\dot{P}^2} ds. \quad (3.39)$$

Therefore, the parametrization of any rotational binormal evolution surface for  $d = 0$  in  $\mathbb{H}^3(\rho)$  is,

$$x(s, u) = \left( \frac{2u\rho^2\dot{P}^2}{(u^2 + v^2(s))\rho^2\dot{P}^2 + b^2}, \frac{2v(s)\rho^2\dot{P}^2}{(u^2 + v^2(s))\rho^2\dot{P}^2 + b^2}, \frac{2\sqrt{b^2\rho^2\dot{P}^2}}{(u^2 + v^2(s))\rho^2\dot{P}^2 + b^2} \right), \quad (3.40)$$

where the curvature of  $\gamma$  is  $\kappa(s)$ ,  $\dot{P} = \frac{dP}{d\kappa}(\kappa(s))$  and  $v(s)$  is given in (3.39). Moreover,  $\gamma(s) = x(s, 0)$ . Notice that above parametrization, (3.40), depends on the parameter  $b \neq 0$  (or, equivalently, on  $a \neq 0$ ). However, it is a straight forward computation to check that the surfaces parametrized by (3.40) are all congruent for any  $b \neq 0$ , that is, there exists basically one rotational binormal evolution surface for  $d = 0$ .

### 3.2.2 Closed Binormal Evolution Surfaces of $M^3(\rho)$

Once we have the parametrizations of the binormal evolution surfaces generated by evolving planar extremals of  $\Theta$ , (1.40), under (3.3) by congruences of  $M^3(\rho)$ , we can obtain conditions for both the initial condition,  $\gamma$ , and the binormal evolution surface,  $S_\gamma$ , to be closed.

Let's begin by developing the conditions that must be verified by  $\gamma$  in order to close up. First of all, we need its curvature  $\kappa(s)$  to be periodic. Then, adapting the computations of [5], if we define the function

$$\Lambda(d) = \int_0^\varrho \frac{\kappa\dot{P} - P}{d - \rho\dot{P}^2} ds, \quad (3.41)$$

where  $\varrho$  is the period of  $\kappa(s)$  and  $d$  is the constant of integration given by (1.58), we have

**Proposition 3.2.6.** *Let  $\gamma \subset M^3(\rho)$  be a planar critical curve of  $\Theta(\gamma) = \int_\gamma (P(\kappa) + \lambda) ds$  with periodic curvature  $\kappa(s)$ , then  $\gamma(s)$  is closed, if and only if, the function  $\Lambda(d)$ , (3.41), vanishes for  $\rho d \leq 0$ , or it is equal  $\frac{2\pi n}{m\sqrt{\rho d}}$  for any integers  $n$  and  $m$ , when  $\rho d > 0$ .*

Notice that the integers  $n$  and  $m$  have a geometrical meaning. The number of rounds the critical curve gives around the pole of the parametrization, that is the point  $(1/\sqrt{\rho}, 0, 0, 0)$ , in order to close up is represented by the integer  $n$ , while  $m$  denotes the number of lobes the curve has, that is, analytically, the number of periods of the curvature needed to close up.

Now, in order the binormal evolution surface,  $S_\gamma$ , to be closed we need the orbits to be closed. Notice that the orbits are closed curves, if and only if, the constant of integration,  $d$ , is positive, as we have proved in Proposition 3.2.5. Moreover, we also need one of the followings, either the profile curve to be closed or that it cuts the axis of rotation. Thus, we conclude

**Corollary 3.2.7.** ([14]) *Let  $S_\gamma \subset M^3(\rho)$  be a binormal evolution surface whose profile curve,  $\gamma$ , is an extremal of  $\Theta$  with  $\tau = 0$  and periodic curvature,  $\kappa(s)$ , which does not meet the axis of rotation. Then,  $S_\gamma$  is a closed surface, if and only if, the function  $\Lambda(d)$ , (3.41), equals  $\frac{2\pi n}{m\sqrt{\rho d}}$ , for some  $d > 0$  and any integers  $n$  and  $m$ , when  $\rho > 0$ ; or,  $\Lambda(d)$ , (3.41) vanishes at some  $d > 0$ , when  $\rho \leq 0$ .*

### 3.2.3 Parametrizations in Minkowski 3-Space

Finally, in this section, we restrict ourselves to the flat Lorentzian space  $\mathbb{L}^3$ , the Minkowski 3-space, see Section 1.2. We say that a surface is a *rotational surface* if it stays invariant under a one-parameter group of rotations. This definition follows the convention of that given in Riemannian 3-space forms, see the beginning of Section 3.2. Notice that in Riemannian settings all rotational surfaces can be constructed by rotating a planar curve. However, this is not true in  $\mathbb{L}^3$ . In fact, there are rotational surfaces that cannot be constructed in this way, see [33]. In any case, rotation of a non-null planar curve generates rotational surfaces. Moreover, the Minkowski 3-space is richer than Riemannian 3-space forms, in the following sense. There are basically three different type of rotations, depending on the causal character of the axis. Here we understand the axis, as the only geodesic that stays point-wise fixed under the action of the group of rotations. If the axis is spacelike, we can assume without loss of generality that is given by  $x_3 = x_4 = 0$ , and the rotation around it can be represented by the matrix

$$\begin{pmatrix} \cosh t & \sinh t & 0 \\ 0 & 0 & 1 \\ \sinh t & \cosh t & 0 \end{pmatrix}.$$

Now, if the axis is, for instance,  $x_2 = x_3 = 0$ , then, it is timelike and the matrix corresponding with rotations around it is expressed as

$$\begin{pmatrix} \cos t & \sin t & 0 \\ -\sin t & \cos t & 0 \\ 0 & 0 & 1 \end{pmatrix}.$$

Finally, there is another possibility for the causal character of the axis. Let's assume that our axis is given by  $x_2 = 0$  and  $x_3 = x_4$ , then this represents a null-geodesic, and its correspondence rotations can be represented as

$$\begin{pmatrix} t & 1 - \frac{t^2}{2} & \frac{t^2}{2} \\ 1 & -t & t \\ t & -\frac{t^2}{2} & 1 + \frac{t^2}{2} \end{pmatrix}.$$

If  $P(\kappa) = \nu\kappa$ ,  $\nu \in \mathbb{R}$ , then any planar curve  $\gamma$  is critical for  $\Theta$ , (1.40), [6] and  $S_\gamma$  must be a right cylinder shaped on  $\gamma$ . Assume then that  $P(\kappa) \neq \nu\kappa$ ,  $\nu \in \mathbb{R}$ . Then the Killing field along  $\gamma$ ,  $\mathcal{I}$ , can be written as  $\mathcal{I} = \dot{P}B = \lambda_1(\gamma \times V) + \lambda_2 V$ , for some  $\lambda_1, \lambda_2 \in \mathbb{R}$ ,  $\lambda_1 \neq 0$  and a constant vector  $V$  in  $\mathbb{R}^3$ . By scalar multiplication of the covariant derivative of  $\mathcal{I} = \dot{P}B = \lambda_1(\gamma \times V) + \lambda_2 V$  with  $V$  we obtain  $\lambda_2 = 0$  and, then,  $S_\gamma$  is a rotational surface in  $\mathbb{L}^3$  with profile curve  $\gamma$ .

Moreover, if  $P(\kappa) \neq \nu\kappa$ ,  $\nu \in \mathbb{R}$ , it is not difficult to see that, identifying the plane containing  $\gamma$  and  $\mathbb{R}^2$  or  $\mathbb{L}^2$ , choosing a coordinate system containing  $V$ , and using  $\mathcal{I} = \dot{P}B$ , it is possible to find a coordinate system in this plane where  $\gamma = (\gamma_1, \gamma_2)$  and  $\gamma_1 = c\dot{P}$ , for some constant  $c \in \mathbb{R}$ .

In particular, take an extremal curve of  $\int_\gamma (P(\kappa) + \lambda) ds$  either in  $\mathbb{R}^2$  or in  $\mathbb{L}^2$  and choose a coordinate system where  $\gamma = (\gamma_1, \gamma_2)$  and  $\gamma_1 = c\dot{P}$ , for some constant  $c \in \mathbb{R}$ . Assuming  $c \neq 0$ , then

$$\begin{aligned} x(s, t) &= \left( c\dot{P} \sin(t), c\dot{P} \cos(t), a(s) \right), \quad \text{if } \varepsilon_1^\delta \varepsilon_2^\delta = 1, \\ x(s, t) &= \left( c\dot{P} \sinh(t), a(s), c\dot{P} \cosh(t) \right), \quad \text{if } \varepsilon_1^\delta = -1, \quad \text{and} \\ x(s, t) &= \left( c\dot{P} \cosh(t), a(s), c\dot{P} \sinh(t) \right), \quad \text{if } \varepsilon_2^\delta = -1, \end{aligned}$$

where  $a(s)$  verifies  $\varepsilon_2^\delta ((c\dot{P})')^2 + \varepsilon_3^\delta (a'(s))^2 = \varepsilon_1$ , are rotation surfaces with planar filaments evolving by (3.3).

Finally, if the extremal curve lies in the Minkowski plane  $\mathbb{L}^2$ , then choosing the same coordinate system as before one could also construct a surface with planar filaments evolving by (3.3) just rotating  $\gamma$  around a lightlike axis. In fact, suppose without loss of generality that the lightlike axis is determined by  $\frac{\partial}{\partial x_3} + \frac{\partial}{\partial x_4}$  then, the parametrization of  $S_\gamma$  is given by,

$$x(s, t) = \left( c\dot{P} + (a(s) - c\dot{P})\frac{t^2}{2}, (a(s) - c\dot{P})t, a(s) + (a(s) - c\dot{P})\frac{t^2}{2} \right),$$

where  $a(s)$  verifies  $((c\dot{P})')^2 - (a'(s))^2 = \varepsilon_1$ . In this case, fibers are spacelike curves with null acceleration.

### 3.3 Evolution with Non-Zero Constant Torsion

Take now  $\tau_o \neq 0$ . If  $\kappa(s, t)$  is also constant, filaments are Frenet helices. Then, as proved in [7] and [57] (see also Section 1.3.1), Frenet helices are critical curves for  $\Theta(\gamma) = \int_{\gamma} (\kappa + \lambda) ds$ . Therefore, by Proposition 1.3.2, the unit binormal  $B$  is a Killing vector field on Frenet helices, hence, their evolution under the  $B$ -flow satisfy

$$x_t = B. \quad (3.42)$$

Moreover, the function  $\dot{P} = \mathcal{F}$  is also constant, and a generalization of Proposition 3.2.3 can be proved arguing in the same way. That is,

**Proposition 3.3.1.** ([12]) *Let  $\gamma$  be a Frenet helix, then the binormal evolution surface generated by evolving  $\gamma$  under (3.42) by congruences is a flat isoparametric surface.*

Thus, we assume  $\kappa(s, t)$  is not constant. Then, (3.11) suggests to study traveling wave solutions of the form  $\kappa(s - \varepsilon_1 \varepsilon_3 \mu t)$ ,  $\mu \in \mathbb{R}$ , what implies  $\mathcal{F}(\kappa(s, t)) = \frac{\varepsilon_1 \varepsilon_3 \mu}{2\tau_o} \kappa + \lambda$ , for some  $\lambda \in \mathbb{R}$ . Call  $\iota = s - \varepsilon_1 \varepsilon_3 \mu t$ . Then, by substitution in (3.12) we obtain

$$0 = \frac{\varepsilon_1 \varepsilon_2 \mu}{2\tau_o} \kappa_{\iota} + \frac{\mu}{4\tau_o} \kappa^3 + \frac{(-1)^r \mu}{2\tau_o} \kappa (\varepsilon_1 \varepsilon_3 \rho - \varepsilon_2 \tau_o^2) + \lambda ((-1)^r \rho - \tau_o^2). \quad (3.43)$$

**Proposition 3.3.2.** ([10]) *Assume that  $\gamma(\iota)$  is a curve in  $M_r^3(\rho)$  with non-constant curvature and constant torsion  $\tau = \tau_o \neq 0$  which is an extremal of the energy*

$$\Theta(\gamma) = \int_{\gamma} \left( \frac{\varepsilon_1 \varepsilon_3 \mu}{4\tau_o} \kappa^2 + \lambda \kappa + \mu \tau + \nu \right) ds,$$

where  $\mu \neq 0$  and  $\lambda, \nu \in \mathbb{R}$ . Then, there exists a one-parameter group of isometries of  $M_r^3(\rho)$ ,  $\{\phi_t, t \in \mathbb{R}\}$ , such that a suitable parametrization of the surface  $S_{\gamma} := \phi_t(\gamma(\iota))$  is a solution of (3.3) with  $\mathcal{F}(\kappa(s, t)) = \frac{\varepsilon_1 \varepsilon_3 \mu}{2\tau_o} \kappa + \lambda$ .

*Proof.* It is easy to verify from (3.43) that  $\kappa(\iota)$  and  $\tau = \tau_o$  satisfy the Euler-Lagrange equations for the above energy  $\Theta$ , (1.62) and (1.63), for a suitable  $\nu \in \mathbb{R}$ .

Consider  $\kappa(\iota)$  a solution of (3.43) (observe that (3.43) can be explicitly solved with the aid of Jacobi elliptic functions, see Appendix A), then  $\kappa(\iota)$  and  $\tau = \tau_o$  determine a curve  $\gamma(\iota)$  in  $M_r^3(\rho)$  which is an extremal for  $\Theta$ . Now, the vector field  $\mathcal{I}(\iota) := \varepsilon_1 \varepsilon_3 \mu T(\iota) + \mathcal{F}(\iota) B(\iota)$  is a Killing field along  $\gamma(\iota)$  (see Proposition 1.3.3).

As in previous arguments,  $\mathcal{I}$  can be extended to a Killing field on  $M_r^3(\rho)$  with one-parameter group of isometries  $\{\phi_t, t \in \mathbb{R}\}$ . Consider the surface  $S_{\gamma} := y(\iota, t) = \phi_t(\gamma(\iota))$ ,  $t \in \mathbb{R}$ . Then, the reparametrization  $x(s, t) := y(s - \varepsilon_1 \varepsilon_3 \mu t, t)$  satisfies  $x_t = \left( \frac{\varepsilon_1 \varepsilon_3 \mu}{2\tau_o} \kappa + \lambda \right) B$ , having all filaments constant torsion  $\tau = \tau_o$ .  $\square$

## 3.4 A Few Consequences

Finally, in this last section we are going to apply our findings about binormal evolution surfaces to some special cases. Depending on the velocity  $\mathcal{F} = \dot{P}$  of the evolution we will have different properties on the surface.

### 3.4.1 Pure Binormal Evolution and Hopf Cylinders

We first choose a constant velocity  $\dot{P}$ . In this case, the binormal evolution equation can be considered to be  $x_t = B$ . These constant velocity binormal evolution surfaces have already appeared along this chapter, see Section 3.3. In fact, if for instance,  $\gamma$  is a Frenet helix, then by Proposition 3.3.1, the generated surface must be a flat isoparametric surface.

On the other hand, if  $\gamma$  has non-constant curvature and constant torsion, the congruence solutions of Gauss-Codazzi equations can be obtained by taking  $\mu = 0$  in (3.43). Notice that then,  $\kappa(s, t) = \kappa(s)$  and  $\mathcal{F}(\kappa(s)) = \lambda$  and  $S_\gamma$  is flat.

Moreover, (3.43) implies that  $\rho = (-1)^r \tau_o^2$ . Thus  $M_r^3(\rho)$  has to be either  $\mathbb{S}^3(\rho)$  or  $\mathbb{H}_1^3(\rho)$ . Flat surfaces in  $\mathbb{S}^3(\rho)$  can be locally described as the product, with respect to the Lie group structure of  $\mathbb{S}^3(\rho)$ , of two curves with torsions  $\rho$  and  $-\rho$ , respectively, [61]. In order to construct explicit parametrizations solving (3.3) in this case, we take the complex plane,  $\mathbb{C}$ , and consider the maps  $\pi_\varepsilon : \mathbb{C}^2 \rightarrow \mathbb{C}^2$  defined by  $\pi_\varepsilon(z_1, z_2) = \frac{1}{2c}(\bar{z}_1 z_1 - \varepsilon \bar{z}_2 z_2, 2z_2 \bar{z}_1)$ , where,  $z_i \in \mathbb{C}, i \in \{1, 2\}$ ,  $\bar{z}_i$  denotes complex conjugate,  $\varepsilon = \pm 1$  and  $c \in \mathbb{R}$ . Endow  $\mathbb{C}^2$  with the semi-Riemannian metric  $\langle z, w \rangle = \text{Real}(z_1 \bar{w}_1 + \varepsilon z_2 \bar{w}_2)$ . Then, the restriction of  $\pi_\varepsilon$  to the hyperquadrics  $\langle z, z \rangle = \varepsilon c^2$ ,  $\varepsilon = \pm 1$ , gives two maps which are known as the *standard Hopf mappings*

$$\pi_+ : \mathbb{S}^3\left(\frac{1}{c^2}\right) \rightarrow \mathbb{S}^2\left(\frac{4}{c^2}\right), \quad \text{and} \quad \pi_- : \mathbb{H}_1^3\left(\frac{-1}{c^2}\right) \rightarrow \mathbb{H}^2\left(\frac{-4}{c^2}\right).$$

Let  $\gamma$  be a curve in either  $\mathbb{S}^2\left(\frac{4}{c^2}\right)$  or  $\mathbb{H}^2\left(\frac{-4}{c^2}\right)$ . Then, the complete lift  $\mathbb{T}_\gamma^+ = \pi_+^{-1}(\gamma)$  (respectively,  $\mathbb{T}_\gamma^- = \pi_-^{-1}(\gamma)$ ) is a Riemannian (respectively, Lorentzian) flat (zero Gaussian curvature) surface in  $\mathbb{S}^3\left(\frac{1}{c^2}\right)$  (respectively, in  $\mathbb{H}_1^3\left(\frac{-1}{c^2}\right)$ ) which is called the *Hopf cylinder on  $\gamma$* . The covering maps  $\Psi^+ : \mathbb{R}^2 \rightarrow \mathbb{T}_\gamma^+$  and  $\Psi^- : \mathbb{L}^2 \rightarrow \mathbb{T}_\gamma^-$  defined by

$$\Psi^\pm(t, s) = e^{it} \bar{\gamma}(s), \tag{3.44}$$

where  $\bar{\gamma}(s)$  denotes a *horizontal lift* of  $\gamma$  can be used to parametrize  $\mathbb{T}_\gamma^\pm$ . Assuming without loss of generality  $c = 1$ , that is,  $\rho = \pm 1$ , critical curves of  $\int_\gamma \kappa$  in  $\mathbb{S}^3(1)$  or  $\mathbb{H}_1^3(-1)$  are characterized by having torsion  $\tau^2 = 1$ , [6] and [22]; and, therefore, they must be horizontal lifts via Hopf maps. Hence,

**Proposition 3.4.1.** ([10]) *Horizontal lifts via the Hopf map  $\pi_\pm$  of arbitrary curves  $\gamma$  of  $\mathbb{S}^2(4)$  or  $\mathbb{H}^2(-4)$  parametrized by (3.44) evolve under  $x_t = B$  by rigid motions and the*

corresponding binormal evolution surface is a Hopf cylinder of  $\mathbb{S}^3(1)$  or  $\mathbb{H}_1^3(-1)$  shaped on  $\gamma$ ,  $\mathbb{T}_\gamma^\pm$ .

Thus, explicit parametrizations of  $\mathbb{T}_\gamma^\pm$  are obtained as follows. Take an arbitrary curve  $\gamma(s) = (A_1(s), 0, A_2(s), A_3(s))$  in  $\mathbb{S}^2(4)$  or  $\mathbb{H}^2(-4)$ , then horizontal lifts of  $\gamma$  via  $\pi_+$  or  $\pi_-$  are given by

$$\begin{aligned} \bar{\gamma}(s) = (\alpha_1(s) \cos \beta(s), \alpha_1(s) \sin \beta(s), \alpha_2(s) \cos \beta(s) - \alpha_3(s) \sin \beta(s), \\ \alpha_2(s) \sin \beta(s) + \alpha_3(s) \cos \beta(s)), \end{aligned}$$

where

$$\alpha_1(s) = \frac{\sqrt{2A_1(s) + 1}}{\sqrt{2}}, \quad \alpha_2(s) = \frac{\sqrt{2}A_2(s)}{\sqrt{2A_1(s) + 1}}, \quad \alpha_3(s) = \frac{\sqrt{2}A_3(s)}{\sqrt{2A_1(s) + 1}},$$

and

$$\beta(s) = \pm 2 \int \frac{A_3(s)A_2'(s) - A_2(s)A_3'(s)}{2A_1(s) + 1} ds.$$

Hence, one uses (3.44) to obtain a solution of (3.3). Notice that if the curve  $\gamma$  is embedded in either  $\mathbb{S}^2(4)$  or  $\mathbb{H}^2(-4)$ , then so is  $\mathbb{T}_\gamma^\pm$  in  $\mathbb{S}^3(1)$  or  $\mathbb{H}_1^3(-1)$  and we have binormal Hopf cylinders with no self-intersections. Moreover, if  $\gamma$  is a closed curve then  $\mathbb{T}_\gamma^\pm$  is a closed surface (a flat Hopf Tori) but the evolving filament  $\bar{\gamma}(s)$  may not be closed because of the non-trivial holonomy. However, if, in addition, the area enclosed by  $\gamma(s)$  in either  $\mathbb{S}^2(4)$  or  $\mathbb{H}^2(-4)$  is a rational multiple of  $\pi$ , then there are  $m \in \mathbb{Z}$  such that the horizontal lift of an  $m$ -cover of  $\gamma(s)$  is a closed filament, [6].

Finally, in this case  $\Theta$  given in (1.61) is nothing but

$$\Theta(\gamma) = \int_\gamma \kappa + \mu\tau + \lambda.$$

Critical curves for Lagrangians of the form  $\Theta_{\nu\mu\lambda}(\gamma) = \int_\gamma \nu\kappa(s) + \mu\tau(s) + \lambda$ , where  $\nu, \mu, \lambda \in \mathbb{R}$ , have been used to construct models of spinning relativistic particles, both massive and massless, in Lorentzian backgrounds, [57]. If the ambient space is a Riemannian space form,  $M^3(\rho)$ , it is known that a curve  $\gamma \in M^3(\rho)$  is critical for  $\Theta_{\nu\mu\lambda}$ , if and only if,  $\gamma$  is a Lancret helix in  $M^3(\rho)$ , [7]. Hence, Lancret curves evolve under (3.3) by congruence and slippage. The most interesting case is when  $M^3(\rho) = \mathbb{S}^3(\rho)$ , since it is the only case in which the variational problem associated to the *total curvature energy*,  $\mu = \lambda = 0$ , makes sense, [7].

### 3.4.2 Hasimoto Surfaces and Elasticae

We choose now  $\zeta \equiv 1$  in (3.2). In other words, we are going to consider the evolution in  $M_r^3(\rho)$  of a unit speed Frenet curve,  $\gamma(s)$ , of rank 2 or 3 under the extension of the

localized induction equation, (3.2). Let  $x(s, t)$  describe the evolution of  $\gamma(s)$  under (3.2). Since our curves  $\gamma$  are arc-length parametrized, (3.2) can be simplified in terms of the binormal flow, (3.3)

$$x_t = \varepsilon_2 \varepsilon_3 \kappa B$$

and the corresponding evolution surfaces are known as *Hasimoto surfaces*. In this case, we have  $\dot{P} = \varepsilon_2 \varepsilon_3 \kappa$ . Moreover, Gauss-Codazzi equations, (3.11) and (3.12) reduce to

$$\kappa_t = -\varepsilon_2 \varepsilon_3 (2\kappa_s \tau + \kappa \tau_s), \quad (3.45)$$

$$\tau_t = \varepsilon_2 \left( \varepsilon_2 \frac{\kappa_{ss}}{\kappa} - \varepsilon_3 \tau^2 + \frac{1}{2} \varepsilon_1 \kappa^2 + \varepsilon_1 \varepsilon_2 \rho \right)_s. \quad (3.46)$$

Notice that if we were considering evolution under localized induction equation, (3.1), in the standard Euclidean case, then  $\varepsilon_i = 1$ , for  $i = 1, 2, 3$ , and (3.45) and (3.46) would be precisely the *Da Rios equations*, [130]. In other words, in the Euclidean case Da Rios equations are nothing but the Gauss-Codazzi equations of Hasimoto surfaces expressed with respect to the geodesic coordinate system (1.20). By this reason the Gauss-Codazzi equations of the general case, (3.45) and (3.46), will be referred to as the *Codazzi-Da Rios equations in space forms*. Remember that Da Rios equations first appeared when the movement of a thin vortex filament in a viscous fluid by the motion of a curve propagating in  $\mathbb{R}^3$  according to the localized induction equation, (3.1), was modeled by Da Rios, [130]. Later on, Hasimoto discovered [73] that the localized induction equation is equivalent to the *nonlinear Schrödinger equation* which is a well-known example of soliton equation.

Furthermore, in this case the complex wave equation corresponding to (3.45) and (3.46) boils down to (see (3.15))

$$(1 - \varepsilon_2 \varepsilon_3) \frac{\Psi}{|\Psi|} |\Psi|_{ss} = i \varepsilon_2 \varepsilon_3 \Psi_t + \Psi_{ss} + \varepsilon_1 \varepsilon_3 \left( \frac{|\Psi|^2}{2} + \varepsilon_3 \rho \right) \Psi. \quad (3.47)$$

So we see that in the Euclidean space,  $M_r^3(\rho) = \mathbb{R}^3$ , (3.47) is nothing but the focusing nonlinear Schrödinger equation, recovering the correspondence found by Hasimoto. Now, in the Minkowski 3-space case,  $M_r^3(\rho) = \mathbb{L}^3$ , we obtain the defocusing nonlinear Schrödinger equation if  $\varepsilon_2 \varepsilon_3 = 1$ .

Finally, notice that for Hasimoto surfaces the energy  $\Theta$  given in (1.61) is nothing but  $\Theta(\gamma) = \int_\gamma \kappa^2 + \mu \tau + \lambda$ . In  $\mathbb{R}^3$ , extremals of this functional are known to be centerlines of Kirchhoff elastic rods, [93]. The converse is also true [81]. In other words, in  $\mathbb{R}^3$  traveling wave solutions of the Gauss-Codazzi-Da Rios equations (3.45) and (3.46) determine Hasimoto surfaces  $S_\gamma$  whose initial conditions  $\gamma$  are centerlines of Kirchhoff rods. They evolve under the localized induction equation, (3.1), by rigid motions and slippage in  $\mathbb{R}^3$ , [93]. In [86] the notion of Kirchhoff elastic rods is extended to Riemannian 3-space forms,  $M^3(\rho)$ , and it is shown that centerlines of Kirchhoff elastic rods provide solutions to the Euler-Lagrange equations for  $\Theta(\gamma) = \int_\gamma \kappa^2 + \mu \tau + \lambda$  in  $M^3(\rho)$ . This is the reason why



in Section 1.3.2 we have used that name. Moreover, classical elasticae in  $M^3(\rho)$  evolve by rigid motions and correspond to soliton solutions of the localized induction equation. We also remark that centerlines of Kirchhoff elastic rods can be identified with magnetic trajectories of Killing magnetic fields in  $M^3(\rho)$ , [19].

On the other hand, in Lorentzian backgrounds (3.2) has been studied in [21] and [49], while long time existence of closed solutions in Riemannian ambient spaces are analyzed in [90].



## Chapter 4

# Invariant Constant Mean Curvature Surfaces in 3-Space Forms

The concept *mean curvature* was first introduced by Germain in 1831, [66], who applied the total mean curvature to describe elastic shells. In many cases, the mean curvature gives us enough information to understand the extrinsic geometry of an immersed surface into the ambient space. In fact, for a surface immersed in  $M_r^3(\rho)$ , the most important extrinsic invariant is, probably, the mean curvature.

Of special interest are surfaces of *constant mean curvature* (CMC, for short), which have played a prominent role in Analysis and Differential Geometry. Among them, if the mean curvature vanishes, these surfaces are usually called *minimal surfaces* of  $M_r^3(\rho)$ . The study of minimal surfaces in 3-space forms is one of the oldest subjects in Differential Geometry. Indeed, minimal surfaces in  $\mathbb{R}^3$  have played a major role in Mathematics since the 1800's, as evidenced by the names of many outstanding mathematicians who got involved in their early developments (Weirstrass, Riemann, Enneper, Scherk,...).

On the other hand, invariant surfaces have rich symmetry which make them ideal for modeling physical systems. Therefore, these two things have stimulated the interest of many authors in studying invariant surfaces with constant mean curvature along the centuries. For instance, a nice application of surfaces of revolution with CMC in  $\mathbb{R}^3$ , regarding liquid bridges between vertical walls, is obtained in [139].

In 1841, Delaunay introduced a way of constructing rotationally symmetric CMC surfaces in  $\mathbb{R}^3$ , by proving that, basically, *a surface of revolution in  $\mathbb{R}^3$  is a CMC surface, if and only if, its profile curve is the roulette of a conic*, [47]. An explicit parametrization of Delaunay surfaces was given by Kenmotsu in 1980, [88], using an approach from complex analysis. Three years later, following this method Do Carmo and Dajczer, [35], gave the parametrization of CMC surfaces of the Euclidean 3-space,  $\mathbb{R}^3$ , invariant under one-parameter groups of isometries, that is, invariant under helicoidal motions. There are many works in the literature using different approaches to study rotational type CMC surfaces both, in Riemannian and Lorentzian 3-space forms (for more details, see [48],

[72], [80], [98], [131], [135],... and the references therein).

Moreover, one of the roulette curves in  $\mathbb{R}^2$  is the catenary which generates the catenoid, the minimal non-trivial surface of revolution. Catenaries are known to be solutions of a classical variational problem. In fact, *they have the shape of a rope when fixing the extremes of it and letting gravity acts on the other part*. However, in 1930, Blaschke proved that catenaries are also a solution of another variational problem ([29], pp. 38-39). To be more precise, Blaschke studied smooth immersed curves in  $\mathbb{R}^3$  which are extremal for the curvature energy functional  $\Theta(\gamma) = \int_{\gamma} \sqrt{\kappa} ds$ ,  $\kappa$  being the curvature of the curve, and he showed that *catenaries are critical for  $\Theta$  when it is acting on planar curves*.

The above facts motivated us to study CMC surfaces in Riemannian and Lorentzian 3-space forms,  $M_r^3(\rho)$ , which are invariant under the flow of a Killing vector field of the ambient space. Along the first part of this chapter, we first describe any CMC invariant surface locally as a binormal evolution surface, which allows us to understand them as *warped product surfaces*, so that their local intrinsic geometry is totally determined by the *warping function*. Moreover, we show that warping functions of invariant CMC surfaces are solutions of an *Ermakov-Milne-Pinney* (EMP) equation with constant coefficients, [54] and [127]. Then, an extension of Blaschke's variational problem is studied. Namely, we will introduce the functional  $\Theta_{\mu}(\gamma) = \int_{\gamma} \sqrt{\kappa - \mu} ds$ , for a fixed  $\mu \in \mathbb{R}$  (notice that this functional falls into the family of generalized elastic functionals (2.2)), and consider the associated variational problem when  $\Theta_{\mu}$  is acting on a certain space of smooth curves immersed in a Riemannian or Lorentzian 3-space form. The corresponding Euler-Lagrange equations, which are expressed in terms of the curvature and the torsion of the critical curves, are integrated. This solves the variational problem geometrically, since curves are completely determined by curvature and torsion (and the Frenet frame causal characters, in the Lorentzian case) in 3-space forms. As a consequence, we will see that extremals (recall the convention introduced in Section 1.3) of  $\Theta_{\mu}$  include roulettes of both the Euclidean plane,  $\mathbb{R}^2$ , and also those of  $\mathbb{L}^2$ , the Minkowski plane. In particular, if  $\mu = 0$ , we will recover Blaschke's result on catenaries of  $\mathbb{R}^2$ .

Furthermore, we also prove that extremals of  $\Theta_{\mu}$  evolving under an associated Killing field,  $\xi$ , produce invariant CMC surfaces in  $M_r^3(\rho)$ . On the other hand, a CMC surface  $N^2$  of  $\mathbb{R}^3$  which is invariant by a one-parameter group of rigid motions is shown to be, locally, spanned by an extremal curve of  $\Theta_{\mu}(\gamma) = \int_{\gamma} \sqrt{\kappa - \mu} ds$  while evolving by  $\xi$ . In particular, if  $N^2$  is a surface of revolution in  $\mathbb{R}^3$ , then it has to be a Delaunay's surface and roulettes of conics (other than lines) are critical for  $\Theta_{\mu}$ . Moreover, this is also true in general backgrounds. We are going to prove that invariant CMC surfaces in 3-space forms are locally foliated by geodesics of the surface being extremals of  $\Theta_{\mu}$ , for a given  $\mu \in \mathbb{R}$ , as curves in the ambient space.

In the second part of this chapter, we use our previous findings to extend two classical results on CMC in  $\mathbb{R}^3$ . In particular, we construct two-parameter families of isometric

deformations preserving the constant mean curvature. This generalizes the well-known isometric deformation of the catenoid into the helicoid and the corresponding extension to CMC surfaces of  $\mathbb{R}^3$ , [35]. Also, in this part, we extend the correspondence between CMC surfaces in different Riemannian 3-space forms described by Lawson [96].

Finally, in the last part of the chapter, by restricting ourselves to Riemannian ambient spaces, we use the variational characterization of profile curves of invariant CMC surfaces to study global properties of these surfaces. More precisely, after describing the local classification of CMC rotational surfaces in Riemannian 3-space forms,  $M^3(\rho)$ , we prove the existence of compact and embedded CMC rotational tori in  $\mathbb{S}^3(\rho)$ , by analyzing the simplicity and closure of planar critical curves for the extension of Blaschke's variational problem.

## 4.1 Characterization as Binormal Evolution Surfaces

Along this section, assume that  $S_\gamma$  is a local description of a  $\xi$ -invariant surface of  $M_r^3(\rho)$  with constant mean curvature,  $H$ , where  $\xi$  denotes a Killing vector field on  $M_r^3(\rho)$  (see Section 1.2.3). Then, following the notation introduced in that section and Chapter 3, we have

**Theorem 4.1.1.** ([12]) *Let  $\xi$  be a non-null Killing vector field on  $M_r^3(\rho)$  and assume that  $S_\gamma$  is a local description of a  $\xi$ -invariant surface of  $M_r^3(\rho)$  with constant mean curvature,  $H$ . Then, locally,  $S_\gamma$  is either a ruled surface or it is spanned by a critical curve  $\gamma(s)$  of  $\Theta_\mu(\gamma) = \int_\gamma \sqrt{\kappa - \bar{\mu}} ds$ ,  $\mu = -\varepsilon_1 \varepsilon_2 H$ , in the sense of Section 1.3, evolving by the flow of  $\xi$ . Moreover, in the latter case,  $S_\gamma$  is a binormal evolution surface with initial condition  $\gamma(s)$  and velocity  $\frac{1}{2\sqrt{\kappa(s) + \varepsilon_1 \varepsilon_2 H}}$ .*

*Proof.* Consider  $N_\nu^2 \subset M_r^3(\rho)$  an isometrically immersed  $\xi$ -invariant surface in any semi-Riemannian 3-space form  $M_r^3(\rho)$ , then, using the notation of Section 1.2.3, we have that  $N_\nu^2$  can locally be described as the warped product  $S_\gamma$  with metric given by  $g = \varepsilon_1 ds^2 + \varepsilon_3 G^2(s) dt^2$ , where  $G^2(s) = \tilde{\varepsilon} \langle \xi, \xi \rangle$ ,  $\tilde{\varepsilon}$  being the causal character of  $\xi$ . Moreover, it must satisfy the PDE system (1.29)-(1.31). The compatibility conditions for this system are given by the Gauss-Codazzi equations (3.11) and (3.12), which in our case, since  $\phi_t$  are isometries, can be shown to boil down to

$$0 = -2G_s \tau - \tau_s G, \quad (4.1)$$

$$0 = \left( \frac{1}{\kappa} (\varepsilon_2 \varepsilon_3 G_{ss} + \varepsilon_1 \varepsilon_3 G(\kappa^2 - \varepsilon_1 \varepsilon_3 \tau^2 + \varepsilon_2 \rho)) \right)_s - \varepsilon_1 \varepsilon_3 \kappa_s G, \quad (4.2)$$

where the involved functions depend only on  $s$ . Now, using (1.39), the mean curvature  $H$  can be computed, so that we get

$$G_{ss} - G(\varepsilon_1 \varepsilon_2 \kappa^2 + \varepsilon_2 \varepsilon_3 \tau^2 - \varepsilon_1 \rho) = 2H \kappa G, \quad (4.3)$$

for some constant  $H \in \mathbb{R}$ .

First, assume that  $\gamma$  has constant curvature  $\kappa \neq 0$  in  $M_r^3(\rho)$ . We combine (4.1) and (4.2) to obtain  $2\varepsilon_3 G(\kappa + \varepsilon_1 \varepsilon_2 H) = \varepsilon_3 c$ . Thus, if  $\kappa = -\varepsilon_1 \varepsilon_2 H$ ,  $\gamma$  has constant curvature making it a global minimum of  $\Theta_{-\varepsilon_1 \varepsilon_2 H}$  (see Section 2.1) and we are done.

If  $\kappa \neq -\varepsilon_1 \varepsilon_2 H$ , then substituting (4.3) into (4.2) we obtain that  $G$  is constant, so that (4.1) means that  $\tau$  must be constant too, and  $S_\gamma$  is a flat isoparametric surface foliated by congruent Frenet helices (see Proposition 3.3.1). Moreover,  $\kappa > 0$  and the sign of  $H$  can be inverted by changing the local orientation, so solving (4.3) for  $\kappa$  we get

$$\kappa = -\varepsilon_1 \varepsilon_2 H + \sqrt{H^2 - \varepsilon_1 \varepsilon_3 \tau^2 + \varepsilon_2 \rho}. \quad (4.4)$$

Thus, following (1.52) and (1.53), we obtain that  $\gamma$  is a constant curvature extremal for  $\Theta_\mu$  with  $\mu = -\varepsilon_1 \varepsilon_2 H$ , since it verifies (2.4) and (2.5).

Finally, suppose that  $\kappa$  is not constant. Locally, by the Inverse Function Theorem we can suppose that  $s$  is a function of  $\kappa$ , and, calling  $G(\kappa) = \dot{P}(\kappa)$ , where the upper dot denotes derivative with respect to  $\kappa$ , we have that (4.1)-(4.3) can be expressed in the following way

$$\left( \dot{P}^2 \tau \right)_s = 0, \quad (4.5)$$

$$\dot{P}_{ss} + \varepsilon_1 \varepsilon_2 \dot{P} (\kappa^2 - \varepsilon_1 \varepsilon_3 \tau^2 + \varepsilon_2 \rho) - \varepsilon_1 \varepsilon_2 \kappa (P + \lambda) = 0, \quad (4.6)$$

$$\dot{P}_{ss} - \varepsilon_1 \varepsilon_2 \dot{P} (\kappa^2 + \varepsilon_1 \varepsilon_3 \tau^2 - \varepsilon_2 \rho) - 2H\kappa \dot{P} = 0, \quad (4.7)$$

for some  $\lambda \in \mathbb{R}$ . Now, substituting (4.7) in equations (4.5) and (4.6), we obtain (1.52) and (1.53) what imply that  $\gamma(s)$  is critical for  $\Theta(\gamma) = \int_\gamma (P(\kappa) + \lambda) ds$ . Since  $H$  is constant, substitution of (4.6) into (4.7) and solving the resulting differential equation gives

$$P(\kappa) = c\sqrt{\kappa + \varepsilon_1 \varepsilon_2 H} - \lambda.$$

Thus,  $\gamma$  is critical for  $\Theta_\mu$ ,  $\mu = -\varepsilon_1 \varepsilon_2 H$ . This finishes the proof.  $\square$

Notice that the restriction of  $\xi$  to  $\gamma(s)$  is  $\xi(s) = \frac{1}{2\sqrt{\kappa(s) + \varepsilon_1 \varepsilon_2 H}} B(s)$ , where  $\kappa(s)$ ,  $B(s)$  and  $\varepsilon_i$ ,  $i \in \{1, 2, 3\}$  are the curvature, the Frenet binormal of  $\gamma(s)$ , and the causal characters of its Frenet frame, respectively. Hence, with the notation of above proof, we have that, locally, a  $\xi$ -invariant surface of  $M_r^3(\rho)$  can be seen as a warped product surface,  $S_\gamma$ , parametrized by (1.32) with warped metric (1.22) and warping function  $G(s) = \mathcal{F}(s, t)$  given by

$$G(s) = \sqrt{\tilde{\varepsilon} \langle \xi, \xi \rangle}, \quad (4.8)$$

where  $\tilde{\varepsilon}$  is the causal character of the Killing field  $\xi$ . Thus, the intrinsic geometry of  $S_\gamma$  is totally determined by  $G(s)$ , that is, by the length of the Killing field along the profile curve  $\gamma$ , (4.8).

As it turns out, for the local description of the CMC  $\xi$ -invariant surfaces,  $S_\gamma$ , the function  $G(s)$  is a solution of the Ermakov-Milne-Pinney (EMP, for short) equation with constant coefficients [127]

$$G''(s) + \alpha G(s) = \frac{\varpi}{G^3(s)}, \quad (4.9)$$

$\alpha$  and  $\varpi \in \mathbb{R}$ . A generalization of this connection has been studied in [63] (see also Section 5.1.1). In fact, if  $G(s)$  is constant, then by Proposition 3.3.1,  $S_\gamma$  is a flat isoparametric surface, and it trivially satisfies (4.9) for certain  $\alpha, \varpi \in \mathbb{R}$ . On the other hand, if  $G(s)$  is not constant, we have the following

**Theorem 4.1.2.** ([12]) *Let  $\xi$  be a non-null Killing vector field on  $M_r^3(\rho)$  and  $N_\nu^2$  be a  $\xi$ -invariant CMC  $H$  surface of  $M_r^3(\rho)$ . Assume that  $S_\gamma$  is a local description of  $N_\nu^2$  with profile curve  $\gamma$ , as an evolving curve with metric (1.22) and warping function  $G(s)$ , (4.8). Then, if  $S_\gamma$  is not flat,  $G(s)$  is a solution of the following EMP equation*

$$G''(s) + \varepsilon_1 \varepsilon_2 G(s)(H^2 + \varepsilon_2 \rho) = \frac{\varpi}{G^3(s)}, \quad (4.10)$$

where  $\varpi \in \mathbb{R}$  and  $\varepsilon_i, i \in \{1, 2, 3\}$  are the causal characters of the Frenet frame on  $\gamma$ .

*Proof.* Let's begin by taking  $\gamma$  a geodesic of  $M_r^3(\rho)$ . In this case, we must consider the frame introduced in Section 1.2.3. Now, since  $G(s)$  is not constant and  $S_\gamma$  has constant mean curvature (in particular,  $h_{22}$  is constant), then (1.37) gives  $h_{22} = 0$ , and therefore the mean curvature vanishes,  $H = 0$ . Hence, from (1.36) we get  $f(s) = \frac{\omega}{G^2(s)}$  with  $\omega \in \mathbb{R}$ . Finally, substituting this value of  $f(s)$  in the Gauss equation (1.35) we obtain

$$G_{ss} + \varepsilon_1 \rho G - \varepsilon_2 \varepsilon_3 \frac{\omega^2}{G^3} = 0, \quad (4.11)$$

which falls under (4.10) replacing the derivative notation there by subscripts and taking  $H = 0$ . Now, if  $\gamma$  has constant curvature,  $\kappa(s) = -\varepsilon_1 \varepsilon_2 H$ , then (4.1) and (4.2) reduce to

$$\tau(s)G^2(s) = \omega, \quad (4.12)$$

$$G_{ss} + \varepsilon_1 \varepsilon_2 G(H^2 + \varepsilon_2 \rho) - \varepsilon_2 \varepsilon_3 \frac{\omega^2}{G^3} = 0, \quad (4.13)$$

where  $\omega \in \mathbb{R}$ , and, again, the second equation, (4.13), is a particular case of (4.10). So, finally we assume that  $\kappa(s)$  is not constant. Then, from the proof of Theorem 4.1.1 we have that  $\gamma$  is a critical curve of  $\Theta_\mu(\gamma) = \int_\gamma \sqrt{\kappa + \varepsilon_1 \varepsilon_2 H} ds$ , with  $\mu = -\varepsilon_1 \varepsilon_2 H$ , and  $G$  is given by

$$G(s) = \frac{1}{2\sqrt{\kappa(s) + \varepsilon_1 \varepsilon_2 H}}. \quad (4.14)$$

Now, combining (4.1) and (4.2) with (4.14) we obtain

$$\tau(s)G^2(s) = \omega, \quad (4.15)$$

$$G_{ss} + \varepsilon_1\varepsilon_2G(H^2 + \varepsilon_2\rho) - \varepsilon_2\frac{\varepsilon_1 + 16\varepsilon_3\omega^2}{16G^3} = 0, \quad (4.16)$$

for some constant  $\omega \in \mathbb{R}$ . This finishes the proof.  $\square$

Thus, according to above results, if  $\xi$  is a non-null Killing field of  $M_r^3(\rho)$ , a  $\xi$ -invariant surface  $N_\nu^2 \subset M_r^3(\rho)$  with constant mean curvature  $H$  admits a local description  $S_\gamma$ , the  $\xi$ -orthogonal evolution of an extremal curve of  $\Theta_\mu$ ,  $\gamma$ , (with non-null velocity and acceleration vectors) along the flow of  $\xi$ .  $S_\gamma$  is a warped product surface whose intrinsic geometry is determined by the length of  $\xi$  along the profile curve  $\gamma(s)$ ,  $G(s) = |\xi(s)|$ , (4.8). The extrinsic geometry of  $S_\gamma$  is determined by  $\gamma$  and the value of  $\xi$  along it. But the profile curve itself is determined, in turn, by its curvature  $\kappa(s)$ , torsion  $\tau(s)$  and causal character of the Frenet frame. Hence, we have the following four cases for  $S_\gamma$

(i)  $\kappa(s)$  is constant.

- (a)  $\kappa(s) = 0$ . Then  $\tau$  is not defined and  $G(s)$  is solution of the EMP equation (4.11).  $S_\gamma$  is a ruled surface and, if  $G$  is constant, it is flat.
- (b)  $\kappa(s) = -\varepsilon_1\varepsilon_2H$ . In this case,  $\tau = \frac{\omega}{G^2(s)}$ ,  $\omega \in \mathbb{R}$  and  $G(s)$  is solution of the EMP equation (4.13). If  $G$  is constant,  $S_\gamma$  is flat.
- (c)  $\kappa$  and  $\tau$  are two constants satisfying (4.4)

$$(\kappa + \varepsilon_1\varepsilon_2H)^2 = H^2 - \varepsilon_1\varepsilon_3\tau^2 + \varepsilon_2\rho.$$

Then, the profile curve  $\gamma$  is a Frenet helix in  $M_r^3(\rho)$  and  $S_\gamma$  is always flat in this case. Indeed,  $S_\gamma$  is a flat isoparametric surface (see Proposition 3.3.1).

- (ii)  $\kappa(s)$  is not constant. Now,  $G(s)$  is given by (4.14) and so, the torsion is  $\tau(s) = e(\kappa(s) + \varepsilon_1\varepsilon_2H)$  for some  $e \in \mathbb{R}$ . Moreover,  $G(s)$  is a solution of the EMP equation (4.16).  $S_\gamma$  is never flat in this case.

Now, calling  $\mu = -\varepsilon_1\varepsilon_2H$ , we have that in the second part of case (i), (b), the profile curve  $\gamma$  is a global minimum for the energy  $\Theta_\mu(\gamma) = \int_\gamma \sqrt{\kappa - \mu} ds$  acting on a suitable space of curves, see Section 2.1. Finally, in the last part of case (i), (c), and in (ii), we have that the profile curve  $\gamma(s)$  is a critical curve for the energy  $\Theta_\mu(\gamma) = \int_\gamma \sqrt{\kappa - \mu} ds$  and the restriction of  $\xi$  to  $\gamma(s)$  is  $\xi(s) = \frac{1}{2\sqrt{\kappa(s) + \varepsilon_1\varepsilon_2H}} B(s)$ , where  $B(s)$ ,  $\varepsilon_i$ ,  $i \in \{1, 2, 3\}$  are the Frenet binormal of  $\gamma(s)$ , and the causal character of its Frenet frame, respectively.



## 4.2 Extension of Blaschke's Variational Problem

Notice that from the last remark of previous section, §4.1, it makes sense to study the functional  $\Theta_\mu(\gamma) = \int_\gamma \sqrt{\kappa - \mu} ds$ , in order to geometrically obtain all its critical curves. This functional corresponds with the generalized elastic functional  $\Theta_\mu^{\epsilon,p}$ , (2.2), for the particular choices  $p = \frac{1}{2}$  and  $\epsilon = 1$ .

For this purpose, we will assume from now on that all our curves are Frenet curves, and for a fixed constant  $\mu \in \mathbb{R}$  we will consider the following *curvature energy functional*  $\Theta_\mu = \Theta_\mu^{1,1/2}$ , (2.2),

$$\Theta_\mu(\gamma) := \int_\gamma \sqrt{\kappa - \mu} = \int_0^L \sqrt{\kappa(s) - \mu} ds, \quad (4.17)$$

where, as usual, the arc-length or natural parameter is represented by  $s \in [0, L]$ ,  $L$  being the length of  $\gamma$ . As a particular case of (2.2), observe that any curve with  $\kappa = \mu$  will be a global minimum among curves with  $\sqrt{\kappa - \mu} \in L^1([0, L])$ . Then, we consider  $\Theta_\mu(\gamma) \geq 0$  acting on  $\Omega_{p_0 p_1}^{r\rho*}$ , which was defined in Section 2.1.1 as

$$\Omega_{p_0 p_1}^{r\rho*} = \{\beta : [0, 1] \rightarrow M_r^3(\rho) \mid \beta(i) = p_i, i \in \{0, 1\}, \frac{d\beta}{dt}(t) \neq 0, \forall t \in [0, 1], \kappa > \mu\}, \quad (4.18)$$

where  $p_i \in M_r^3(\rho)$ ,  $i \in \{0, 1\}$ , are arbitrary given points of  $M_r^3(\rho)$ .

This is a generalization of the problem studied by Blaschke in the Euclidean 3-space  $\mathbb{R}^3$  with  $\mu = 0$ , [29]. Actually, the above variational problem can be considered on curves of  $M_r^n(\rho)$ , but, as we have already mentioned in Proposition 1.3.1, a curve critical for  $\Theta_\mu$  must lie in a totally geodesic  $M_r^3(\rho) \subset M_r^n(\rho)$ . As a consequence, it will be enough to study our functional (4.17) acting on the space of smooth immersed curves of  $M_r^3(\rho)$ ,  $\Omega_{p_0 p_1}^{r\rho*}$ , (4.18). Moreover, if  $\beta$  lies fully in  $M_r^3(\rho)$ , then  $\kappa$  is positive and, for our purposes  $\mu$  can be considered to be non-positive, then the restriction  $\kappa > \mu$  in the definition of  $\Omega_{p_0 p_1}^{r\rho*}$ , (4.18), can be omitted. On the other hand, if  $\beta$  lies fully in  $M_r^2(\rho)$ , then  $\kappa$  is considered to be the signed curvature.

Then, following the arguments and notation of Section 2.1.1, a critical curve  $\gamma \in \Omega_{p_0 p_1}^{r\rho*}$  of  $\Theta_\mu(\gamma) = \int_\gamma \sqrt{\kappa - \mu} ds$  is characterized by  $\mathcal{E}(\gamma) = 0$ , where  $\mathcal{E}$  is the Euler-Lagrange operator defined in (1.51). Thus, substituting the value of  $P(\kappa) = \sqrt{\kappa - \mu}$  in (1.52) and (1.53) (also using (2.4) and (2.5)),  $\mathcal{E}(\gamma) = 0$  boils down to

$$\frac{d^2}{ds^2} \left( \frac{1}{\sqrt{\kappa - \mu}} \right) + \frac{1}{\sqrt{\kappa - \mu}} (\varepsilon_1 \varepsilon_2 \kappa^2 - \varepsilon_2 \varepsilon_3 \tau^2 + \varepsilon_1 \rho) - 2\varepsilon_1 \varepsilon_2 \kappa \sqrt{\kappa - \mu} = 0, \quad (4.19)$$

$$\frac{d}{ds} \left( \frac{\tau}{\kappa - \mu} \right) = 0, \quad (4.20)$$

which are the *Euler-Lagrange* equations of the curvature energy functional  $\Theta_\mu(\gamma) = \int_\gamma \sqrt{\kappa - \mu} ds$  acting on  $\Omega_{p_0 p_1}^{r\rho*}$ , (4.18).

In order to integrate (4.19) and (4.20) we define the following parameters in terms of the sectional curvature  $\rho$ , the energy index  $\mu$ , and the two constants of integration  $d, e \in \mathbb{R}$ , (1.57) and (1.58),

$$a = -\varepsilon_1\rho - \varepsilon_1\varepsilon_2\mu^2, \quad b = 4\varepsilon_2d + 2\varepsilon_1\varepsilon_2\mu, \quad c = -\varepsilon_1\varepsilon_2 - \varepsilon_2\varepsilon_3e^2, \quad \Delta = 4ac - b^2. \quad (4.21)$$

Now, we have

**Proposition 4.2.1.** ([12]) *Let  $\gamma$  be an extremal for  $\Theta_\mu(\gamma) = \int_\gamma \sqrt{\kappa - \mu} ds$  acting on  $\Omega_{p_0 p_1}^{r\rho*}$ , (4.18). If  $\gamma$  has constant curvature  $\kappa_o$ , then  $\gamma$  is a Frenet helix with curvature given by*

$$\kappa_o = \mu + \sqrt{\mu^2 - \varepsilon_1\varepsilon_3\tau_o^2 + \varepsilon_2\rho}, \quad (4.22)$$

and where  $\tau_o$  (the torsion of  $\gamma$ ) can be any constant verifying  $\varepsilon_1\varepsilon_3\tau_o^2 < \mu^2 + \varepsilon_2\rho$ . Now, assume that  $\gamma$  has non-constant curvature  $\kappa(s)$ . Then, with the notation introduced in (4.21),  $\kappa(s)$  depends on two parameters  $d, e$  and we have

(i) If  $\Delta \neq 0$  and  $a \neq 0$ ,

$$\kappa(s) = \frac{2a}{-b + \sqrt{|\Delta|}f(2\sqrt{|a|}s)} + \mu, \quad (4.23)$$

where,  $f(x) = \sinh x$ , if  $\Delta > 0$  and  $a > 0$ ;  $f(x) = \cosh x$ , if  $\Delta < 0$  and  $a > 0$ ; and  $f(x) = \sin x$ , if  $\Delta < 0$  and  $a < 0$ .

(ii) If  $\Delta = 0$  and  $a > 0$

$$\kappa(s) = \frac{2a}{1 - b \exp(2\sqrt{a}s)} + \mu. \quad (4.24)$$

(iii) If  $\Delta < 0$  and  $a = 0$

$$\kappa(s) = \frac{b}{b^2s^2 - c} + \mu. \quad (4.25)$$

(iv) Finally, if  $\Delta = 0$  and  $a = 0$ , the curvature is given by,

$$\kappa(s) = \frac{1}{2\sqrt{c}s} + \mu. \quad (4.26)$$

Moreover, in all above cases the torsion of the curve  $\gamma$  is  $\tau = e(\kappa - \mu)$ ,  $e \in \mathbb{R}$ .

*Proof.* If  $\kappa$  is constant, then (4.20) implies that  $\tau$  must also be constant, and then equation (4.19) gives

$$\kappa_o = \mu + \sqrt{\mu^2 - \varepsilon_1\varepsilon_3\tau_o^2 + \varepsilon_2\rho}.$$

Observe, that this relation between the constant curvature  $\kappa_o$  and torsion  $\tau_o$  of critical Frenet helices already appeared in (4.4). Now, if  $\kappa$  is not constant, we know that (2.8)

and (2.9) are first integrals of the Euler-Lagrange equations (2.4) and (2.5). Then, by substituting  $P(\kappa) = \sqrt{\kappa - \mu}$  in (2.8) and (2.9) and simplifying one gets

$$\left(\frac{d\kappa}{ds}\right)^2 = 4\varepsilon_2(\kappa - \mu)^2(4d(\kappa - \mu) - \varepsilon_3e^2(\kappa - \mu)^2 - \varepsilon_1(\kappa - 2\mu)^2 - \varepsilon_1\varepsilon_2\rho), \quad (4.27)$$

$$\tau = e(\kappa - \mu). \quad (4.28)$$

In order to solve these equations, we make the change of variable,  $x = \kappa - \mu$ . Then, we see that (4.27) reduces to  $x_s^2 = 4x^2Q(x)$ , where  $Q(x) = cx^2 + bx + a$ . Thus, equation (4.27) only makes sense if  $Q(x) \geq 0$  what imposes some conditions on the parameters. That is, the following two cases are not possible; first,  $\Delta \geq 0$  and  $c < 0$ ; and, second,  $a \leq 0$ ,  $2d = -\varepsilon_1\mu$  and  $e^2 = -\varepsilon_1\varepsilon_3$ . Then, after lengthy computations with the aid of suitable formulas in [68], equation (4.27) can be solved for the rest of cases obtaining (4.23)-(4.26). Finally, the torsion of the curve is determined by (4.28).  $\square$

**Remark 4.2.2.** *The integration constants  $d$  and  $e$  are not entirely arbitrary. They are constrained by (1.57) and (1.58). Thus, for instance, when  $M_r^3(\rho) = M^3(\rho)$ , the Riemannian case, then  $\Delta$  must be negative, so that if  $a \leq 0$  we obtain  $d > \frac{-\mu + \sqrt{\mu^2 + \rho}}{2}$ .*

Notice that the Fundamental Theorem for Frenet Curves tells us that the Frenet curvatures  $\kappa(s)$  and  $\tau(s)$  (and the causal character of the Frenet frame in  $M_r^3(\rho)$  in the Lorentzian case,  $r = 1$ ) completely determine the curve up to isometries. Thus, the solutions of the Euler-Lagrange equations given in Proposition 4.2.1 provide the extremal curves of our variational problem (under suitable boundary conditions).

In the Riemannian setting,  $M^3(\rho)$ , things can be made simpler. Now, we get from equation (4.21) that  $\Delta$  must be negative and the non-constant solutions of (4.19) are

**Corollary 4.2.3.** *([12]) Assume that  $M^3(\rho)$  is a Riemannian 3-space form. Let  $\gamma$  be an extremal (with non-constant curvature) for  $\Theta_\mu(\gamma) = \int_\gamma \sqrt{\kappa - \mu} ds$  acting on  $\Omega_{p_0 p_1}^{\rho*}$ , (4.18). Then*

(i) *If  $-\rho = \mu^2$ , then  $a = 0$  and*

$$\kappa(s) = \frac{b}{b^2s^2 - c} + \mu. \quad (4.29)$$

(ii) *If  $-\rho < \mu^2$ , then  $a < 0$  and*

$$\kappa(s) = \frac{2a}{-b + \sqrt{-\Delta} \sin(2\sqrt{-a}s)} + \mu. \quad (4.30)$$

(iii) *If  $-\rho > \mu^2$ , then  $a > 0$  and*

$$\kappa(s) = \frac{2a}{-b + \sqrt{-\Delta} \cosh(2\sqrt{a}s)} + \mu. \quad (4.31)$$

Again, the torsion of  $\gamma$  is given by  $\tau = e(\kappa - \mu)$ ,  $e \in \mathbb{R}$ .

Case (i) of Corollary 4.2.3 ( $\mu = 0$  and  $M^3(\rho) = \mathbb{R}^3$ ) was obtained by Blaschke in [29]. Moreover, in this case the equation (4.20) implies that  $\tau = e\kappa$ ,  $e \in \mathbb{R}$ , and the solutions are all *Lancret curves* in  $\mathbb{R}^3$  with non-constant curvature and torsion. See also [119]. In particular, in the planar case setting,  $\tau = 0 = e$ , we see that the curvature obtained in (i) of Corollary 4.2.3 is precisely that of a *catenary* in  $\mathbb{R}^2$ . Catenaries can be generated by the trace of the focus of a parabola when rolling it along a line. More generally, the loci of a focus of a conic as the point of contact rolls along a straight line without slipping in a plane are called *roulettes of conics* in  $\mathbb{R}^2$ . A *line* is generated when the conic is a circle since its focus coincides with its center. If the conic is a parabola, as we have just said, its focus traces a *catenary*. For a hyperbola we get a *nodary*; for a proper ellipse, an *undulary*; and, finally, if our conic is degenerate we obtain a *circle*. Then, we obtain the geometric characterization of critical curves of  $\Theta_\mu$  in the plane. In fact, curves with constant curvature are either lines or circles, and they are also roulettes of conic foci. As for the critical curves with non-constant curvature one has

**Corollary 4.2.4.** ([12] and [64]) *Non-constant curvature critical curves for  $\Theta_\mu(\gamma) = \int_\gamma \sqrt{\kappa - \mu}$  in  $\mathbb{R}^2$  are, precisely, the roulettes of conic foci with non-constant curvature (that is, other than lines and circles).*

*Proof.* From the first two items in Corollary 4.2.3, (4.29) and (4.30), the planar critical curves of  $\Theta_\mu$  have curvature

$$\kappa(s) = \frac{4d}{1 + 16d^2s^2}, \quad (4.32)$$

for every  $d > 0$  if  $\mu = 0$ , and if  $\mu \neq 0$ , we have that,

$$\kappa(s) = \frac{2\mu(\omega^2 + \omega \sin(2\mu s))}{1 + \omega^2 + 2\omega \sin(2\mu s)}, \quad (4.33)$$

where  $\omega^2 = 1 + \frac{\mu}{d}$ . Since planar curves are totally determined by their curvature, it is enough to compute the curvature of the roulettes of conic foci. It is known that (4.32) corresponds to the curvature of the catenary. On the other hand, a direct computation of the curvatures of the roulettes using the parametrizations

$$\beta(s, \mu, \omega) = \left( \int_0^s \frac{1 + \omega \sin(2\mu t)}{\sqrt{1 + \omega^2 + 2\omega \sin(2\mu t)}} dt, \frac{\sqrt{1 + \omega^2 + 2\omega \sin(2\mu s)}}{2\mu} \right)$$

gives (4.33) for the curvature of the others. □

In particular, above curvature functions (4.32) and (4.33) represent a catenary for the case  $\mu = 0$ , a *nodary* for  $\mu \neq 0$  and  $\omega < 1$  and an *undulary* for  $\mu \neq 0$  and  $\omega > 1$ . Lines

and circles correspond to the global minima obtained when  $\kappa = \mu$ . If  $\mu = 0$  we have the real line. If  $\mu \neq 0$  and  $\kappa = \mu$  we get a circle. Notice, that circles with curvature  $\kappa = 2\mu$  for non-zero constant  $\mu$  also appear as extremal curves. Rolling constructions for generating curves of CMC surfaces in  $\mathbb{S}^3(\rho)$  and  $\mathbb{H}^3(\rho)$  have been developed in [135].

Another connection of our extremal curves with rolling curves can be given in  $\mathbb{L}^2$ . In fact, Hano and Nomizu, [72], defined spacelike roulettes of quadratic curves foci in  $\mathbb{L}^2$ , and show that CMC spacelike rotational surfaces in  $\mathbb{L}^3$  which are generated by rotating a planar curve, with spacelike or timelike axis, are obtained by rotating these roulettes. When the mean curvature is a constant  $H$  and the polar form of the profile curve is given by  $(r(\theta) \sinh \theta, r(\theta) \cosh \theta)$ , then, they show that  $r$  has to be of one of the following types;

- (i)  $r = \frac{1}{\nu}$  and  $H = \frac{-\nu}{2}$ ;
- (ii)  $\frac{1}{r} = \pm \lambda \cosh \theta + \nu$ ,  $\lambda > 0$  and  $H = \frac{(\lambda^2 - \nu^2)}{2\nu}$ ;
- (iii)  $\frac{1}{r} = \lambda \sinh \theta + \nu$ ,  $\lambda > 0$  and  $H = \frac{-(\lambda^2 + \nu^2)}{2\nu}$ ; or
- (iv)  $\frac{1}{r} = \eta \exp^{-\theta} + \nu$ , where  $\nu \neq 0$ .

On the other hand, if  $s$  denotes the arc-length parameter, then, it can be seen from formula (3) of [72] that the curvature of the profile curve  $\kappa(s)$  must satisfy  $\kappa(s) = \theta'(s) - \frac{1}{r(s)}$  and  $2\kappa(s) = \theta'(s) + 2H$ . By combining these two equations and substituting the values of  $r$  given in (i) to (iv) we obtain a ODE in  $\theta(s)$  which can be solved and, then, the curvature for spacelike roulettes of quadratic curves foci,  $\kappa(s)$ , is obtained. After suitable reparametrizations, it can be checked that these curvature functions fall under cases (i) to (iii) of Proposition 4.2.1. Profile curves,  $\gamma$ , for CMC spacelike rotational surfaces in  $\mathbb{L}^3$  of type  $S_\gamma$ , with lightlike axis of revolution are also given in [72]. It is a straightforward computation to check that the curvatures of these curves are also included in Proposition 4.2.1. Thus

**Corollary 4.2.5.** ([12]) *If  $\gamma$  lies in a Lorentzian plane,  $\gamma \subset \mathbb{L}^2$ , the locus of the origin when a part of a spacelike quadratic curve is rolled along a spacelike line is a spacelike critical curve for  $\Theta_\mu(\gamma) = \int_\gamma \sqrt{\kappa - \mu} ds$  in  $\mathbb{L}^2$ .*

### 4.2.1 Binormal Evolution of Extremal Curves

We have seen in Section 4.1 that the local description  $S_\gamma$  of any  $\xi$ -invariant CMC surface is spanned by an extremal curve of the extension of Blaschke's variational problem. Furthermore, in what follows we are going to prove the converse, giving a way of constructing CMC invariant surfaces from critical curves; namely the binormal evolution procedure introduced in Chapter 3.

Therefore, now we are going to consider a suitable binormal evolution in any 3-dimensional Riemannian or Lorentzian space form,  $M_r^3(\rho)$ , of a Frenet curve of rank

2 or 3,  $\gamma(s)$ , which is critical for the extension of the Blaschke's variational problem. In Proposition 1.3.2, we have proved that critical curves have an associated Killing vector field in the direction of the binormal which can be uniquely extended to a Killing vector field  $\mathcal{I}$  on the whole space,  $M_r^3(\rho)$ . Let's consider the one-parameter group of isometries determined by the flow of  $\mathcal{I}$ ,  $\{\phi_t, t \in \mathbb{R}\}$ , and define the surface  $S_\gamma := \{\phi_t(\gamma(s))\}$  obtained as the binormal evolution of  $\gamma$  under the  $\mathcal{I}$ -flow.

Observe that in our case, the velocity of the binormal evolution is given by  $\dot{P}(\kappa) = \frac{1}{2\sqrt{\kappa(s)-\mu}}$ , where  $\kappa(s)$  is the curvature of the critical curve and falls inside one of the cases of Proposition 4.2.1. Then, these  $\mathcal{I}$ -invariant surfaces  $S_\gamma$  have a very nice property. In fact, we have

**Theorem 4.2.6.** ([12]) *Let  $\gamma$  be an extremal curve of the energy  $\Theta_\mu(\gamma) = \int_\gamma \sqrt{\kappa - \mu} ds$  and let  $S_\gamma$  denote the  $\mathcal{I}$ -invariant surface in  $M_r^3(\rho)$  obtained by evolving  $\gamma$  under the flow of the Killing field  $\mathcal{I}$  which extends (2.6) (for our particular choices of  $\epsilon = 1$  and  $p = \frac{1}{2}$ ) to  $M_r^3(\rho)$ . Then  $S_\gamma$  has constant mean curvature  $H = -\epsilon_1\epsilon_2\mu$ .*

*Proof.* We know that our critical curve  $\gamma$  evolves by isometries of  $M_r^3(\rho)$ , sweeping out a surface,  $S_\gamma$ , which is not only a binormal evolution surface with velocity  $\dot{P}$ , but also a  $\mathcal{I}$ -invariant surface.

Then, as explained in Section 1.2.3, with respect to the coordinate system given by (1.32), the mean curvature function can be written as (1.39). Finally, by substitution of (4.19) and (4.20) into (1.39) and after some simplifications, we obtain  $H = -\epsilon_1\epsilon_2\mu$ . That is, as  $\mu \in \mathbb{R}$  is fixed,  $S_\gamma$  has constant mean curvature  $H = -\epsilon_1\epsilon_2\mu$ .  $\square$

Theorem 4.2.6 is particularly illuminating in  $\mathbb{R}^3$ . In fact, in 1841 Delaunay classified the surfaces of revolution with constant mean curvature, called *Delaunay surfaces*, and proved that they are obtained by rotating the roulette of a conic over the basic line; *a curve  $\gamma$  in the  $x_1x_2$ -plane generates a surface of constant mean curvature when rotated about the  $x_1$ -axis, if and only if,  $\gamma$  is the roulette of a conic rolling along the  $x_1$ -axis*, [47]. On the other hand, the classification of constant mean curvature helicoidal surfaces of  $\mathbb{R}^3$ , that is, surfaces invariant under a one-parameter group of helicoidal transformations, is given in [35]. Now, from Theorem 4.2.6, if  $\gamma$  is an extremal for  $\Theta_\mu(\gamma) = \int_\gamma \sqrt{\kappa - \mu} ds$ , then it evolves under  $x_t = \dot{P}B$  by rigid motions following the one-parameter group of isometries associated to the extension of  $\mathcal{I} = \dot{P}B$  to  $\mathbb{R}^3$ , sweeping out a surface with constant mean curvature. If  $\gamma$  is planar ( $\tau = 0$ ) and its curvature is constant, then  $\mathcal{I}$  is constant on  $\gamma$  and it sweeps out a circular cylinder by translations. If the curvature of  $\gamma$  is not constant, then the one-parameter group of  $\mathcal{I}$  is a group of rotations and  $\gamma$  spans a Delaunay surface. Now, if  $\gamma$  is a non-planar critical curve of  $\Theta_\mu(\gamma) = \int_\gamma \sqrt{\kappa - \mu} ds$  in  $\mathbb{R}^3$ , then its evolution under the flow of  $\mathcal{I}$  is driven by helicoidal motions and  $\gamma$  spans a helicoidal surface with constant mean curvature in  $\mathbb{R}^3$ , that is, one of the surfaces classified by Do Carmo and Dajczer [35].

## 4.2.2 Bour's Families of Invariant CMC Surfaces

From previous characterization we have that, basically, CMC  $\xi$ -invariant surfaces of  $M_r^3(\rho)$ , are locally either ruled surfaces  $S_\gamma$ ,  $\gamma$  being a geodesic; or, surfaces  $S_\gamma$  swept out by extremals  $\gamma$  of  $\Theta_\mu$  in the sense of Section 1.3. If  $\gamma$  has constant curvature, then  $S_\gamma$  can be either a flat isoparametric surface or it is determined by a solution of the EMP equations (4.11) or (4.13), according to whether the curvature of  $\gamma$  vanishes or not. Moreover, by manipulating both equations (4.11) and (4.13), it is easy to check that if  $\omega = 0$ , then we have that  $S_\gamma$  is a totally geodesic surface when  $\kappa = 0$ , or a totally umbilical surface if  $\kappa = \mu \neq 0$ . On the other hand, if  $\omega \neq 0$  in (4.11) or (4.13), one obtains a two-parameter family  $\mathcal{F}_{\omega\beta} = \{S_\gamma\}_{\omega\beta}$  where  $\beta$  is a constant of integration. Along this section, all the subscripts will denote the dependence of the corresponding function on them, do not confuse with the notation of the derivatives used in other parts of the memory.

If  $\gamma$  has non-constant curvature, then  $S_\gamma$  can be constructed, basically, by using just one function and Proposition 4.2.1 in the following manner. Given  $M_r^3(\rho)$  with  $r = 0, 1$ , let us fix a constant  $\mu \in \mathbb{R}$  and three numbers  $\{\varepsilon_i, i = 1, 2, 3\}$  satisfying (1.13). Take  $a, b, c, \Delta$  as defined in (4.21) with parameters  $d, e \in \mathbb{R}$  subjected to certain natural conditions as observed in Remark 4.2.2. Consider the corresponding functions  $\kappa(s) = \kappa_{de}(s)$  as defined in formulas (4.23)-(4.26) and  $\tau(s) = \tau_{de}(s) = e(\kappa_{de}(s) - \mu)$ . Once  $\kappa_{de}, \tau_{de}$  and  $\varepsilon_i, i = 1, 2, 3$  have been set up, consider  $\gamma_{d,e}$ , the only Frenet curve (up to congruences) of  $M_r^3(\rho)$  with curvature  $\kappa_{de}$ , torsion  $\tau_{de}$  and the following causal characters of its Frenet frame,  $\{T, N, B\}$ ;  $\langle T, T \rangle = \varepsilon_1$ ,  $\langle N, N \rangle = \varepsilon_2$ , and  $\langle B, B \rangle = \varepsilon_3$ . Now,  $\gamma_{d,e}$  is an extremal curve of  $\Theta_\mu$  under suitable boundary conditions and denote by  $S_{\gamma_{d,e}}$  the surface obtained as the evolution of  $\gamma_{d,e}$  under the Killing field  $\mathcal{I} = \xi_{de}$  determined in (2.6). Then, from Theorem 4.2.6 we know that  $S_{\gamma_{d,e}}$  is  $\xi_{de}$ -invariant surface of constant mean curvature  $H = -\varepsilon_1\varepsilon_2\mu$  with profile curve  $\gamma_{d,e}$ .

In this way, according to Theorem 4.2.6, for each possible choice of the ambient space,  $M_r^3(\rho)$ , constant  $\mu \in \mathbb{R}$ , and  $\{\varepsilon_i, i = 1, 2, 3\}$  satisfying (1.13), we have a two-parameter family of surfaces in  $M_r^3(\rho)$ ,  $\mathcal{F}_{d,e} := \{S_{\gamma_{d,e}} \mid d, e \in \mathbb{R}\}$ , with the same constant mean curvature  $H = -\varepsilon_1\varepsilon_2\mu$ . Moreover, any surface of  $\mathcal{F}_{d,e}$  is  $\xi_{de}$ -invariant for a certain Killing field  $\xi_{de}$  and is shaped on a critical curve  $\gamma_{d,e}$  of  $\Theta_\mu(\gamma) = \int_\gamma \sqrt{\kappa - \mu} ds$  with non-constant curvature  $\kappa_{de}$ .

Now, generalizing a classical result of Lawson in  $\mathbb{R}^3$  [96], we are going to see that for some cases, within each of these two-parameter families  $\mathcal{F}_{d,e}$  it is possible to find one-parameter subfamilies representing isometric deformations with the same constant mean curvature. Recall we are using the notation of (4.21) and Proposition 4.2.1.

**Theorem 4.2.7.** ([12]) *Choose  $r = 0$  or  $r = 1$  and two real constants  $\rho$  and  $\mu$ . Take  $\{\varepsilon_i, i = 1, 2, 3\}$  three numbers satisfying (1.13). For any real constant  $\nu$ , consider the conic  $\mathcal{C}_\nu$  in the  $(d, e)$ -plane defined by*

$$\mathcal{C}_\nu \equiv 1 + \varepsilon_1\varepsilon_3e^2 = \nu(2d + \varepsilon_1\mu)^2. \quad (4.34)$$

When points  $(d, e)$  are moving on a fixed conic,  $(d, e) \in \mathcal{C}_\nu$ , the above family  $\mathcal{F}_{d,e}$  becomes a one-parameter family, denoted here by  $\mathcal{F}_d^\nu$ . Assume that one of the two following conditions is satisfied

- (i)  $d \neq -\varepsilon_1 \frac{\mu}{2}$  and  $1 + \varepsilon_1 \varepsilon_2 a \nu > 0$ .
- (ii)  $\varepsilon_1 \rho < -\varepsilon_1 \varepsilon_2 \mu^2$ ,  $d \neq -\varepsilon_1 \frac{\mu}{2}$  and  $1 + \varepsilon_1 \varepsilon_2 a \nu < 0$ .

Then, if  $\mathcal{F}_d^\nu$  is not empty, it represents a one-parameter isometric deformation of  $\xi_{d,e}$ -invariant surfaces,  $\xi_{d,e}$  being Killing fields on  $M_r^3(\rho)$ , with the same mean curvature  $H = -\varepsilon_1 \varepsilon_2 \mu$ .

*Proof.* Observe that, apart from  $a$  which is constant, under condition (4.34) all other parameters defined in (4.21) depend only on  $d$ :  $b_d, c_d, \Delta_d$ . First assume  $\Delta_d \neq 0$ . Then, combining (4.21) and (4.34), we obtain  $\Delta_d = \varpi b_d$ , where  $\varpi$  is another constant given by  $\varpi = (\varepsilon_2(\rho + \varepsilon_2 \mu^2)\nu - 1)$ . Now, remember that the metric of  $S_{\gamma_{de}}$  is defined by  $g = \varepsilon_1 ds^2 + \varepsilon_3 G_d(s)^2 dt^2$ , where  $G_d(s)$ , given in (4.14), is  $G_d(s) = \frac{1}{2\sqrt{\kappa_d(s) - \mu}}$ .

Suppose  $a \neq 0$ , that is, we are in the first case of Proposition 4.2.1. Hence, using formula (4.23) we have

$$G_d^2(s) = b_d \frac{\sqrt{\varpi} f(2\sqrt{|a|s}) - 1}{8|a|} := b_d G_o^2(s).$$

Thus, we see that, after a suitable reparametrization, all  $S_{\gamma_{de}}$  within this family are isometric surfaces with the same constant mean curvature  $H = -\varepsilon_1 \varepsilon_2 \mu$ , what finishes this case.

Now, under the above assumptions (i) and (ii), only two more cases for  $\Delta_d$  are possible; *i)*  $\Delta_d < 0$  and  $a = 0$ , and *ii)*  $\Delta_d = a = 0$ . A similar argument shows that the corresponding values of  $G_d(s)$  under the deformation along the conic  $\mathcal{C}_\nu$  are, respectively,  $G_d(s) = \sqrt{b_d} G_o(s)$ , and,  $c G_o^4(s) = G_d^4(s)$ , for certain  $b_d, c \in \mathbb{R}$  and function  $G_o(s)$ . This finishes the proof.  $\square$

Notice that for the surface family corresponding to a profile curve of constant curvature with  $\omega \neq 0$ , the relation (4.34) becomes  $\omega^2 = \nu^2 \beta^2$ . Then, under the same conditions (i) and (ii) of Theorem 4.2.7, it can be seen that for each fixed  $\nu$  the family of surfaces  $\mathcal{F}_{\omega\beta}$  (introduced in the first paragraph of this section, §4.2.2) verifying  $\omega^2 = \nu^2 \beta^2$ , are all congruent among them and, in addition, they are isometric to  $\mathcal{F}_d^\nu$ . Moreover, making  $d, e$  tend to  $\infty$ , we find that the curvatures of the profile curves  $\gamma$  of the family  $\mathcal{F}_d^\nu$  approaches to  $\kappa = \mu$ , which is, precisely, the curvature of the profile curves for the surfaces in  $\mathcal{F}_{\omega\beta}$  with  $\omega^2 = \nu^2 \beta^2$ . In other words, *the surface obtained from a profile curve  $\gamma$  of constant curvature with  $\omega \neq 0$  can be understood as the "limit" surface of the family  $\mathcal{F}_d^\nu$* . This reflects what happens in the well-known catenoid-helicoid classical deformation, where the helicoid corresponds to a surface obtained from  $\omega \neq 0$ .



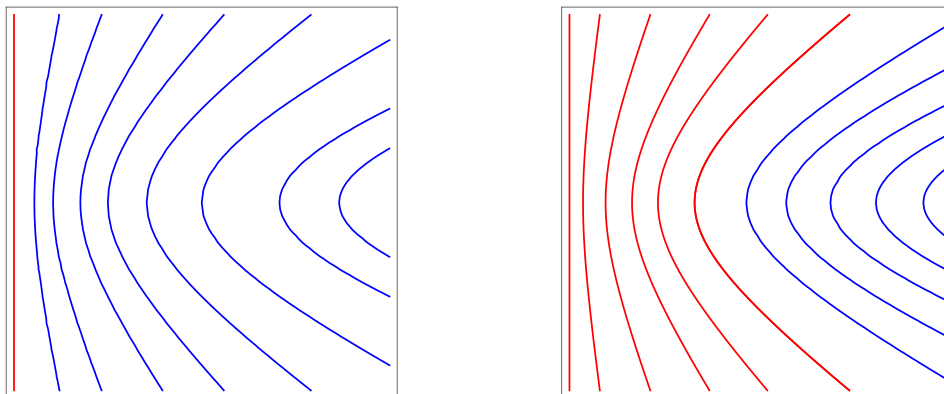


Figure 4.1: Conics  $\mathcal{C}_\nu$  of type (4.34) for: minimal surfaces in  $\mathbb{R}^3$  (Left); and, non-minimals in  $\mathbb{R}^3$  and all cases in  $\mathbb{S}^3(\rho)$  (Right).

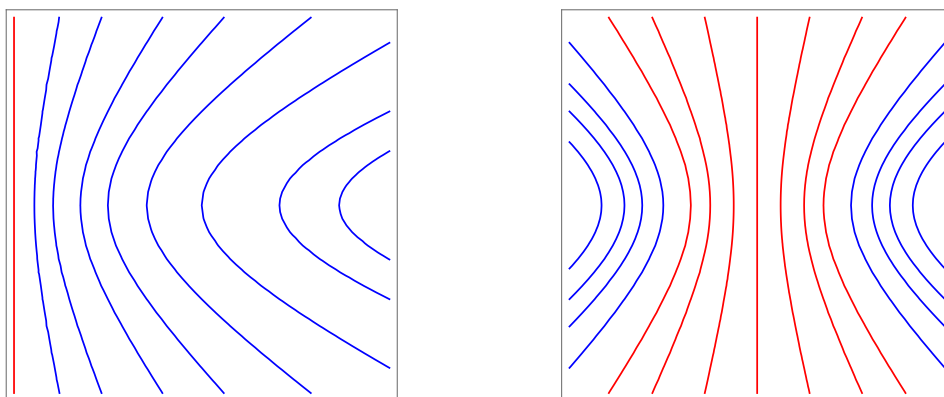


Figure 4.2: Conics  $\mathcal{C}_\nu$  of type (4.34) for:  $\rho + \mu^2 \leq 0$  in  $\mathbb{H}^3(\rho)$  (Left); and,  $\rho + \mu^2 > 0$  in  $\mathbb{H}^3(\rho)$  (Right).

Several families of conics  $\mathcal{C}_\nu$  of type (4.34) are drawn in Figures 4.1 to 4.5, for different values of the parameters. Profile curves  $\gamma_{d,e}$  of the surfaces  $\{S_{\gamma_{d,e}}\}$  belonging to one-parameter families  $\mathcal{F}_d^\nu$  included in Theorem 4.2.7 are determined by the curvature and torsion given in cases (i) and (iv) of Proposition 4.2.1. These  $\mathcal{F}_d^\nu$  correspond to conics  $\mathcal{C}_\nu$  satisfying conditions (i) and (ii) of Theorem 4.2.7 and which are painted in blue in Figures 4.1 to 4.5. Solutions of type (ii) in Proposition 4.2.1 are the curvature and torsion of profile curves  $\gamma_{de}$  for CMC surfaces  $S_{\gamma_{de}}$  which appear when the point  $(d, e)$  is moving on conics  $\mathcal{C}_\nu$  satisfying

$$d \neq -\varepsilon_1 \frac{\mu}{2}, \quad \nu a = -\varepsilon_1 \varepsilon_2, \quad \varepsilon_2 \varepsilon_3 e^2 < -\varepsilon_1 \varepsilon_2, \quad (4.35)$$

but this time the deformation along these conics does not provide isometric surfaces. These conics only appear in Lorentzian backgrounds and are painted in orange in Figures 4.3 and 4.5.

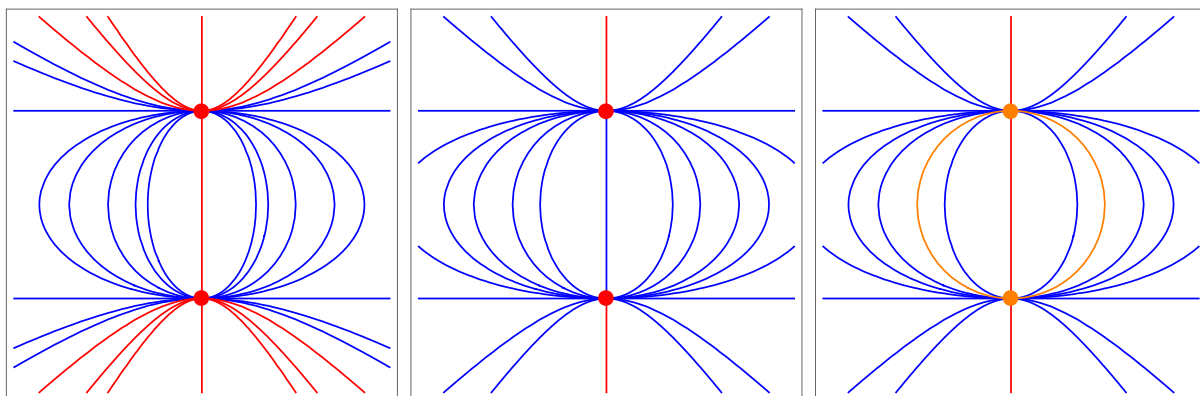


Figure 4.3: Conics  $\mathcal{C}_\nu$  of type (4.34) with  $\varepsilon_1 = -1$  for:  $\rho + \mu^2 < 0$  in  $\mathbb{H}_1^3(\rho)$  (Left);  $\rho + \mu^2 = 0$  in  $\mathbb{L}^3$  and  $\mathbb{H}_1^3(\rho)$  (Center); and,  $\rho + \mu^2 > 0$  in  $\mathbb{L}^3$ ,  $\mathbb{S}_1^3(\rho)$  and  $\mathbb{H}_1^3(\rho)$  (Right).

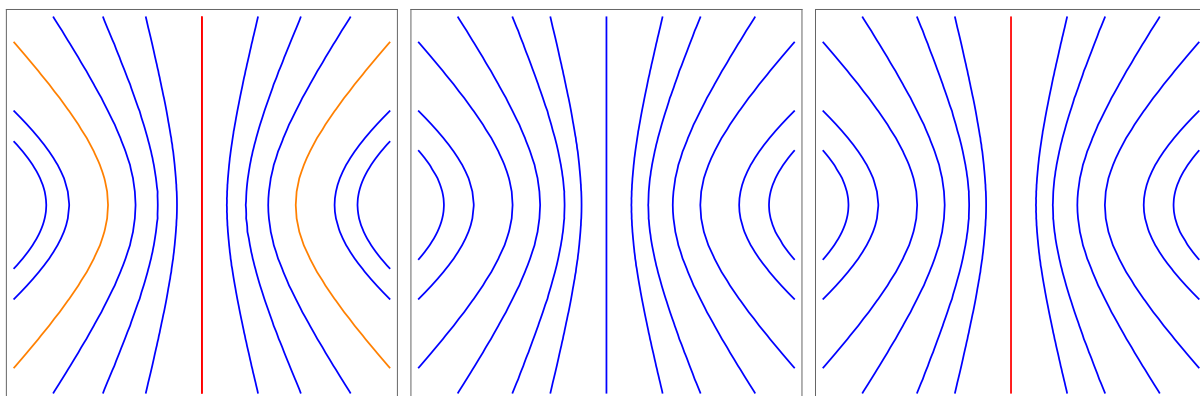


Figure 4.4: Conics  $\mathcal{C}_\nu$  of type (4.34) with  $\varepsilon_2 = -1$  for:  $\rho < \mu^2$  in  $\mathbb{L}^3$ ,  $\mathbb{S}_1^3(\rho)$  and  $\mathbb{H}_1^3(\rho)$  (Left);  $\rho = \mu^2$  in  $\mathbb{L}^3$  and  $\mathbb{S}_1^3(\rho)$  (Center); and,  $\rho > \mu^2$  in  $\mathbb{S}_1^3(\rho)$  (Right).

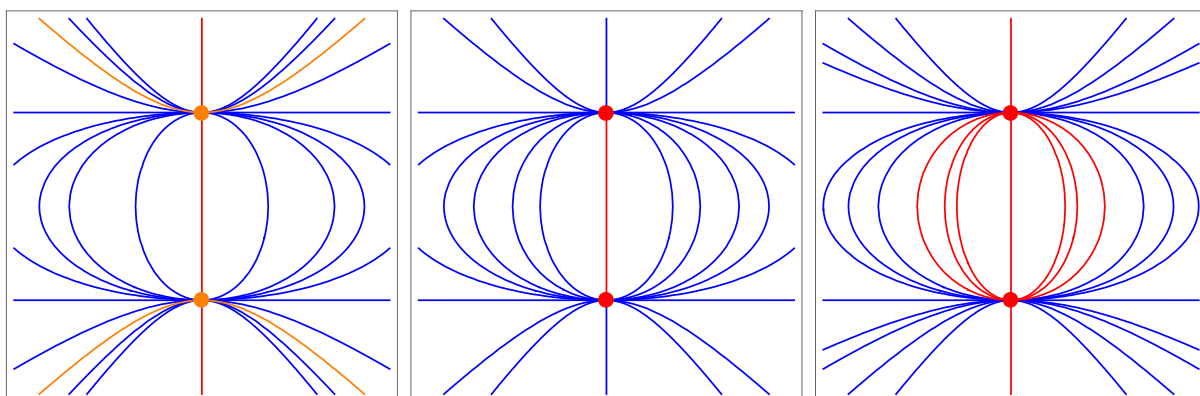


Figure 4.5: Conics  $\mathcal{C}_\nu$  of type (4.34) with  $\varepsilon_3 = -1$  for:  $\rho + \mu^2 < 0$  in  $\mathbb{H}_1^3(\rho)$  (Left);  $\rho + \mu^2 = 0$  in  $\mathbb{L}^3$  and  $\mathbb{H}_1^3(\rho)$  (Center); and,  $\rho + \mu^2 > 0$  in  $\mathbb{L}^3$  and  $\mathbb{S}_1^3(\rho)$  (Right).

If  $d = -\varepsilon_1 \frac{\mu}{2}$  and  $e^2 = -\varepsilon_1 \varepsilon_3$ , we also have solutions of type (ii) in Proposition 4.2.1, but now the conic degenerates to one point. On the other hand, if  $d = -\varepsilon_1 \frac{\mu}{2}$ ,  $\varepsilon_2 \varepsilon_3 e^2 < -\varepsilon_1 \varepsilon_2$  and  $\rho = -\varepsilon_2 \mu^2$  the conic degenerates to a piece of a line and the deformation along it also gives an isometric deformation. This case corresponds to surfaces  $S_{\gamma,d,e}$  whose profile curves have curvature and torsion of type (iv) in Proposition 4.2.1. Notice that for any other choices of the parameters  $d, e$  the conics  $\mathcal{C}_\nu$  (red conics in Figures 4.1 to 4.5) do not correspond to solutions of the extended Blaschke's problem solved in Proposition 4.2.1.

As we have just mentioned, families of surfaces  $\mathcal{F}_d^\nu$  corresponding to conics satisfying (4.35) provide an interesting difference between Riemannian and Lorentzian ambient spaces, since they only appear in the latter case and the deformation along the conics  $\mathcal{C}_\nu$  is not isometric but preserves the mean curvature  $H$ . In fact, conditions (4.35) amount to  $\Delta = 0$  and  $a > 0$  in (4.21). Let's take the unique curve  $\gamma$  (up to rigid motions and causal character of the Frenet frame) determined by a solution of the first integrals of the Euler-Lagrange equations with  $\Delta = 0$  and  $a > 0$ . The curvature and torsion of  $\gamma$  are given by (see Proposition 4.2.1)

$$\kappa(s) = \frac{2a}{1 - b \exp(2\sqrt{a}s)} + \mu, \quad \tau(s) = \frac{2ea \exp(2\sqrt{a}s)}{1 - b \exp(2\sqrt{a}s)}. \quad (4.36)$$

Thus, the binormal evolution surface generated by evolving  $\gamma$  under the extension of its associated Killing vector field  $\mathcal{I} = G(s)B(s, t)$ , where  $G(s)$  is

$$G(s) = \sqrt{\frac{1 - b \exp(2\sqrt{a}s)}{8a \exp(2\sqrt{a}s)}}, \quad (4.37)$$

defines a surface  $S_\gamma$  whose first fundamental form is given by

$$g = \varepsilon_1 ds^2 + \varepsilon_3 \frac{1 - b \exp(2\sqrt{a}s)}{8a \exp(2\sqrt{a}s)} dt^2,$$

while the second fundamental form is given in (1.27) where  $h_{22}$  is given by (1.28),  $G(s)$  is defined in (4.37) and  $\kappa(s)$  and  $\tau(s)$  are those of (4.36). These surfaces have constant mean curvature  $H = -\varepsilon_1 \varepsilon_2 \mu$  since they are generated by a critical curve of the extended Blaschke's variational problem, and they only appear in Lorentzian space forms,  $M_1^3(\rho)$ . Moreover, from the first fundamental form we see that  $\mathcal{F}_d^\nu$  does not give an isometric deformation of these  $\xi$ -invariant surfaces.

### 4.2.3 Lawson's Correspondence for Invariant CMC Surfaces

To finish this section, a couple of consequences of Theorem 4.2.7 are given; an extension of the so called Lawson's correspondence and an extension of a Do Carmo-Dajczer result on rotational CMC cousins.

There exists an elementary correspondence between CMC surfaces in the different 3-space forms, described by Lawson in the Riemannian case [96] and often attributed to him although it was known to Riccati. In Lorentzian space forms, there are also Lawson's type correspondences between spacelike CMC surfaces [118] and between timelike CMC surfaces [59]. Such CMC surfaces are called *cousins* of each other. The following version of Lawson's type correspondence for  $\xi$ -invariant surfaces can be obtained from our computations

**Theorem 4.2.8.** ([12]) *Take  $r = 0$  or  $r = 1$ . Choose real numbers  $\rho, \mu, \hat{\rho}, \hat{\mu}$  and  $\varepsilon$ , satisfying  $\varepsilon^{r+1} = 1$  and*

$$\rho + \varepsilon\mu^2 = \hat{\rho} + \varepsilon\hat{\mu}^2. \quad (4.38)$$

*Then, for each  $\nu \in \mathbb{R}$  with non-empty associated one-parameter family  $\mathcal{F}_d^\nu$ , there exists a warped product surface  $S^\nu$ , such that  $S^\nu$  admits both*

- (i) *A one-parameter family of isometric immersions in  $M_r^3(\rho)$  with the same mean curvature  $|H| = |\mu|$ , and*
- (ii) *A one-parameter family of isometric immersions in  $M_r^3(\hat{\rho})$  with the same mean curvature  $|\hat{H}| = |\hat{\mu}|$ .*

*Proof.* Take  $r, \rho, \mu, \hat{\rho}, \hat{\mu}$  and  $\varepsilon$  as stated above. Consider the following data  $r, \rho, \mu$  and three numbers  $\{\varepsilon_i, i = 1, 2, 3\}$  satisfying (1.13) and such that  $\varepsilon_2 = \varepsilon$ . For  $d, e$  real numbers satisfying suitable conditions (see Remark 4.2.2), define  $a, b, c, \Delta$  as in (4.21). Consider the corresponding functions  $\kappa_{de}(s)$  as defined in formulas (4.23)-(4.26) and the induced surface  $S_{\gamma_{d,e}}$  constructed at the beginning of this section.  $S_{\gamma_{d,e}}$  is a warped surface with metric determined by  $G_{de}(s) = \frac{1}{2\sqrt{\kappa_{de}(s) - \mu}}$ . Now, for  $\nu \neq 0$  take the conic  $\mathcal{C}_\nu$  (4.34), and assume that the one-parameter family of surfaces  $\mathcal{F}_d^\nu$  (defined in Theorem 4.2.7) is non-empty. For a fixed  $(d_o, e_o) \in \mathcal{C}_\nu$ , denote by  $S^\nu$  the corresponding surface of  $\mathcal{F}_d^\nu$ . Then, from Theorem 4.2.7,  $\mathcal{F}_d^\nu$  can be seen as a one-parameter family of isometric immersions of  $S^\nu$  into  $M_r^3(\rho)$  with constant mean curvature  $H = -\varepsilon_1\varepsilon_2\mu$ .

Now, for  $(d, e) \in \mathcal{C}_\nu$ , consider  $\hat{d}$  such that

$$2d + \varepsilon_1\mu = 2\hat{d} + \varepsilon_1\hat{\mu}. \quad (4.39)$$

Observe that  $(d, e) \in \mathcal{C}_\nu$ , if and only if,  $(\hat{d}, e) \in \mathcal{C}_\nu$  in the  $(\hat{d}, e)$ -plane.

Finally, for initial data  $r, \hat{\rho}, \hat{\mu}$  and  $\{\varepsilon_i, i = 1, 2, 3\}$  as before, consider the corresponding parameters defined in (4.21) and call them  $\hat{a}, \hat{b}, \hat{c}, \hat{\Delta}$ . Repeating the process we obtain a one-parameter family of isometric immersions of a warped surface  $\hat{S}^\nu$  into  $M_r^3(\hat{\rho})$ ,  $\mathcal{F}_{\hat{d}}^\nu$ , with constant mean curvature  $\hat{H} = -\varepsilon_1\varepsilon_2\hat{\mu}$ . Then, one can check that conditions (4.38) and (4.39) imply  $a = \hat{a}$ ,  $b = \hat{b}$ ,  $c = \hat{c}$ ,  $\Delta = \hat{\Delta}$ . Hence, from (4.23)-(4.26) we see that

$$G_{de}(s) = \frac{1}{2\sqrt{\kappa_{de}(s) - \mu}} = \frac{1}{2\sqrt{\hat{\kappa}_{de}(s) - \hat{\mu}}} = \hat{G}_{de}(s),$$

so that  $S^\nu$  and  $\widehat{S}^\nu$  are isometric and we are done.  $\square$

On the other hand, as mentioned before, in 1982 Do Carmo and Dajczer [35] investigated surfaces of constant mean curvature in  $\mathbb{R}^3$  which are generated from a plane curve by the action of a helicoidal group. They proved the following theorem; *a complete immersed CMC surface is helicoidal, if and only if, it is in the associated family of a Delaunay surface.* They proved this result by introducing for each helicoidal CMC immersion the two-parameter family of helicoidal surfaces given by Bour's Lemma and evaluating the constant mean curvature condition for the elements of these families [35]. Now, we can give the following extension of the above result to Riemannian 3-space forms

**Theorem 4.2.9.** ([12]) *Assume that  $S_\gamma$  is a local description of a  $\xi$ -invariant CMC  $H$  surface of a Riemannian 3-space form  $M^3(\rho)$ , verifying that its profile curve,  $\gamma$ , has non-constant curvature,  $\kappa$ . Then,  $S_\gamma$  can be isometrically deformed into a rotational surface with the same mean curvature  $H$ .*

*Proof.* The local description of any  $\xi$ -invariant CMC  $H$  surface belongs to a one-parameter family  $\mathcal{F}_d^\nu$ , associated to a conic  $\mathcal{C}_\nu$ , for a fixed  $\nu$ . In the Riemannian case,  $\mathcal{C}_\nu$  are hyperbolas in the  $(d, e)$ -plane. See Figures 4.1 and 4.2. All members of  $\mathcal{F}_d^\nu$  are isometric and have the same mean curvature  $H$ .

For a fixed  $\nu$ , consider  $S_\gamma$  the member of the family  $\mathcal{F}_d^\nu$  which corresponds to  $e = 0$ , that is, corresponding to the point in which  $\mathcal{C}_\nu$  crosses the horizontal axis in the  $(d, e)$ -plane. Since the torsion of  $\gamma$ , the profile curve of  $S_\gamma$ , is given by  $\tau(s) = e(\kappa(s) - \mu)$ , we have that  $\tau = 0$ , what means that  $\gamma$  is planar, that is, it is contained in a totally geodesic surface  $M^2(\rho)$  of  $M^3(\rho)$ .

Therefore, by applying Proposition 3.2.4, we conclude that  $S_\gamma$  is a rotational surface.  $\square$

Above Proposition does not hold in the Lorentzian case. In fact, on the one hand, as we noticed before, families of surfaces  $\mathcal{F}_d^\nu$  corresponding to conics satisfying (4.35) provide a deformation along the conics  $\mathcal{C}_\nu$  which is not isometric although it preserves the mean curvature  $H$ . On the other hand, there are values of  $\mu$  and  $\rho$  for which two types of conics  $\mathcal{C}_\nu$  appear, depending on the value of  $\nu$  (see Figures 4.3 and 4.5). In fact, in these cases we might have ellipses  $\mathcal{C}_\nu$ , as those shown in the central parts of the pictures given in Figures 4.3 and 4.5, or hyperbolas  $\mathcal{C}_\nu$  which correspond to the upper and lower part of the same pictures. In the latter case, the hyperbolas do not cross the  $d$ -axis, so that  $e$ , and therefore  $\tau$ , is never 0.

### 4.3 Delaunay Surfaces in Riemannian 3-Space Forms

Observe that the result proved in Theorem 4.2.9 highlights the importance of rotational CMC surfaces of Riemannian 3-space forms. As we have mentioned in the introduction

of this chapter, Delaunay constructed rotationally symmetric CMC surfaces of  $\mathbb{R}^3$  from roulettes of conics [47]. These roulettes have been proved to be planar critical curves of  $\Theta_\mu$ , (4.17), in Corollary 4.2.4. Moreover, in previous sections, we have also proved that the profile curves of local descriptions of rotational CMC surfaces in Riemannian 3-space forms are planar critical curves of  $\Theta_\mu$ , (4.17) (see Theorem 4.1.1 and Theorem 4.2.6). For this reason, along this section we are going to call *Delaunay surfaces* to all CMC rotational surfaces of any Riemannian 3-space form,  $M^3(\rho)$ .

In the Euclidean 3-space,  $\mathbb{R}^3$ , Delaunay surfaces are globally well-known, since they are Euclidean planes, catenoids (these two for the minimal case), spheres, cylinders, nodoids and unduloids.

On the other hand, CMC surfaces immersed in the 3-sphere,  $\mathbb{S}^3(\rho)$ , have played a major role in Mathematics in last decades. In 1966, Almgren [1] proved that *any immersed minimal 2-sphere in  $\mathbb{S}^3(\rho)$  must be totally geodesic* and, therefore, congruent to the equator. Moreover, in 1970, Lawson [96] proved that, *given any positive integer  $m$ , there exist at least one compact embedded minimal surface in  $\mathbb{S}^3(\rho)$  with genus  $m$* . In fact, if the genus of the CMC surface is 1, he conjectured that *the only embedded minimal tori, up to rigid motions in  $\mathbb{S}^3(\rho)$ , is the Clifford torus*, [97]. Lawson's conjecture was recently proved by Brendle in [30]. Furthermore, adapting the technique of this proof, Andrews and Li [3] proved the Pinkall-Sterling conjecture; *any CMC tori embedded in  $\mathbb{S}^3(\rho)$  must be rotationally symmetric*, [126]. In fact, these rotational CMC surfaces were completely classified by Perdomo, [121] and [122], and Andrews and Li [3].

The study of CMC surfaces in the hyperbolic 3-space,  $\mathbb{H}^3(\rho)$ , depends greatly on the value of the mean curvature,  $H$ . *For a surface with CMC  $H \geq \sqrt{-\rho}$ , it was shown that there is a corresponding cousin CMC surface in both  $\mathbb{R}^3$  and  $\mathbb{S}^3(\rho)$* . Due to the existence of Lawson's correspondence, there have been many articles about these CMC surfaces. For instance, Bryant constructed a Weierstrass type representation for surfaces with CMC  $H = \sqrt{-\rho}$  using the Lawson's correspondence [31]. However, there have been relatively few papers when CMC verifies  $H < \sqrt{-\rho}$ . In [123], Perdomo characterized these CMC rotational surfaces in terms of solutions of an ordinary differential equation. Moreover, using tools from equivariant geometry, Gomes described rotational CMC surfaces of  $\mathbb{H}^3(\rho)$  of spherical type, [67].

In this last part of the chapter we use the local characterization of rotational CMC surfaces of  $M^3(\rho)$  as binormal evolution surfaces swept out by planar critical curves of  $\Theta_\mu$ , in order to develop a new approach to study Delaunay surfaces in  $M^3(\rho)$ . Indeed, we give the local classification of CMC rotational surfaces in each 3-space form,  $M^3(\rho)$ .

Moreover, although the characterization introduced in previous sections is local in nature, it can be used to make a global analysis of these surfaces. In particular, in the round 3-sphere,  $\mathbb{S}^3(\rho)$ , we prove the existence of closed planar extremal curves for some particular cases, and, we also study when these critical curves are embedded in  $\mathbb{S}^2(\rho)$ , obtaining that the constant  $\mu$  plays an essential role. Finally, applying the properties obtained from the analysis of the planar critical curves, we recover many results about the

global properties of rotational CMC surfaces of  $\mathbb{S}^3(\rho)$ , previously obtained using different tools.

### 4.3.1 Local Classification of CMC Rotational Surfaces

In Section 4.1 we have proved that the profile curve of a local description of a CMC rotational surface of any Riemannian 3-space form,  $M^3(\rho)$ , is locally a planar critical curve of the extended Blaschke's variational problem  $\Theta_\mu$ , (4.17). Therefore, these profile curves are completely characterized by the curvatures given in Corollary 4.2.3, (4.29)-(4.31). Moreover, rotational CMC surfaces of  $M^3(\rho)$  can be locally described as binormal evolution surfaces swept out by these critical curves.

However, notice that in Proposition 4.2.1 there was another option for the curvature  $\kappa(s)$ , namely (4.22), which represents a constant solution of Euler-Lagrange equations, (4.19) and (4.20). In Proposition 3.2.3, it has been proved that the binormal evolution surfaces with this initial condition are flat isoparametric surfaces, and, therefore, in  $M^3(\rho)$ , they are spherical cylinders.

Furthermore, for the sake of completeness, we recall that  $\kappa = \mu$  was a global minimum of  $\Theta_\mu$ , (4.17), when acting on a different space of curves, see Section 4.2. As explained in the beginning of Section 4.2.2, the binormal evolution surfaces with initial condition of this type are totally umbilical surfaces.

Taking this into account, we are in conditions to state the main results of this section.

**Theorem 4.3.1.** ([14]) *Let  $S_\gamma$  be a rotational surface of  $\mathbb{R}^3$  with CMC  $H$ , and let's denote by  $\kappa(s)$  the curvature of the profile curve of  $S_\gamma$ ,  $\gamma$ . Then, locally,  $S_\gamma$  is a piece of one of the followings*

- (i) *A totally geodesic plane,  $\mathbb{R}^2$ ; if  $\kappa(s) = H = 0$ .*
- (ii) *A totally umbilical sphere; if  $\kappa(s) = |H| \neq 0$ .*
- (iii) *A circular cylinder; if  $\kappa(s) = 2|H| \neq 0$ .*
- (iv) *A binormal evolution surface parametrized by (3.30) where the initial condition  $\gamma$  has curvature  $\kappa(s)$  given by (4.29) or (4.30), the velocity is  $\dot{P}(\kappa) = \frac{1}{2\sqrt{\kappa-\mu}}$  and  $|\mu| = |H|$ .*

*Proof.* From Theorem 4.1.1, we have that the profile curve of  $S_\gamma$  must be, locally, a planar extremal curve for  $\Theta_\mu$ , (4.17), where  $|H| = |\mu|$ . Therefore, its curvature must be either  $\kappa(s) = |H|$ , or given by Proposition 4.2.1 (see also Corollary 4.2.3). We first recall that the case  $\kappa(s) = |H|$  represents totally umbilical surfaces, thus points (i) and (ii) are clear. On the other hand, if  $\kappa(s)$  is given in Proposition 4.2.1 and it is constant, (4.22), then  $S_\gamma$  must be a spherical cylinder, point (iii), as explained just before.

The other possible curvatures of Proposition 4.2.1 are also included in Corollary 4.2.3,

and are given by, (4.29) and (4.30). They give rise to binormal evolution surfaces with velocity  $\dot{P}(\kappa) = \frac{1}{2\sqrt{\kappa-\mu}}$ . For the parametrizations of these surfaces see Section 3.2.1.  $\square$

Notice that in the last point of previous theorem we get a *catenoid* if  $H = 0$ ; and a *nodoid* and an *unduloid*, if  $H \neq 0$ . The nodoid comes from (4.30) with  $\mu > 0$ , whereas the unduloid is given by a profile curve with curvature (4.30) and  $\mu < 0$ . This can also be checked from Corollary 4.2.4.

The particular case where  $H = 0$  has special interest, since it represents minimal rotational surfaces of  $\mathbb{R}^3$ . From Theorem 4.3.1, we obtain the following well-known classical result

**Corollary 4.3.2.** ([14]) *Let  $S_\gamma$  be a rotational minimal surface of  $\mathbb{R}^3$ . Then,  $S_\gamma$  must be congruent to either the plane, if the profile curve of  $S_\gamma$ ,  $\gamma$ , is a geodesic of  $\mathbb{R}^3$ ; or to the catenoid.*

Now, we are going to state a similar classification result for rotational CMC surfaces of the round 3-sphere,  $\mathbb{S}^3(\rho)$ .

**Theorem 4.3.3.** ([14]) *If we denote by  $S_\gamma$  a rotational surface of CMC  $H$  in  $\mathbb{S}^3(\rho)$  and by  $\kappa(s)$  the curvature of its profile curve,  $\gamma$ , then,  $S_\gamma$  must be locally congruent to a piece of one of the followings*

- (i) *The equator  $\mathbb{S}^2(\rho)$ ; if  $\kappa(s) = H = 0$ .*
- (ii) *A totally umbilical sphere; if  $\kappa(s) = |H| \neq 0$ .*
- (iii) *A Hopf Torus*

$$\mathbb{S}^1\left(\sqrt{\rho + \kappa^2}\right) \times \mathbb{S}^1\left(\frac{\sqrt{\rho}}{\kappa}\sqrt{\rho + \kappa^2}\right),$$

$$\text{if } \kappa(s) = -|H| + \sqrt{H^2 + \rho}.$$

- (iv) *A binormal evolution surface parametrized by (3.32) where the initial condition  $\gamma$  has curvature (4.30), the velocity is given by  $\dot{P} = \frac{1}{2\sqrt{\kappa-\mu}}$  and where  $|\mu| = |H|$ .*

*Proof.* This proof is similar to that of Theorem 4.3.1.  $\square$

Finally, we are going to develop a similar classification for the hyperbolic 3-space,  $\mathbb{H}^3(\rho)$ . Observe that, as it is clear from the different types of Killing vector fields, (3.22) and (3.23), the group of motions of this space is richer than those of  $\mathbb{R}^3$  and  $\mathbb{S}^3(\rho)$ , and because of this reason there are more options for the rotational CMC surface.

**Theorem 4.3.4.** ([14]) *Consider a rotational surface  $S_\gamma \subset \mathbb{H}^3(\rho)$  with CMC  $H$ . Assume that  $\kappa(s)$  is the curvature of the profile curve,  $\gamma$ . Then,  $S_\gamma$  is locally congruent to a piece of one of the following surfaces*



- (i) A totally geodesic hyperbolic plane,  $\mathbb{H}^2(\rho)$ ; if  $\kappa(s) = H = 0$ .
- (ii) A totally umbilical sphere when  $\kappa(s) = |H| > \sqrt{-\rho}$ .
- (iii) An equidistant surface when  $0 \neq \kappa(s) = |H| < \sqrt{-\rho}$ .
- (iv) An horosphere; if  $\kappa(s) = |H| = \sqrt{-\rho}$ .
- (v) An hyperbolic cylinder; if  $\kappa(s) = |H| + \sqrt{H^2 + \rho}$ .
- (vi) A binormal evolution surface with velocity  $\dot{P} = \frac{1}{2\sqrt{\kappa-\mu}}$ , parametrized by (3.35), if  $d > 0$ ; (3.37), if  $d < 0$ ; or (3.40), when  $d = 0$ . Furthermore, in all these cases, the initial condition  $\gamma$  has curvature (4.29), (4.30) or (4.31) and  $|\mu| = |H|$ .

*Proof.* We can prove this result arguing as in the proof of Theorem 4.3.1. □

As we can see, in the hyperbolic 3-space,  $\mathbb{H}^3(\rho)$ , things are a little bit more complicated. On one hand, we have three different types of rotations, as studied in Section 3.2.1, and on the other hand, there is another possibility for the curvature of the profile curve  $\kappa(s)$ , (4.31). If we restrict our attention to minimal rotational surfaces, we have that  $H = \mu = 0$ , so the only options are; the totally geodesic hyperbolic plane,  $\mathbb{H}^2(\rho)$ , and the binormal evolution surfaces given in point (vi) of Theorem 4.3.4, where  $\kappa(s)$  comes from (4.31). Thus, we obtain

**Corollary 4.3.5.** ([14]) *A minimal rotational surface,  $S_\gamma$ , of  $\mathbb{H}^3(\rho)$  with profile curve  $\gamma$  is locally congruent to a piece of either,  $\mathbb{H}^2(\rho)$  if  $\gamma$  is a geodesic of  $\mathbb{H}^3(\rho)$ ; or to one of the three binormal evolution surfaces described in point (vi) of Theorem 4.3.4, with  $\mu = 0$ , if  $\gamma$  has non-constant curvature.*

From the similarity with the Euclidean 3-Space, some authors [36] call *catenoids* of first, second and third type, respectively, to the binormal evolution surfaces appearing in Corollary 4.3.5.

To end up this section, notice that from the well-known global classification of CMC rotational surfaces of Euclidean 3-space,  $\mathbb{R}^3$ , which is locally given in Theorem 4.3.1, *the only closed surface is the totally umbilical sphere*. Moreover, in [2], the same result was proved for the hyperbolic 3-space,  $\mathbb{H}^3(\rho)$ , which means that *the binormal evolution surfaces for  $d > 0$  of point (vi) in Theorem 4.3.4 have non-closed profile curves*. However, in the round 3-sphere,  $\mathbb{S}^3(\rho)$ , the first points of Theorem 4.3.3, (i)-(iii), give local descriptions of closed rotational surfaces with CMC in  $\mathbb{S}^3(\rho)$ , which are not only spheres, but also tori (see for instance point (iii) in Theorem 4.3.3). Moreover, these surfaces are not only closed, but they are also embedded in  $\mathbb{S}^3(\rho)$ . On the other hand, the last case, (iv), depends greatly on the profile curve. In fact, if the profile curve is closed, then the surface  $S_\gamma$  would also be closed.

### 4.3.2 Embedded CMC Tori in the Round 3-Sphere

Now, we want to understand which of the rotational CMC surface of  $\mathbb{S}^3(\rho)$ , locally classified in point (iv) of Theorem 4.3.3, are closed. Then, using the results presented in Section 3.2.2, we have that there are two possibilities to obtain closed rotational CMC surfaces. The first one corresponds with planar critical curves that meet the axis of rotation, and the second one comes from planar closed critical curves. However, from equation (3.33), in this particular case we have

$$\bar{\kappa}_\delta^2 = \kappa_\delta^2 + \rho = \frac{d}{\dot{P}^2} = 4d(\kappa - \mu) > 0.$$

Therefore, the Euclidean radius of curvature of the orbits (taking into account the immersion of  $\mathbb{S}^3(\rho)$  into  $\mathbb{R}^4$ , see Section 1.2) is never zero, since  $\kappa$  is bounded (see (4.30)), what means that planar critical curves of the extended Blaschke's energy never cut the axis of rotation. Observe that this result can also be obtained by considering the fixed points of the binormal evolution, and checking that the evolution restricted to the initial curve  $\mathcal{I} = \dot{P}B$ , (2.6) for  $\epsilon = 1$  and  $p = 1/2$ , is never zero, that is, there are no fixed points along planar critical curves. Thus, we draw the same conclusion.

By the remark made just above, it is clear that it may be interesting to study closure conditions for profile curves of  $\Theta_\mu$ , (4.17), when acting on curves immersed in  $\mathbb{S}^2(\rho)$ , since closed planar critical curves with curvature given by (4.30) will generate CMC rotational tori, and these are the only possible non-isoparametric closed CMC rotational surfaces in  $\mathbb{S}^3(\rho)$ . Moreover, by the recently proved Pinkall-Sterling's conjecture, these are the only possible non-isoparametric CMC tori embedded in  $\mathbb{S}^3(\rho)$ .

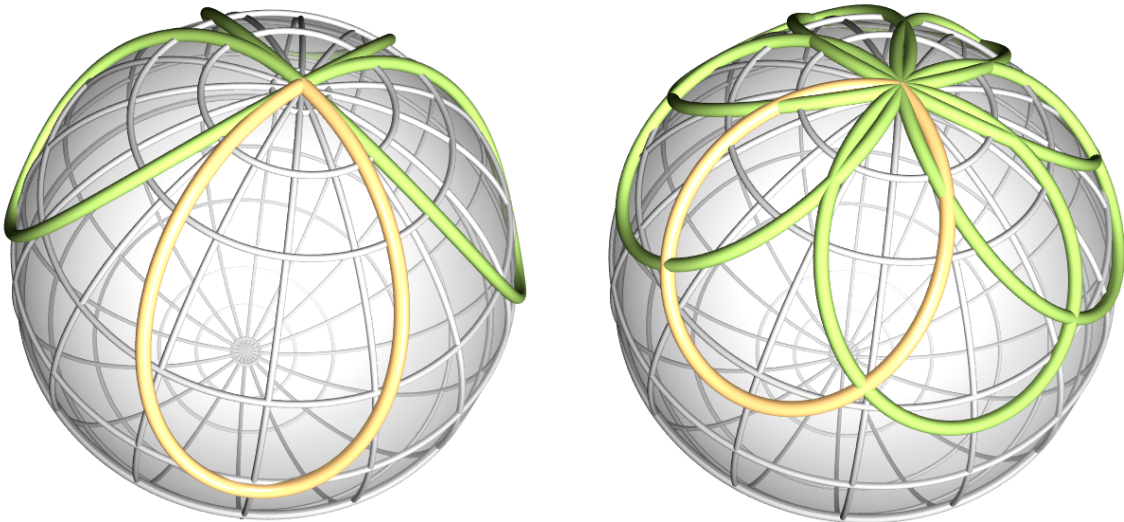


Figure 4.6: Closed planar extremal curves in  $\mathbb{S}^2(1)$  passing through the pole ( $4\mu d = 1$ ) for  $\mu \simeq 0.312$  (Left) and  $\mu \simeq 0.634$  (Right).

Therefore, along this section we are going to restrict ourselves to  $M^3(\rho) = \mathbb{S}^3(\rho)$ , the round 3-sphere. In this case, planar critical curves of  $\Theta_\mu$ , (4.17), are completely determined by the curvature  $\kappa(s)$ , (4.30). Notice that this curvature is periodic of period  $\varrho = \frac{\pi}{\sqrt{\rho+\mu^2}}$ .

Now, using (4.30), it is easy to check that whenever  $4\mu d \neq \rho$ , at maximum and minimum curvatures, the vector field  $\mathcal{J}$ , (2.7), has only component in  $T$ , which means that the critical curve is bounded between two parallels, which are the integral curves of  $\mathcal{J}$  at the maximum and minimum curvatures, respectively. What is more, the length of  $\mathcal{J}$  vanishes, if and only if,  $\kappa(s)$  reaches its minimum and  $4\mu d = \rho$  (observe that since  $d > 0$ , this equality can only occur for positive values of  $\mu$ ). In this particular case, the critical curve crosses the pole of the parametrization (see the parametrization given in (3.32) and Figure 4.6). However, notice that it is possible to find a reparametrization of the critical curve in order to delete this singularity. For instance, in Lemma 3.1 of [122] it has been done when  $\rho = 1$ .

In Figure 4.6 and 4.7, we can see some plots of closed critical curves of  $\Theta_\mu$ , (4.17) in  $\mathbb{S}^2(1)$ . These curves have periodic curvature,  $\kappa(s)$ , given by (4.30). The yellow part of these pictures corresponds with the part of the curve covered in one period of the curvature. Notice that, as the curvature is the same for each period of it, our critical curve is nothing but congruent copies of the yellow part, that is, the whole curve can be constructed by gluing smoothly as many copies of the trace covered in one period of the curvature as needed to close up the curve.

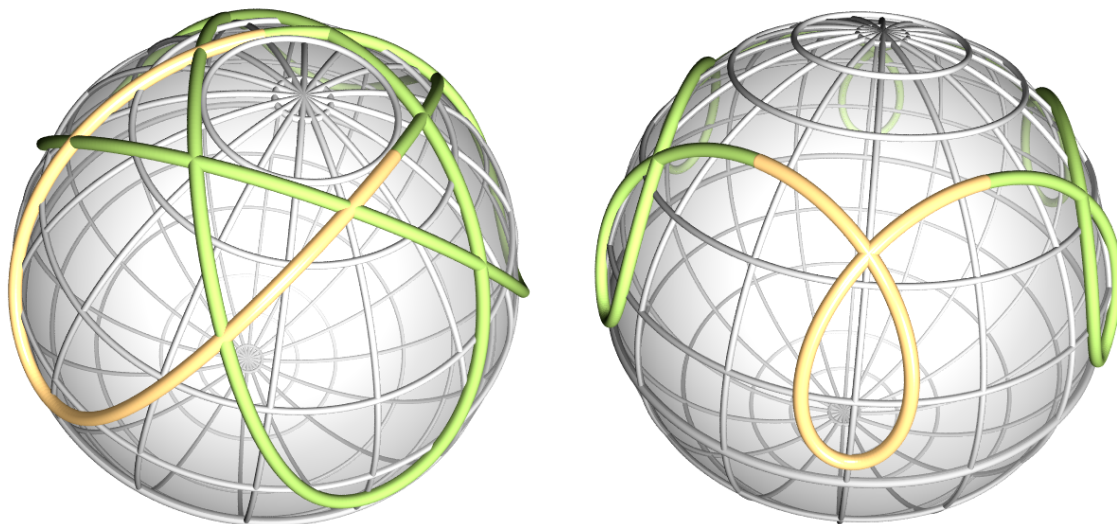


Figure 4.7: Closed planar extremal curves in  $\mathbb{S}^2(1)$  for:  $\mu = -0.1$  and  $d \simeq 1.27$  (Left); and,  $\mu = 1$  and  $d \simeq 1.81$  (Right). They close up for the values  $m = 5$  and  $n = 3$  (resp.,  $m = 6$  and  $n = 1$ ).

However, not every critical curve with periodic curvature (4.30) is closed. In fact, as Proposition 3.2.6 states, we need the closure condition to be satisfied. Now, since we are working in the round 3-sphere,  $\mathbb{S}^3(\rho)$ , by (1.58) we have that the constant of integration  $d$  must be positive (see also Remark 4.2.2). Moreover, in this case, the closure condition boils down to

$$I = -\frac{1}{2}\sqrt{\rho d}\Lambda(d) = \sqrt{\rho d} \int_0^{\varrho} \frac{(\kappa(s) - 2\mu) \sqrt{\kappa(s) - \mu}}{4d(\kappa(s) - \mu) - \rho} ds = \frac{n\pi}{m}, \quad (4.40)$$

for any integers  $n$  and  $m$ . We recall that  $n$  denotes the number of rounds the critical curve gives around the pole of the parametrization in order to close up, and that  $m$  is the number of lobes the critical curve has. Then, we can prove the existence of closed planar critical curves with non-constant curvature,  $\kappa(s)$ , given by (4.30), for any values of  $\mu$ .

Let  $\gamma$  be a planar ( $\tau = 0$ ) critical curve of  $\Theta_\mu$ , (4.17), completely determined by the curvature,  $\kappa(s)$ , given by (4.30). As these curvatures are periodic functions with period  $\varrho = \frac{\pi}{\sqrt{\rho + \mu^2}}$ , if we call  $\alpha$  to the maximum curvature of  $\kappa(s)$  and  $\beta$  to the minimum curvature, we obtain

$$\alpha = \kappa\left(\frac{\pi}{4\sqrt{\rho + \mu^2}}\right) \geq \kappa\left(-\frac{\pi}{4\sqrt{\rho + \mu^2}}\right) = \beta.$$

Then, we can rewrite the function on the left hand side of (4.40). By symmetry,

$$I = 2\sqrt{\rho d} \int_{-\frac{\pi}{4\sqrt{\rho + \mu^2}}}^{\frac{\pi}{4\sqrt{\rho + \mu^2}}} \frac{(\kappa(s) - 2\mu) \sqrt{\kappa(s) - \mu}}{4d(\kappa(s) - \mu) - \rho} ds. \quad (4.41)$$

Now, differentiating equation (4.30), we get that  $\kappa_s = 2(\kappa - \mu)\sqrt{4d(\kappa - \mu) - (\kappa - 2\mu)^2 - \rho}$ , which can be written in terms of the maximum and minimum curvatures,  $\alpha$  and  $\beta$ , respectively, as

$$\kappa_s = 2(\kappa - \mu)\sqrt{(\alpha - \kappa)(\kappa - \beta)}. \quad (4.42)$$

If we use above equation, (4.42), to make a change of variable in (4.41), we get

$$I = \sqrt{\rho d} \int_\beta^\alpha \frac{\kappa - 2\mu}{(4d(\kappa - \mu) - \rho) \sqrt{(\kappa - \mu)(\alpha - \kappa)(\kappa - \beta)}} d\kappa.$$

This integral can be written as a linear combination of complete elliptic integrals, see Appendix A. As  $d > 0$ , we have the following relation,  $4d(\kappa - 2\mu) = (4d(\kappa - \mu) - \rho) + \rho - 4\mu d$ , and, therefore, we conclude that

$$I = \frac{\sqrt{\rho}}{4\sqrt{d}} \left( \int_\beta^\alpha \frac{d\kappa}{\sqrt{(\kappa - \mu)(\alpha - \kappa)(\kappa - \beta)}} + (\rho - 4\mu d) \int_\beta^\alpha \frac{d\kappa}{(4d(\kappa - \mu) - \rho) \sqrt{(\kappa - \mu)(\alpha - \kappa)(\kappa - \beta)}} \right). \quad (4.43)$$

Take into account that  $\rho = 4\mu d$  is a special case since the second integral does not appear. Indeed if  $\rho = 4\mu d$ , then the critical curve passes through the pole, as we have explained in the beginning of the section.

Now, following the notation of [68], we define

$$p = \sqrt{\frac{\alpha - \beta}{\alpha - \mu}}, \quad q = \sqrt{1 - p^2}, \quad \nu = \frac{(\alpha - \beta)(\alpha + \beta - 4\mu)}{(\alpha - \mu)(\alpha + \beta - 4\mu) - \rho}. \quad (4.44)$$

Then, from (4.42), we know that  $4d(\kappa - \mu) - (\kappa - 2\mu)^2 - \rho = (\alpha - \kappa)(\kappa - \beta)$  which gives us  $\alpha + \beta = 4(d + \mu)$  and  $\alpha\beta = 4\mu^2 + 4\mu d + \rho$ . Thus, finally, we obtain that

$$\alpha = \frac{\sqrt{\rho + \mu^2}}{q} + \mu, \quad \beta = q\sqrt{\rho + \mu^2} + \mu. \quad (4.45)$$

Therefore, using above relations (4.45), we reduce (4.43) to (see Appendix A)

$$I = \frac{2\sqrt{\rho}}{\sqrt{\alpha + \beta - 4\mu}\sqrt{\alpha - \mu}} \left( K(p) + \frac{\rho - \mu(\alpha + \beta - 4\mu)}{(\alpha - \mu)(\alpha + \beta - 4\mu) - \rho} \Pi(\nu, p) \right), \quad (4.46)$$

where  $K(p)$  and  $\Pi(\nu, p)$  denote the complete elliptic integrals of first and third kind, respectively.

Then, we have the following result

**Theorem 4.3.6.** ([14]) *In the round 3-sphere,  $\mathbb{S}^3(\rho)$ , there exist closed planar critical curves of  $\Theta_\mu$ , (4.17), with non-constant curvature,  $\kappa(s)$ , given by (4.30), for any value of  $\mu$ .*

*Proof.* Consider a planar critical curve  $\gamma$  of  $\Theta_\mu$ , (4.17), with non-constant periodic curvature  $\kappa(s)$ , (4.30). Now, we need to check whether the conditions of Proposition 3.2.6 are verified or not. Remember that we have written the function  $I$ , (4.40), in terms of elliptic integrals, (4.46).

We first begin by translating the different values of the parameter  $d$  into the new parameter  $q$  introduced in (4.44). The value  $d = \frac{-\mu + \sqrt{\rho + \mu^2}}{2}$  corresponds with  $q = 1$ , while, the limit  $d \rightarrow \infty$ , now reads  $q \rightarrow 0$ . Moreover,  $d = \frac{\rho}{4\mu}$ , that is, when the critical curve passes through the pole, is represented by  $q = \frac{\mu}{\sqrt{\rho + \mu^2}}$ .

Then, with the notation introduced in (4.44), it can be checked that  $p^2 < \nu < 1$ . Moreover, as mentioned in Remark 4.2.2,  $d > \frac{-\mu + \sqrt{\rho + \mu^2}}{2} > 0$  and using (4.46) and formula (A.1) of the Appendix A, we get

$$I = q\phi K(p) + \frac{\pi}{2} \epsilon \Lambda_o(\arcsin \phi, p), \quad (4.47)$$

where  $\epsilon$  represents the sign of  $\rho - 4\mu d$  and  $\phi$  is given by

$$\phi = \sqrt{\frac{\nu - p^2}{\nu(1 - p^2)}} = \frac{1}{q} \sqrt{\frac{\rho}{4d(\alpha - \mu)}}.$$

If  $\mu \leq 0$ , then necessarily  $\epsilon = 1$  and for any  $d \in \left(\frac{-\mu + \sqrt{\rho + \mu^2}}{2}, \infty\right)$ ,  $I$ , (4.40), is a monotonically decreasing function on  $d$  bounded by (see Lemmas A.0.1 and A.0.2 of Appendix A)

$$\arcsin \sqrt{\frac{\rho}{\rho + \mu^2}} < I < \frac{\pi}{(\rho + \mu^2)^{\frac{1}{4}}} \sqrt{2 \frac{\rho}{(-\mu + \sqrt{\rho + \mu^2})}}. \quad (4.48)$$

On the other hand, if  $\mu > 0$ , we need to take out the case  $d = \frac{\rho}{4\mu}$  and  $d \in \left(\frac{-\mu + \sqrt{\rho + \mu^2}}{2}, \frac{\rho}{4\mu}\right) \cup \left(\frac{\rho}{4\mu}, \infty\right)$ . Then, taking into account the sign of  $\epsilon$ , we obtain that  $I$ , (4.40), is a monotonically decreasing function on  $d$ , which is bounded by (see Lemmas A.0.1 and A.0.3 of Appendix A)

$$-\arcsin \sqrt{\frac{\rho}{\rho + \mu^2}} < I < \frac{\mu}{\sqrt{\rho + \mu^2}} K \left( \sqrt{\frac{\rho}{\rho + \mu^2}} \right) - \frac{\pi}{2}, \quad (4.49)$$

if  $\epsilon = -1$ , or, in the case  $\epsilon = 1$  we have the following upper and lower bounds

$$\frac{\mu}{\sqrt{\rho + \mu^2}} K \left( \sqrt{\frac{\rho}{\rho + \mu^2}} \right) + \frac{\pi}{2} < I < \frac{\pi}{(\rho + \mu^2)^{\frac{1}{4}}} \sqrt{2 \frac{\rho}{(-\mu + \sqrt{\rho + \mu^2})}}. \quad (4.50)$$

Thus, in all the three cases (4.48)-(4.50), we can always find some integers  $m$  and  $n$ , such that,  $mI = n\pi$ , that is, there are closed critical curves.

To end up the proof, we are going to consider now the case where the critical curve passes through the pole. That is, when  $\rho = 4\mu d$ . As mentioned before, for this case we only have the first integral in (4.43). Moreover, in this case,  $q = \frac{\mu}{\sqrt{\rho + \mu^2}}$  and  $\mu$  can have values in  $(0, \infty)$ , since  $\rho > 0$ . In this case, by (4.46),

$$I = \frac{\mu}{\sqrt{\rho + \mu^2}} K \left( \sqrt{\frac{\rho}{\rho + \mu^2}} \right). \quad (4.51)$$

Then, from the result proved in Lemmas A.0.1 and A.0.3 of Appendix A,  $I$  is increasing in  $\mu$  and  $0 < I < \pi/2$ . Therefore, there are also closed critical curves passing through the pole.  $\square$

Notice that planar critical curves of  $\Theta_\mu$ , (4.17), are all immersed in the totally geodesic sphere  $\mathbb{S}^2(\rho)$  (see Figures 4.6 and 4.7). However, in order to study embeddedness of the associated binormal evolution surfaces, we need to get under what conditions planar critical curves are embedded in  $\mathbb{S}^2(\rho)$ , that is, when these critical curves are simple.

**Theorem 4.3.7.** ([14]) *Assume that  $\gamma$  is a planar critical curve of  $\Theta_\mu$ , (4.17), with non-constant curvature,  $\kappa(s)$ , (4.30), immersed in  $\mathbb{S}^2(\rho)$ . Then, if  $\mu > 0$ ,  $\gamma$  is not simple. Moreover, if  $\mu \leq 0$ ,  $\gamma$  will be simple, if and only if, it is closed and it closes up in one round around the pole.*

*Proof.* Let  $\gamma$  be a planar critical curve of (4.17), with curvature,  $\kappa(s)$  (which is given by (4.30)). Then, the function

$$\tilde{I}(s) = \frac{(\kappa(s) - 2\mu) \sqrt{\kappa(s) - \mu}}{4d(\kappa(s) - \mu) - \rho}, \quad (4.52)$$

verifies that;

- (i) If  $\mu \leq 0$  or,  $\mu > 0$  and  $4\mu d \leq \rho$ , then it never changes sign.
- (ii) If  $\mu > 0$  and  $4\mu d > \rho$ , it changes sign.

Now, by Remark 4.2.2, we have that  $2d > -\mu + \sqrt{\rho + \mu^2}$ . Moreover, notice that if  $\mu \leq 0$ , then  $\tilde{I}(s)$ , (4.52), does not change sign and, therefore, the function  $\psi(s)$ , (3.31), is monotone. Furthermore, the planar critical curve  $\gamma$  will be simple, unless it closes up in more than one round. Thus,  $\gamma \subset \mathbb{S}^2(\rho)$  is simple, if and only if, it closes up in one round, that is, by checking the image of  $I$ , (4.48), if there exists an integer  $m$ , such that,

$$\arcsin \sqrt{\frac{\rho}{\rho + \mu^2}} < \frac{\pi}{m} < \frac{\pi}{(\rho + \mu^2)^{\frac{1}{4}}} \sqrt{2(-\mu + \sqrt{\rho + \mu^2})},$$

and verifying  $mI = \pi$ .

Now, if  $\mu > 0$  and  $4\mu d < \rho$ , the function  $\tilde{I}(s)$ , (4.52), has always the same sign. That is, by monotonicity of  $\psi(s)$ , (3.31),  $\gamma$  will be simple, if and only if, it closes up in one round. Attending to the limits obtained in Lemma A.0.2 of Appendix A, the absolute value of the total angular variation,  $|2I|$ , of  $\gamma$  in  $\mathbb{S}^2(\rho)$ , (4.50), is always bigger than  $\pi$ , but smaller than  $2\pi$ . Thus,  $\gamma$  cannot close up in one period, and from the second period it travels more than one round, so it cuts itself. That is,  $\gamma$  is not simple.

Let's study now the case  $\mu > 0$  and  $4\mu d = \rho$ . In this case,  $\gamma$  passes through the pole exactly once in each period of its curvature, therefore the only option for  $\gamma$  to be simple is that it closes up in just one period. But, if we look at the absolute value of the total angular variation,  $|2I|$ , for this case,  $(0, \pi)$ , we realize that  $\gamma \subset \mathbb{S}^2(\rho)$  does not travel one whole round in each period, since  $|2I|$  is always smaller than  $\pi$ .

Finally, if  $\mu > 0$  and  $4\mu d > \rho$ , we have that  $\tilde{I}(s)$ , (4.52), has changes of sign, what it means that  $\gamma$  goes back, and as a consequence from (3.32), it is clear that  $\gamma$  is not simple.  $\square$

Notice that what Theorem 4.3.7 tells us is that there exist closed critical curves embedded in  $\mathbb{S}^2(\rho)$ . In fact, the condition in this case reduces to  $\gamma$  closing up in one round and not having self-intersections in one period of its curvature.

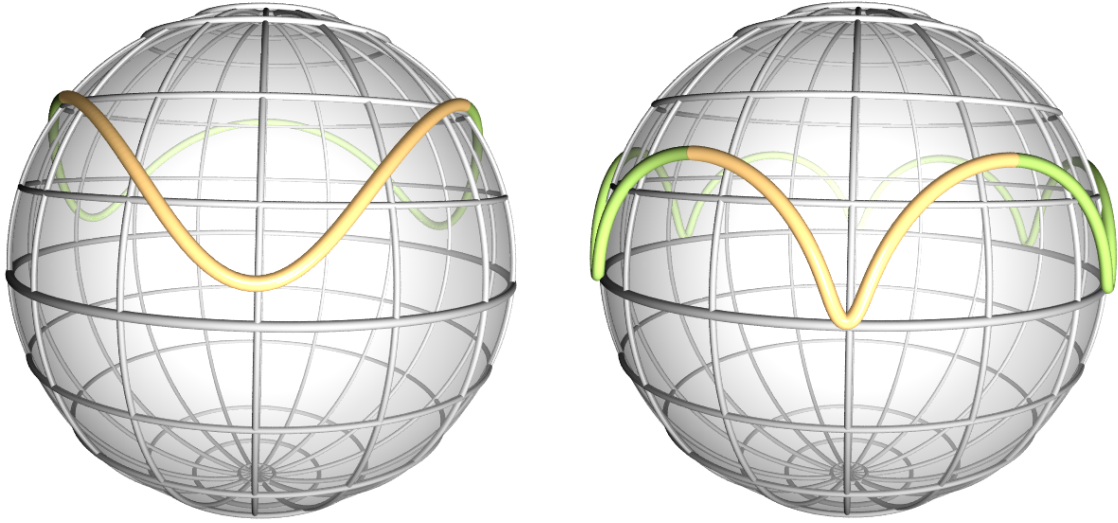


Figure 4.8: Closed and simple planar extremal curves in  $\mathbb{S}^2(1)$  for:  $\mu = -1$  and  $d \simeq 2.48$  (Left); and,  $\mu = -2$  and  $d \simeq 16.19$  (Right).

The condition of closing up in just one round means that the angular variation,  $I$ , must be equal  $\pi/m$ , for any integer  $m$ . This function has been proved to be bijective in Appendix A (Lemma A.0.1), since the analysis made with elliptic integrals leads to  $I$  being monotone. A different proof when  $\rho = 1$  can be found in [3]. This bijection means that for each  $m$ , there exist just one  $d$  such that  $mI = \pi$ . However, the election of the integer  $m$  is not totally free, since it is constrained by  $\mu$ . Indeed, if we combine Theorem 4.3.6 and Theorem 4.3.7 to obtain closed and simple planar critical curves we get that  $\mu < 0$  and that for any  $m > 1$

$$\mu \in \left( -\sqrt{\rho} \frac{m^2 - 2}{2\sqrt{m^2 - 1}}, -\sqrt{\rho} \cot \frac{\pi}{m} \right). \quad (4.53)$$

Finally, we sum up all this information in the following Corollary,

**Corollary 4.3.8.** ([14]) *Let  $\gamma$  be a planar closed critical curve of  $\Theta_\mu$ , (4.17), with non-constant curvature,  $\kappa(s)$ , (4.30), embedded in  $\mathbb{S}^2(\rho)$ . Then,  $\mu \neq -\sqrt{\frac{\rho}{3}}$  is negative.*



*Proof.* From Theorem 4.3.7, we know that necessarily  $\mu \leq 0$ . Moreover, as explained above, it must verify (4.53), for any  $m > 1$ . Then, we can check that for any strictly negative  $\mu \neq -\sqrt{\frac{\rho}{3}}$ , there exist such  $m > 1$ .  $\square$

Observe that these results can be translated to the binormal evolution surfaces. In fact, as we have already mentioned, if the initial condition is closed, then  $S_\gamma$  would also be closed (see Figure 4.9), and, what is more, if the planar critical curve is simple and closed, then the evolution under the binormal flow sweeps out a closed surface embedded in  $\mathbb{S}^3(\rho)$ .

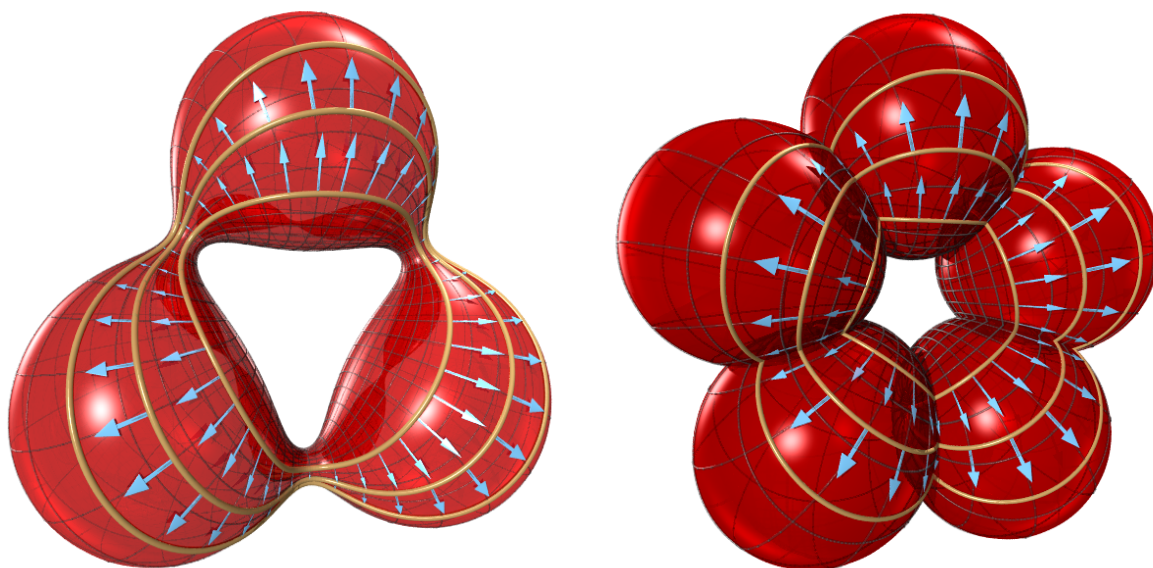


Figure 4.9: Stereographic projections of two closed CMC rotational surfaces in  $\mathbb{S}^3(\rho)$  showing the binormal evolution (in blue) of the filaments (in yellow).

With this argument, the local classification theorem (Theorem 4.3.3) and the bijection of  $I$ , we have that once we fix the CMC  $H$ , for each  $m > 1$ , there exist at most one compact embedded non-isoparametric rotational surface of CMC  $H$  in  $\mathbb{S}^3(\rho)$ .

Observe that since critical curves with non-constant curvature do not meet the axis of rotation, the binormal evolution surfaces of point (iv) of Theorem 4.3.3 are all local descriptions of topological torus, therefore, both the Hopf tori and the binormal evolution surfaces have genus one. Moreover, notice that the interval (4.53), is precisely the interval given by Perdomo in [121]. In fact, for each possible value  $H$  and any  $m > 1$  such that

$$|H| \in \left( \sqrt{\rho} \cot \frac{\pi}{m}, \sqrt{\rho} \frac{m^2 - 2}{2\sqrt{m^2 - 1}} \right),$$

there exist a compact embedded non-isoparametric surface of genus one given by point (iv) of Theorem 4.3.3 (see some of them in Figures 4.9 and 4.10). Moreover, our construction

here gives a way of proving Ripoll's Theorem [128], which states that *for any  $H \neq 0$ ,  $\pm\sqrt{\frac{\rho}{3}}$ , there exist a non-isoparametric torus of CMC  $H$* . In Figure 4.10, we can see the stereographic projection of three of these surfaces for  $m = 3, 4$  and  $5$ , respectively.

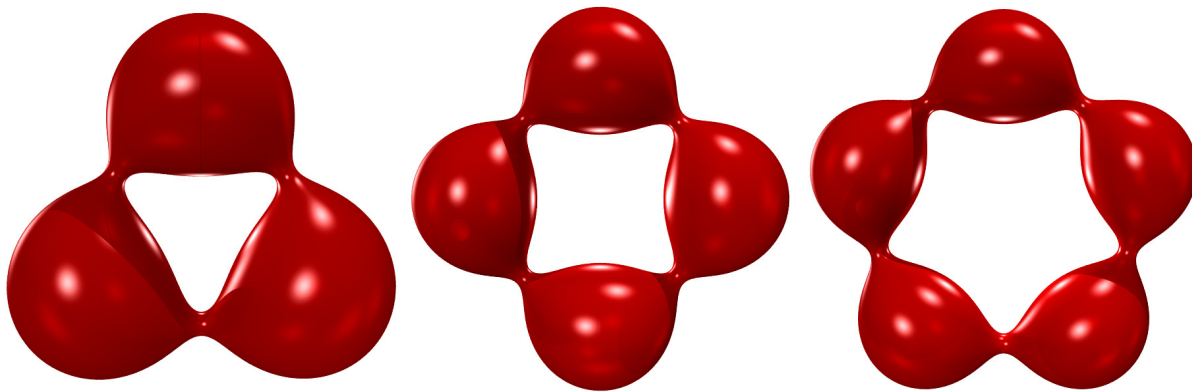


Figure 4.10: Stereographic projections of embedded CMC rotational surfaces in  $\mathbb{S}^3(\rho)$ .

Furthermore, the Pinkall-Sterling's conjecture [126] (recently proved in [3]) asserts that *any CMC tori embedded in  $\mathbb{S}^3(\rho)$  must be rotationally symmetric*. Therefore, points (iii) and (iv) in Theorem 4.3.3 (together with the restriction from Corollary 4.3.8) give rise to a complete classification of CMC tori embedded in  $\mathbb{S}^3(\rho)$ . In particular, the Lawson's conjecture (see [30] and [97]) is verified. Indeed, if a rotational torus is minimal, then  $\mu$  must be zero and there are no closed simple planar critical curves of  $\Theta_\mu$ , (4.17), (see Corollary 4.3.8), therefore, the only minimal torus embedded in  $\mathbb{S}^3(\rho)$  is locally given in point (iii) of Theorem 4.3.3,

$$\mathbb{S}^1(\sqrt{2\rho}) \times \mathbb{S}^1(\sqrt{2\rho}),$$

which is a Hopf torus, usually called the *Clifford torus*.

# Chapter 5

## Invariant Linear Weingarten Surfaces in 3-Space Forms

In the introduction of Chapter 4, we have mentioned that the mean curvature,  $H$ , is one of the most important extrinsic invariants for a surface immersed in any Riemannian or Lorentzian 3-space form,  $M_r^3(\rho)$ . Moreover, as we have seen in Chapter 1, all the intrinsic and extrinsic information of an immersion of a surface,  $N_\nu^2$ , into any 3-space form,  $M_r^3(\rho)$ , is encoded in the two fundamental forms. In particular, a combination of them gives rise to the shape operator,  $A_\eta$ .

Take into account that in Riemannian backgrounds, the shape operator is symmetric and that its eigenvalues are usually called *principal curvatures*. Therefore, it is well-known that in Riemannian ambient spaces the principal curvatures of  $N^2$  always exist. However, in Lorentzian 3-space forms, the shape operator may not be diagonalizable, so, in general, the principal curvatures are not well-defined. For this reason, from now on, we are going to restrict ourselves to surfaces immersed in Riemannian 3-space forms,  $M^3(\rho)$ .

In this setting, it can be checked that the mean curvature,  $H$ , verifies  $2H = \kappa_1 + \kappa_2$ ,  $\kappa_1$  and  $\kappa_2$  being the principal curvatures. In Chapter 4, we have considered CMC invariant surfaces. Notice that the CMC condition expressed in terms of the principal curvatures gives rise to a relation of the type  $\Upsilon(\kappa_1, \kappa_2) = 0$ . Surfaces verifying a certain relation  $\Upsilon(\kappa_1, \kappa_2) = 0$  between their principal curvatures are usually called *Weingarten surfaces*. These surfaces were introduced by Weingarten in [142] and its study occupies an important role in classical Differential Geometry.

The simplest relation of the type  $\Upsilon(\kappa_1, \kappa_2) = 0$  which extends the CMC condition is the affine relation, often called linear relation in the literature. That is

$$a \kappa_1 + b \kappa_2 = c,$$

where  $a$ ,  $b$  and  $c$  are three real constants, such that,  $a^2 + b^2 \neq 0$ . We are going to call *linear Weingarten surfaces* to the surfaces whose principal curvatures verify this linear relation. Trivial examples appear whenever  $a$  and  $c$  (or, equivalently,  $b$  and  $c$ ) are both

zero, or, also when the surface has one constant principal curvature. Thus, from now on, we are going to discard them.

After these examples, without loss of generality, we can rewrite above linear relation as

$$\kappa_1 = a \kappa_2 + b,$$

where  $a, b \in \mathbb{R}$  and  $a \neq 0$ . Well-known families of linear Weingarten surfaces are the following;

- (i) *Totally Umbilical Surfaces.* This is the case where  $a = 1$  and  $b = 0$ .
- (ii) *Isoparametric Surfaces.* In this case both principal curvatures are constant. Besides the umbilical surfaces, the surface may be a spherical cylinder.
- (iii) *Constant Mean Curvature Surfaces.* This is the case when  $a = -1$  and the surface has constant mean curvature  $H = b/2$ . Observe that in Chapter 4 we have been able to study invariant CMC surfaces also in Lorentzian 3-space forms,  $M_1^3(\rho)$ , by considering  $H = H_o$  instead of above linear relation.

Finally, we remind that in the literature the name linear Weingarten surfaces has also been used to denote surfaces verifying a linear relation between their Gaussian and mean curvatures,  $K$  and  $H$ , respectively. However, we point out that, in general, these surfaces do not coincide with those ones satisfying a linear relation of above type.

In this chapter we are going to apply the binormal evolution procedure described in Chapter 3, in order to study invariant linear Weingarten surfaces of Riemannian 3-space forms,  $M^3(\rho)$ . We begin by analyzing the critical curves of a particular generalized elastic energy ( $\epsilon = 1$  in (2.2)), which along this chapter is going to be called p-elastic energy following the notation of [63]. Moreover, we are also going to see that there exist a correspondence between critical curves of this energy and a generalization of a famous nonlinear equation, namely the Ermakov-Milne-Pinney (EMP) equation. This correspondence can be used as an alternative route for obtaining exact solutions of the generalized EMP equation.

Then, in the second part of the chapter, we variationally characterize the profile curves of rotational linear Weingarten surfaces of Riemannian 3-space forms,  $M^3(\rho)$ . Indeed, we prove that they are planar critical curves of two curvature energy functionals. Mainly, they are p-elastic curves, that is, critical curves of the generalized elastic energy  $\Theta_\mu^{\epsilon,p}$ , (2.2), with  $\epsilon = 1$ . However, for the case  $a = 1$  in the linear relation, a completely different curvature energy functional appears.

Moreover, we can prove that the binormal evolution of these critical curves generates an invariant linear Weingarten surface. In fact, as critical curves are planar, the invariance is given by a one-parameter group of rotations, and, therefore, the binormal evolution surfaces with these planar critical curves as initial filaments are going to be rotational linear Weingarten surfaces.

Then, we are going to restrict ourselves to the Euclidean 3-space,  $\mathbb{R}^3$ , proving that there are no rotational linear Weingarten tori for  $b = 0$ , that is, for the pure linear relation. However, by giving the full geometric description of all rotational linear Weingarten surfaces in  $\mathbb{R}^3$ , we are going to see that for other topological types of surfaces, there may exist closed rotational linear Weingarten surfaces, as, for instance, the Mylar balloon proves.

In the last part of the chapter, a nice application of this characterization to another type of variational problems is described. Indeed, we characterize the profile curves of non-CMC biconservative surfaces as generalized elasticae. What is more, locally, all these non-CMC biconservative surfaces are binormal evolution surfaces with initial condition a planar generalized elastica. Finally, using this new description of the non-CMC biconservative surfaces, we are going to prove that in both  $\mathbb{R}^3$  and  $\mathbb{H}^3(\rho)$ , there are no closed non-CMC biconservative surfaces. On the other hand, in  $\mathbb{S}^3(\rho)$ , we will see that the closure condition plays an essential role.

## 5.1 The $p$ -Elastic Energy of Curves in Riemannian 3-Space Forms

As we have just explained, for our purposes it is sufficient to consider Riemannian ambient spaces along this section. That is, we are going to work with Riemannian 3-space forms,  $M^3(\rho)$ . Then, for  $p \neq 0$  and  $\mu \in \mathbb{R}$ , we define the curvature energy functional

$$\Theta_{\mu}^p(\gamma) = \int_o^L (\kappa(s) - \mu)^p ds. \quad (5.1)$$

Notice that if we fix  $\epsilon = 1$  in the generalized elastic functional (2.2), we recover (5.1). Moreover, in the flat ambient space,  $\mathbb{R}^3$  (and also in the Minkowski 3-space,  $\mathbb{L}^3$ ) this functional has been studied in [63], where its critical curves have been called *p-elastic curves*. Therefore, along this section, we are going to refer to  $\Theta_{\mu}^p$ , (5.1), as the *p-elastic energy*.

On the other hand, as a particular case of a generalized elastic energy obtained by fixing  $\epsilon = 1$  in (2.2), the case  $p = 1$  is, basically, the total curvature functional, whose extremals are any planar curves whenever  $\rho + \mu = 0$  (see equations (2.4) and (2.5)). This result was also obtained in [7] (check also the references therein). Notice that in the definition of  $\Theta_{\mu}^p$  we have required  $p \neq 0$  since, as explained in Section 2.1, the case  $p = 0$  corresponds with the length functional. From now on, we discard these two cases, so  $p \neq 0, 1$ .

Now, adapting the Euler-Lagrange equations (2.4) and (2.5) for the case  $\epsilon = 1$  and  $M^3(\rho)$  (that is,  $\varepsilon_i = 1$ , for  $i = 1, 2, 3$ ) we obtain the Euler-Lagrange equations of  $\Theta_{\mu}^p$ ,

(5.1), acting on  $\Omega_{p_0 p_1}^{\rho*}$ , (4.18),

$$\frac{d^2}{ds^2} ((\kappa - \mu)^{p-1}) + (\kappa - \mu)^{p-1} (\kappa^2 - \tau^2 + \rho) - \frac{1}{p} \kappa (\kappa - \mu)^p = 0, \quad (5.2)$$

$$2 \frac{d}{ds} ((\kappa - \mu)^{p-1}) \tau + (\kappa - \mu)^{p-1} \frac{d\tau}{ds} = 0. \quad (5.3)$$

We also recall that for the space of curves  $L^1([0, L])$ , any curve with  $\kappa = \mu$  (whenever it makes sense) will be a global minimum of  $\Theta_\mu^p$ , (5.1). For details see Section 2.1.

Moreover, by the same argument of Section 1.3.1, equations (2.8) and (2.9) are the first integrals of the Euler-Lagrange equations. In our case, by substituting  $\epsilon = 1$  in (2.8) and (2.9), we get

$$\left( \frac{d}{ds} ((\kappa - \mu)^{p-1}) \right)^2 + \frac{1}{p^2} (\kappa - \mu)^{2(p-1)} ((p-1)\kappa + \mu)^2$$

$$+ (\tau^2 + \rho) (\kappa - \mu)^{2(p-1)} = d, \quad (5.4)$$

$$p^2 (\kappa - \mu)^{2(p-1)} \tau = e, \quad (5.5)$$

with  $d$  and  $e$  being real constants.

To end up this section, notice that for  $p$ -elastic curves we also have naturally associated Killing vector fields. Indeed, the vector fields along  $\gamma$ ,  $\mathcal{I}$  and  $\mathcal{J}$ , (2.6) and (2.7) with  $\epsilon = 1$ , can be extended to the whole  $M^3(\rho)$ . We are going to use the same letters for these extensions (see Proposition 1.3.2 and the argument after it). Finally, the extension of the Killing vector field along  $\gamma$ ,  $\mathcal{I}$ , given by

$$\mathcal{I} = p (\kappa - \mu)^{p-1} B \quad (5.6)$$

will play an essential role in following sections.

### 5.1.1 A New Approach to the Generalized EMP Equation

Nonlinear equations have been of an increasing interest in Physics during the last decades and one of the simplest examples is the today called *Ermakov-Milne-Pinney* (EMP) equation, that is, the second order nonlinear differential equation

$$x''(t) + q(t)x(t) = \frac{\hbar}{x^3(t)}, \quad (5.7)$$

$\hbar$  being constant. If  $\hbar = 0$ , this is a particular instance of the one-dimensional linear Schrödinger equation and for  $\hbar \neq 0$  and  $q(t) = w^2(t)$  it describes the radial equation of motion for a two-dimensional time-dependent linear oscillator, [52]. It was introduced by Ermakov as a way of looking for a first integral for the time-dependent harmonic oscillator [54] and it may be regarded as the simplest case of an Ermakov system [133].

Recently, various authors have shown that, for a number of pure scalar fields and other classes of cosmological models, Einstein's gravitational field equations can be equivalently reformulated in terms of the so called *generalized EMP* (GEMP) equation

$$x''(t) + q(t)x(t) = \sum_{i=0}^m \frac{\lambda_i(t)}{x^{b_i}(t)}, \quad (5.8)$$

for functions  $q(t)$ ,  $\lambda_i(t)$  and  $b_i \in \mathbb{R}$ ,  $i \in \{0, 1, \dots, m\}$  (see, for instance, [46] and [76]). Observe that in Chapter 4 equation (5.8) already appeared and it described the warping function of a local description of a  $\xi$ -invariant CMC surface, see Section 4.1.

Along this section, we are going to show the existence of a correspondence between a certain family of generalized EMP equations and  $p$ -elastic curves of Riemannian 3-space forms, which were introduced in Section 5.1. In particular, solutions of these generalized EMP equations are going to be geometrically characterized, in the sense that they are going to be completely described by the curvature of a  $p$ -elastic curve. The results of this section are an extension of those given in [63] to any Riemannian 3-space form.

Thus, if we define the function  $\zeta(s)$  as

$$\zeta(s) = (\kappa(s) - \mu)^{p-1}, \quad (5.9)$$

$\kappa(s)$  being the curvature of a  $p$ -elastic curve,  $\gamma(s)$ , we will see in the following theorem that  $\zeta(s)$  satisfies a generalized EMP equation with constant coefficients of the type

$$\zeta''(s) + \alpha \zeta(s) + \frac{\varpi}{\zeta^3(s)} = \nu \zeta^a(s) - \frac{1}{a} \zeta^{2a-1}(s), \quad (5.10)$$

for certain values of the parameters  $a$ ,  $\alpha$ ,  $\varpi$  and  $\nu$  in  $\mathbb{R}$ .

**Theorem 5.1.1.** (Extension of [63]) *Assume that  $\gamma \in \Omega_{p_0 p_1}^{\rho*}$  is a unit speed immersed curve in any Riemannian 3-space form,  $M^3(\rho)$ , which is a critical curve of the  $p$ -elastic energy  $\Theta_\mu^p$ , (5.1). Then, the function  $\zeta(s)$ , defined in (5.9), is a solution of the generalized EMP equation with constant coefficients*

$$\zeta''(s) + (\rho + \mu^2) \zeta(s) - \frac{e^2}{p^4 \zeta^3(s)} = \frac{1-p}{p} \zeta^{\frac{p+1}{p-1}}(s) + \mu \frac{1-2p}{p} \zeta^{\frac{p}{p-1}}(s). \quad (5.11)$$

*Proof.* Take  $\gamma \in \Omega_{p_0 p_1}^{\rho*}$  a  $p$ -elastic curve and denote by  $\kappa(s)$  and  $\tau(s)$  to its curvature and torsion, respectively. Now, since  $\gamma$  is a  $p$ -elastic curve, its curvature and torsion must verify the Euler-Lagrange equations (5.2) and (5.3). Then, if we define  $\zeta(s)$  by formula (5.9), we obtain

$$\begin{aligned} \zeta''(s) + \zeta(s) \left( \left( \zeta^{\frac{1}{p-1}}(s) + \mu \right)^2 - \tau^2 + \rho \right) - \frac{1}{p} \zeta^{\frac{p}{p-1}} \left( \zeta^{\frac{1}{p-1}}(s) + \mu \right) &= 0, \\ 2\zeta'(s)\tau(s) + \zeta(s)\tau'(s) &= 0. \end{aligned}$$

Second equation above can be integrated and we have  $p^2 \zeta^2(s) \tau = e$ , where the constant of integration has been chosen so that it coincides with (5.5). Finally, substituting this expression for  $\tau(s)$  in the first equation of above system we conclude the proof.  $\square$

Notice that the expression (5.10) is obtained from (5.11) after the following choice of parameters

$$a = \frac{p}{p-1}, \quad \alpha = \rho + \mu^2, \quad \varpi = -\frac{e^2}{p^4}, \quad \nu = \mu \frac{1-2p}{p}. \quad (5.12)$$

We recall that the relations (5.12) can be softened by considering the  $p$ -elastic energy acting on a space of curves immersed in Lorentzian 3-space forms. Moreover, by the Lagrange's Multipliers Principle, restricting the length of the critical curves another extra term appears in (5.11). For this more general cases in both the Euclidean 3-space,  $\mathbb{R}^3$ , and the Minkowski 3-space,  $\mathbb{L}^3$ , see [63].

Conversely, for any  $p \neq 0, 1$  consider real constants  $\rho, \mu, \varpi \in \mathbb{R}$  such that  $\varpi \leq 0$ . Take any solution  $\zeta(s)$  of the generalized EMP equation

$$\zeta''(s) + (\rho + \mu^2) \zeta(s) + \frac{\varpi}{\zeta^3(s)} = -\mu \frac{a+1}{a} \zeta^a(s) - \frac{1}{a} \zeta^{2a-1}(s), \quad (5.13)$$

with  $a = p/(p-1)$ . Now, formula (5.9) defines a function,  $\kappa(s)$ , and then another function,  $\tau(s)$ , can be defined from

$$p^2 \zeta^2(s) \tau = e,$$

$e \in \mathbb{R}$  being a constant verifying  $e^2 = -\varpi p^4$ . Then, up to congruences in  $M^3(\rho)$ , there exists a unique Frenet curve,  $\gamma(s)$ , having  $\kappa(s)$  and  $\tau(s)$  as curvature and torsion, respectively. Hence, we obtain

**Theorem 5.1.2.** (Extension of [63]) *Under the previous conditions, the curve  $\gamma(s)$  of  $M^3(\rho)$  constructed out of a solution of (5.13) is a critical curve of the energy functional  $\Theta_\mu^p$ , (5.1).*

*Proof.* By combining (5.2), (5.3) and (5.13), it is a straightforward computation to check that the curvature and torsion of  $\gamma(s)$ ,  $\kappa(s)$  and  $\tau(s)$ , respectively, verify the Euler-Lagrange equations (5.2) and (5.3). Then,  $\gamma$  is a critical curve of  $\Theta_\mu^p$ , (5.1), in the sense explained in Section 1.3.  $\square$

To end up this section, recall that Ermakov used (5.7) to obtain a first integral for the one-dimensional linear Schrödinger equation. Therefore, motivated by this fact, we are going to use the connection we have just introduced between the generalized EMP equation with constant coefficients of type (5.13) and the  $p$ -elastic curves in Riemannian 3-space forms to get a first integral of these nonlinear generalized EMP equations.



Indeed, by substituting the value of  $\zeta(s)$ , (5.9), in the first integrals of the Euler-Lagrange equations, (5.4) and (5.5), we obtain after some long direct computations

$$\left(\zeta'(s)\right)^2 = d - \frac{e^2}{p^4 \zeta^2(s)} - \frac{\zeta^2(s)}{p^2} \left( \left( (p-1)\zeta^{\frac{1}{p-1}}(s) + \mu p \right)^2 + p^2 \rho \right), \quad (5.14)$$

for some constants  $d, e \in \mathbb{R}$ . Hence, it is easy to check that equation (5.14) is a first integral of (5.13).

## 5.2 Planar p-Elasticae and Rotational Linear Weingarten Surfaces

Here, we are going to understand that a surface  $N^2$  immersed in  $M^3(\rho)$  is a *linear Weingarten surface* if its principal curvatures,  $\kappa_1$  and  $\kappa_2$ , verify the linear relation

$$\kappa_1 = a \kappa_2 + b, \quad (5.15)$$

where  $a$  and  $b$  are real constants such that  $a \neq 0$ . The case  $a = 0$  has been discarded by the arguments given in the introduction of the chapter.

In this section, we are going to consider rotational linear Weingarten surfaces verifying (5.15) in Riemannian 3-space forms,  $M^3(\rho)$ . As mentioned before, in Riemannian ambient spaces the principal curvatures of a surface always exist. Moreover, since the initial condition is planar, the shape operator  $A_\eta$  is directly diagonal, and, therefore, using the first and second fundamental forms (see Chapter 1), we can check that the principal curvatures are  $-\kappa(s)$  and  $h_{22}(s)$ , respectively. Then, we are going to characterize variationally the profile curve of these particular invariant surfaces of 3-space forms, generalizing the results of [103] (and also those given in [120]).

As it will be clear after Theorem 5.2.1, for our purpose we also need to define the energy

$$\Theta^\nu(\gamma) = \int_o^L \exp(\nu\kappa(s)) ds \quad (5.16)$$

among curves immersed in  $\Omega_{p_0 p_1}^\rho$ , (1.49), and where  $\nu \in \mathbb{R} - \{0\}$ . In fact, if  $\nu$  happens to be zero, above energy, (5.16), is once more the length functional. Notice that the energy  $\Theta^\nu$ , (5.16), is not included in the family of generalized elastic functionals. Even though, by making use of the formulas presented in Section 1.3 and writing  $P(\kappa) = \exp(\nu\kappa)$ , we can obtain the corresponding general Euler-Lagrange equations (1.52) and (1.53), which, in our case, boil down just to

$$\frac{d^2}{ds^2} (\exp(\nu\kappa)) + \exp(\nu\kappa) (\kappa^2 + \rho) - \frac{1}{\nu} \kappa \exp(\nu\kappa) = 0,$$

since for our purposes we are working with planar curves, that is,  $\tau = 0$ , in Riemannian 3-space forms,  $M^3(\rho)$ .

Let  $N^2$  be a rotational linear Weingarten surface. As explained in Section 3.2, it will be denoted by  $S_\gamma$ , where  $\gamma$  is the profile curve. Let us assume first that  $\gamma$  is a geodesic of  $M^3(\rho)$ . Then, the Gauss-Codazzi equations for  $S_\gamma$  are given by (1.35)-(1.37). Moreover, the principal curvatures in this case can both be written in terms of  $G(s)$ , the length of the rotational Killing vector field. Indeed, from equation (1.36) and (1.37), we get that the products  $f(s)G^2(s)$  and  $h_{22}(s)G^2(s)$  are both constant. Then, combining properly the fundamental forms (see (1.34) and the beginning of Section 1.2.3), we get that the principal curvatures only depend on  $G(s)$ .

Now, by applying the linear relation between these principal curvatures, we necessarily conclude that  $G(s)$  is constant, and thus,  $S_\gamma$  is a flat ruled isoparametric surface. Therefore, we assume now that  $\gamma(s)$  is not a geodesic, then we obtain

**Theorem 5.2.1.** (Extension of [103]) *Let  $S_\gamma$  be a rotational surface of  $M^3(\rho)$  with profile curve  $\gamma$  and such that its principal curvatures verify the relation (5.15). Then,*

(i) *If  $a \neq 1$ ,  $\gamma$  is an extremal curve of  $\Theta_\mu^p$ , (5.1), for*

$$\mu = \frac{b}{a-1} \quad \text{and} \quad p = \frac{a}{a-1}.$$

(ii) *If  $a = 1$  and  $b \neq 0$ , then  $\gamma$  satisfies the Euler-Lagrange equation of  $\Theta^\nu$ , (5.16), for*

$$\nu = -\frac{1}{b}.$$

*Proof.* Let  $S_\gamma$  be a rotational surface, with profile curve  $\gamma$ , verifying (5.15) between its principal curvatures. If the curvature of  $\gamma$ ,  $\kappa(s)$ , is constant, then by (5.15) and (1.28),  $\kappa$  must be a solution of  $\kappa^2 + b\kappa + \rho a = 0$ . Notice that a planar curve with such a constant curvature falls inside points (i) and (ii), since it trivially verifies the Euler-Lagrange equations for those cases. Assume now that the curvature of  $\gamma$ ,  $\kappa(s)$ , is not constant. Furthermore, recall that since  $S_\gamma$  is rotational,  $\gamma$  is planar, that is, its torsion,  $\tau(s)$ , vanishes.

Now, by the Inverse Function Theorem, we can locally assume that  $s$  is a function of  $\kappa$ , and, then we call  $G(\kappa) = \dot{P}(\kappa)$ . For this case, the Gauss-Codazzi equations of  $S_\gamma$ , (3.11) and (3.12), can be written as

$$\dot{P}_{ss} + \dot{P}(\kappa^2 + \rho) - \kappa(P + \lambda) = 0, \quad (5.17)$$

for some real constant  $\lambda$ , since  $\phi$  is a rotation. Notice that (5.17) is the Euler-Lagrange equation of  $\Theta$ , (1.40). Moreover, using (1.28) and  $G(\kappa) = \dot{P}(\kappa)$ , equation (5.15) can be expressed as

$$-\kappa = a \frac{1}{\kappa} \left( \frac{\dot{P}_{ss}}{\dot{P}} + \rho \right) + b. \quad (5.18)$$

Therefore, combining (5.17) with (5.18), we end up with an ordinary differential equation (ODE),

$$((a-1)\kappa - b)\dot{P} = a(P + \lambda). \quad (5.19)$$

Let's consider first the case  $a = 1$ , in this case solving above ODE, (5.19), we get

$$P(\kappa) = c \exp\left(-\frac{1}{b}\kappa\right) - \lambda,$$

for some  $c \in \mathbb{R}$ . Thus, point (ii) is clear. On the other hand, if  $a \neq 1$ , the ODE, (5.19), gives

$$P(\kappa) = c \left(\kappa - \frac{b}{a-1}\right)^{\frac{a}{a-1}} - \lambda,$$

for any  $c \in \mathbb{R}$ . This corresponds with (i), and it concludes the proof.  $\square$

Moreover, the converse of Theorem 5.2.1 is also true. Indeed, suppose  $\gamma$  is a critical curve of either  $\Theta_\mu^p$ , (5.1), or  $\Theta^\nu$ , (5.16), with constant curvature and vanishing torsion. Then, by Proposition 3.2.3, the binormal evolution surface swept out by  $\gamma$  is a flat isoparametric surface, and, as a consequence, it trivially verifies (5.15) for some suitable constants  $a$  and  $b \in \mathbb{R}$ .

On the other hand, for the non-constant curvature case, we have

**Theorem 5.2.2.** (Extension of [103]) *Let  $\gamma$  be a critical curve of either  $\Theta_\mu^p$ , (5.1), or  $\Theta^\nu$ , (5.16), with non-constant curvature and vanishing torsion. Then, the binormal evolution surface with initial condition  $\gamma$  is a rotational surface that satisfies the linear Weingarten relation (5.15), where*

$$a = \frac{p}{p-1} \quad \text{and} \quad b = \frac{\mu}{p-1},$$

if  $\gamma$  is critical for the the functional  $\Theta_\mu^p$ , (5.1), or

$$a = 1 \quad \text{and} \quad b = -\frac{1}{\nu},$$

if  $\gamma$  is critical for  $\Theta^\nu$ , (5.16).

*Proof.* Take  $\gamma$  a planar critical curve of either  $\Theta_\mu^p$ , (5.1), or  $\Theta^\nu$ , (5.16), with non-constant curvature,  $\kappa(s)$ . Then, by Proposition 3.2.4, the binormal evolution surface generated by evolving  $\gamma$  under the flow of  $\mathcal{L}$ , (1.55), is a rotational surface with warped product metric (1.22) where  $\mathcal{F}(s, t) = G(s) = \dot{P}(\kappa(s))$  for the suitable choice of  $P(\kappa)$ . Moreover, as  $\gamma$  is critical for a curvature energy, it must verify the corresponding Euler-Lagrange equations. Let's assume first that  $\gamma$  is critical for  $\Theta_\mu^p$ , (5.1), then, we have the following Euler-Lagrange equation (see (5.2) and (5.3))

$$\frac{d^2}{ds^2} ((\kappa - \mu)^{p-1}) + (\kappa - \mu)^{p-1} (\kappa^2 + \rho) - \frac{1}{p}\kappa(\kappa - \mu)^p = 0.$$

Now, if we substitute the value of  $G(s) = p(\kappa - \mu)^{p-1}$ , it boils down to

$$G'''(s) + G(s) (\kappa^2(s) + \rho) - \frac{1}{p} \kappa(s) (\kappa(s) - \mu) G(s) = 0.$$

On the other hand, if we use this equation in the linear relation  $-\kappa = a h_{22} + b$ , where  $h_{22}$  is given in (1.28), we end up with

$$a = \frac{p}{p-1} \quad \text{and} \quad b = \frac{\mu}{p-1},$$

as desired. Finally, if  $\gamma$  is critical for  $\Theta^\nu$ , (5.16), the corresponding Euler-Lagrange equation, once we have used  $G(s) = \nu \exp(\nu\kappa)$  to simplify it, is

$$G'''(s) + G(s) (\kappa^2(s) + \rho) - \frac{1}{\nu} \kappa(s) G(s) = 0. \quad (5.20)$$

Therefore, using (5.20) and  $h_{22}$ , (1.28), in  $-\kappa = h_{22} + b$ , we get  $a = 1$  and

$$b = -\frac{1}{\nu},$$

proving the result. □

### 5.2.1 Rotational Linear Weingarten Surfaces in the Euclidean 3-Space

The cases discarded in the introduction of the chapter are those where one principal curvature is constant. If  $\kappa_1 = 0$  (equivalently, if  $\kappa_2 = 0$ ), in the Euclidean 3-space,  $\mathbb{R}^3$ , then the surface is developable. Moreover, if  $\kappa_1$  is a non-zero constant (equivalently,  $\kappa_2$ ), these surfaces were classified in [134]. In particular, since we are just concerned with rotational surfaces, then they must be either a sphere or a tori of revolution.

Apart from these examples and those ones described in (i)-(iii) in the introduction, a first result due to Chern proves that the sphere is the only ovaloid with the property that  $\kappa_1$  is a decreasing function of  $\kappa_2$  [42] (this happens, for example, if  $a < 0$ ). Later, Hopf proved in [79] that there are no closed analytic surfaces of genus greater or equal than 2 unless  $a = -1$ , that is, the surface has constant mean curvature and if the genus is 0 and the surface is analytic and rotational, then  $a$  or  $1/a$  must be an odd integer. Indeed, for each  $a > 1$ , Hopf proved the existence of a non-spherical closed convex rotational  $\mathcal{C}^2$ -surfaces. The particular case  $a = -1$  is exceptional. Hopf proved that the sphere is the only closed surface of genus 0 with constant mean curvature [78]. In fact, during many years, it was conjectured that the sphere was the only closed surface with constant mean curvature until in 1986 Wente found an immersed torus in  $\mathbb{R}^3$  with constant mean

curvature [143]. Later, Kapouleas proved the existence of closed surfaces for arbitrary genus [85].

Moreover, Hopf proved in [79] the existence of convex closed rotational surfaces for any  $a > 0$ . When  $a = 2$  and  $b = 0$ , Mladenov and Oprea have named this surface as the Mylar balloon [110]. If  $a > 0$  and  $b = 0$ , they have also given parametrizations of the closed surfaces in terms of elliptic and hypergeometric functions and show that the surface is a critical point of a variational problem [109]. For any  $a$  and  $b = 0$ , Barros and Garay proved that all the parallels of these rotational surfaces are critical points for an energy functional involving the normal curvature and acting on the space of closed curves immersed in the surface [24]. On the other hand, in [102], López studied linear Weingarten surfaces foliated by a uniparametric group of circles, proving that the surface is rotational or that the surface is one of the minimal examples of Riemann.

In Section 5.2, we have variationally characterize the planar profile curves of rotational linear Weingarten surfaces in any Riemannian 3-space form,  $M^3(\rho)$ . Now, restricting ourselves to the Euclidean case,  $\mathbb{R}^3$ , Theorem 5.2.1 and Theorem 5.2.2 give us the characterization of profile curves of rotational linear Weingarten surfaces of  $\mathbb{R}^3$ . As a consequence of this variational characterization, we prove that, there are no topological torus for the pure linear case, that is, for  $b = 0$  in (5.15) (see also Theorem 5.2.4). In fact, let  $S_\gamma$  be a closed rotational linear Weingarten surface. First, notice that if  $a = 1$  and  $b = 0$ , then  $S_\gamma$  must be a totally umbilical surface. Therefore, we assume now  $a \neq 1$ , and then, from our variational characterization, its generating curve  $\gamma$  is critical for  $\Theta_\mu^p$ , (5.1). If the critical curve  $\gamma$  has constant curvature, then as mentioned above, it generates a flat isoparametric surface, that is, either a plane, a cylinder or a sphere. Thus, up to here, the only closed surface is the sphere, which has genus 0.

From now on, we are going to consider that  $\gamma$  has non-constant curvature. In order  $S_\gamma$  to be closed, we need either  $\gamma$  to be closed or that it cuts the axis of rotation (see Section 3.2.2). In the latter,  $S_\gamma$  cannot be a torus. Therefore, in order to look for rotational linear Weingarten tori for  $b = 0$ , we must look for closed critical curves of  $\Theta_\mu^p$ , (5.1). Thus, we are going to apply Proposition 3.2.6, in order to prove

**Proposition 5.2.3.** ([103]) *There are no closed critical curves with non-constant curvature of  $\Theta_\mu^p$  for  $\mu = 0$ . And, as a consequence, there are no topological torus satisfying  $\kappa_1 = a \kappa_2$ .*

*Proof.* Critical curves with non-constant curvature of  $\Theta_\mu^p$  will be closed, if and only if,  $\kappa(s)$  is a periodic function of period  $\varrho$  and the closure condition of Proposition 3.2.6 is verified. If  $\mu = 0$ , (3.41) simplifies to

$$\Lambda(d) = \frac{p-1}{d} \int_o^\varrho \kappa^p ds.$$

Then, the closure condition in the Euclidean 3-space,  $\mathbb{R}^3$ , ( $\rho = 0$  and  $d > 0$ ) reads

$$\int_0^e \kappa^p(s) ds = 0.$$

Finally, since the orientation can be locally fixed, say  $\kappa(s) > 0$ , the closure condition cannot be verified and, therefore, we obtain a contradiction.  $\square$

However, notice that the condition imposed to  $S_\gamma$  of being a torus is essential. On the contrary, as explained above,  $S_\gamma$  can be closed if a non-closed critical curve cuts the axis of rotation. For the pure linear relation, there exist these type of surfaces as we can see in the following geometric description. See also [24].

We now summarize the complete description of the rotational linear Weingarten surfaces (see Figures 5.1, 5.2 and 5.3). Denote by  $\gamma$  the generating curve. If the surface does not meet the axis of rotation, we have the next type of surfaces;

- (i) *Catenoid-Type Surfaces.* The curve  $\gamma$  is a concave graph on some interval  $I$  of the axis. These surfaces only appear when  $a < 0$  and  $b = 0$ . There are two types depending if  $I = \mathbb{R}$  ( $-1 \leq a < 0$ ) or if  $I$  is a bounded interval ( $a < -1$ ). The plane is included here as an extremal case.
- (ii) *Unduloid-Type Surfaces.* Embedded surfaces which are periodic in the direction of the axis. Circular cylinders belong to this family.
- (iii) *Nodoid-Type Surfaces.* Non embedded surfaces which are periodic in the direction of the axis and the curve  $\gamma$  has loops towards the axis.
- (iv) *Antinodoid-Type Surfaces.* Non embedded surfaces which are periodic in the direction of the axis and the curve  $\gamma$  has loops facing away from the axis.
- (v) *Cylindrical Antinodoid-Type Surfaces.* Non embedded surfaces asymptotic to a circular cylinder. The curve  $\gamma$  has a single loop facing away from the axis.

Then, we turn to those surfaces that meet (necessarily orthogonally) the axis of rotation. All the surfaces have genus 0 except in one case that the surface touches the axis at exactly one point (case (iii) below).

- (i) *Ovaloids.* They are convex surfaces. The shape is like an oblate spheroid being more flat close to the axis as the parameter  $a$  gets bigger. This case only occurs when  $a > 0$ . Round spheres are included here.
- (ii) *Vesicle-Type Surfaces.* Embedded closed surfaces where the two poles of the profile curve are close so the meridian presents two inflection points. These surfaces have concave regions around the poles.

- (iii) *Pinched Spheroids*. Limit case of vesicle-type surfaces when the two poles coincide. The surface is tangentially immersed on the axis and bounds a solid 3-dimensional torus.
- (iv) *Immersed Spheroids*. Closed surfaces of genus 0 that appear when the two poles of the vesicle-type surface pass their-self through the axis.

Finally, for the sake of completeness, we recall that in [103], using a different tool the classification of all rotational linear Weingarten surfaces has been proved. In fact, let  $(x_1, x_2, x_3)$  be the canonical coordinates in the Euclidean space  $\mathbb{R}^3$  and let  $S_\gamma \subset \mathbb{R}^3$  be a rotational surface. Without loss of generality, we may assume that the axis of rotation is the  $x_3$ -axis and that its generating curve  $\gamma$  is contained in the  $x_1x_3$ -plane. Let  $\gamma(s) = (x_1(s), 0, x_3(s))$ ,  $s \in I \subset \mathbb{R}$ , be parametrized by the arc-length, and thus  $x_1'(s) = \cos \theta(s)$  and  $x_3'(s) = \sin \theta(s)$  for a certain function  $\theta$ . If  $x(s, \psi) = (x_1(s) \cos \psi, x_1(s) \sin \psi, x_3(s))$  is a parametrization of  $S_\gamma$ , then the principal curvatures are

$$\kappa_1(s) = \kappa(s) = \theta'(s), \quad \kappa_2(s) = \frac{\sin \theta(s)}{x_1(s)}, \quad s \in I.$$

Notice that they are independent of the rotation angle  $\psi$ . Therefore, a surface of revolution  $S_\gamma$  satisfying the linear relation (5.15) is characterized by the following system of ordinary differential equations

$$x_1'(s) = \cos \theta(s), \quad (5.21)$$

$$x_3'(s) = \sin \theta(s), \quad (5.22)$$

$$\theta'(s) = a \frac{\sin \theta(s)}{x_1(s)} + b. \quad (5.23)$$

Now, we give the classification of the rotational surfaces satisfying the linear relation  $\kappa_1 = a \kappa_2$  with  $a \neq 0$ . The study of this class of surfaces has been first done in [24] where the authors have characterized the parallels of these surfaces from a variational viewpoint and different from our Theorem 5.2.1.

**Theorem 5.2.4.** ([103]) *The rotational linear Weingarten surfaces satisfying the relation  $\kappa_1 = a \kappa_2$ ,  $a \neq 0$ , are planes, ovaloids (including spheres) and catenoid-type surfaces. More precisely, if  $\gamma$  is the generating curve, we have (see Figure 5.1);*

- (i) *Case  $a > 0$ . The curve  $\gamma$  is a concave graph on the  $z$ -axis of a function defined on a bounded interval. The rotational surface is an ovaloid. If  $a = 1$ , then the surface is a round sphere.*
- (ii) *Case  $a < 0$ . The curve  $\gamma$  is a convex graph on the  $z$ -axis. If  $-1 \leq a < 0$ , then  $\gamma$  is a graph of a function defined on the entire  $z$ -axis and if  $a < -1$ , the function is defined on a bounded interval of the  $z$ -axis being asymptotic to two parallel lines. In both cases, the surface is of catenoid-type.*

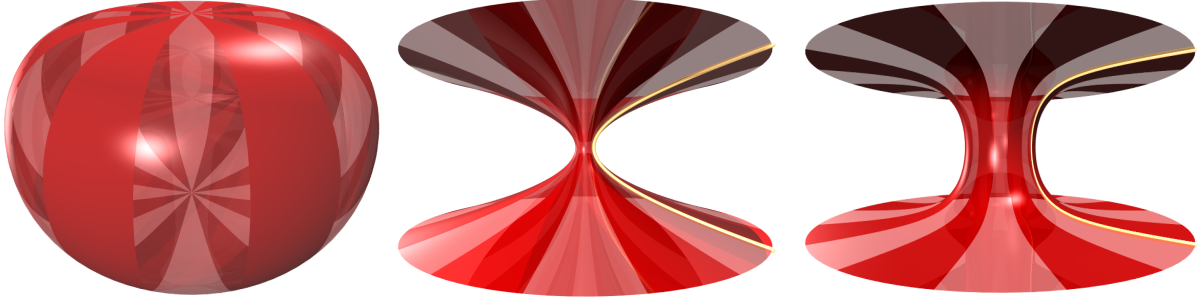


Figure 5.1: Rotational linear Weingarten surfaces for  $b = 0$  in  $\mathbb{R}^3$ . From left to right: Ovaloid ( $a > 0$ ), Catenoid-Type Surface with  $a \in [-1, 0)$  and Catenoid-Type Surface with  $a < -1$ .

To end up this section, we consider the general case  $b \neq 0$  in the linear Weingarten relation  $\kappa_1 = a\kappa_2 + b$  (see Figures 5.2 and 5.3). The classification of the rotational linear Weingarten surfaces is given by studying the solutions of (5.21)-(5.23) for all possible values on the initial conditions. The classification will be done according to the sign of the parameter  $a$ .

**Theorem 5.2.5.** ([103]) *Let  $a > 0$  and  $b \neq 0$ . The rotational linear Weingarten surfaces are ovaloids, vesicle-type surfaces, pinched spheroids, immersed spheroids, cylindrical antinodoid-type surfaces, antinodoid-type surfaces and circular cylinders.*

**Theorem 5.2.6.** ([103]) *Let  $a < 0$  and  $b \neq 0$ . The rotational linear Weingarten surfaces are unduloid-type surfaces, circular cylinders, spheres and nodoid-type surfaces.*

For a proof of above theorems (Theorem 5.2.4, Theorem 5.2.5 and Theorem 5.2.6) see [103].

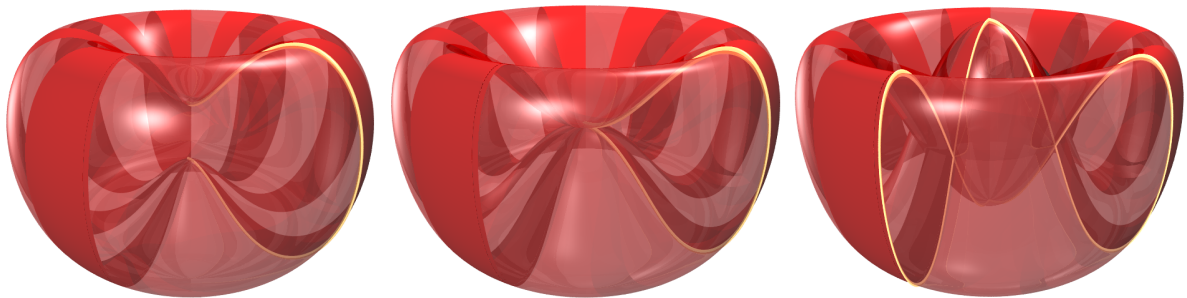


Figure 5.2: Rotational linear Weingarten surfaces for  $b \neq 0$  in  $\mathbb{R}^3$  that meet the axis of rotation apart from Ovaloids (see Figure 5.1 on the left). From left to right: Vesicle-Type Surface, Pinched Spheroid and Immersed Spheroid.



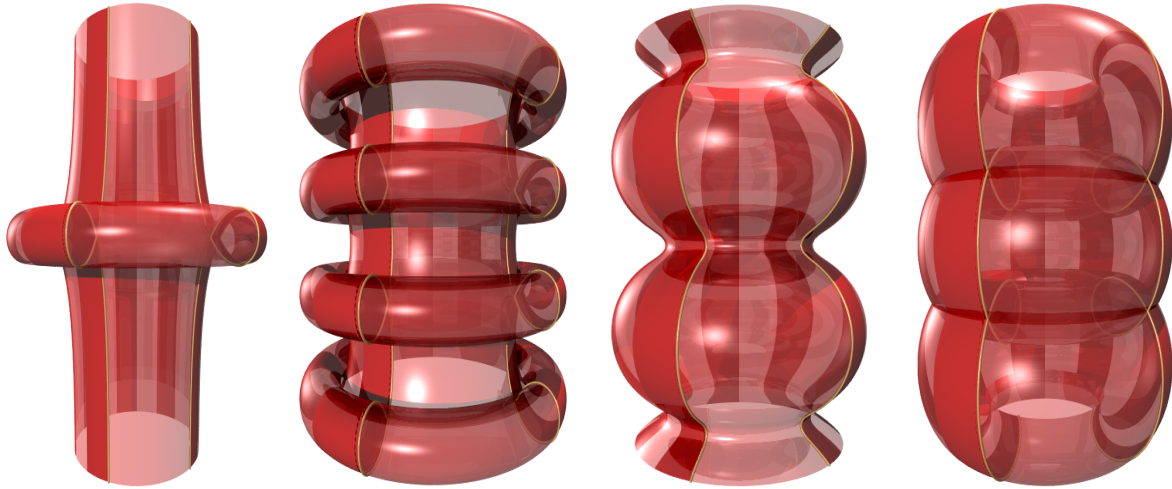


Figure 5.3: Rotational linear Weingarten surfaces for  $b \neq 0$  in  $\mathbb{R}^3$  that do not meet the axis of rotation. From left to right: Cylindrical Antinodoid-Type Surface, Antinodoid-Type Surface, Unduloid-Type Surface and Nodoid-Type Surface.

### 5.3 Application to Biconservative Surfaces

Harmonic maps  $\varphi : N^m \rightarrow M^n$  between Riemannian manifolds are the critical points of the energy functional

$$E(\varphi) = \frac{1}{2} \int_{N^m} |d\varphi|^2 v_g, \quad (5.24)$$

acting on the space of all maps between  $N^m$  and  $M^n$ . Their corresponding Euler-Lagrange equation is given by the vanishing of the tension field

$$\tilde{\tau}(\varphi) = \text{trace grad } d\varphi. \quad (5.25)$$

In [51], Eells and Sampson suggested to study *biharmonic maps*, which are the critical points of the *bienergy* functional

$$E_2(\varphi) = \frac{1}{2} \int_{N^m} |\tilde{\tau}(\varphi)|^2 v_g. \quad (5.26)$$

The first variation formula of the bienergy was derived by Jiang, [84]. Moreover, he showed that the Euler-Lagrange equation for  $E_2$  is

$$\tilde{\tau}_2(\varphi) = -J(\tilde{\tau}(\varphi)) = -\Delta \tilde{\tau}(\varphi) + \text{trace } R^M(d\varphi, \tilde{\tau}(\varphi))d\varphi = 0, \quad (5.27)$$

where  $J$  is the Jacobi operator of  $\varphi$ ,  $\Delta$  represents the rough Laplacian on sections  $\varphi^{-1}(TM)$  and  $R^M$  denotes the curvature operator on  $M^n$ . The equation  $\tilde{\tau}_2(\varphi) = 0$  is called the *biharmonic equation*.

Let  $\varphi : N^{n-1} \rightarrow M^n$  be an isometric immersion of an hypersurface  $N^{n-1}$  into a Riemannian manifold  $M^n$  of dimension  $n$  with unit normal vector field  $\eta$  and mean curvature vector field  $\mathbf{H} = H\eta$ . The decomposition of the bitension field for hypersurfaces is given in [34]. In fact, the normal and tangential components of  $\tilde{\tau}_2(\varphi)$ , (5.27), are respectively

$$\Delta H + H|A_\eta|^2 - HRic(\eta, \eta) = 0, \quad (5.28)$$

$$2A_\eta(\text{grad}H) + (n-1)H\text{grad}H - 2HRic(\eta)^T = 0, \quad (5.29)$$

where  $A_\eta$  is the shape operator and  $Ric(\eta)^T$  is the tangent component of the Ricci curvature of  $N^{n-1}$  in the direction of the vector field  $\eta$ . Notice that studying hypersurfaces that only verify the second equation of this system, (5.29), makes sense by its own. Indeed, as described by Hilbert in [77], the *stress-energy* tensor associated with a variational problem is a symmetric 2-covariant tensor  $\mathcal{S}$  which is conservative at critical points, that is, with  $\text{div } \mathcal{S} = 0$ .

Let  $\varphi : (N^m, g) \rightarrow (M^n, \tilde{g})$  be an harmonic map between two Riemannian manifolds, that is a critical point of the *energy* functional (5.24). In this context, the stress-energy tensor was studied in detail by Baird and Eells in [16]. Moreover, the tensor

$$\mathcal{S} = \frac{1}{2}|d\varphi|^2g - \varphi^*\tilde{g}$$

satisfies  $\text{div } \mathcal{S} = -\langle \tilde{\tau}(\varphi), d\varphi \rangle$ , where  $\tilde{\tau}(\varphi)$  is given by (5.25). Therefore, we have that  $\text{div } \mathcal{S} = 0$  when the map is harmonic. Moreover, when  $\varphi$  is any isometric immersion, the condition  $\text{div } \mathcal{S} = 0$  is always satisfied, since the tension field  $\tilde{\tau}(\varphi)$  is normal to the submanifold.

On the other hand, the study of the stress-energy tensor for the bienergy, (5.26), was initiated in [83] and afterwards developed in [101]. It is given by

$$\mathcal{S}_2(X, Y) = \frac{1}{2}|\tilde{\tau}(\varphi)|^2\langle X, Y \rangle + \langle d\varphi, \tilde{\nabla}\tilde{\tau}(\varphi) \rangle\langle X, Y \rangle - \langle d\varphi(X), \tilde{\nabla}_Y\tilde{\tau}(\varphi) \rangle - \langle d\varphi(Y), \tilde{\nabla}_X\tilde{\tau}(\varphi) \rangle,$$

and it satisfies the condition

$$\text{div } \mathcal{S}_2 = -\langle \tilde{\tau}_2(\varphi), d\varphi \rangle, \quad (5.30)$$

where  $\tilde{\tau}_2(\varphi)$  is the bitension field, (5.27). Due to (5.30), we have the conforming to the principle of a stress-energy tensor for the bienergy.

Now, if  $\varphi$  is an isometric immersion, (5.30) boils down to

$$(\text{div } \mathcal{S}_2)^\sharp = -\tilde{\tau}_2(\varphi)^T, \quad (5.31)$$

where  $\sharp$  denotes the musical isomorphism sharp. We say that an isometric immersion is *biconservative* if the corresponding stress-energy tensor  $\mathcal{S}_2$  is conservative, that is, if  $\text{div } \mathcal{S}_2 = 0$ . From (5.31), biconservative isometric immersions correspond to immersions with vanishing tangential part of the corresponding bitension field. That is, an isometric

immersion of a hypersurface  $\varphi : N^{n-1} \rightarrow M^n$  is *biconservative*, if and only if,  $\varphi$  satisfies the condition

$$2A_\eta(\text{grad}H) + (n-1)H \text{grad}H - 2H\text{Ric}(\eta)^T = 0, \quad (5.32)$$

where  $A_\eta$  denotes the shape operator,  $H$  is the mean curvature function and  $\eta$  is a unit normal vector field. The hypersurface  $N^{n-1}$  immersed in this way is usually called a *biconservative hypersurface*. Observe that, in particular, when the ambient space is any Riemannian space form of dimension  $n$ ,  $M^n(\rho)$ , the tangential part of the Ricci curvature vanishes, and therefore equation (5.32) simplifies to

$$2A_\eta(\text{grad}H) + (n-1)H \text{grad}H = 0.$$

### 5.3.1 Biconservative Surfaces in Riemannian 3-Space Forms

Now, let  $M^3(\rho)$  denote a Riemannian 3-space form. In [34], it was proved that a biconservative surface of a 3-space form,  $M^3(\rho)$ , is either a CMC surface or a rotational surface. Moreover, in the same paper, a relation between the Gaussian curvature,  $K$ , and the mean curvature,  $H$ , of the non-CMC biconservative surfaces of  $M^3(\rho)$  was stated. Indeed, these rotational surfaces verify

$$K = -3H^2 + \rho. \quad (5.33)$$

This relation implies that non-CMC biconservative surfaces are linear Weingarten surfaces as it was first pointed out by Fu and Li in [60]. In this particular case, equations (5.32) and (5.33), implies that the relation between the principal curvatures is given by

$$3\kappa_1 + \kappa_2 = 0.$$

Thus, we have the following

**Proposition 5.3.1.** ([111]) *Non-CMC biconservative surfaces of  $M^3(\rho)$  are rotational linear Weingarten surfaces verifying*

$$3\kappa_1 + \kappa_2 = 0. \quad (5.34)$$

*Moreover, let  $N^2 \subset M^3(\rho)$  be a rotational linear Weingarten surface verifying (5.34), then,  $N^2$  is a biconservative surface.*

Along this section we are going to assume that  $N^2$  is a non-CMC biconservative surface of a Riemannian 3-space form,  $M^3(\rho)$ . Then, as mentioned above,  $N^2$  is locally rotational and can be denoted by  $S_\gamma$ , see Section 3.2. Now, particularizing the result of Theorem 5.2.1, we have that profile curves of these rotational surfaces have a nice geometric property.

**Theorem 5.3.2.** ([111]) *Let  $N^2$  be a non-CMC biconservative surface of  $M^3(\rho)$ . Then, locally,  $N^2$  is a warped product surface,  $S_\gamma$ , whose profile curve verifies the Euler-Lagrange equations for the functional  $\Theta_o^{1/4}(\gamma) = \int_\gamma \kappa^{1/4} ds$ , (5.1).*

In fact, the converse of Theorem 5.3.2 is also true, and gives us a way of constructing all non-CMC biconservative surfaces of 3-space forms, as we have seen in Theorem 5.2.2.

We summarize this result in the following Theorem.

**Theorem 5.3.3.** ([111]) *Let  $\gamma$  be a planar extremal curve with non-constant curvature of the energy  $\Theta_o^{1/4}(\gamma) = \int_\gamma \kappa^{1/4} ds$ , (5.1), and let  $S_\gamma$  denote the  $\mathcal{I}$ -invariant surface in  $M^3(\rho)$  obtained by evolving  $\gamma$  under the flow of the Killing field  $\mathcal{I}$  which extends (5.6) for  $\mu = 0$  and  $p = 1/4$  to  $M^3(\rho)$ . Then,  $S_\gamma$  is a rotational linear Weingarten surface of  $M^3(\rho)$  verifying (5.34), that is,  $S_\gamma$  is a non-CMC biconservative surface.*

We remind that Theorem 5.3.3 gives a way of constructing all non-CMC biconservative surfaces of  $M^3(\rho)$ . And, in fact, together with Theorem 5.3.2, it characterizes non-CMC biconservative surfaces as the binormal evolution surfaces swept out by a planar extremal of  $\Theta_o^{1/4}$ , (5.1). This characterization also allows us to analyze global properties of the binormal evolution surfaces based on topological facts about the profile curves. For instance, we can study the existence of non-CMC closed biconservative surfaces.

### 5.3.2 Non-CMC Closed Biconservative Surfaces

Along this section, let  $S_\gamma$  be a local description of a non-CMC biconservative surface immersed in a Riemannian 3-space form,  $M^3(\rho)$ . As we have just seen,  $S_\gamma$  is locally a binormal evolution surface with initial condition,  $\gamma$ , being a planar critical curve of  $\Theta_o^{1/4}$ , (5.1). Now, as explained in Section 3.2.2, in order to look for closed surfaces we need  $d > 0$ , since for these values of  $d$ , the orbits of the evolution are Euclidean circles. Moreover, we also need either that  $\gamma$  cuts the axis of rotation or that it is closed. Notice that  $\gamma$  is completely determined (up to rigid motions) by its curvature,  $\kappa(s)$ , which must be a solution of the first integral (5.4) for  $p = 1/4$  and  $\mu = 0$ , that is, after long direct computations,

$$\kappa_s^2 = \frac{16}{9} \kappa^2 \left( 16 d \kappa^{3/2} - 9 \kappa^2 - \rho \right). \quad (5.35)$$

For simplicity on the notation, let's call  $u = \kappa^{1/2}$ . Therefore, above first integral reads,

$$u_s^2 = \frac{4}{9} u^2 \left( 16 d u^3 - 9 u^4 - \rho \right). \quad (5.36)$$

Now, observe that we need the right hand side of (5.36) to be positive. That is, the following polynomial,  $Q(u)$ , must be positive for some values of  $u$ ,

$$Q(u) = 16 d u^3 - 9 u^4 - \rho > 0. \quad (5.37)$$

Moreover, we have that  $Q(u)$  tends to  $-\infty$ , whenever  $u$  tends to  $\pm\infty$ . It has a local maximum at  $u = 4/(3d)$ , so condition (5.37) can be verified for some values of  $u$ , if and

only if,  $Q(4/(3d)) > 0$ , which gives an extra constraint on the parameter  $d$ . See the plot of  $Q(u)$  in Figure 5.4.

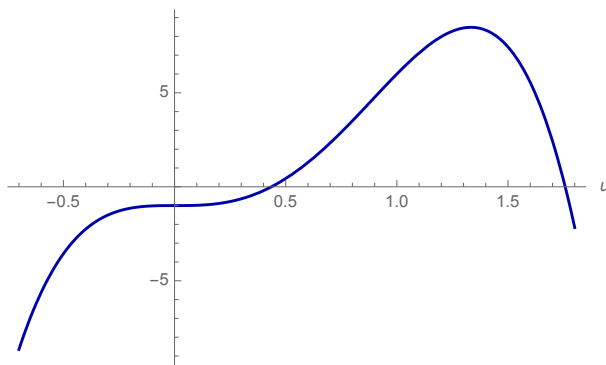


Figure 5.4: Plot of the polynomial  $Q(u)$  for  $\rho = 1$  and  $d = 1$ .

To be more precise, this extra constraint only appears when  $\rho > 0$  (since for  $\rho \leq 0$  is always true), and in this case we have

$$d > d_* = \frac{(27\rho)^{\frac{1}{4}}}{4}. \quad (5.38)$$

Notice that this argument also shows the existence of just two roots of  $Q(u)$ . Let's call  $\alpha_u$  and  $\beta_u$  to these roots, such that  $\alpha_u > \beta_u$ . After reversing the change of variable, they will represent the maximum and minimum curvatures of  $\gamma$ , respectively. Indeed, we have

$$\beta_u < u < \alpha_u$$

for any  $u$ , that verifies (5.37).

Now, from the equation of Proposition 3.2.5, (3.33), we obtain  $\bar{\kappa}_\delta^2 = \kappa_\delta^2 + \rho = 16du^3$ , where  $\bar{\kappa}_\delta^2$  represents the curvature of the orbit  $\delta$  in the semi-space  $\mathbb{E}_\delta^4$  where  $M^3(\rho)$  is immersed (see Section 1.2). Furthermore, since  $u$  is bounded, the Euclidean radius of  $\delta$  is never zero, which means that our critical curves never meet their respective axis of rotation. For a different way of proving this fact, one can adapt the computations of the beginning of Section 4.3.2, which involve the fixed points of the evolution.

Therefore, we can apply Corollary 3.2.7 and see if there exist closed critical curves. Let's assume for a moment that there exist periodic solutions that are critical for  $\Theta_o^{1/4}$ , (5.1), then we can obtain conditions for both  $\gamma$  and  $S_\gamma$  to be closed.

The function  $\Lambda(d)$  defined in (3.41) for this particular case, is precisely,

$$\Lambda(d) = -12 \int_o^e \frac{\kappa_\delta^{\frac{7}{4}}}{16d\kappa_\delta^{\frac{3}{2}} - \rho} ds, \quad (5.39)$$

where  $\varrho$  is the period of  $\kappa(s)$  (remember that we have assumed that there exist critical curves with periodic curvatures, and therefore, we are considering them) and  $d$  is the constant of integration given by (1.58). Now, making use of Corollary 3.2.7, the following result is clear, since for  $\rho \leq 0$ , the integrand of (5.39) is always negative, and therefore,  $\Lambda(d)$  never vanishes. That is, there are no closed critical curves, and, as a consequence, we have

**Proposition 5.3.4.** ([111]) *There are no closed non-CMC biconservative surfaces in 3-space forms,  $M^3(\rho)$ , with  $\rho \leq 0$ .*

Thus, it makes no sense to look for periodic solutions of the Euler-Lagrange equation, (5.35), in neither  $\mathbb{R}^3$  nor  $\mathbb{H}^3(\rho)$ , since even if they exist by Proposition 5.3.4 it will be impossible to find closed non-CMC biconservative surfaces in these spaces. On the other hand, if  $M^3(\rho) = \mathbb{S}^3(\rho)$ , we are going to prove the existence of periodic solutions. Consider the phase plane of the Euler-Lagrange equation, (5.35) in  $\mathbb{S}^3(\rho)$ . In order to simplify the computations, we will denote  $x = \kappa^{1/4}$ . Then, (5.35) can be written as the system

$$x' = y, \quad (5.40)$$

$$y' = 4\frac{y^2}{x} - x^9 + \frac{\rho}{3}x. \quad (5.41)$$

Now, since  $x \neq 0$ , the only critical point of the system (5.40) and (5.41) is  $(x_\rho, 0) = ((\rho/3)^{1/8}, 0)$ , and it only appears if  $\rho > 0$ , which is our case. The orbits of the phase plane of (5.35) are determined by the equation

$$\frac{dy}{dx} = 4\frac{y}{x} - \frac{x^9}{y} + \frac{\rho x}{3y},$$

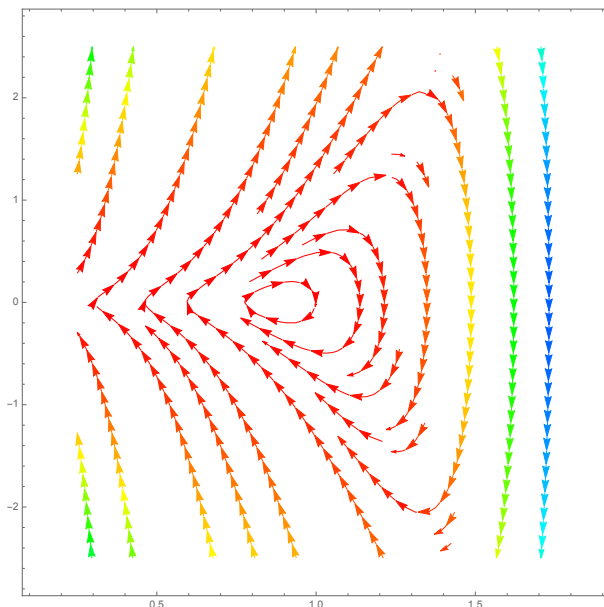
which can be integrated obtaining

$$\frac{y^2}{x^8} + x^2 + \frac{\rho}{9x^6} = \alpha,$$

for some constant  $\alpha$ . Let's denote now,  $F(x, y) = \frac{y^2}{x^8} + x^2 + \frac{\rho}{9x^6}$ . Then,  $F(x, y)$  is a Morse function in a neighborhood of the critical point  $(x_\rho, 0)$ . Moreover, we can compute

$$\left. \frac{\partial^2 F}{\partial x^2} \right|_{(x_\rho, 0)} = \frac{6 + 14\rho}{3x_\rho^8} > 0, \quad \left. \frac{\partial^2 F}{\partial x \partial y} \right|_{(x_\rho, 0)} = 0, \quad \left. \frac{\partial^2 F}{\partial y^2} \right|_{(x_\rho, 0)} = \frac{2}{x_\rho^8} > 0.$$

That is,  $(x_\rho, 0)$  is a non-degenerate critical point of  $F$ , and, then, applying the Morse's Lemma, there are closed orbits around it (see Figure 5.5). Therefore, (5.35) admits periodic solutions on  $\mathbb{R}$ .

Figure 5.5: Phase plane of the system (5.40) and (5.41) for  $\rho = 1$ .

Of course, since the profile curve has periodic curvature and the orbits are Euclidean circles, the binormal evolution surface it generates is complete. The existence of complete non-CMC biconservative in the round 3-sphere was first proved in [113] (see also [114]). Notice that the existence of complete ones in  $\mathbb{R}^3$  and  $\mathbb{H}^3(\rho)$  is clear from the geometric description given in [24]. Moreover, for the Euclidean case one can also see the classification of Section 5.2.1 and Figure 5.1. However, to assure closure in  $\mathbb{S}^3(\rho)$ , Corollary 3.2.7 tells that a binormal evolution surface of  $\mathbb{S}^3(\rho)$  whose profile curve,  $\gamma$ , has periodic curvature,  $\kappa(s)$ , is a closed surface, if and only if, the function

$$I = -\frac{1}{2}\sqrt{\rho d}\Lambda(d) = 6\sqrt{\rho d}\int_0^{\varrho}\frac{\kappa^{\frac{7}{4}}}{16d\kappa^{\frac{3}{2}}-\rho}ds = \frac{n\pi}{m} \quad (5.42)$$

for any  $d > d_*$ , (5.38), and any integers  $n$  and  $m$ , where  $n$  is the number of rounds and  $m$  the number of lobes, see Section 3.2.2.

Now, from the differential equation that satisfies  $u = \kappa^{1/2}$ , (5.36), it is easy to check that when  $u = \alpha_u$  or  $u = \beta_u$  the vector field  $\mathcal{J}$  has only component in  $T$ , that is, the profile curve  $\gamma$  is parallel to the integral curves of the Killing vector field  $\mathcal{J}$  in that points. Therefore, our critical curve is bounded between those parallels. What is more, in those points the length of  $\mathcal{J}$  is never zero, since, both  $\alpha_u$  and  $\beta_u$  are positive. This means that  $\gamma$  does not cross over the pole of the parametrization. Moreover, since the component in  $T$  of the Killing vector field  $\mathcal{J}$  is a non-zero multiple of  $u^{1/2}$  and  $u$  is always positive (it varies from  $\alpha_u$  to  $\beta_u$ , which in the spherical case are positive since  $Q(0) < 0$ ), we get that  $\gamma$  is never orthogonal to the integral curves of  $\mathcal{J}$ , that is,  $\gamma$  is always going forward.

Consequently, it does not cut itself in one period of its curvature, unless it gives more than one round in that period. Thus, a critical curve  $\gamma$  can only be simple if it is closed and if it closes up in just one round, that is, if it verifies the closure condition, (5.42), for  $n = 1$ . For more details about the existence of non-CMC biconservative surfaces in  $\mathbb{S}^3(\rho)$  see [111].



## Chapter 6

# Invariant Willmore Tori in Killing Submersions

In 1811, Germain pointed out that the free energy controlling the physical system associated to an elastic plate is the *total squared curvature* or *bending energy*. In other words, the bending energy of a surface  $N^2$  in  $\mathbb{R}^3$  is given by

$$\mathcal{W}(N^2) = \int_{N^2} H^2 dA,$$

where  $H$  denotes the mean curvature of the surface. Notice that for curves  $\gamma$  isometrically immersed in a Riemannian manifold,  $H$  is nothing but the geodesic curvature of  $\gamma$ ,  $\kappa$ , and  $\mathcal{W}(N^2)$  boils down to

$$\Theta_o^{2,1}(\gamma) = \int_{\gamma} \kappa^2 ds.$$

According to the classical model of Bernoulli, planar curves minimizing the bending energy  $\Theta_o^{2,1}$  can be thought of as the equilibrium positions of thin elastic rods (or *elasticae*). Observe that this energy acting on curves has been studied in Section 2.1.

On the other hand, the analysis of the variational problem associated to  $\mathcal{W}(N^2)$  for surfaces in  $\mathbb{R}^3$  goes back to Blaschke's school in the 1920s. Some years later, Willmore reintroduced the problem in [144] and this is the reason why  $\mathcal{W}(N^2)$  is also known as the *Willmore energy* of a surface in  $\mathbb{R}^3$  and its critical points are known as *Willmore surfaces*. The Willmore energy is a conformal invariant, a property that was already known to Blaschke. In the last years, there has been an intensive investigation of Willmore surfaces in connection with the so called Willmore Problem, that is, the determination of the minima for the Willmore energy within a given topological class. In particular, Willmore proposed in 1965 the following conjecture; *for every smooth immersed torus,  $N^2$ , in  $\mathbb{R}^3$ ,  $\mathcal{W}(N^2) \geq 2\pi^2$  and the equality is obtained at the Clifford torus*. The conjecture has been recently proved in [108], although prior to this proof the Willmore conjecture had already

been shown for many special cases (see [91], [129], [137],... and references therein). As a result, there is a huge literature concerning Willmore surfaces, specially within real space form backgrounds (for more details in this respect, see, for instance, [62]).

A generalization of the Willmore energy is due to Chen [40]. He extended the Willmore functional to any submanifold  $N^m$  of any Riemannian manifold  $M^n$  so that the conformal invariance property is preserved. Given a Riemannian submanifold  $N^m$  of  $M^n$  the *Chen-Willmore functional* is defined by

$$\mathcal{CW}(N^m) = \int_{N^m} (H^2 - \tau_e)^{\frac{m}{2}} dV ,$$

where  $H$  and  $\tau_e$  denote the *mean curvature* and the *extrinsic scalar curvature* of  $N^m$ , respectively. The energy  $\mathcal{CW}$  is conformally invariant and its critical points are known as *Chen-Willmore submanifolds*, [40] and [41]. In contrast to the case of Willmore surfaces in ambient spaces of constant curvature, there are no many results concerning Chen-Willmore submanifolds in background spaces with non-constant sectional curvature. Nevertheless, Willmore surfaces and submanifolds have strong connections in Physics with applications to the analysis of elastic plates and biological membranes, [75] and [115], and to bosonic string theories and sigma models, [18] and references therein, just to mention a few. Several of these applications are based on a beautiful link between Willmore surfaces and elastica which can be established by using a symmetry reduction procedure [125].

Along this chapter we are going to consider a generalization of Willmore surfaces, what we are going to call Willmore-like surfaces, by introducing a potential in  $\mathcal{W}(N^2)$ . These Willmore-like surfaces, following the idea of [125], will allow us to describe a connection between elastic curves with potential in the base surfaces of Killing submersions, studied in Section 1.3.3, and invariant Willmore-like tori in total spaces of Killing submersions.

In the first part of the chapter, the First Variation Formula and the Euler-Lagrange equation associated to this generalization of the Willmore energy, the Willmore-like energy, are computed in any Riemannian 3-spaces.

Then, as we are mainly interested in studying these surfaces in total spaces of Killing submersions, along the second part of the chapter, we are going to introduce the basic facts of Killing submersions, as well as an existence result that softens the simply connected condition of the base surface.

Finally, the connection between invariant Willmore-like tori in total spaces of Killing submersions and elastic curves with related potentials in the base surfaces is described. This connection is exploited in the last part of the chapter in order to analyze Willmore tori in Killing submersions and to construct foliations of Killing submersions made up of Willmore tori with constant mean curvature.

## 6.1 Willmore-Like Surfaces in Riemannian 3-Spaces

In this section we are going to study the following generalization of the Willmore energy, which will be called *Willmore energy with a potential*  $\Phi$  (or, simply, *Willmore-like energy*)

$$\mathcal{W}_\Phi(N^2) = \int_{N^2} (H^2 + \Phi|_{N^2}) dA,$$

where  $N^2$  is a surface of a 3-dimensional Riemannian manifold  $M^3$ ,  $H$  denotes the mean curvature of  $N^2$ , and  $\Phi \in \mathcal{C}^\infty(M^3)$ . More precisely, let  $(M^3, g = \langle \cdot, \cdot \rangle)$  be a 3-dimensional Riemannian manifold,  $\Phi \in \mathcal{C}^\infty(M^3)$  a smooth function and  $N^2$  a compact surface with no boundary. In the space of isometric immersions of  $N^2$  in  $M^3$ ,  $Imm(N^2, M^3)$ , we define the following Willmore-like energy

$$\mathcal{W}_\Phi(N^2) \equiv \mathcal{W}_\Phi(N^2, \varphi) = \int_{N^2} (H_\varphi^2 + \Phi|_{\varphi(N^2)}) dA_\varphi, \quad (6.1)$$

where  $\varphi \in Imm(N^2, M^3)$ ,  $H_\varphi$  denotes the mean curvature function of  $\varphi$  and  $dA_\varphi$  is the induced element of area via the immersion  $\varphi$ .

### 6.1.1 Field Equations

To compute the field equations associated with these kind of functionals, we consider a *variation* of  $\varphi \in Imm(N^2, M^3)$ . That is, a smooth map  $\Gamma : N^2 \times (-\varepsilon, \varepsilon) \rightarrow M^3$  satisfying the following conditions

- (i) For any  $\varsigma \in (-\varepsilon, \varepsilon)$  the map  $\varphi_\varsigma : N^2 \rightarrow M^3$  defined by  $\varphi_\varsigma(p) = \Gamma(p, \varsigma)$  belongs to  $Imm(N^2, M^3)$ .
- (ii)  $\varphi_0 = \varphi$ .

Then, the vector field along  $\Gamma$  given by

$$W(p, \varsigma) = \Gamma_* \left( \frac{\partial}{\partial \varsigma} (p, \varsigma) \right)$$

determines a vector field along  $\varphi$ ,  $W(p) := W(p, 0)$ , which is called the *variational vector field* associated to the variation  $\Gamma$ . Thus, we can identify the tangent space  $T_\varphi(Imm(N^2, M^3))$  with that of vector fields along  $\varphi$  and, consequently, we have

$$\partial \mathcal{W}_\Phi(N^2, \varphi)[W] = \frac{\partial}{\partial \varsigma} \left( \int_{N^2} (H_{\varphi_\varsigma}^2 + \Phi) dA_{\varphi_\varsigma} \right) \Big|_{\varsigma=0}.$$

Now, using similar computations to those included in [18] and [141], we can obtain the following formulae

(i) Let  $\mathbf{H}(p, \varsigma)$  be the mean curvature vector field of  $\varphi_\varsigma$  at  $p \in N^2$ , then

$$D_\varsigma \mathbf{H} \Big|_{\varsigma=0} = \frac{1}{2} \left( \Delta V^\perp + \tilde{A}(V^\perp) + \text{Ric}(\eta, \eta) \right) + D_{V^\perp} \mathbf{H},$$

where  $\Delta$  is the rough Laplacian associated with the connection  $D^\perp$  in the normal bundle of  $\varphi(N^2)$ ,  $\tilde{A}$  stands for the Simons operator,  $\text{Ric}$  is the Ricci curvature of  $M^3$  and  $\eta$  denotes the unit normal vector field of  $\varphi$ . Here  $(\ )^\top$  and  $(\ )^\perp$  denote tangential part and normal part, respectively.

(ii) The variation of the area element is given by the following formula

$$\frac{\partial}{\partial \varsigma} dA_{\varphi_\varsigma} \Big|_{\varsigma=0} = -2\langle \mathbf{H}, V \rangle dA_\varphi + d\theta,$$

where  $\theta$  is the one-form defined by  $\theta(X) = dA_\varphi(V^\top, X)$ .

In both cases, for the sake of simplicity, we have omitted the symbol  $\varphi$ . Then, combining the above two formulae and an argument involving integration by parts, we obtain the First Variation Formula of the first term in (6.1)

$$\frac{\partial}{\partial \varsigma} \left( \int_{N^2} (H_{\varphi_\varsigma}^2) dA_{\varphi_\varsigma} \right) \Big|_{\varsigma=0} = \int_{N^2} \langle \Delta \mathbf{H} + (2H^2 - 2K_{N^2} + 2R + \text{Ric}(\eta, \eta)) \mathbf{H}, V \rangle dA, \quad (6.2)$$

where  $K_{N^2}$  denotes the Gaussian curvature of  $N^2$  endowed with the induced metric associated with the initial immersion  $\varphi$ , and  $R$  stands for its *extrinsic Gaussian curvature* (that is, the sectional curvature of  $M^3$  on the tangent plane of  $\varphi$ ).

Now, using once more above formulas to compute the First Variation Formula of the second term in (6.1), we get

$$\frac{\partial}{\partial \varsigma} \left( \int_{N^2} \Phi dA_{\varphi_\varsigma} \right) \Big|_{\varsigma=0} = \int_{N^2} \langle \text{grad } \Phi, V \rangle dA - 2 \int_{N^2} \Phi \langle \mathbf{H}, V \rangle dA - \int_{N^2} d\Phi \wedge \theta.$$

Take into account that  $d\Phi \wedge \theta = V^\top(\Phi) dA$  and then

$$\frac{\partial}{\partial \varsigma} \left( \int_{N^2} \Phi dA_{\varphi_\varsigma} \right) \Big|_{\varsigma=0} = \int_{N^2} \langle (\text{grad } \Phi)^\perp - 2\Phi \mathbf{H}, V \rangle dA. \quad (6.3)$$

Finally, we combine (6.2) and (6.3) to characterize the extremals of  $\mathcal{W}_\Phi(N^2)$  as the solutions of the following Euler-Lagrange equation

$$\Delta H + H(2H^2 - 2K_{N^2} + 2R + \text{Ric}(\eta, \eta) - 2\Phi) + \eta(\Phi) = 0. \quad (6.4)$$

Along this PhD memory, closed surfaces solution of (6.4), that is extremals of  $\mathcal{W}_\Phi(N^2)$ , will be called *Willmore-like surfaces*. Notice that if the potential  $\Phi$  is a constant function, say  $\rho$  (in particular, the case in which  $\mathcal{W}_\Phi(N^2)$  is the Willmore energy in a space of constant curvature  $\rho$ ), then every minimal surface is automatically a Willmore-like surface. However, if the potential is not constant, it follows from (6.4) that a minimal surface,  $N^2$ , is Willmore-like, if and only if,  $\text{grad } \Phi$  is tangent to  $N^2$  everywhere.

From now on, our analysis of Willmore-like surfaces will be focused mainly on surfaces living in the total space of a *Killing submersion*.

## 6.2 Killing Submersions

A *submersion* is a smooth map between smooth manifolds whose differential is everywhere surjective. Moreover, submersions equipped with compatible Riemannian metrics are called *Riemannian submersions*. Then, a Riemannian submersion  $\pi : M \rightarrow B$  of a 3-dimensional Riemannian manifold  $M$  over a surface  $B$  will be called a *Killing submersion* if its fibers are the trajectories of a complete unit Killing vector field  $\xi$  (for more details, see [55] and [107]). Fibers of Killing submersions are geodesics in  $M$  and form a foliation called the *vertical foliation*.  $M$  is usually referred as the *total space* of the Killing submersion, while,  $B$  is called the *base surface*.

Most of the geometry of a Killing submersion is encoded in a pair of functions;  $K_B$  and  $\tau_\pi$ . Here  $K_B$  represents the *Gaussian curvature* function of the base surface,  $B$ , while  $\tau_\pi$  denotes the so called *bundle curvature* which is defined as follows. Do not confuse the notation with the one used for the torsion of a Frenet curve,  $\tau$ , (1.10)-(1.12).

Since  $\xi$  is a (vertical) unit Killing vector field, then it is clear that for any vector field,  $Z$ , on  $M$ , there exists a function  $\tau_\pi^Z$  (which a priori depends on the chosen vector field  $Z$ ) such that  $\tilde{\nabla}_Z \xi = \tau_\pi^Z Z \times \xi$ , where, as always,  $\tilde{\nabla}$  denotes the Levi-Civita connection in  $M$  and  $\times$  denotes the cross product. Actually, it is not difficult to see that  $\tau_\pi^Z$  does not depend on the vector field  $Z$  (see [55] for details) so we get a function  $\tau_\pi \in \mathcal{C}^\infty(M)$ , the bundle curvature, satisfying

$$\tilde{\nabla}_Z \xi = \tau_\pi Z \times \xi.$$

Notice that the bundle curvature is obviously constant along the fibers and, consequently, it can be seen as a function on the base surface,  $\tau_\pi \in \mathcal{C}^\infty(B)$ . Sometimes, we will denote by  $M(K_B, \tau_\pi)$  to the total space, in order to give explicitly both  $K_B$  and  $\tau_\pi$ .

Existence of Killing submersions over a given simply connected surface  $B$  for a prescribed bundle curvature,  $\tau_\pi \in \mathcal{C}^\infty(B)$ , has been proved in [107]. Uniqueness of these submersions, up to isomorphisms, is guaranteed under the assumption that the total space is also simply connected. This fact leads to the classification of Killing submersions on a simply connected surface as quotients of simply connected total spaces under vertical translations. In particular, we can suppose that fibers have finite length since, if necessary, we can always take a suitable quotient under a vertical translation in order to get a

circle bundle over  $B$ . The following result provides existence of Killing submersions with prescribed bundle curvature over arbitrary Riemannian surfaces

**Theorem 6.2.1.** ([25]) *Let  $B$  be a Riemannian surface with Gaussian curvature  $K_B$  and choose any function  $\tau_\pi \in \mathcal{C}^\infty(B)$ . Then there exists a Killing submersion over  $B$  with bundle curvature  $\tau_\pi$ ,  $M(K_B, \tau_\pi)$ . Moreover,  $M(K_B, \tau_\pi)$  can be chosen having compact fibers.*

*Proof.* If  $B$  is simply connected, then the result was proved in [107]. Therefore we assume that  $B$  is not simply connected and, thus, it has a non trivial fundamental group  $\pi_1(B)$ . Denote by  $B_o$  its universal covering and by  $p : B_o \rightarrow B$  the universal covering map. Now, if  $g$  is the metric on  $B$ , then we consider  $B_o$  endowed with the metric  $g_o = p^*(g)$  so that  $p$  is a Riemannian covering map. Denote by  $\Upsilon$  the group of deck transformations of  $(B_o, p)$  which is a subgroup of the group of isometries  $Isom(B_o, g_o)$  isomorphic to  $\pi_1(B)$ , the fundamental group of  $B$ .

Consider  $\tau_{\pi_o} = \tau_\pi \circ p \in \mathcal{C}^\infty(B_o)$ . Since  $B_o$  is simply connected, we know there exists a unique (up to isomorphisms) Killing submersion  $\pi_o : M_o \rightarrow B_o$  with simply connected  $M_o$  and bundle curvature  $\tau_{\pi_o}$  (see [107] for details). Now, if  $h \in \Upsilon$ , then it is obvious that  $\tau_{\pi_o} \circ h = \tau_{\pi_o}$ . Consequently, once an initial condition has been chosen, there exists a unique isometry  $\tilde{h} \in Isom(M_o, \tilde{g}_o)$  preserving the Killing fiber flow ( $\tilde{h}_*\xi = \xi$ ) and satisfying  $\pi_o \circ \tilde{h} = h \circ \pi_o$ . Then, we have a monomorphism from  $\Upsilon$  into  $Isom(M_o, \tilde{g}_o)$  whose image  $\tilde{\Upsilon}$  is isomorphic to  $\Upsilon$ . It is not difficult to see that this determines a properly discontinuous action of  $\tilde{\Upsilon}$  on  $M_o$ , defining a Riemannian covering map  $\tilde{p} : (M_o, \tilde{g}_o) \rightarrow (M = M_o/\tilde{\Upsilon}, \tilde{g})$ . Finally we define  $\pi : M \rightarrow B$  by  $\pi(\tilde{p}(\bar{a})) = p(\pi_o(\bar{a}))$  which satisfies  $\pi^*(g) = \tilde{g}$ . It can be checked that it provides a Killing submersion over  $B$  with bundle curvature  $\tau_\pi$ .  $\square$

Finally, we notice that any Killing submersion is locally isometric to one of the following canonical examples, [107], which include, as we will show later, the so called *Bianchi-Cartan-Vranceanu spaces* for suitable choices of the functions  $\lambda, a, b$ .

### 6.2.1 Canonical Examples

Given an open set  $\Omega \subset \mathbb{R}^2$  and  $\lambda, a, b \in \mathcal{C}^\infty(\Omega)$  with  $\lambda > 0$ , the Killing submersion

$$\pi : (\Omega \times \mathbb{R}, ds_{\lambda,a,b}^2) \rightarrow (\Omega, ds_\lambda^2), \quad \pi(x_1, x_2, x_3) = (x_1, x_2),$$

where

$$ds_{\lambda,a,b}^2 = \lambda^2(dx_1^2 + dx_2^2) + (dx_3 - \lambda(a dx_1 + b dx_2))^2 \quad (6.5)$$

and

$$ds_\lambda^2 = \lambda^2(dx_1^2 + dx_2^2),$$

will be called the *canonical example* associated to  $(\lambda, a, b)$ . Regardless of the values of the functions  $a, b \in C^\infty(\Omega)$ , the Riemannian metric given by equation (6.5) satisfies that  $\pi$  is a Killing submersion over  $(\Omega, ds_\lambda^2)$  with  $\xi = \partial_{x_3}$  as unit vertical Killing field.

The bundle curvature and the Gaussian curvature are given by

$$2\tau_\pi = \frac{1}{\lambda^2} ((\lambda b)_{x_1} - (\lambda a)_{x_2}), \quad K_\Omega = -\frac{1}{\lambda^2} \Delta_o(\log \lambda), \quad (6.6)$$

where  $\Delta_o$  represents the Laplacian with respect to the standard metric in the plane.

### 6.2.2 Bianchi-Cartan-Vranceanu Spaces

Fix  $\rho \in \mathbb{R}$ , then, particularizing the above construction one can get models for all Killing submersions over  $\mathbb{R}^2$ , if  $\rho = 0$ ;  $\mathbb{H}^2(\rho)$ , if  $\rho < 0$ ; and the punctured sphere,  $\mathbb{S}_*^2(\rho)$ , when  $\rho > 0$ . In fact, if we define  $\lambda_\rho \in C^\infty(\Omega_\rho)$  as

$$\lambda_\rho(x_1, x_2) = \left(1 + \frac{\rho}{4}(x_1^2 + x_2^2)\right)^{-1},$$

where  $\Omega_\rho = \{(x_1, x_2) \in \mathbb{R}^2 \mid 1 + \frac{\rho}{4}(x_1^2 + x_2^2) > 0\}$ , we obtain that the metric in  $\Omega_\rho = B$  given by (6.6) has constant Gaussian curvature  $K_B = \rho$ . If, in addition, we choose  $2a = -lx_2$  and  $2b = lx_1$  for some real constant  $l$ , then  $2\tau_\pi = l$ , and we deal with the *Bianchi-Cartan-Vranceanu spaces*,  $M(\rho, l)$ . Thus, the Bianchi-Cartan-Vranceanu spaces can be seen as the canonical models of Killing submersions with constant bundle curvature,  $\tau_\pi$ , and constant Gaussian curvature,  $K_B$ .

These spaces (see [38] and [140]) are described by the following two-parameter family of Riemannian metrics

$$g_{\rho, l} = \frac{dx_1^2 + dx_2^2}{\left(1 + \frac{\rho}{4}(x_1^2 + x_2^2)\right)^2} + \left(dx_3 + \frac{l}{2} \frac{x_2 dx_1 - x_1 dx_2}{\left(1 + \frac{\rho}{4}(x_1^2 + x_2^2)\right)}\right)^2, \quad \rho, l \in \mathbb{R} \quad (6.7)$$

defined on  $M = \{(x_1, x_2, x_3) \in \mathbb{R}^3 \mid 1 + \frac{\rho}{4}(x_1^2 + x_2^2) > 0\}$ . Their geometric interest lies in the following fact; *the family of metrics (6.7) includes all three-dimensional homogeneous metrics whose group of isometries has dimension 4 or 6, except for those of constant negative sectional curvature*. We recall that a Riemannian manifold  $(M^n, g)$  is said to be *homogeneous* if for every two points  $p$  and  $q$  in  $M^n$ , there exists an isometry of  $M^n$  mapping  $p$  into  $q$ . Cartan in [38] showed that the examples above cover in fact all possible 3-dimensional homogeneous spaces with 4-dimensional isometry group. These family also includes two real space forms, which have 6-dimensional isometry group. The full classification of these spaces is as follows (see, for instance [107])

- (i) If  $\rho = l = 0$ ,  $M(\rho, l) \cong \mathbb{R}^3$ .
- (ii) If  $\rho = l^2$ , then  $M(\rho, l) \cong \mathbb{S}^3(\frac{\rho}{4}) - \{\infty\}$ .

- (iii) If  $l \neq 0$  and  $\rho = 0$ , we have that  $M(\rho, l) \cong \mathbb{H}_3$ , the *Heisenberg group*.
- (iv) If  $\rho > 0$  and  $l = 0$ ,  $M(\rho, l)$  represents a model for the product space  $(\mathbb{S}^2(\rho) - \{\infty\}) \times \mathbb{R}$ .
- (v) If  $\rho < 0$  and  $l = 0$ ,  $M(\rho, l) \cong \mathbb{H}^2(\rho) \times \mathbb{R}$ .
- (vi) If  $\rho > 0$ ,  $l \neq 0$  and  $\rho \neq l^2$ , then  $M(\rho, l) \cong SU(2) - \{\infty\}$ .
- (vii) And, finally, if  $\rho < 0$  and  $l \neq 0$ , we have that  $M(\rho, l) \cong \tilde{S}l(2, \mathbb{R})$ .

For homogeneous 3-manifolds there are three possibilities for the degree of rigidity, since they may have an isometry group of dimension 6, 4 or 3. The maximum rigidity, 6, corresponds to the space forms, which have been introduced in Section 1.2. On the other hand, the homogeneous 3-dimensional spaces with isometry group of dimension four include, amongst its simply connected members, the product spaces  $\mathbb{S}^2(\rho) \times \mathbb{R}$  and  $\mathbb{H}^2(\rho) \times \mathbb{R}$ ; the Berger spheres; the Heisenberg group; and, the universal covering of the special linear group  $Sl(2, \mathbb{R})$  (see points (iii)-(vii) above). Finally, if the dimension of the isometry group is 3, the homogeneous 3-space is isometric to a general simply connected Lie group with left invariant metric.

Therefore, the above family contains the eight model geometries appearing in the famous conjecture of Thurston on the classification of 3-manifolds, recently proved. Moreover,  $M(\rho, l)$  spaces are the only simply connected homogeneous 3-manifolds admitting the structure of a Killing submersion, [107].

### 6.2.3 Bundle-Like Metrics

Let  $M$  be the 3-dimensional total space of a principal fiber bundle on a surface,  $B$ , and denote by  $\pi : M \rightarrow B$  the natural projection. Consider a principal connection  $\omega$  and denote by  $dt^2$  the metric on the fiber. Now, given a positive smooth function  $f \in C^\infty(B)$  and any Riemannian metric,  $g$ , on  $B$ , we can define the following *generalized Kaluza-Klein Riemannian metric* on  $M$

$$\tilde{g} = \pi^*(g) + (f \circ \pi)^2 \omega^*(dt^2).$$

In particular, if the function  $f$  is constant, then  $\tilde{g}$  is called a *Kaluza-Klein metric* or a *bundle-like metric*. As it is well-known, the following properties are satisfied by the above class of metrics;

- (i) The natural action of the structure group,  $G$ , on  $M$  is carried out by isometries of  $(M, \tilde{g})$ . Consequently, the fiber flow is associated with a Killing vector field of  $(M, \tilde{g})$ .
- (ii) The natural projection  $\pi : (M, \tilde{g}) \rightarrow (B, g)$  is a Riemannian submersion. Furthermore, its leaves are geodesics in  $(M, \tilde{g})$ , if and only if,  $f$  is a constant function, that is,  $\tilde{g}$  is a bundle-like metric.



(iii) Setting

$$\bar{g} = \frac{1}{(f \circ \pi^2)} \tilde{g} = \pi^* \left( \frac{1}{f^2} g \right) + \omega^*(dt^2)$$

one sees that generalized Kaluza-Klein metrics are conformal to bundle-like metrics.

Hence, once a suitable conformal change has been made (if necessary), every bundle-like metric provides a Riemannian submersion whose fiber flow is associated with a vertical unit Killing vector field. In other words, we have a Killing submersion.

### 6.3 Willmore-Like Tori in Killing Submersions

Assume we have a Killing submersion  $\pi : M \rightarrow B$  of a 3-dimensional Riemannian manifold  $M$  over a surface  $B$ . Let  $\gamma$  be an immersed curve in  $(B, g)$ , then  $S_\gamma = \pi^{-1}(\gamma)$  is a surface isometrically immersed in  $M$  (by the natural inclusion  $i = \varphi$ ) which is invariant under  $\mathcal{G} := \{\phi_t, t \in \mathbb{R}\}$ , the one-parameter group of isometries associated to the Killing vector field  $\xi$ . In fact, any  $\xi$ -invariant surface in  $M$ ,  $N^2$ , is obtained in this way;  $N^2 = \pi^{-1}(\gamma)$ , for some curve  $\gamma$  of  $B$ . It is usual to call  $S_\gamma$  *the vertical tube (or vertical cylinder) shaped on the curve  $\gamma$* . Notice that  $S_\gamma$  is embedded if  $\gamma$  is a simple curve, and it is a torus when  $\gamma$  is closed and  $\mathcal{G} \cong \mathbb{S}^1$  is a circle group. If  $\gamma$  is parametrized by its arc-length, then any horizontal lift of  $\gamma$ ,  $\bar{\gamma}$ , is also arc-length parametrized. Now, using as coordinate curves the horizontal lifts of  $\gamma$  and the fibers of the submersion, vertical tubes  $S_\gamma$  can be parametrized by  $x(s, t) = \phi_t(\bar{\gamma}(s))$  and, as a consequence,  $S_\gamma$  are flat. It is also known that the mean curvature of these surfaces  $H$  is related with the curvature function of the corresponding cross sections by the formula (for details, see [17])

$$H = \frac{1}{2} \kappa \circ \pi, \quad (6.8)$$

$\kappa$  denoting the geodesic curvature of  $\gamma$  in  $B$ . Then, we have

**Theorem 6.3.1.** ([25]) *Consider a Willmore-like energy  $\mathcal{W}_\Phi(N^2) = \int_{N^2} (H^2 + \Phi) dA$ , (6.1), with invariant potential  $\Phi$  ( $\Phi = \bar{\Phi} \circ \pi$ ) defined on the space of surface immersions in a Killing submersion  $\pi : M \rightarrow B$  with compact fiber, that is,  $\mathcal{G} \cong \mathbb{S}^1$ . If  $\gamma$  is a closed curve in  $B$ , then, its vertical torus  $S_\gamma = \pi^{-1}(\gamma)$  is a Willmore-like surface, if and only if,  $\gamma$  is an extremal of the following elastic energy with potential  $\Theta_{4\bar{\Phi}}(\gamma) = \int_\gamma (\kappa^2 + 4\bar{\Phi}) ds$ , (1.66).*

*Proof.* Let  $S_\gamma$  be a torus over  $\gamma$ . The  $\mathbb{S}^1$ -action on  $M$  can be naturally extended to  $Imm(N^2, M)$  by  $\mathcal{W}_\Phi(\varphi) = \mathcal{W}_\Phi(\phi_t \circ \varphi)$ , for all  $t \in \mathbb{R}$ ,  $\varphi \in Imm(N^2, M)$ . On the other hand the space,  $\Sigma$ , of the  $\mathbb{S}^1$ -invariant immersions can be identified with

$$\Sigma = \{S_\gamma = \pi^{-1}(\gamma) \mid \gamma \text{ is a closed curve in } B\}.$$

In this setting, we can apply the symmetric criticality principle of Palais [117] to reduce symmetry and then  $S_\gamma = \pi^{-1}(\gamma)$  is a Willmore-like torus, if and only if, it is an extremal of  $\mathcal{W}_\Phi$  restricted to  $\Sigma$ . Finally, we use (6.8) to conclude that this happens, precisely, when  $\gamma$  is a critical curve for  $\Theta_{4\bar{\Phi}}$ .  $\square$

Notice that the Euler-Lagrange equation of the elastic energy with potential  $4\bar{\Phi}$  has been introduced in Section 1.3.3, (1.67), obtaining

$$2\kappa_{ss} + \kappa (\kappa^2 + 2K_B - 4\bar{\Phi}) + 4N(\bar{\Phi}) = 0.$$

However, observe that this equation can also be derived as an application of Theorem 6.3.1. Indeed, we have

**Corollary 6.3.2.** ([25]) *A closed unit speed curve  $\gamma(s)$  of a Riemannian surface  $B$  is an extremal of the elastic energy with potential  $\Theta_{4\bar{\Phi}}(\gamma) = \int_\gamma (\kappa^2 + 4\bar{\Phi}) ds$ , if and only if,*

$$2\kappa_{ss} + \kappa (\kappa^2 + 2K_B - 4\bar{\Phi}) + 4N(\bar{\Phi}) = 0,$$

where  $N$  denotes the unit normal of  $\gamma$  in  $B$ .

*Proof.* If  $K_B$  is the Gaussian curvature of  $B$ , choose any  $\tau_\pi \in \mathcal{C}^\infty(B)$  and a Killing submersion  $\pi : M(K_B, \tau_\pi) \rightarrow B$  with compact fibers, as guaranteed by Theorem 6.2.1. Define  $\Phi = \bar{\Phi} \circ \pi$  on  $M(K_B, \tau_\pi)$ . Now, from Theorem 6.3.1, we have that  $\gamma$  is an extremal of the elastic energy with potential  $\Theta_{4\bar{\Phi}}(\gamma) = \int_\gamma (\kappa^2 + 4\bar{\Phi}) ds$ , if and only if,  $S_\gamma$  is a critical point of  $\mathcal{W}_\Phi(N^2) = \int_{N^2} (H^2 + \Phi) dA$ . Since  $S_\gamma$  is flat  $K_{S_\gamma} = 0$ , moreover, a straightforward computation shows that on these vertical flat tori  $2R + \text{Ric}(\eta, \eta) = K_B$ ,  $\eta$  being the unit normal along  $S_\gamma$ . Hence (6.4) gives that  $S_\gamma$  must provide a solution of the following differential equation

$$\Delta H + H(2H^2 + K_B - 2\Phi) + \eta(\Phi) = 0. \quad (6.9)$$

where  $H$  is the mean curvature function of  $S_\gamma$  in  $M(K_B, \tau_\pi)$ . Finally we combine (6.8) and (6.9) to conclude that the curvature of the elastica with  $4\bar{\Phi}$ -potential must satisfy the desired equation.  $\square$

### 6.3.1 Vertical Willmore Tori in Killing Submersions

As indicated in the introduction of the chapter, in the context of Killing submersions the Willmore problem can be described as the variational problem associated with the so called *Chen-Willmore energy*

$$\mathcal{CW}(N^2) \equiv \mathcal{CW}(N^2, \varphi) = \int_{N^2} (H_\varphi^2 + R) dA_\varphi, \quad (6.10)$$

where  $\varphi \in \text{Imm}(N^2, M)$ , and  $R$  denotes the *extrinsic Gaussian curvature* associated with the immersion  $\varphi$ , that is the sectional curvature of  $M$  restricted to the tangent bundle  $d\varphi(TN^2)$  of the corresponding surface. Recall that extremals of  $\mathcal{CW}$ , (6.10), are known as *Willmore surfaces*.

However, it should be noticed that, in general, the energy (6.10) does not coincide with those given in (6.1), because the potential in (6.10) is defined on the Grassmanian of two planes, but if  $(M, \tilde{g})$  has constant sectional curvature,  $\rho$ , then the Willmore energy (6.10) would correspond to a Willmore-like energy with constant potential  $\Phi = \rho$ . Nevertheless, the situation for vertical cylinders shaped on closed curves of the base surface changes and we have the following

**Theorem 6.3.3.** ([25]) *Assume that  $\pi : M(K_B, \tau_\pi) \rightarrow B$  is a Killing submersion with compact fiber, that is,  $\mathcal{G} \cong \mathbb{S}^1$ . Then, a vertical torus over a closed curve  $\gamma$  in  $B$ ,  $S_\gamma = \pi^{-1}(\gamma)$ , is a Willmore surface in  $M(K_B, \tau_\pi)$ , if and only if,  $S_\gamma$  is an extremal of the following Willmore-like energy*

$$\mathcal{W}_{\tau_\pi^2}(N^2) = \int_{N^2} (H^2 + \tau_\pi^2) dA.$$

And this happens in turn, if and only if,  $\gamma$  is an elastica with potential  $4\tau_\pi^2$  in  $B$ .

*Proof.* The extrinsic Gaussian curvature of vertical cylinders  $S_\gamma$  is related to the bundle curvature by

$$R(\bar{X}, \xi, \xi, \bar{X}) = \tau_\pi^2, \quad (6.11)$$

where  $\bar{X}$  denotes the horizontal lift of the unit tangent vector field  $X = \gamma'$ . Now, combining (6.10) and (6.11) and applying similar arguments to those used in Theorem 6.3.1 and the symmetric criticality principle of Palais, we draw the conclusion.  $\square$

It is well-known that compact minimal surfaces in spaces of constant curvature are examples of Willmore surfaces. The Euclidean 3-space,  $\mathbb{R}^3$ , does not contain compact minimal surfaces. However, the round 3-sphere,  $\mathbb{S}^3(\rho)$ , has plenty of compact minimal surfaces (for all rotational examples see Chapter 4). These Willmore surfaces can be conformally projected by the stereographic projection to the Euclidean 3-space,  $\mathbb{R}^3$ , (see, for instance, Figure 4.10 of Chapter 4) obtaining in this way examples of Willmore surfaces in the Euclidean 3-space,  $\mathbb{R}^3$ , because the Willmore energy is invariant under conformal changes in the surrounding metric.

Moreover, both the Euclidean 3-space,  $\mathbb{R}^3$ , and the round 3-sphere,  $\mathbb{S}^3(\rho)$ , provide examples of total 3-spaces associated with Killing submersions. In the former case,  $K_B = \tau_\pi = 0$  and  $\pi$  is just the projection over a plane, see point (i) of Section 6.2.2. In the spherical case,  $K_B = 4\tau_\pi^2$  is a constant and  $\pi$  is the well-known Hopf map from  $\mathbb{S}^3$  on  $\mathbb{S}^2$ , this is the case (ii) of Section 6.2.2 (see also Section 3.4.1). As it has been said previously, besides these spaces (whose group of isometries has dimension 6) the class of homogeneous

three spaces with 4-dimensional group of isometries provides also nice examples of Killing submersions with both  $K_B$  and  $\tau_\pi$  being constant. In this case vertical minimal tori are automatically Willmore (see [20] and references therein). In contrast, for general Killing submersions we have the following direct consequence of Theorem 6.3.3 and (6.11)

**Corollary 6.3.4.** ([25]) *Let  $\pi : M(K_B, \tau_\pi) \rightarrow B$  be a Killing submersion and  $\gamma(s)$  be a closed geodesic in  $B$ , then  $S_\gamma = \pi^{-1}(\gamma)$  is a Willmore torus in  $M(K_B, \tau_\pi)$ , if and only if,  $\gamma(s)$  is a tangent line of  $\tau_\pi^2$ .*

As an application, let us consider, for example, the unit round 2-sphere,  $\mathbb{S}^2(1) \subset \mathbb{R}^3$ , which we assume to be centered at the point  $p_o = (0, 0, 1)$ . Now, choose the non-negative function  $h \in \mathcal{C}^\infty(\mathbb{S}^2(1))$  obtained as the restriction of the height function, in  $\mathbb{R}^3$ , to the plane  $x_3 = 0$ . It is clear that the gradient flow associated with  $\text{grad } h$  is made up of the great circles through the origin, which obviously are geodesics. On the other hand, we know that there exists a Killing submersion  $M(K_B = 1, h) \rightarrow \mathbb{S}^2(1)$  with bundle curvature  $h$ , [107]. This Killing submersion is unique up to isomorphism and, in this case, it coincides with the Hopf map  $\pi : \mathbb{S}^3(1/4) \rightarrow \mathbb{S}^2(1)$  where the 3-sphere is endowed with a suitable metric. Therefore, in the corresponding conformal class, we get a class of minimal Willmore tori having a pair of great circles in common.

To end up this section, we consider frame bundles of surfaces as a particular case of Killing submersions and study Willmore surfaces in this context. Let  $B$  be a surface endowed with a Riemannian metric  $g$  and Gaussian curvature  $K_B$ . Denote by  $\mathbf{FB}$  its orthonormal frame bundle. Then, the natural projection,  $\pi : \mathbf{FB} \rightarrow B$  gives a principal bundle with structure group  $\mathbf{O}(2)$ . Now,  $\mathbf{FB}$  can be endowed with bundle-like metrics as follows

$$\tilde{g} = \pi^*(g) + \omega^*(dt^2),$$

providing a large class of Killing submersions. The corresponding bundle curvature  $\tau_\pi$  can be computed using (6.11) and [70]

$$\tau_\pi^2 = R(\bar{X}, \xi, \xi, \bar{X}) = \frac{1}{4} \frac{|R_{\Xi(\xi)}X|^2}{|X|^2 |\Xi(\xi)|^2} \circ \pi, \quad (6.12)$$

where  $\Xi$  is the third O'Neill invariant [116] defined in terms of the connection form  $\omega = (\omega_{ij})$  by

$$\Xi(\xi)(f) = \sum_{i \neq j}^2 \omega_{ij}(\xi) f_i \wedge f_j = 2\omega_{12}(\xi) f_1 \wedge f_2, \quad f = (f_1, f_2) \in \mathbf{FB}.$$

But  $1 = \bar{g}(\xi, \xi) = \langle \omega(\xi), \omega(\xi) \rangle = \sum_{i \neq j}^2 (\omega_{ij}(\xi))^2 = 2(\omega_{12}(\xi))^2$  and consequently  $(\omega_{12}(\xi))^2 = 1/2$ . Therefore,  $|\Xi(\xi)|^2 = 2$ . Moreover, we have

$$R_{\Xi(\xi)} = 2\omega_{12}(\xi) R_{f_1 f_2} \bar{X} = \sqrt{2} K_B (\langle X, f_2 \rangle f_1 - \langle X, f_1 \rangle f_2),$$

and we obtain

$$|R_{\Xi(\xi)}X|^2 = 2K_B^2 (\langle X, f_1 \rangle^2 + \langle X, f_2 \rangle^2) = 2K_B^2,$$

where  $|X| = 1$ . Hence, from (6.12) we see that the bundle curvature of the frame bundle Killing submersion is given by

$$\tau_\pi^2 = \frac{1}{4} K_B^2 \circ \pi. \quad (6.13)$$

Thus, combining Theorem 6.3.3 and (6.13) we have

**Corollary 6.3.5.** ([25]) *Let  $\gamma$  be a closed curve in a Riemannian surface,  $B$ , with Gaussian curvature  $K_B$ . Then  $S_\gamma = \pi^{-1}(\gamma)$  is a Willmore torus in the orthonormal frame bundle  $\mathbf{FB}$ , if and only if,  $\gamma$  is an extremal of the following elastic energy with potential (1.66)*

$$\Theta_{K_B^2}(\gamma) = \int_\gamma (\kappa^2 + K_B^2) ds,$$

acting on the space of closed curves in  $B$ .

## 6.4 Willmore Tori Foliations of Killing Submersions

In this last part we are going to exploit the characterization given in previous section of vertical Willmore tori in the total space of a Killing submersion in terms of elasticae with potential in the base surface.

On one hand, we are going to use the particular case of Killing submersions described above, that is, orthonormal frame bundles of surfaces, together with Corollary 6.3.5, to foliate these bundles by Willmore tori. Moreover, these tori will have constant mean curvature. On the other hand, strongly using Theorem 6.3.3 and the existence of Killing submersions given in Theorem 6.2.1, we are going to be able to construct some special cases of Killing submersions whose total spaces may be foliated by Willmore tori with constant mean curvature.

### 6.4.1 Willmore Tori Foliations of Orthonormal Frame Bundles

We first show how one can get minimal Willmore tori families foliating the frame bundle of compact rotational surfaces in  $\mathbb{R}^3$ .

**Proposition 6.4.1.** ([25]) *The orthonormal frame bundle of any compact rotational surface in  $\mathbb{R}^3$  admits a foliation by minimal Willmore tori.*

*Proof.* Let  $S_\gamma$  be the rotation torus which is swept out by rotating a closed curve  $\gamma$  contained in the half plane  $x_3 = 0$ ,  $x_1 > 0$ , around the  $x_3$ -axis. Denote by  $\phi_t(\gamma)$  the meridian obtained by rotating an angle  $t$  the profile curve  $\gamma$ . It is obvious that  $\pi^{-1}(\phi_t(\gamma))$

is a minimal torus in  $\mathbf{FS}_\gamma$ . However, meridians are not only geodesic, but they are also extremals of the elastic energy  $\Theta_{K_B^2}$  because  $T(K_B) = 0$  (see Corollary 6.3.5 and (1.66)). Consequently,  $\{\pi^{-1}(\phi_t(\gamma)), t \in \mathbb{R}\}$  constitutes a foliation of  $\mathbf{FS}_\gamma$  by minimal Willmore tori.  $\square$

Now we want to obtain orthonormal frame bundles of surfaces, which admit foliations by non-minimal Willmore tori. To this end, we consider the following construction. Let  $f(s)$  be a smooth function defined on a real interval  $I$  endowed with the warped product metric  $ds^2 + f(s)dt^2$ . The corresponding Riemannian surface is a warped product surface simply denoted by  $S_f = I \times_f \mathbb{S}^1$ . The group  $\mathbb{S}^1$  acts trivially on  $S_f$  by isometries and the orbits of this action,  $\delta_s(t) = \{s\} \times \mathbb{S}^1$ , are the corresponding fibers of  $S_f$ . We first want to determine the warped product surfaces for which all fibers are extremals of

$$\Theta_{K_{S_f}^2}(\delta) = \int_\delta \left( \kappa^2 + K_{S_f}^2 \right) dt, \quad (6.14)$$

$K_{S_f}$  denoting the Gaussian curvature of  $S_f$ . Then, we have

**Proposition 6.4.2.** ([25]) *Let  $S_f := I \times_f \mathbb{S}^1$  be a warped product surface all whose fibers are critical for the energy functional (6.14). Then, locally, either  $f$  is constant and  $S_f$  is a Riemannian product surface, or  $f(s)$  is determined by*

$$\frac{\lambda s}{2} = \pm \int \frac{df}{\sqrt{-1 + \frac{4}{\lambda}f - 2\text{Lam}\left(-\frac{1}{\lambda} \exp\left(d_1 - \frac{2}{\lambda}f\right)\right) - \text{Lam}^2\left(-\frac{1}{\lambda} \exp\left(d_1 - \frac{2}{\lambda}f\right)\right)}},$$

where  $\lambda \in \mathbb{R}^+$  and  $\text{Lam}$  denotes the Lambert function [43].

*Proof.* As mentioned above, the Euler-Lagrange equation for closed extremals of (6.14) in a surface has been obtained in Section 1.3.3 (see also Corollary 6.3.2), and it reads

$$2\kappa''(t) + \kappa^3(t) + 2K(t)\kappa(t) - K^2(t)\kappa(t) + N(K^2(t)) = 0, \quad (6.15)$$

where just in this proof  $t$  is the arc-length parameter of the curve,  $(\cdot)' = \frac{d}{dt}$ ,  $K(t)$  is the Gaussian curvature of the surface along the curve and  $N$  is the normal vector to the curve in the surface.

Assume that every orbit of  $S_f$  is critical for (6.14). In  $S_f$  the geodesic curvature of any orbit  $\kappa_\delta(s, t) = -\frac{\dot{f}(s)}{f(s)}$  is constant on it (where now we are using overdots for  $\frac{d}{ds}$ ) while the Gaussian curvature is given by  $K(s, t) = -\frac{\ddot{f}(s)}{f(s)}$ . Observe that  $N \equiv \frac{d}{ds}$  is the normal vector field to the orbits on the surface. Since, all orbits are critical, equation (6.15) tells us that

$$2f(s)\dot{f}(s)\ddot{f}(s) - \dot{f}^3(s) + 2f(s)\ddot{f}(s)\ddot{\dot{f}}(s) - \dot{f}(s)\dot{f}^2(s) = 0, \quad (6.16)$$

for  $s \in I$ . If  $f(s)$  is constant, then  $S_f$  is locally a Riemannian product which is a flat surface with every orbit being a geodesic. Therefore, orbits of Riemannian products satisfy (6.15) so that they are critical for (6.14). If  $f(s)$  is not constant, we divide (6.16) by  $f^2(s)$  obtaining

$$\frac{d}{ds} \left( \frac{\dot{f}^2(s)}{f(s)} + \frac{\ddot{f}^2(s)}{f(s)} \right) = 0.$$

and therefore

$$\dot{f}^2(s) + \ddot{f}^2(s) = \lambda f(s), \quad (6.17)$$

for some  $\lambda \in \mathbb{R}^+$ . For simplicity, in the following manipulations we put  $y(s) := f(s)$ . Then, (6.17) can be written as

$$\frac{1}{2} \frac{d}{dy} (\dot{y}^2(s)) = \pm \sqrt{\lambda y(s) - \dot{y}^2(s)}.$$

Thus, setting  $z(s) = \dot{y}^2(s)$ ,  $p(y) = \frac{dz}{dy}$ , one gets

$$\frac{1}{2} \frac{dz}{dy} = \pm \sqrt{\lambda y - z}, \quad y = \frac{1}{\lambda} \left( \frac{1}{4} p^2 + z \right). \quad (6.18)$$

Differentiating with respect to  $z$  the second identity in (6.18), we have

$$dz = \frac{1}{2} \frac{p^2}{\lambda - p} dp.$$

Integrating this we get

$$z + c_1 = -\frac{\lambda}{2} p - \frac{1}{4} p^2 - \frac{\lambda^2}{2} \log(\lambda - p), \quad (6.19)$$

with  $c_1 \in \mathbb{R}$ . Unwinding the changes of variable (6.19) reduces to

$$c_1 = \mp \lambda \sqrt{\lambda y - \dot{y}^2} - \lambda y - \frac{\lambda^2}{2} \log \left( \lambda \mp 2 \sqrt{\lambda y - \dot{y}^2} \right). \quad (6.20)$$

Manipulating the equation (6.20), we obtain

$$-\frac{1}{\lambda} \exp \left( d_1 - \frac{2}{\lambda} y \right) = -\frac{1}{\lambda} \left( \lambda \mp 2 \sqrt{\lambda y - \dot{y}^2} \right) \exp \left( -\frac{1}{\lambda} \left( \lambda \mp 2 \sqrt{\lambda y - \dot{y}^2} \right) \right),$$

for a certain constant  $d_1 \in \mathbb{R}$ . In other words

$$\text{Lam} \left( -\frac{1}{\lambda} \exp \left( d_1 - \frac{2}{\lambda} y \right) \right) = -\frac{1}{\lambda} \left( \lambda \mp 2 \sqrt{\lambda y - \dot{y}^2} \right), \quad (6.21)$$

where Lam denotes the Lambert function (see [43]). Finally, from (6.21) we have

$$\dot{y}^2 = \frac{\lambda}{4} \left( -1 + \frac{4}{\lambda} y - 2 \operatorname{Lam} \left( -\frac{1}{\lambda} \exp \left( d_1 - \frac{2}{\lambda} y \right) \right) - \operatorname{Lam}^2 \left( -\frac{1}{\lambda} \exp \left( d_1 - \frac{2}{\lambda} y \right) \right) \right).$$

This concludes the proof.  $\square$

Observe that according to the results in previous section, the warped product surfaces described in Proposition 6.4.2 give rise to orthonormal frame bundles admitting foliations by Willmore tori with constant mean curvature.

### 6.4.2 Construction of Killing Submersions Foliated by Willmore Tori

The purpose of this section is to introduce a way of constructing special Killing submersion whose total spaces admit foliations by Willmore tori. In order to achieve this goal, we are going to consider elastic curves with potential, as suggested by Theorem 6.3.3. In particular, one possible potential may be a constant one, that is,  $\bar{\Phi} = \lambda \in \mathbb{R}$ . This will give us, precisely, critical curves of the bending energy for variations with a restriction on the length of the curves, due to a version of the Lagrange's Multipliers Principle.

Now, a natural problem is the following; *given a generalized elastica, critical curve of the energy  $\Theta_{-\lambda}^{2,o}$ , (2.2), say  $\gamma(s)$ , in  $B$ , determine those potentials  $\bar{\Phi} \in C^\infty(B)$  for which  $\gamma(s)$  is an extremal of  $\Theta_{\bar{\Phi}}$ , in other words, a solution of (1.67).* It is clear that these potentials must satisfy the following differential equation along the curve  $\gamma(s)$

$$N(\ln(\bar{\Phi} - \lambda)) = \kappa.$$

Therefore, in a neighborhood of  $\gamma(s)$  in  $B$ , they must have the following form

$$\bar{\Phi}(s, t) = \exp(\kappa(s)t + \varpi(s)) + \lambda,$$

where  $\varpi(s)$  is an arbitrary function along  $\gamma(s)$ . Consequently, we have

**Theorem 6.4.3.** ([25]) *Let  $\gamma(s)$  be an elastic curve with constant potential  $\lambda$  and with curvature function  $\kappa(s)$  lying on a surface  $B$  with Gaussian curvature  $K_B$ . For an arbitrary function  $\varpi(s)$  along  $\gamma(s)$  consider*

$$\bar{\Phi}(s, t) = \exp(\kappa(s)t + \varpi(s)) + \lambda,$$

*defined on a certain neighborhood  $t \in (-\epsilon, \epsilon)$  of  $\gamma(s)$ . Let  $\pi : M(K_B, \tau_\pi) \rightarrow B$  be a Killing submersion with closed fibers and bundle curvature,  $\tau_\pi$ , satisfying  $4\tau_\pi^2 = \bar{\Phi}(s, t)$  on the chosen neighborhood. Then,  $S_\gamma = \pi^{-1}(\gamma)$  is a Willmore torus in  $M(K_B, \tau_\pi)$ .*



Finally, as an illustration we analyze the following problem. In  $B = \mathbb{R}^2 - \{(0,0)\}$  consider the family of circles  $\{C_t, t > 0\}$  defined by  $C_t = \{(x_1, x_2) \in \mathbb{R}^2 \mid x_1^2 + x_2^2 = t^2\}$ . It is obvious that this family constitutes the leaves of a foliation in  $B$ . Now, we wish to determine those potentials  $\bar{\Phi} \in \mathcal{C}^\infty(B)$  that make the whole family of circles extremals of the energy (1.66). Notice that we are considering  $B$  as the once-punctured Euclidean plane and obviously endowed with the Euclidean metric, so  $K_B = 0$  and the curvature of  $C_t$  is  $1/t$ . Hence, from (1.67) we must determine those functions  $\bar{\Phi}(s, t)$  which are solutions of the following differential equation

$$\frac{\partial}{\partial t} \bar{\Phi} = \frac{1}{t} \bar{\Phi} - \frac{1}{t^3}. \quad (6.22)$$

But, the general solution of this (6.22) is

$$\bar{\Phi}(s, t) = f(s)t + \frac{1}{3t^2}, \quad f \in \mathcal{C}^\infty(\mathbb{S}^1). \quad (6.23)$$

As a consequence, we have the following statement

**Corollary 6.4.4.** ([25]) *Let  $B = \mathbb{R}^2 - \{(0,0)\}$  be the once-punctured Euclidean plane,  $f$  a smooth periodic positive function and define  $\bar{\Phi}$  by (6.23). Then, there exists a Killing submersion  $\pi : M(0, \tau_\pi) \rightarrow B$  with bundle curvature given by  $4\tau_\pi^2 = \bar{\Phi}$  which admits a foliation by Willmore tori with constant mean curvature.*

*Proof.* Positivity of the function  $f$  allows to ensure the existence of  $\tau_\pi \in \mathcal{C}^\infty(B)$  satisfying  $4\tau_\pi^2 = \bar{\Phi}$ , where  $\bar{\Phi}$  is defined in (6.23). Now, we use Theorem 6.4.3 to obtain a Killing submersion, say  $\pi : M(0, \tau_\pi) \rightarrow B$ , with compact fibers over  $B$  and bundle curvature  $\tau_\pi$ . Since the circles  $C_t, t > 0$  are extremals of the energy action (1.66), we obtain that  $S_t = \pi^{-1}(C_t)$  are Willmore tori in  $M$  (see Proposition 6.23).  $\square$



# Appendix A

## Computations Involving Elliptic Integrals

The main purpose of this appendix is to introduce a brief survey about elliptic integrals and to prove some results involving long computations that have been used along the whole PhD memory, to be more precise in Section 4.3.2.

We begin by introducing well-known definitions and properties concerning elliptic integrals. We define the *incomplete elliptic integrals* of first, second and third kind, respectively by

$$F(\chi, p) = \int_0^{\sin \chi} \frac{dx}{\sqrt{(1-x^2)(1-p^2x^2)}}, \quad E(\chi, p) = \int_0^{\sin \chi} \frac{\sqrt{1-p^2x^2}}{\sqrt{1-x^2}} dx,$$

and

$$\Pi(\chi, \nu, p) = \int_0^{\sin \chi} \frac{dx}{(1-\nu x^2)\sqrt{(1-x^2)(1-p^2x^2)}},$$

where  $p$  is the *modulus* and the number  $\nu$  represents the *parameter* of the integral of third kind.

We will denote by  $K(p)$ ,  $E(p)$  and  $\Pi(\nu, p)$  to the *complete elliptic integrals* of first, second and third kind, respectively, where  $\chi = \pi/2$ ; that is,

$$K(p) = F\left(\frac{\pi}{2}, p\right), \quad E(p) = E\left(\frac{\pi}{2}, p\right), \quad \Pi(\nu, p) = \Pi\left(\frac{\pi}{2}, \nu, p\right).$$

Complete elliptic integrals have some distinguished values. In the following formulas we recall some of them (for more details see [68])

$$K(0) = \frac{\pi}{2}, \quad E(0) = \frac{\pi}{2} \quad \text{and} \quad E(1) = 0.$$

Notice that along the memory, as  $p^2 < \nu < 1$  (see Section 4.3.2), we have made use of the following alternative description for  $\Pi(\nu, p)$ ,

$$\Pi(\nu, p) = \frac{\pi}{2} \sqrt{\frac{\nu}{(1-\nu)(\nu-p^2)}} \Lambda_o \left( \arcsin \sqrt{\frac{\nu-p^2}{\nu(1-p^2)}}, p \right), \quad (\text{A.1})$$

where  $\Lambda_o$  represents the *Heuman's Lambda*, (similar descriptions for this and other relations between  $p$  and  $\nu$  can be found in Appendix B of [5]).

As happened with the complete elliptic integrals, there are some distinguished values for the Heuman's Lambda too, these main values are (see Appendix B of [5])

$$\Lambda_o(\phi, 0) = \sin \phi, \quad \Lambda_o(\phi, 1) = \frac{2\phi}{\pi} \quad \text{and} \quad \Lambda_o\left(\frac{\pi}{2}, p\right) = 1.$$

It is also important to have in mind that Heuman's Lambda is antisymmetric in  $\phi$  and that

$$\Lambda_o(\phi + m\pi, p) = 2m\pi + \Lambda_o(\phi, p), \quad (\text{A.2})$$

for any integer  $m \in \mathbb{Z}$ .

Moreover, along the memory, we have also made use of the derivatives of the elliptic integrals and of the Heuman's Lambda with respect to their modulus. These derivatives are given by the following formulas

- (i)  $\frac{dK(p)}{dp} = \frac{1}{p(1-p^2)} (E(p) - (1-p^2)K(p)),$
- (ii)  $\frac{dE(p)}{dp} = \frac{1}{p} (E(p) - K(p))$  and
- (iii)  $\frac{d\Lambda_o(\phi, p)}{dp} = \frac{\sin 2\phi}{\pi p \sqrt{1-(1-p^2)\sin^2 \phi}} (E(p) - K(p)).$

Now, following the notation of [68], we call

$$q = \sqrt{1-p^2} \quad \text{and} \quad \nu = \frac{4d(\alpha-\beta)}{4d(\alpha-\mu)-\rho},$$

where  $\alpha$  and  $\beta$  are given in Section 4.3.2 and  $4d = \alpha + \beta - 4\mu$ . One may check that this definitions coincide with those given in (4.44). Then, let's consider the function

$$I = \sqrt{\frac{\nu-p^2}{\nu}} K(p) + \frac{\pi}{2} \epsilon \Lambda_o \left( \arcsin \frac{1}{q} \sqrt{\frac{\nu-p^2}{\nu}}, p \right), \quad (\text{A.3})$$

where  $\epsilon$  can be  $-1, 0$  or  $1$ , since it will represent the sign of  $\rho - 4\mu d$ . Observe that the function  $I$ , (A.3), corresponds with (4.47) if  $\epsilon = \pm 1$ , and with (4.51), if  $\epsilon = 0$ ; and that it is expressed as a linear combination of complete elliptic integrals after making use of the relation (A.1).

In the following lemmas, we are going to state the main results of this appendix.

**Lemma A.0.1.** *The function  $I$  defined in (A.3) is monotonically decreasing in  $p$ .*

*Proof.* In order to prove this result, we compute the derivative of  $I$  with respect to  $p$  and see that it is always negative. For the sake of simplicity and following the notation of Section 4.3.2, we call  $q$  to  $\sqrt{1-p^2}$  and

$$\phi = \frac{1}{q} \sqrt{\frac{\nu - p^2}{\nu}}.$$

Then, we observe that  $\phi$  is not monotone. Indeed, since

$$\frac{d\phi}{dq} = -\frac{\phi}{\sqrt{\alpha - 2\mu}} (\beta - 2\mu),$$

it changes monotonicity at  $q = \frac{\mu}{\sqrt{\rho + \mu^2}}$ , that is, precisely at  $\rho = 4\mu d$ . This means that the sign  $\epsilon$  for each possible value disappears when differentiating. Notice that this can also be obtained as a consequence of the property of the Heuman's Lambda given in (A.2). Let's begin by considering first the case  $\epsilon = 0$ . Computing the derivative of  $I$ , (A.3), with respect to  $p$  we obtain after straight forward computations

$$\frac{dI}{dp} = \frac{1}{pq} (E(p) - K(p)) < 0,$$

which concludes the proof for this case.

Now, if  $\epsilon \neq 0$ , differentiating  $I$ , (A.3), with respect to  $p$  and using previous argument about monotonicity of  $\phi$  to delete  $\epsilon$ , we get after long computations for both  $\epsilon = 1$  and  $\epsilon = -1$  that

$$\frac{dI}{dp} = \frac{\phi}{pq} (2E(p) - (1 + q^2)K(p)).$$

Moreover, calling  $G(p) = 2E(p) - (1 + q^2)K(p)$ , we get that  $G(p) < 0$ , for any  $p \in (0, 1)$ , since  $G(0) = 0$  and

$$G'(p) = p \left( K(p) - \frac{1}{q^2} E(p) \right) < 0$$

implies that  $G(p)$  is decreasing and, therefore,  $G(p) < G(0) = 0$ . That is,  $I$  is decreasing in  $p$ , as desired.  $\square$

The main consequence that can be obtained from previous lemma is that the function  $I$  is bijective, since it is monotonically decreasing. Therefore, it is clear that its range decreases from the maximum value, obtained as the limit when  $p$  is the smallest possible value, to the maximum one, which is reached at the biggest possible value of  $p$ .

Thus, now we want to obtain the maximum and minimum values of  $I$ . Indeed, as explained above, it is sufficient to take limits for the maximum and minimum values of  $p$

for each correspondence case. This is a direct long computation where we must use the different distinguished values presented before. We sum up these results in the following lemmas,

**Lemma A.0.2.** *Consider  $\mu \leq 0$ , then  $p \in (0, 1)$  and the maximum and minimum values of  $I$ , (A.3), are respectively*

$$\lim_{p \rightarrow 0} I = \frac{\pi}{(\rho + \mu^2)^{\frac{1}{4}}} \sqrt{\frac{\rho}{2(-\mu + \sqrt{\rho + \mu^2})}} \quad \text{and} \quad \lim_{p \rightarrow 1} I = \arcsin \sqrt{\frac{\rho}{\rho + \mu^2}}.$$

*Proof.* Since  $\mu \leq 0$ , then necessarily  $\epsilon = 1$  and  $p \in (0, 1)$ . Then, taking limits in (A.3) we obtain the statement.  $\square$

**Lemma A.0.3.** *Let  $\mu > 0$ , then  $\epsilon$  can be either 0, 1 or  $-1$ , and we have the following cases;*

- (i)  $\epsilon = 1$ , if and only if,  $p \in \left(0, \sqrt{\frac{\rho}{\rho + \mu^2}}\right)$ ; and, the maximum and minimum values of  $I$ , (A.3), are respectively

$$\begin{aligned} \lim_{p \rightarrow 0} I &= \frac{\pi}{(\rho + \mu^2)^{\frac{1}{4}}} \sqrt{\frac{\rho}{2(-\mu + \sqrt{\rho + \mu^2})}} \quad \text{and} \\ \lim_{p \rightarrow \frac{\rho}{\sqrt{\rho + \mu^2}}^-} I &= \frac{\mu}{\sqrt{\rho + \mu^2}} K \left( \sqrt{\frac{\rho}{\rho + \mu^2}} \right) + \frac{\pi}{2}. \end{aligned}$$

- (ii)  $\epsilon = -1$ , if and only if,  $p \in \left(\sqrt{\frac{\rho}{\rho + \mu^2}}, 1\right)$ ; and, we have the following limits for  $I$ , (A.3)

$$\lim_{p \rightarrow \frac{\rho}{\sqrt{\rho + \mu^2}}^+} I = \frac{\mu}{\sqrt{\rho + \mu^2}} K \left( \sqrt{\frac{\rho}{\rho + \mu^2}} \right) - \frac{\pi}{2} \quad \text{and} \quad \lim_{p \rightarrow 1} I = -\arcsin \sqrt{\frac{\rho}{\rho + \mu^2}}.$$

- (iii) Finally,  $\epsilon = 0$ , if and only if,  $p = \sqrt{\frac{\rho}{\rho + \mu^2}}$ . In this case, for the possible values of  $\mu \in (0, \infty)$ ,  $p$  varies from zero to one, and we have

$$\lim_{p \rightarrow 0} I = \frac{\pi}{2} \quad \text{and} \quad \lim_{p \rightarrow 1} I = 0.$$

*Proof.* Observe that since  $\epsilon$  represents the sign of  $\rho - 4\mu d$  and  $\mu > 0$ , we have that the three options for  $\epsilon$  may be possible. Then, using the definition of  $p$ , (4.44), we obtain

the three different intervals. Finally, by taking the correspondence limits in  $I$ , (A.3), and making use of the distinguished values of elliptic integrals and Heuman's Lambda we conclude the proof.  $\square$

In Figure A.1 we have painted in light blue the different regions where the function  $I$  may have values. The upper regions correspond with the two possible cases for  $\epsilon = 1$ , while the region in the negative part of the  $I$ -axis corresponds with  $\epsilon = -1$ . The functions drawn in dark blue are the corresponding limit functions of previous lemmas. Notice that a similar picture was drawn in [122]. Finally, in Figure A.1 two horizontal red lines have been plotted at  $\pi/2$  and  $-\pi/3$ , respectively, and they bound the rectangular region where there may be values of the type  $mI = \pi$ , for some integer  $m$ . For more details see Theorem 4.3.7.

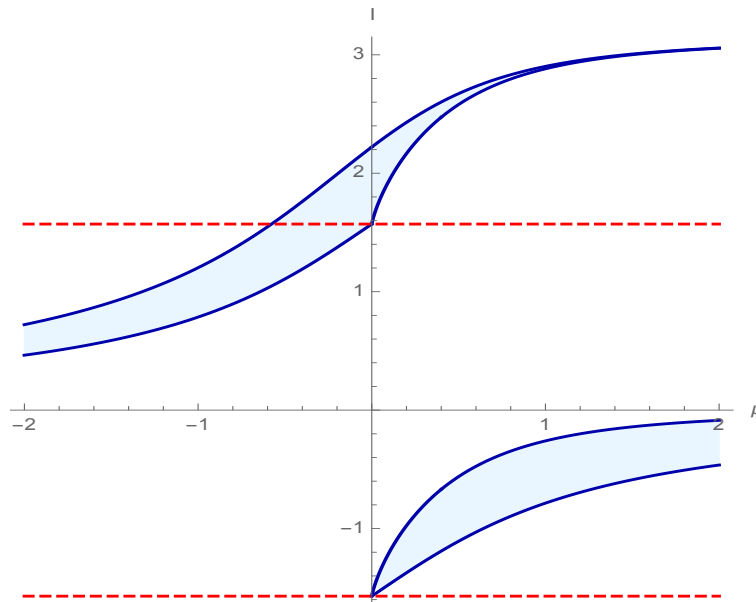


Figure A.1: Regions for the range of the function  $I$ , (A.3).





# Appendix B

## Gradient-Descent Method

In this appendix we are going to introduce a brief description of the gradient descent based method we have developed in [9] (which we call *XEL-platform*) to localize minima of an ample family of functionals defined on certain spaces of curves satisfying both affine and isoperimetric constraints. First, we are going to describe the formalism which serves as base for the numerical treatment.

Let  $H_0(I, \mathbb{R}^m) = L^2(I, \mathbb{R}^m)$  be the set of square integrable functions from  $I$  to  $\mathbb{R}^m$ , where  $I$  is an interval  $[a, b]$ . Let  $H_1(I, \mathbb{R}^m)$  denote the set of absolutely continuous maps  $\mathbf{x} : I \rightarrow \mathbb{R}^m$  such that  $\mathbf{x}^{(1)} \in H_0(I, \mathbb{R}^m)$ , where  $\mathbf{x}^{(1)}$  stands for the first derivative of the function. Finally, denote by  $H_n(I, \mathbb{R}^m)$  the set of maps  $\mathbf{x} : I \rightarrow \mathbb{R}^m$  such that  $\mathbf{x}^{(k)} \in H_1(I, \mathbb{R}^m)$ ,  $k \in \{0, \dots, n-1\}$ , where  $\mathbf{x}^{(k)}$  denotes the  $k$ -th derivative of  $\mathbf{x}$ . Then,  $H_n(I, \mathbb{R}^m)$  is a Hilbert space with the following family of inner products [9]

$$\begin{aligned} \langle \mathbf{x}(t), \mathbf{y}(t) \rangle_{n,a,b} := & \int_a^b \langle \mathbf{x}^{(n)}(t), \mathbf{y}^{(n)}(t) \rangle dt + \sum_{k=0}^{n-1} \eta_a^k \langle \mathbf{x}^{(k)}(a), \mathbf{y}^{(k)}(a) \rangle \\ & + \sum_{k=0}^{n-1} \eta_b^k \langle \mathbf{x}^{(k)}(b), \mathbf{y}^{(k)}(b) \rangle, \end{aligned} \quad (\text{B.1})$$

where  $\langle \cdot, \cdot \rangle$  is the standard inner product in  $\mathbb{R}^m$  and,  $\eta_a^k \geq 0$ ;  $\eta_b^k \geq 0$ ; and,  $\eta_a^k + \eta_b^k > 0$ . To simplify the notation, from now on the above inner product (B.1) and the space  $H_n(I, \mathbb{R}^m)$  will be denoted simply by  $\langle \cdot, \cdot \rangle_n$  and  $X^n$ , respectively.

We want to analyze the variational problem associated to a certain family of energy functionals  $\mathcal{F} : X^n \rightarrow \mathbb{R}$  defined on  $X^n$  or on suitable subspaces of curves in  $X^n$ . We

consider functionals of the form

$$\begin{aligned} \mathcal{F}(\mathbf{x}) &= \int_a^b f\left(t, \dots, x_i, \dots, x_i^{(1)}, \dots, x_i^{(n)}, \dots\right) dt \\ &\quad + A\left(a, \dots, x_i(a), \dots, x_i^{(n-1)}(a), \dots\right) \\ &\quad + B\left(b, \dots, x_i(b), \dots, x_i^{(n-1)}(b), \dots\right) \end{aligned} \quad (\text{B.2})$$

where  $\mathbf{x} = (x_j(t)) \in X^n$ ,  $j = 1, \dots, m$  and  $f: W \subset \mathbb{R}^{m(n+1)+1} \rightarrow \mathbb{R}$ ,  $A, B: \widetilde{W} \subset \mathbb{R}^{mn+1} \rightarrow \mathbb{R}$  are continuously differentiable functions defined on a sufficiently large domains  $W, \widetilde{W}$ . We also assume that  $f, A, B$  satisfy suitable additional conditions which guarantee the Fréchet differentiability of  $\mathcal{F}$  and the (local) convergence of the gradient steepest descent method (for more details see [9]).

As usual, one may consider  $\mathcal{F}$  acting on subspaces of functions  $\mathbf{x} = (x_1, \dots, x_m) \in X^n$  satisfying, together with their derivatives  $\mathbf{x}^{(i)} = (x_1^{(i)}, \dots, x_m^{(i)})$ , given boundary conditions at the endpoints of the interval (they will be referred to as *affine constraints*). For instance, for a given  $i \in \{0, 1, \dots, n-1\}$ , fix  $\mathbf{p}^i = (p_1^i, \dots, p_m^i)$  and  $\mathbf{q}^i = (q_1^i, \dots, q_m^i)$ , points in  $\mathbb{R}^m$ . Then, for any arbitrary choice of a finite number of indexes  $i \in \{0, 1, \dots, n-1\}$  and  $j \in \{1, 2, \dots, m\}$ , the intersection of the following family of subspaces

$$X_{a,b,j}^{(i)} = \left\{ \mathbf{y}: [a, b] \rightarrow \mathbb{R}^m; y_j^{(i)}(a) = p_j^i, y_j^{(i)}(b) = q_j^i \right\},$$

is an affine subspace of  $X^n$ . So endpoint constraints lead to spaces of functions which are not linear but they are affine spaces instead what causes minor computational additional difficulties.

In contrast, suppose that we are seeking functions which not only satisfy affine constraints but also verify extra restrictions of the form (which will be called *isoperimetric restrictions*)

$$\begin{aligned} \mathcal{G}(\mathbf{x}) &= \int_a^b g\left(t, \dots, x_i, \dots, x_i^{(1)}, \dots, x_i^{(n)}, \dots\right) dt \\ &\quad + A^{\mathcal{G}}\left(a, \dots, x_i(a), \dots, x_i^{(n-1)}(a), \dots\right) \\ &\quad + B^{\mathcal{G}}\left(b, \dots, x_i(b), \dots, x_i^{(n-1)}(b), \dots\right) = c, \end{aligned} \quad (\text{B.3})$$

where,  $g, A^{\mathcal{G}}, B^{\mathcal{G}}$  are, at least, continuously differentiable functions and  $c \in \mathbb{R}$ . Now any candidate to be a solution must lie in the hypersurface  $X_{\mathcal{G}}^n = \mathcal{G}^{-1}(c) \subseteq X^n$ , which is not an affine subspace. Of course, more than one isoperimetric restriction may appear at the same time, and then any solution to the variational problem must lie in  $X_{\mathcal{G}}^n = X_{\mathcal{G}_1}^n \cap \dots \cap X_{\mathcal{G}_h}^n$ .

For simplicity, in the rest of this appendix we focus on the unconstrained problem. Thus, we assume that the above functional (B.2) is defined on  $X^n$ . The gradient of  $\mathcal{F}$

at  $\mathbf{x}$  is defined to be the unique  $\nabla\mathcal{F}_{\mathbf{x}} \in X^n$  that satisfies  $\langle \nabla\mathcal{F}_{\mathbf{x}}, \mathbf{w} \rangle_n = D\mathcal{F}_{\mathbf{x}}(\mathbf{w})$ , for all  $\mathbf{w} \in X^n$ . The existence and uniqueness of  $\nabla\mathcal{F}_{\mathbf{x}}$  is guaranteed by the Riesz Representation Theorem. Actually, as it has been proved in [9], for a functional  $\mathcal{F}: X^n \rightarrow \mathbb{R}$  of the type (B.2) (satisfying suitable conditions as those mentioned before), then the gradient is given by  $\nabla\mathcal{F}_{\mathbf{x}} = (\nabla\mathcal{F}_{x_1}, \dots, \nabla\mathcal{F}_{x_m})$  and

$$\nabla\mathcal{F}_{x_j} = \int_a^t \overset{\cdot}{\cdot} \overset{\cdot}{\cdot} \overset{\cdot}{\cdot} \int_a^t E_{x_j, n}^f dt + P_{x_j, 2n-1}(t), \quad (\text{B.4})$$

where  $E_{x_j, n}^f$  are defined recursively as

$$E_{x_j, 0}^f = \frac{\partial f}{\partial x_j} = f_{x_j}, \quad E_{x_j, i}^f = f_{x_j^{(i)}} - \int_a^t E_{x_j, i-1}^f ds = \sum_{k=0}^i (-1)^{i-k} \int_a^t \overset{\cdot}{\cdot} \overset{\cdot}{\cdot} \overset{\cdot}{\cdot} \int_a^t f_{x_j^{(k)}} ds.$$

and  $P_{x_j, 2n-1}(t) = \sum_{k=0}^{2n-1} c_{j,k} t^k$  are polynomials of degree  $2n-1$ , whose coefficients  $c_{j,k}$  are completely determined as the solutions of  $2n \times 2n$  linear systems which depend on the concrete choice of the metric  $\langle \cdot, \cdot \rangle_n$  and the affine boundary constraints. Notice that then, while an extremal is a zero of the gradient for any choice of the metric (B.1), the gradient itself depends on the metric and, therefore the metric choice is crucial in our computation.

If  $\mathcal{F}$  is considered acting on a subspace satisfying additional constraints  $X_{\mathcal{G}}^n$ , the gradient  $\nabla_*\mathcal{F}_{\mathbf{x}}$  is the orthogonal projection of  $\nabla\mathcal{F}_{\mathbf{x}}$  onto the corresponding tangent space and computation of the gradient requires a more elaborated process.

On the other hand, one of the most common methods for minimization of  $\mathcal{F}$  is the *gradient steepest descent method*. Basically, the essence of this method is to analyze the behavior of the sequence  $\{\mathbf{x}_k, k \in \mathbb{N}\}$  of successive approximations for the local minimum points of  $\mathcal{F}$  given by the formula

$$\mathbf{x}_{k+1} = \mathbf{x}_k + t_k \mathbf{h}_k, \quad k \in \mathbb{N},$$

where  $t_k$  is a sequence of positive numbers, the so called *control parameters*, which lie in a closed interval of the real line. In order to construct the sequence  $\{\mathbf{x}_k, k \in \mathbb{N}\}$ , start with an arbitrary point  $\mathbf{x}_o \in X^n$  (where, of course,  $\nabla\mathcal{F}_{\mathbf{x}_o} \neq 0$ ), then, assuming that  $\mathbf{x}_o, \mathbf{x}_1, \dots, \mathbf{x}_k$  have already been constructed, proceed by choosing a sequence  $\mathbf{h}_k \in X^n$  such that  $\langle \nabla\mathcal{F}_{\mathbf{x}_k}, \mathbf{h}_k \rangle < 0$  (usually,  $\mathbf{h}_k = -\nabla\mathcal{F}_{\mathbf{x}_k}$ ) and then take  $\mathbf{x}_{k+1} = \mathbf{x}_k + t_k \mathbf{h}_k$ .

A numerical method to locate minimizers of this general class of variational problems under both affine and isoperimetric constraints is implemented in [9] (see also, the webpage of the research group [www.ikergeometry.org](http://www.ikergeometry.org)). The method is suitable for application to the energy functionals described in Chapters 1 and 2, in particular it will be applicable to Frenet-Serret actions after some convenient adjustments.



# References

- [1] F. J. Almgren, Some Interior Regularity Theorems for Minimal Surfaces and an Extension of Bernstein's Theorem, *Ann. of Math.*, **84** (1966), 277-292.
- [2] J. A. Aledo and J. A. Gálvez, Some Rigidity Results for Compact Spacelike Surfaces in the 3-Dimensional De Sitter Space, *Differential Geometry, Valencia*, (2001).
- [3] L. Andrews and H. Li, Embedded Constant Mean Curvature Tori in the Three-Sphere, *J. Diff. Geom.*, **99** (2015), 169-189.
- [4] G. Arreaga, R. Capovilla and J. Guven, Frenet-Serret Dynamics, *Class. Quantum Grav.*, **18** (2001), 5065-5084.
- [5] J. Arroyo, Presión Calibrada Total: Estudio Variacional y Aplicaciones al Problema de Willmore-Chen, *PhD Thesis*, UPV-EHU (2001).
- [6] J. Arroyo, M. Barros and O. J. Garay, Some Examples of Critical Points for the Total Mean Curvature Functional, *Proc. Edinb. Math. Soc.*, **43** (2000), 587-603.
- [7] J. Arroyo, M. Barros and O. J. Garay, Models of Relativistic Particle with Curvature and Torsion Revisited, *Gen. Relativ. Gravit.*, **36** (2004), 1441-1451.
- [8] J. Arroyo, O. J. Garay and J. Mencía, A Note on Closed Generalized Elastic Curves in  $\mathbb{S}^2(1)$ , *J. Geom. Phys.*, **48** (2003), 339-353.
- [9] J. Arroyo, O. J. Garay, J. J. Mencía and A. Pámpano, A Gradient-Descent Method for Lagrangian Densities depending on Multiple Derivatives, *preprint*, (2018).
- [10] J. Arroyo, O. J. Garay and A. Pámpano, Binormal Motion of Curves with Constant Torsion in 3-Spaces, *Adv. Math. Phys.*, **2017** (2017).
- [11] J. Arroyo, O. J. Garay and A. Pámpano, Boundary Value Problems for Euler-Bernoulli Planar Elastica. A Solution Construction Procedure, *submitted*, (2018).
- [12] J. Arroyo, O. J. Garay and A. Pámpano, Constant Mean Curvature Invariant Surfaces and Extremals of Curvature Energies, *J. Math. Anal. App.*, **462** (2018), 1644-1668.

- [13] J. Arroyo, O. J. Garay and A. Pámpano, Curvature-Dependent Energies Minimizers and Visual Curve Completion, *Nonlinear Dyn.*, **86** (2016), 1137-1156.
- [14] J. Arroyo, O. J. Garay and A. Pámpano, Delaunay Surfaces in Riemannian 3-Space Forms, *preprint*, (2018).
- [15] J. Arroyo, O. J. Garay and A. Pámpano, Extremal Curves of a Total Curvature Type Energy, *Proc. Int. Conf. NOLASC15*, (2015), 103-112.
- [16] P. Baird and J. Eells, A Conservation Law for Harmonic Maps, Geometry Symposium Utrecht 1980, 1-25, *Lecture Notes in Mathematics*, Springer, **894** (1981).
- [17] M. Barros, Willmore Tori in Non-Standard 3-Spheres, *Math. Proc. Camb. Phil. Soc.*, **121** (1997), 321-324.
- [18] M. Barros, M. Caballero and M. Ortega, Rotational Surfaces in  $L^3$  and Solutions of the Nonlinear Sigma Model, *Comm. Math. Phys.*, **290** (2009), 437-477.
- [19] M. Barros, J. L. Cabrerizo, M. Fernández and A. Romero, Magnetic Vortex Filament Flows, *J. Math. Phys.*, **48** (2007), 082904.
- [20] M. Barros, A. Ferrández and O. J. Garay, Equivariant Willmore Surfaces in Conformal Homogeneous Three Spaces, *J. Math. Anal. Appl.*, **431-1** (2015), 342-364.
- [21] M. Barros, A. Ferrández, P. Lucas and M.A. Meroño, General Helices in the 3-dimensional Lorentzian Space Forms, *Rocky Mount. J. Math.*, **31** (2001), 373-388.
- [22] M. Barros, A. Ferrández, P. Lucas and M.A. Meroño, Solutions of the Betchov-Da Rios Soliton Equations: A Lorentzian Approach, *J. Geom. Phys.*, **31** (1999), 217-228.
- [23] M. Barros, A. Ferrández, P. Lucas and M.A. Meroño, Willmore Tori and Willmore-Chen Submanifolds in Pseudo-Riemannian Spaces, *J Geom. Phys.*, **28** (1998), 45-66.
- [24] M. Barros and O.J. Garay, Critical Curves for the Total Normal Curvature in Surfaces of 3-dimensional Space Forms, *J. Math. Anal. Appl.*, **389** (2012), 275-292.
- [25] M. Barros, O. J. Garay and A. Pámpano, Willmore-like Tori in Killing Submersions, *Adv. Math. Phys.*, **2018** (2018).
- [26] G. Ben-Yosef and O. Ben-Shahar, A Tangent Bundle Theory for Visual Curve Completion, *IEEE Trans. Pattern Anal. Mach. Intell.*, **34-7** (2012), 1263-1280.
- [27] G. Ben-Yosef and O. Ben-Shahar, Tangent Bundle Elastica and Computer Vision, *IEEE Trans. Pattern Anal. Mach. Intell.*, **37-1** (2015), 164-174.

- 
- [28] W. A. Blankinship, The Curtain Rod Problem, *Amer. Math. Monthly*, **50** (1943), 186-189.
- [29] W. Blaschke, Vorlesungen über Differentialgeometrie und Geometrische Grundlagen von Einsteins Relativitätstheorie I: Elementare Differentialgeometrie, *Springer*, (1930).
- [30] S. Brendle, Embedded Minimal Tori in  $S^3$  and the Lawson Conjecture, *Acta Math.*, **211** (2013), 177-190.
- [31] R. Bryant, Surfaces of Mean Curvature One in Hyperbolic Space, *Asterisque*, **154-155** (1987), 341-347.
- [32] R. Bryant and P. Griffiths, Reduction of Order for Constrained Variational Problems and  $\int_{\gamma} \frac{\kappa^2}{2} ds$ , *Am. J. Math.*, **108** (1986), 525-570.
- [33] M. Caballero, Superficies Willmore con Borde y Sigma Modelos No Lineales, *PhD Thesis*, Univ. Granada (2008).
- [34] R. Caddeo, S. Montaldo, C. Oniciuc and P. Piu, Surfaces in Three-Dimensional Space Forms with Divergence-Free Stress-Bienergy Tensor, *Annali di Matematica*, **193** (2014), 529-550.
- [35] M. P. do Carmo and M. Dajczer, Helicoidal Surfaces with Constant Mean Curvature, *Tohoku Math. J.*, **34** (1982), 425-435.
- [36] M. do Carmo and M. Dajczer, Rotation Hypersurfaces in Spaces of Constant Curvature, *Trans. Amer. Math. Soc.*, **277** (1983), 685-709.
- [37] E. Cartan, Familles de Surfaces Isoparamétriques dans les Espaces à Courbure Constante, *Annali di Mat.*, **17** (1938), 177-191.
- [38] E. Cartan, *Leçons sur la Géométrie des Espaces de Riemann*, Gauthier Villars, Paris, 1946.
- [39] B-Y. Chen, *Pseudo-Riemannian Geometry,  $\delta$ -Invariants and Applications*, World Scientific, Singapore, 2011.
- [40] B-Y. Chen, Some Conformal Invariants of Submanifolds and their Applications, *Boll. Un. Mat. Ital.*, **6** (1974), 380-385.
- [41] B-Y. Chen, *Total Mean Curvature and Submanifolds of Finite Type*, 2<sup>nd</sup> Edition, Series in Pure Mathematics: Volume 27, World Scientific, 2014.
- [42] S. S. Chern, Some New Characterization of the Euclidean Sphere, *Duke Math. J.*, **12** (1945), 279-290.

- [43] R. M. Corless, G. H. Gonnet, D. E. Hare, D. J. Jeffrey and D. E. Knuth, On the Lambert W Function, *Adv. Comp. Math.*, **5-4** (1996), 329-359.
- [44] M. Dajczer, *Submanifolds and Isometric Immersions*, Mathematics Lecture Series 13, Publish or Perish Inc, Houston, Texas 1990.
- [45] M. Dajczer and K. Nomizu, On Flat Surfaces in  $\mathbb{S}_1^3$  and  $\mathbb{H}_1^3$ , *Manifolds and Lie Groups, Notre Dame*, (1980), 71-108.
- [46] J. D'Ambrose, EMP Reformulations of Einstein's Equations as an Application of a Property of Suitable Second Order Differential Equations, *AIP Conf. Proc.*, **1243** (2010), 87-98.
- [47] C. Delaunay, Sur la Surface de Revolution dont la Courbure Moyenne est Constante, *J. Math. Pures Appl.*, **16** (1841), 309-320.
- [48] E. Demir and R. López, Helicoidal Surfaces in Minkowski Space with Constant Mean Curvature and Constant Gauss Curvature, *Cent. Eur. J. Math.*, **12** (2014), 1349-1361.
- [49] Q. Ding, X. Liu and W. Wang, The Vortex Filament in the Minkowski 3-Space and Generalized Bi-Schrodinger Maps, *J. Phys.*, **45** (2012), 455201.
- [50] R. Duits, U. Boscain, F. Rossi and Y. Sachkov, Association Fields via Cuspless Sub-Riemannian Geodesics in  $SE(2)$ , *J. Math. Imaging Vis.*, **49** (2014), 384-417.
- [51] J. Eells and J. H. Sampson, Harmonic Mappings of Riemannian Manifolds, *Amer. J. Math.*, **86** (1964), 109-160.
- [52] C. J. Eliezer and A. Grey, A Note on the Time-Dependent Harmonic Oscillator, *SIAM J. App. Math.*, **30** (1976), 463-468.
- [53] J. Erbacher, Reduction of the Codimension of an Isometric Immersion, *J. Diff. Geom.*, **5** (1971), 333-340.
- [54] V. P. Ermakov, Second-Order Differential Equations. Conditions of Complete Integrability, *Univ. Isz. Kiev Series III*, **9** (1980), 1-25.
- [55] J. M. Espinar and I. S. de Oliveira, Locally Convex Surfaces Immersed in a Killing Submersion, *Bull. Braz. Math. Soc.*, **44** (2013), 155-171.
- [56] L. Euler, Methodus Inveniendi Lineas Curvas Maximi Minimive Proprietate Gaudentes, Sive Solutio Problematis Isoperimetrici Lattissimo Sensu Accepti, *Bousquet, Lausannae et Genevae*, **24** (1744).



- 
- [57] A. Feoli, V. V. Nesterenko and G. Scarpetta, Functionals Linear in Curvature and Statistics of Helical Proteins, *Nucl. Phys. B.*, **705** (2005), 577-592.
- [58] A. Ferrández, J. Guerrero, M.A. Javaloyes and P. Lucas, Particles with Curvature and Torsion in Three-dimensional Pseudo-Riemannian Space Forms, *J. Geom. Phys.*, **56** (2006), 1666-1687.
- [59] A. Fujioka and J. Inoguchi, Timelike Bonnet Surfaces in Lorentzian Space Forms, *Differential Geom. Appl.*, **18-1** (2003), 103-111.
- [60] Y. Fu and L. Li, A Class of Weingarten Surfaces in Euclidean 3-Space, *Abs. App. Anal.*, **2013** (2013).
- [61] J. A. Gálvez, Surfaces of Constant Curvature in 3-dimensional Space Forms, *Math. Contemporanea*, **37** (2009), 1-42.
- [62] O. J. Garay, Riemannian Submanifolds Shaped by the Bending Energy and its Allies, *Proc. of the Sixteenth International Workshop on Diff. Geom.*, **16** (2012), 57-70.
- [63] O. J. Garay and A. Pámpano, A Note on p-Elasticae and the Generalized EMP Equation, *submitted*, (2018).
- [64] O. J. Garay and A. Pámpano, Binormal Evolution of Curves with Prescribed Velocity, *WSEAS Trans. Fluid Mech.*, **11** (2016), 112-120.
- [65] O. J. Garay, A. Pámpano and C. Woo, Hypersurface Constrained Elasticae in Lorentzian Space Forms, *Adv. Math. Phys.*, **2015** (2015).
- [66] S. Germain, Memoire sur la Courbure des Surfaces, *J. Reine Angrew. Math.*, **7** (1831), 1-29.
- [67] M. J. Gomes, Spherical Surfaces with Constant Mean Curvature in Hyperbolic Space, *Bol. Soc. Brasil Mat.*, **18** (1987), 49-73.
- [68] I. S. Gradshteyn and I. M. Ryzhik, *Table of Integrals, Series and Products*, Academic Press London, 2007.
- [69] L. K. Graves, Codimension One Isometric Immersion Between Lorentz Spaces, *Trans. Amer. Math. Soc.*, **252** (1979), 367-392.
- [70] A. Gray, Pseudo-Riemannian Almost Product Manifolds and Submersions, *J. Math. Mech.*, **16** (1967), 715-727.
- [71] J. Hahn, Isoparametric Hypersurfaces in the Pseudo-Riemannian Space Forms, *Math. Z.*, **187** (1984), 195-208.

- [72] J. Hano and K. Nomizu, Surfaces of Revolution with Constant Mean Curvature in Lorentz-Minkowski Space, *Tohoku Math. J.*, **36** (1984), 427-437.
- [73] H. Hasimoto, A Soliton On A Vortex Filament, *J. Fluid Mech.*, **51** (1972), 477-485.
- [74] H. Hasimoto, Motion of a Vortex Filament and its Relation to Elastica, *J. Phy. Soc. Japan*, **31** (1971), 293-294.
- [75] W. Helfrich, Elastic Properties of Lipid Bilayers: Theory and Possible Experiments, *Zeit. Naturfor. C.*, **28** (1973), 693-703.
- [76] R. Hawkins and J. Lidsey, The Ermakov-Pinney Equation in Scalar Field Cosmologies, *Physical Review D.*, **66** (2002), 23523-23531.
- [77] D. Hilbert, Die Grundlagen der Physik, *Math. Ann.*, **92** (1924), 1-32.
- [78] H. Hopf, *Differential Geometry in the Large*, Lecture Notes in Mathematics, 1000, Springer-Verlag, Berlin, 1983.
- [79] H. Hopf, Uber Flächen mit einer Relation Zwischen den Hauptkrümmungen, *Math. Nachr.*, **4** (1951), 232-249.
- [80] W-Y. Hsiang, Generalized Rotational Hypersurfaces of Constant Mean Curvature in the Euclidean Spaces I, *J. Differential Geom.*, **17** (1982), 337-356.
- [81] T. A. Ivey and D. A. Singer, Knot Types Homotopies and Stability of Closed Elastic Rods, *Proc. London Math. Soc.*, **79-3** (1999), 429-450.
- [82] M. A. Javaloyes, Sumersiones Pseudo-Riemannianas y Modelos Geometricos de Particulas Relativistas, *PhD Thesis*, Univ. Murcia (2004).
- [83] G. Y. Jiang, The Conservative Law for 2-Harmonic Maps between Riemannian Manifolds, *Acta Math. Sinica*, **30** (1987), 220-225.
- [84] G. Y. Jiang, 2-Harmonic Maps and their First and Second Variational Formulas, *Chinese Ann. Math. Ser. A*, **7** (1986), 389-402.
- [85] N. Kapouleas, Constant Mean Curvature Surfaces Constructed by Fusing Wente Tori, *Invent. Math.*, **119** (1995), 443-518.
- [86] S. Kawakubo, Kirchhoff Elastic Rods in Three Dimensional Space Forms, *Jap. J. Math.*, **60** (2008), 551-582.
- [87] S. Kawamoto, Codimension Reduction for Real Submanifolds of a Complex Hyperbolic Space, *Rev. Mat. Univ. Complut. Madrid*, **7-1** (1994), 119-128.

- 
- [88] K. Kenmotsu, Surfaces of Revolution with Prescribed Mean Curvature, *Tohoku Math. J.*, **32** (1980), 147-153.
- [89] S. Kida, A Vortex Filament Moving Without Change of Form, *J. Fluid Mech.*, **112** (1981), 397-409.
- [90] N. Koiso, Vortex Filament Equation in a Riemannian Manifold, *Tohoku Math. J.*, **55** (2003), 311-320.
- [91] J. Langer and D. A. Singer, Curves in the Hyperbolic Plane and Mean Curvature of Tori in 3 Space, *Bull. London Math. Soc.*, **18** (1984), 531-534.
- [92] J. Langer and D. A. Singer, Knotted Elastic Curves in  $\mathbb{R}^3$ , *J. London Math. Soc.*, **16** (1984), 512-520.
- [93] J. Langer and D.A. Singer, Lagrangian Aspects of the Kirchhoff Elastic Rod, *SIAM Rev.*, **38** (1996), 605-618.
- [94] J. Langer and D. A. Singer, The Total Squared Curvature of Closed Curves, *J. Diff. Geom.*, **20** (1984), 1-22.
- [95] P. S. Laplace, *Traite de Mecanique Celeste*, Volume 4, Paris, 1805.
- [96] H. B. Lawson, Complete Minimal Surfaces in  $S^3$ , *Ann. of Math.*, **92** (1970), 335-374.
- [97] H. B. Lawson, The Unknottedness of Minimal Embeddings, *Invent. Math.*, **11** (1970), 183-187.
- [98] S. Lee and K. A. Zarske, Surfaces of Revolution with Constant Mean Curvature in Hyperbolic 3-Space, *Differ. Geom. Dynam. Syst.*, **16** (2014), 203-218.
- [99] R. Levien, The Elastica: A Mathematical History, *Technical Report*, No. UCB/EECS-2008-103, Univ. of Berkeley.
- [100] C. Li and J. Wang, The Classification of Isoparametric Surfaces in  $S_1^3$ , *Kobe J. Math.*, **22** (2005), 1-12.
- [101] E. Lobeau, S. Montaldo and C. Oniciuc, The Stress-Energy Tensor for Biharmonic Maps, *Math. Z.*, **259** (2008), 503-524.
- [102] R. López, On Linear Weingarten Surfaces, *Internat. J. Math.*, **19** (2008), 439-448.
- [103] R. López and A. Pámpano, Classification of Rotational Surfaces in Euclidean Space Satisfying a Linear Relation between their Principal Curvatures, *submitted*, (2018).

- 
- [104] A. E. Love, *A Treatise on the Mathematical Theory of Elasticity*, Dover Publications, New York, 1944.
- [105] M. A. Magid, Isometric Immersions of Lorentz Space with Parallel Second Fundamental Forms, *Tsukuba J. Math.*, **8** (1984), 31-54.
- [106] M. A. Magid, Lorentzian Isoparametric Hypersurfaces, *Pacific J. Math.*, **118** (1985), 165-197.
- [107] J. M. Manzano, On the Classification of Killing Submersions and Their Isometries, *Pacific J. Math.*, **270** (2014), 367-392.
- [108] F. C. Marques and A. Neves, Min-Max Theory and the Willmore Conjecture, *Ann. Math. Second Series*, **179-2** (2014), 683-782.
- [109] I. V. Mladenov and J. Oprea, *The Mylar Balloon: New Viewpoints and Generalizations*, Geometry, Integrability and Quantization, 246-263, Sofia, 2007.
- [110] I. V. Mladenov and J. Oprea, The Mylar Balloon Revisited, *Amer. Math. Monthly*, **110** (2003), 761-784.
- [111] S. Montaldo and A. Pámpano, Biconservative Linear Weingarten Surfaces, *preprint*, (2018).
- [112] D. Mumford, *Elastica and Computer Vision*, Algebraic Geometry and its Applications, 491-506, Springer-Verlag, New York, 1994.
- [113] S. Nistor, Complete Biconservative Surfaces in  $\mathbb{R}^3$  and  $\mathbb{S}^3$ , *J. Geom. Phys.*, **110** (2016), 130-153.
- [114] S. Nistor and C. Oniciuc, Global Properties of Biconservative Surfaces in  $\mathbb{R}^3$  and  $\mathbb{S}^3$ , (2017).
- [115] J. C. Nitsche, Boundary Value Problems for Variational Integrals Involving Surface Curvatures, *Q. App. Math.*, **51-2** (1993), 363-387.
- [116] B. O'Neill, The Fundamental Equations of a Submersion, *Michigan Math. J.*, **13** (1966), 459-469.
- [117] R. S. Palais, The Principle of Symmetric Criticality, *Commun. Math. Phys.*, **69** (1979), 19-30.
- [118] B. Palmer, Spacelike Constant Mean Curvature Surfaces in Pseudo-Riemannian Space Forms, *Ann. Global Anal. Geom.*, **8** (1990), 217-226.

- 
- [119] A. Pámpano, Binormal Evolution of Blaschke's Curvature Energy Extremals in the Minkowski 3-Space, *Prooc. Young Res. Work. Diff. Geom.*, (2017), 115-123.
- [120] A. Pámpano, Planar p-Elasticae and Rotational Linear Weingarten Surfaces, *preprint*, (2018).
- [121] O. M. Perdomo, Embedded Constant Mean Curvature Hypersurfaces on Spheres, *Asian J. Math.*, **14** (2010), 73-108.
- [122] O. M. Perdomo, Rotational Surfaces in  $S^3$  with Constant Mean Curvature, *J. Geom. Anal.*, **26** (2016), 2155-2168.
- [123] O. M. Perdomo, Embedded CMC Hypersurfaces on Hyperbolic Spaces, *Rev. Colomb. Mat.*, **45** (2011), 81-96.
- [124] J. Petitot, The Neurogeometry of Pinwheels as a Sub-Riemannian Contact Structure, *J. Physiol.*, **97** (2003), 265-309.
- [125] U. Pinkall, Hopf Tori in  $S^3$ , *Invent. Math.*, **81-2** (1985), 379-386.
- [126] U. Pinkall and I. Sterling, On the Classification of Constant Mean Curvature Tori, *Ann. of Math.*, **130** (1989), 407-451.
- [127] E. Pinney, The Nonlinear Differential Equation  $y'' + p(x)y' + cy^3 = 0$ , *Proc. A. M. S.*, **1** (1950).
- [128] J. B. Ripoll, Superficies Invariantes de Curvatura Media Constante, *PhD Thesis*, IMPA (1986).
- [129] A. Ros, The Willmore Conjecture in the Real Projective Space, *Math. Soc.*, **16-5** (1984), 531-534.
- [130] L. Sante da Rios, Sul Moto d'un Liquido Indefinito con un Fileto Vorticoso di Forma Qualunque, *Rend. Cir. Mat. Palermo*, **22** (1906), 117-135.
- [131] N. Sasahara, Spacelike Helicoidal Surfaces with Constant Mean Curvature in Minkowski 3-Space, *Tokyo J. Math.*, **23** (2000).
- [132] W. K. Schief and C. Rogers, Binormal Motion of Curves of Constant Curvature and Torsion. Generation of Soliton Surfaces, *Proc. R. Soc. Lond.*, **455** (1999), 3163-3188.
- [133] W. K. Schief, C. Rogers and A. P. Bassom, Ermakov System of Arbitrary Order and Dimension: Structure and Linearization, *L. Phys. A: Math. Gen.*, **29** (1996), 903-911.

- [134] K. Shiohama and R. Takagi, A Characterization of a Standard Torus in  $E^3$ , *J. Diff. Geom.*, **4** (1970), 477-485.
- [135] I. Sterling, A Generalization of a Theorem of Delaunay to Rotational W-Hypersurfaces of  $\sigma_\Gamma$ -type in  $S^{n+1}$  and  $H^{n+1}$ , *Pacific J. Math.*, **127** (1987), 187-197.
- [136] G. Thomsen, Uber Konforme Geometrie I: Grundlagen der Konformen Flächentheorie, *Abk. Math. Sem. Univ. Hamburg*, **3** (1923), 31-56.
- [137] P. Topping, Towards the Willmore Conjecture, *Calc. Var. Part. Diff. Eqs.*, **11-4** (2000), 361-393.
- [138] C. Truesdel, The Rational Mechanics of Flexible or Elastic Bodies, *Introd. Vol. X and XI, L. Euleri Opera Omnia*, Birkhuser, Basel-Zurich (1960), 1338-1788.
- [139] T.I. Vogel, Stability of a Liquid Drop Trapped Between Two Parallel Planes, *SIAM J. Applied Math.*, **47-3**, 516-525.
- [140] G. Vranceanu, *Lecons de Geometrie Differentielle*, Ed. Acad. Rep. Pop. Roum., vol I, Bucarest, 1957.
- [141] J. L. Weiner, On a Problem of Chen, Willmore et Al, *Indiana Univ. Math. J.*, **27** (1978), 19-35.
- [142] J. Weingarten, Ueber eine Klasse auf Einander Abwickelbarer Flächen, *J. Reine Angrew. Math.*, **59** (1861), 382-393.
- [143] H. C. Wente, Counterexample to a Conjecture of H. Hopf, *Pacific J. Math.*, **121** (1986), 193-243.
- [144] T. J. Willmore, Mean Curvature of Immersed Surfaces, *An. Sti. Univ. Al. I. Cuza Iasi Sec. I. a Mat. (N.S.)*, **14** (1968), 99-103.
- [145] L. Xiao, Lorentzian Isoparametric Hypersurfaces in  $H_1^{n+1}$ , *Pacific J. Math.*, **189** (1999), 377-397.
- [146] T. Young, An Essay on the Cohesion of Fluids, *Phil. Trans. Royal Soc. London*, **95** (1805), 65-87.